

**Consideration of
Climate Changes in
Biosphere Modelling
for Performance
Assessment**

Consideration of Climate Changes in Biosphere Modelling for Performance Assessment

Nathascha Semioshkina (HMGU)
Christian Staudt (HMGU)
Christian Kaiser (HMGU)
Gerhard Pröhl (GRS)
Christine Fahrenholz (GRS)
Ulrich Noseck (GRS)

December 2012

Acknowledgement:

This report was prepared under contract No. 02 E 10548 by the Federal Ministry of Economics and Technology (BMWi).

The work was conducted by the Gesellschaft für Anlagen- und Reaktorsicherheit (GRS) mbH.

The author is responsible for the content of the report.

Keywords:

Biosphere, Climate change, Modelling, Radionuclides, Safety assessment, Uncertainty analysis

Zusammenfassung

Klimaveränderungen können erheblichen Einfluss auf Biosphärenprozesse und Expositionspfade von Radionukliden haben. Diese müssen in einem Safety Case für Endlager mit radioaktiven Abfällen betrachtet werden. Die hier beschriebenen Arbeiten stellen eine Weiterführung der in /NOS 08/ beschriebenen Studie dar. Um diese Einflüsse abzuschätzen, wurden Biosphärenmodelle entwickelt und Biosphären-Dosiskonversionsfaktoren (BDCFs) ermittelt. Der Ansatz basiert auf einer normierten Radionuklidkonzentration in einem oberflächennahen Grundwasserleiter, aus dem die Radionuklide in die Biosphäre gelangen können. In dieser Arbeit werden zwei Szenarien betrachtet: (i) Grundwasser steigt in die Bodenschichten, die für die Landwirtschaft verwendet werden auf (RGW-Szenario) und (ii) die Böden werden durch Bewässerung mit Grundwasser kontaminiert (Brunnen Szenario). Beide Szenarien wurden bereits in /NOS 08/ für sechs diskrete Klimazustände, für die repräsentative Klimastationen angenommen wurden, betrachtet.

In der hier präsentierten Arbeit wurden in einem ersten Schritt diejenigen Klimazustände, die die potentielle zukünftige Klimaentwicklung in Norddeutschland über einen Zeitraum von 1 Millionen Jahren abdecken, kritisch überprüft und gerechtfertigt. Zu diesem Zweck wurde u. a. auf Ergebnisse des EU-Projekts „Modelling sequential BIOSphere systems under CLIMate change for radioactive waste disposal“ (BIOCLIM) zurückgegriffen. Als Konsequenz wurden insgesamt neun Klimastationen – also drei zusätzliche Stationen zu den in /NOS 08/ betrachteten – ausgewählt, um möglichst umfassend kältere und wärmere Klimate mit unterschiedlichen Niederschlagsmengen zu berücksichtigen. Speziell die Rechnungen für die subtropische Referenzregion Valladolid zeigten gegenüber den bisher berücksichtigten Klimastationen erhöhte BDCFs.

In einem zweiten Schritt wurde eine globale Unsicherheits- und Sensitivitätsanalyse durchgeführt, in der eine große Anzahl an Parametern des Biosphärenmodells für das temperierte und das Mediterrane Klima variiert wurde. Die Unsicherheitsanalyse, speziell die Bandbreite der berechneten BDCFs deuten darauf hin, dass der Einfluss der Unsicherheiten in den Parametern vergleichbar oder für manche Radionuklide sogar höher ist, als der Einfluss verschiedener zukünftiger Klimazustände, der für die neun Klimastationen ermittelt wurde. Allerdings sollte die Unsicherheitsanalyse als eine erste Abschätzung betrachtet werden, da zur Ableitung von Wahrscheinlichkeitsdichtefunktionen (pdfs) für die Parameter und zur Behandlung von Korrelationen zwischen den Pa-

rametern noch weitere FuE-Arbeiten notwendig sind. Die Ergebnisse der Sensitivitätsanalyse stimmen gut mit den Beobachtungen aus deterministischen Rechnungen überein: Die wichtigsten Expositionspfade und die entsprechenden Modellparameter aus den deterministischen Rechnungen zeigten sich auch in den Sensitivitätsanalysen als wichtigste Parameter.

In einem weiteren Schritt wurden die Auswirkungen von Klimaübergängen untersucht, speziell, ob Prozesse, die während Klimaübergängen auftreten, zu einer erhöhten Radionuklidfreisetzung, bzw. -akkumulation führen und dadurch höhere Strahlenexpositionen bewirken können als diejenigen, die für diskrete Klimazustände ermittelt wurden. Ziel war es, entsprechende Prozesse zu identifizieren, wobei die Untersuchungen nicht das Ziel hatten, abdeckend zu sein. Als wichtigste Prozesse stellten sich diejenigen bei Übergängen von kälteren zu wärmeren Klimazuständen heraus. Speziell für redox-sensitive Radionuklide, deren chemische Speziation sich bei trockeneren, stärker oxidierenden Bedingungen verändern kann, wodurch sie für Pflanzen besser verfügbar werden, sind gegenüber den diskreten Klimazuständen erhöhte BDCFs zu erwarten. Zur Untersuchung entsprechender Übergänge wurden exemplarisch zwei Szenarien, die Austrocknung eines Sees und die Trocknung eines Moores betrachtet.

Um die Effekte während der Übergänge, die eine Abfolge von komplexen Prozessen sind, zu quantifizieren wurde versucht, die Modelle so einfach wie möglich zu halten. Die Modellrechnungen zeigen, dass die Kontamination von Pflanzen aufgrund der erheblich höheren Mobilität von redox-sensitiven Radionukliden bei derartigen Übergängen signifikant ansteigen kann. Dieser Effekt wurde anhand der Simulation von Veränderungen der Aktivitäts-Konzentrationen im Sediment sowie im Gras, das auf den Sedimenten eines ausgetrockneten Sees, bzw. eines trocken gelegten Moores wuchs, demonstriert. Eine Auswirkung auf die BDCFs für die effektive Dosis konnte aber nur für die Radionuklide Se-79 und Tc-99 beobachtet werden, bei denen die Expositionspfade über kontaminierten Boden einen vergleichsweise hohen Anteil am BDCF haben. Für diese Rechnungen wurden eine relativ hohe Vorkontamination des Bodens und ein relativ schneller Übergang zwischen reduziertem und oxidiertem Redoxzustand angenommen. Bei einer geringeren Vorkontamination des Bodens nehmen die Effekte ab, da die Beiträge bodenunabhängiger Prozesse, wie Eintrag über die Blätter oder Aufnahme über den Trinkwasserpfad relativ zunehmen. Da die Dauer des Übergangs schwer abzuschätzen ist, wurden Rechnungen für drei verschiedene Übergangszeiträume durchgeführt: 1, 10 und 100 Jahre. Längere Übergangszeiträume führen dabei zu einer Reduktion der Peaks.

Mit den hier vorgestellten Untersuchungen wurde versucht, den Einfluss zukünftiger Klimazustände und Übergangsprozessen zwischen zwei diskreten Klimazuständen auf Biosphärenprozesse und resultierende Strahlenexpositionen anhand von stilisierten Modellen abzuschätzen. Als Fazit ist zu sagen, dass die Bandbreiten für die BDCFs, die sich aus der Variation der potentiellen zukünftigen Klimazustände ergeben, in einer ähnlichen Größenordnung liegen wie die die sich aus generellen Parameterunsicherheiten ergeben. Die Modelle erlaubten auch die vereinfachte Berechnung von Biosphärenprozessen bei Klimaübergängen, die komplexer Natur sein können. Generell zeigen die Ergebnisse, dass Klimaübergänge Strahlenexpositionen (BDCFs) bewirken können, die gegenüber den für diskrete Klimazustände erhöht sein können, aber nicht um mehr als einen Faktor zehn. Relativ hohe Akkumulationspeaks redoxsensitiver Radionuklide in Böden und Pflanzen treten bei den BDCFs nur noch erheblich reduziert auf, da andere Expositionspfade, die unabhängig von der Radionuklidmobilisierung in Böden ebenfalls zu den BDCFs beitragen.

Preface

The assessment of the long-term safety of a repository for radioactive or hazardous waste and therewith the development of a safety case requires a comprehensive system understanding, a continuous development of the methods of a safety case and capable and qualified numerical tools. The objective of the project “Scientific basis for the assessment of the long-term safety of repositories”, identification number 02 E 10548, was to follow national and international developments in this area, to evaluate research projects, which contribute to knowledge, model approaches and data, and to perform specific investigations to improve the methodologies of the safety case and the long-term safety assessment.

This project, founded by the German Federal Ministry of Economics and Technology (BMWi), was performed in the period from 1st August 2008 to 31st July 2012. The results of the key topics investigated within the project are published in the following reports:

- GRS-264: Grundsatzfragen Hydrogeologie – Workshop der GRS in Zusammenarbeit mit dem PTKA-WTE
- GRS-269: Code Viper: Theory and Current Status
- GRS-291: Microbial Processes Relevant for the Long-Term Performance of Radioactive Waste Repositories in Clays
- GRS-294: Radionuclide Inventory of Vitrified Waste from Nuclear Fuel Reprocessing: Basic Issues and Current Status in Germany
- GRS-299: Impact of Different Climates and Climate Transitions on Biosphere Modelling in Long-Term Safety Assessment

The results of the whole project are summarised in the overall final report:

- GRS-298: Scientific Basis for a Safety Case of Deep Geological Repositories

List of contents

1	Introduction.....	1
2	Status of modelling	3
2.1	Transfer processes	8
2.2	Food and feed products considered.....	10
2.3	Main conclusions	12
3	Selection, justification of climate states and modelling results.....	15
3.1	Selection and justification	15
3.1.1	Predicted climate development.....	15
3.1.2	Selected reference climate regions.....	17
3.1.3	Model parameters for the additional reference climate regions and probabilistic models	21
3.1.4	Soil development	23
3.2	Results	24
3.3	Probabilistic uncertainty and sensitivity analysis	33
4	Identification of key transition processes affecting exposure	53
4.1	Selection and justification of climate transitions	54
4.1.1	Discrete climate states.....	56
4.1.2	Cooling	56
4.1.3	Warming.....	58
4.1.4	Redox sensitive radionuclides.....	62
4.1.5	Special scenario	63
4.1.6	Time scale	64

5	Modelling Exposure during Transitions.....	67
5.1	Drying of a Lake	67
5.2	Drying of fen	68
5.2.1	Sorption of radionuclides on peat soil	68
5.2.2	Using fen for agriculture.....	69
5.3	Description of the model	70
5.3.1	General assumptions of the model:	70
5.3.2	Model concept	71
5.3.3	Implementation of the model.....	73
6	Results	75
6.1	Lake.....	75
6.2	Fen	84
6.2.1	Fen for agricultural use	84
6.2.2	Fen peat as fuel.....	85
6.3	Calculation of the Biosphere Dose Conversion Factor (BDCF) for transition between two climates	88
6.4	Desertification.....	90
7	Summary and conclusions	93
	References	97
	List of figures.....	109
	List of tables	115

A	Annexes	119
A.1	Model approaches for exposure calculation	119
A.1.1	Activity in foods.....	119
A.1.2	Dose calculation	142
A.2	Characteristics of considered radionuclides	147
A.2.1	Selenium	147
A.2.2	Technetium.....	153
A.2.3	Neptunium	155
A.2.4	Uranium.....	156
A.2.5	Iodine.....	158
A.2.6	Cesium	160
A.2.7	K_d model.....	161
A.3	Soil classification (FAO).....	167
A.4	Examples of dried out Lakes.....	169
A.4.1	Peatland classification	171
A.5	Group of population considered in reference biosphere assessment	174
	Glossary	175

1 Introduction

For the long-term safety assessment of repositories for radioactive waste generally very long timescales have to be considered. As stated in the German safety requirements governing the final disposal of heat-generating radioactive waste an assessment period of one million years have to be addressed /BMU 10/. During this time frame significant changes of the climate will occur also impacting the environment including geomorphology, hydrology, flora and fauna as well as human habits.

One important aspect of climate changes for the long-term safety assessment of radioactive waste repositories is its impact on exposure pathways for humans in the future, which are dependent on the environmental characteristics mentioned. This topic has been dealt with in international projects like BIOMASS /IAE 03/, BIOMOSA /OLY 05/ and particularly in BIOCLIM /BIO 04/. The topic of BIOMASS describes the development of reference biosphere systems according to a fixed methodology. The methodology begins with defining the assessment context and the identification and justification of the biosphere systems. Those biosphere systems are then described in further detail and potentially exposed groups are considered. Finally the model is developed, calculations are done and further iterations can be used to refine the model. The international project BIOMOSA considered the application of the BIOMASS methodology at specific sites, as compared to a generic methodology application. In the BIOCLIM project the investigation of long-term climate changes and their impact on biosphere modelling was addressed.

Since so far no site for a radioactive waste repository is selected in Germany, a generic approach using analogue stations is applied to estimate the impact of future climatic changes on biosphere modelling, according to the methodology and experiences described in the international projects mentioned above. In our previous work six different discrete climate states, i. e., steppe (BS), Mediterranean (Cs), temperate (Cfb), boreal (Dfa/Dfb), and tundra (ET), have been considered /NOS 08/. For these climate states modelling approaches were developed and data for potential future distribution of temperature, precipitation, and humidity were taken from so-called analogue stations, which are characterized by those climates today: Marrakesh, Rome, Magdeburg, Rostow, Turku and Vardo, respectively. For all six climate states biosphere dose conversion factors (BDCFs) were calculated.

The first step in the work presented here is to check, whether these six climate stations really cover the potential range of climates which could be expected in Northern Germany within the next one million years. Based on paleoclimatic data and model calculations for future climates additional climate states might be selected and, a justification for the selected climate states can be given. Nevertheless, all parameters used for modelling of one single climate state are to some extent uncertain. In order to determine the uncertainty of BDCFs for a single climate state, bandwidths for all input parameters are estimated and a global uncertainty analyses for the current temperate climate and the Mediterranean climate is performed. Based on this the uncertainty of a BDCF can be compared with the magnitude BDCFs are impacted by climate changes and their effect on the environment.

A further important question is, whether the calculation of discrete climate states is sufficient to judge the impact of climate changes on potential radiation exposures of individuals. It is conceivable that effects or processes occurring during climate changes lead to an increased accumulation and/or release of radionuclides in the biosphere resulting in higher doses compared to that calculated for discrete climate states. In order to shed light on this question key processes are identified – by a sensitivity analysis as well as by expert guess – which might lead to such an increased accumulation and/or release of radionuclides. After identification of such processes first modelling approaches are developed to implement the respective processes and to simulate selected examples of transient biosphere systems driven by climate changes.

Simulation of these biosphere transitions based on generic models should firstly increase understanding in the effects occurring during transition states. Further it should clarify, which of the considered transition cases are of importance and which factors are controlling the temporal evolution of the radiation exposure. Particularly, it should be determined, whether a maximum value for the radiation exposure calculated during a transition could exceed the doses calculated for the discrete climate states.

2 Status of modelling

Within performance assessment amongst others, scenarios are considered, where radioactive waste gets into contact with water, containers fail and radionuclides are mobilised from the waste matrix. After release from the repository and transport through geological formations radionuclides can contaminate near-surface aquifers and may enter the biosphere via different geosphere-biosphere interfaces as the withdrawal of water from a well or by contamination of surface soil, if the water table is high /CRO 05/. Once entered the biosphere, radionuclides may cause exposures to humans via ingestion of water and food, inhalation of re-suspended contaminated soil particles as well as via external exposure from contaminated soils. The resulting radiation exposure potentially arising from the contamination of groundwater is an important safety indicator for the long-term safety assessment.

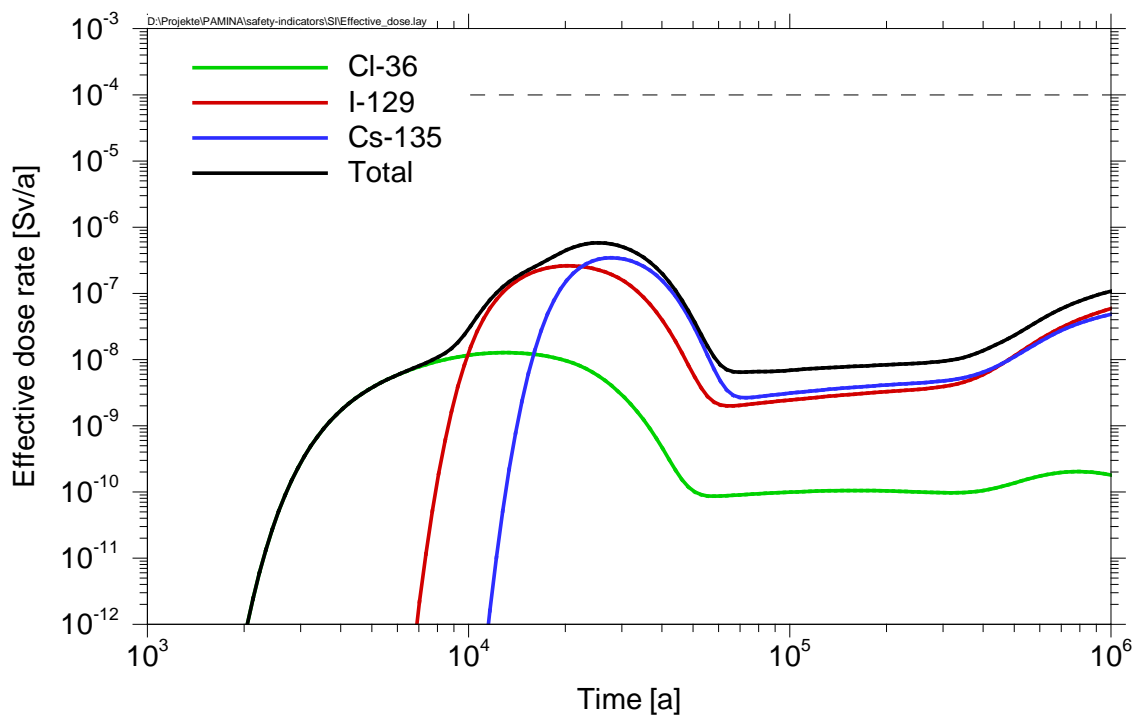


Fig. 2.1 Effective dose rate calculated for /BEX 08/

Fig. 2.1 shows a typical dose curve derived from performance assessment calculations. In this example a repository for HLW in rock salt is considered. The calculation is performed for a case, where the permeability of the shaft seal and the drift seals is increased after a period of 75 years by four orders of magnitude. This pessimistic parameter combination leads to a relatively early outflow of contaminated brine out of the

repository. However, this figure should mainly illustrate a fact, which is valid for most of the PA results, namely that the concentration distribution in surface near aquifers and therewith the calculated dose typically shows a plateau-like behaviour over several 10 000 years. This justifies the use of stationary BDCFs which are reached after relative long time frames, when the stationary state of soil contamination is reached, see section 3.2.

The biosphere characteristics and therewith the exposures to humans depend on environmental and climatic conditions, agricultural practices and the habits of potentially exposed people which are difficult to predict for very long periods. This is a key source of uncertainty in estimating doses in the post-closure period of nuclear waste repositories. Therefore, in a previous work we started to investigate the impact of climate changes on radiation exposures. In this work dose conversion factors for a number of specific situations, which reflect different climate conditions at the reference site were calculated /NOS 08/. The most relevant aspects are shortly summarised here.

In total six different climate states, i. e., steppe (BS), Mediterranean (Cs), temperate (Cfb), boreal (Dfa/Dfb), and tundra (ET), have been considered, respectively. Data for potential future distribution of temperature, precipitation, and humidity were taken from so-called analogue stations, which are characterised by those climates today: Marrakesh, Rome, Magdeburg, Rostow, Turku and Vardo, respectively. The conditions of the reference site have been also considered by the current soil properties and potential developments (see Tab. 2.1).

Tab. 2.1 Climates, analogue stations and GBIs considered in /NOS 08/

Climate	Climate zone	Analogue climate station	GBI	
			Well	Rising groundwater
Current conditions	Cfb: Temperate	Magdeburg (Germany)	X	X
Hot/dry summers, mild/humid winters	Csa: Mediterranean	Rome (Italy)	X	-
Hot summers, warm winters	BS: Steppe	Marrakesh	X	-
Hot summers cold winters	Dfa: Boreal	Rostow (Russia)	X	X
Cold winters, cool and short summers	Dfc: Boreal	Turku (Finland)	X	X
Very cold winter, cool/short summers	ET: Tundra	Vardo (Norway)	X	X

The starting point of the calculation is a reference contamination of the groundwater. From there radionuclides might enter the biosphere via two principal geosphere-biosphere interfaces (GBIs) (see Fig. 2.2): Contaminated groundwater might be withdrawn from a well. It enters the biosphere due the use of well water for drinking and agricultural purposes. In case of high water tables, groundwater may enter the biosphere directly and cause contaminations of soils. After entering the biosphere, radionuclides may cause radiation exposures to humans. The impacts of changing climate and environmental conditions on the transfer of radionuclides through the biosphere for both GBIs have been estimated. The possible geosphere-biosphere interfaces for each climate state are given in Tab. 2.1. The withdrawal of groundwater is likely for all climates. In hot climates, the contamination of surface soils by rising groundwater may in principle be possible, but it is not very likely due to the pronounced aridity. Therefore, the GBI “rising groundwater” is not taken into account for the steppe and the Mediterranean climate.

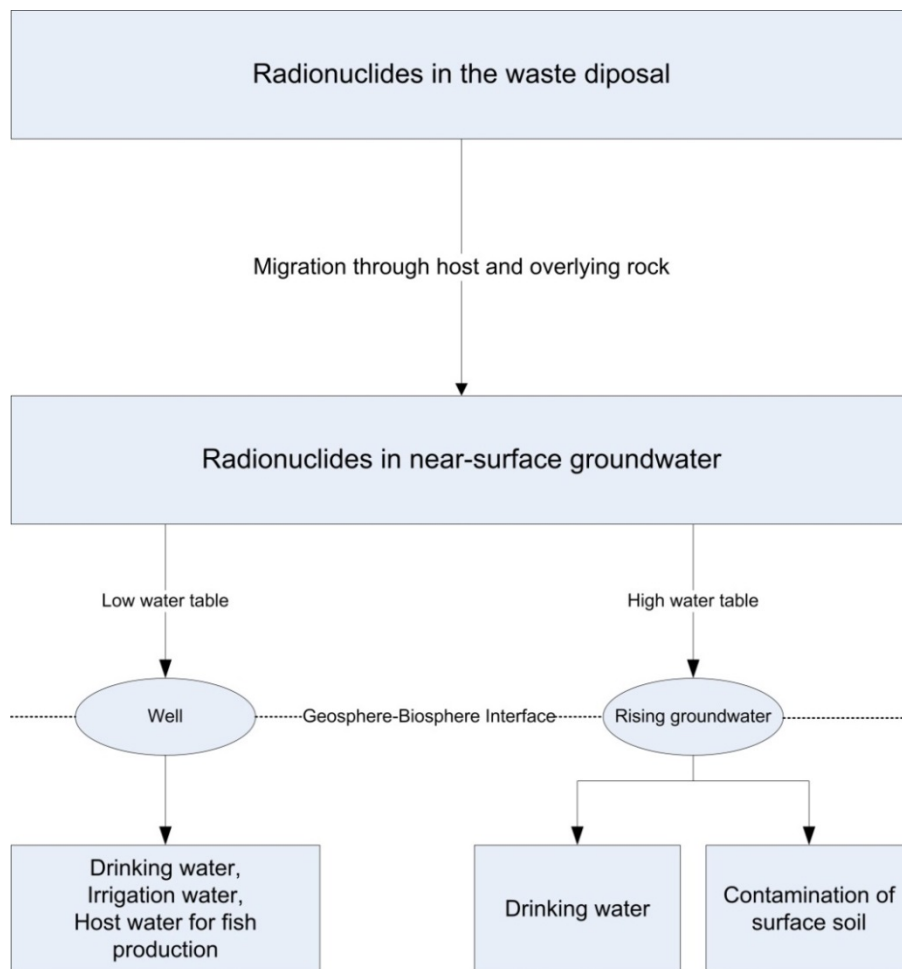


Fig. 2.2 Principal geosphere-biosphere interfaces for radionuclides entering biosphere

In the calculations of the radiation exposure, a normalised activity concentration of 1 Bq m^{-3} for each of the radionuclides is assumed. The endpoints of the calculation are the effective dose of an adult reference person. The conceptual models for estimating exposures are shown in Fig. 2.3 (GBI “well”) and Fig. 2.4 (GBI “rising groundwater”).

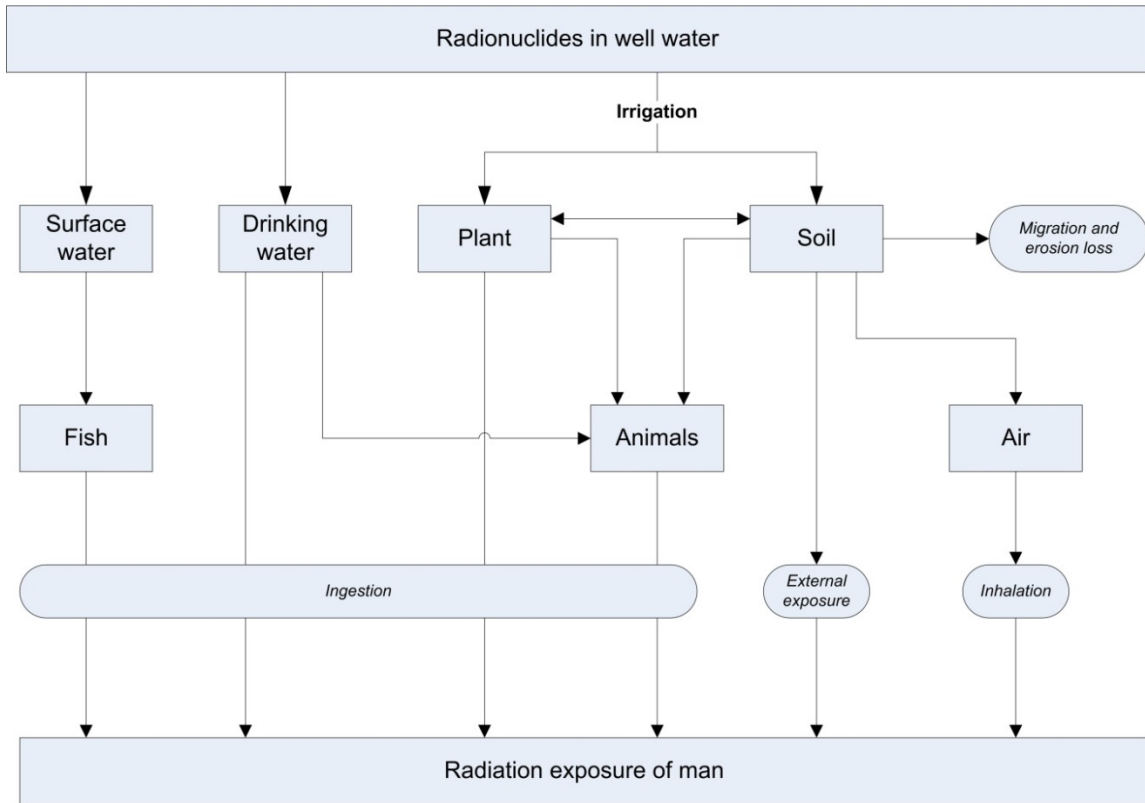


Fig. 2.3 Conceptual model for estimating the radiation exposure to man, if radionuclides enter the biosphere via well water

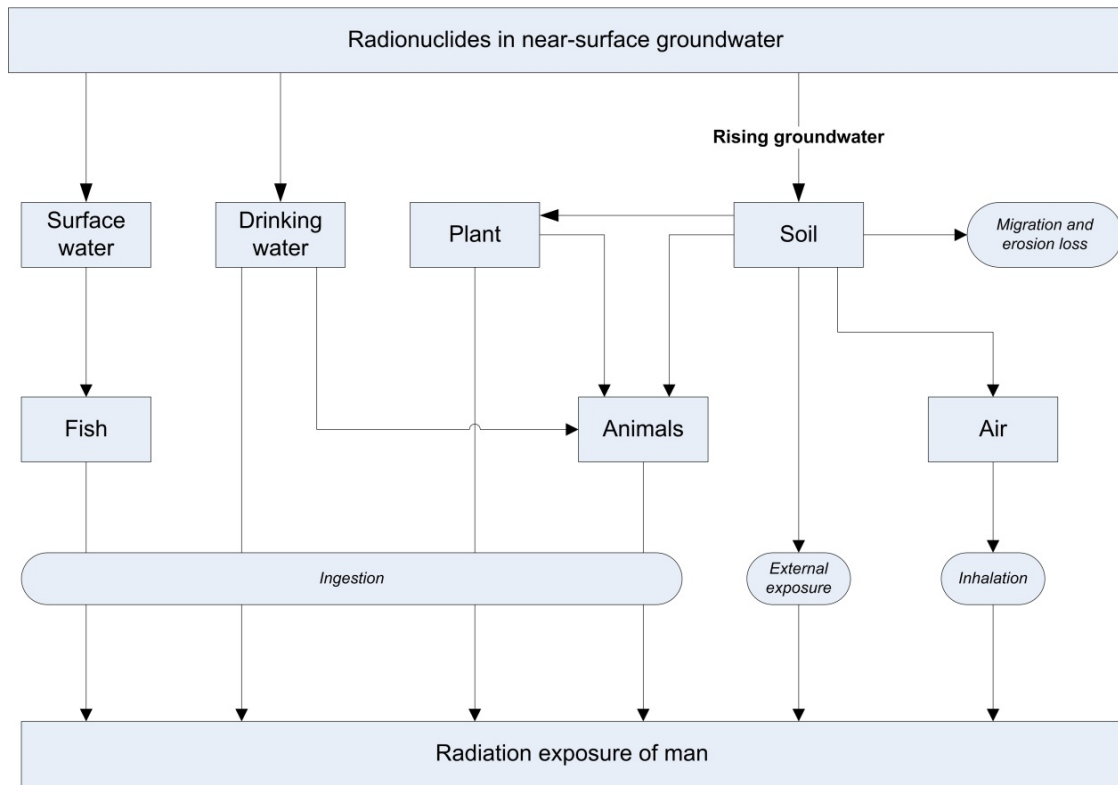


Fig. 2.4 Conceptual model for estimating the radiation exposure to man if radionuclides enter the biosphere via rising groundwater

For both geosphere-biosphere interfaces the following exposure pathways were considered:

- ingestion,
- inhalation of resuspended contaminated soil particles, and
- external exposure due occupation on contaminated land.

Further it is assumed that contaminated groundwater is used for various purposes:

- drinking water for humans,
- drinking water for cattle,
- irrigation of plants, and
- host water for fish production.

2.1 Transfer processes

The input of radionuclides to the biosphere via irrigation or rising of groundwater causes the contamination of food and feed stuffs. The contamination processes taken into account are summarised in Tab. 2.2. The relationships between the compartments involved in the contamination of plants are shown in Fig. 2.5 and Fig. 2.6 for both pathways.

Tab. 2.2 Contamination pathways considered

Contamination process	Geosphere-biosphere interface	
	Well	Rising groundwater
Transfer to plants		
Radionuclide uptake from soil	X	X
Contamination due to resuspension	X	X
Weathering	X	
Interception by plants during application of irrigation water	X	
Translocation (systemic transport within the plant subsequent to foliar deposition)	X	
Loss from soil		
Migration	X	X
Erosion	X	X
Transfer to animals		
Drinking water for cattle	X	X
Use of contaminated feed plants	X	X
Contamination of air by resuspension		
Accumulation of radionuclides in the resuspendable soil fraction	X	X
Transfer to freshwater fish		
Radionuclide uptake by fish	X	X
Attachment of radionuclides to particles and sedimentation	X	X

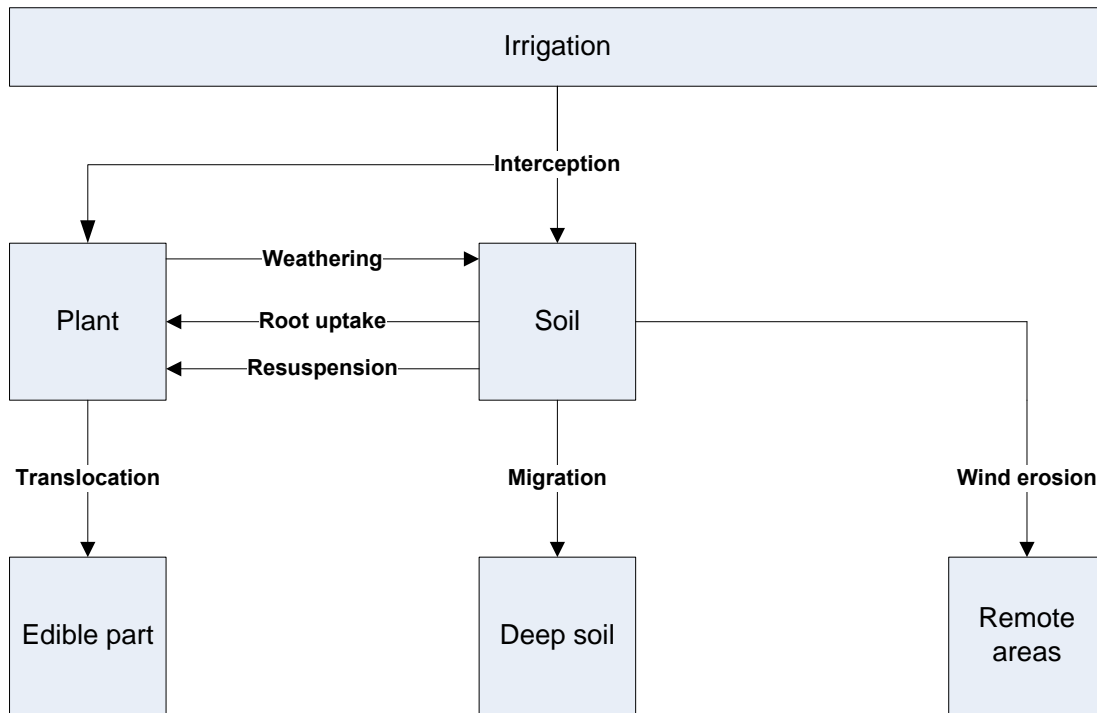


Fig. 2.5 Processes involved in the transfer of radionuclides to plants subsequent to irrigation with contaminated groundwater

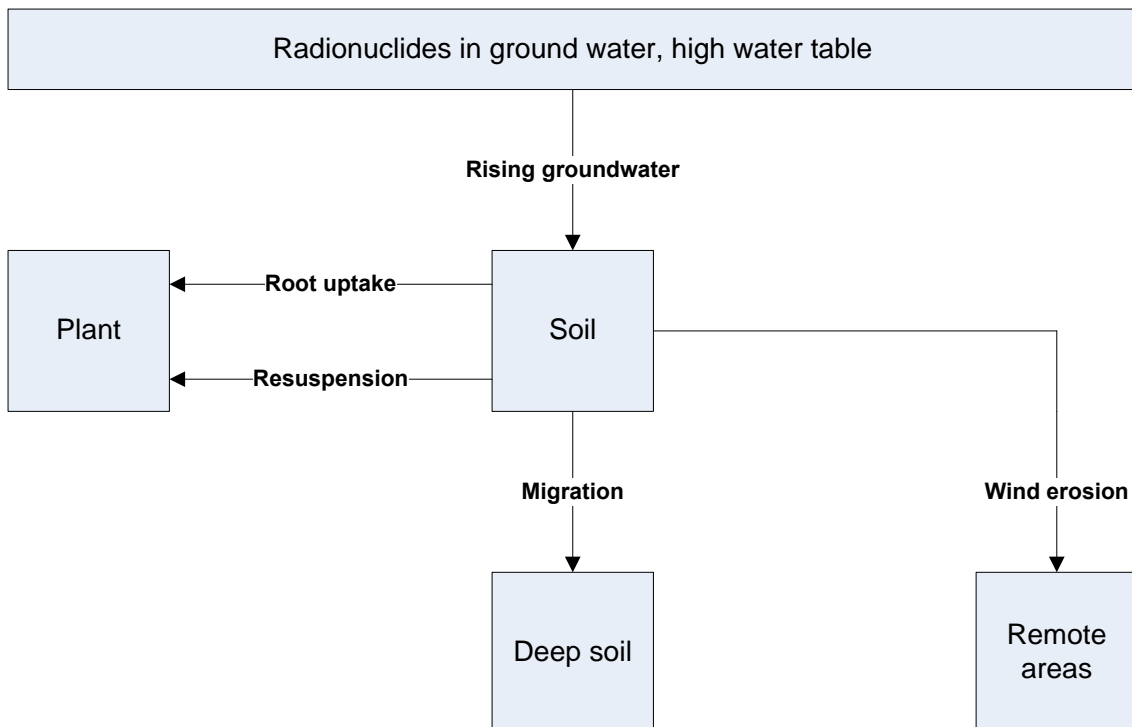


Fig. 2.6 Processes involved in the transfer of radionuclides to plants due to rising of contaminated groundwater

During irrigation of plants with contaminated water, a fraction of radionuclides is initially retained by the foliage; the rest passes through the canopy and contaminates the soil. Once deposited on the foliage, part of these radionuclides is lost from the plant to the soil by weathering. Furthermore, the systemic transport to the edible parts of plants is taken into account. Processes related to direct plant contamination are not relevant, if radionuclides enter the biosphere via rising groundwater. Radionuclides are lost from soil due to erosion and due to migration to deeper soil layers, where they are no longer available for root uptake.

2.2 Food and feed products considered

This study takes into account all crops and group of crops that are currently relevant in Europe like cereals, maize, potatoes, root vegetables, fruit vegetables, leafy vegetables and wild berries. All of the crops represent a group of plants rather than a distinct species. The classification follows similarities in modelling, whereas botanical criteria are not considered in this respect.

- Cereals represent crops as wheat, barley, oats and rye. These species are very similar concerning morphology and growth. Wheat and barley predominate in Southern Europe, whereas rye and oats are more typical for Northern Europe because they are more adapted to cool summers and poor soils.
- Maize represents a crop that is completely used as animal feed.
- Potatoes and root vegetables represent crops with an edible plant part that grows below the soil surface. Besides potatoes, crops as carrots, beetroot, radish, celery are considered here.
- Fruit vegetables: This group includes a wide range of crops with the commonality that all have an edible part growing aboveground as e. g. beans, peas, cucumbers, zucchini, capsicum, and tomatoes.
- Leafy vegetables cover a wide range of plants that are used completely by humans as lettuce, field salad, green cabbage, endive, leaf beet and spinach.
- Wild berries and mushrooms are considered for the tundra climate only. In this case, the radionuclides enter the biosphere via rising groundwater which might affect also natural land. Ingestion exposure might be due to consumption of wild berries and mushrooms.

Animal food products are an important part of the human diet. In this study, the consumption of beef, pork, lamb, chicken and freshwater fish is considered. For the tundra climate, the ingestion of reindeer meat is taken into account. The specific intake rates of these food items depend on environmental conditions of the site considered. Details are given in Chapter A.1.2.1.

All food products that are considered to be used at the different climate states are summarised in Tab. 2.3. The spectrum of products is quite similar for temperate, Mediterranean and boreal climate. For tundra climate the relevance of natural food products as berries, mushrooms and reindeer is of increased importance. In the tundra climate, cereals are not cultivated due to climatic reasons.

Tab. 2.3 Plant and animal products considered for the different climates

Plant/Animal	Climate					
	Cfb: Temperate	BS: Steppe	Csa Mediterranean	Dfa: Boreal	Dfc: Boreal	ET: Tundra
Grass	X	X	X	X	X	X
Maize	X	X	X	X	-	-
Cereals	X	X	X	X	X	-
Potatoes & roots	X	X	X	X	X	X
Leafy veg.	X	X	X	X	X	-
Fruit veg.	X	X	X	X	X	-
Mushrooms	-	-	-	-	-	X
Berries	-	-	-	-	-	-
Milk	X	X	X	X	X	X
Beef	X	X	X	X	X	-
Pork	X	X	X	X	X	-
Reindeer	-	-	-	-	-	X
Lamb	-	X	X	-	-	-
Fish	X	-	-	X	X	X

All other details of the modelling approaches used in /NOS 08/ and also for the deterministic calculations described in section 1, can be found in the appendix A.1.

2.3 Main conclusions

The results show that the variations among all climates for Ra-226, Th-230, Pa-231, U-238, Np-237, Am-243, and Pu-239 are relatively small; mostly the differences are less than a factor of 5. In general, the transfer for these radionuclides through food chains is relatively low, and the mobility within the plant subsequent to foliar deposition is low as well. Therefore, the intake of radionuclides with drinking water dominates over the other ingestion pathways. This does not mean that root uptake and migration are not influenced by environmental conditions, but even under conditions that cause enhanced transfers of actinides, the transfer to man changes only slightly.

The results further show that the dose conversion factors for other radionuclides vary considerably for the different climate states. This variation is strongly dependent on the different geosphere-biosphere interfaces. For the temperate and the boreal climates, the interface “well” causes higher dose conversion factors, whereas in case of the tundra climate, dose conversion factors are higher for the interface “rising groundwater”.

For the GBI “well”, the highest variations between the different climates are found for C-14, Cl-36, Nb-94, Cs-135 and for the redox-sensitive radionuclides Se-79, Tc-99, and I-129. Variations are caused especially by the following factors:

Due to the differences in temperature, precipitation and evapotranspiration at the analogue stations the irrigation rates and therewith the input of radionuclides to soil varies considerably by a factor of about 6, which has a direct impact on the exposure via ingestion of foods, inhalation and external exposure.

The root uptake and migration of Se-79, Tc-99, and I-129 depends largely on the soil characteristics. The root uptake of selenium and technetium is enhanced on well aerated and dry soil, as it is the case for steppe climate. In this case selenate and pertechnetate are the predominating chemical species which are readily available for root uptake. At the same time, due to the aridity, the migration to deeper soil layers is reduced compared to the other climates. On the other hand for I-129, root uptake is highest in wet and water-logged soils which occur especially under cold climates.

The intake rates for the reference climates are different. For steppe climate a daily water consumption of 3 L d⁻¹ is assumed compared to 2 L d⁻¹ for the other climates to account for the higher water demand under hot conditions. Furthermore, in the steppe

climate, the husbandry of small ruminants as sheep and goat is relevant. The transfer of some elements to sheep and goat is much higher than to beef, which causes an increased radionuclide intake by humans. Among the radionuclides considered in the study presented here, this is especially the case for Cs-135 and I-129.

These factors cause maximum differences of more than two orders of magnitude in the dose conversion factors for the interface “well”. Highest differences occur for the radionuclides Se-79, C-14, Tc-99, Cl-36, Nb-94 and Cs-135.

For the GBI “rising groundwater”, the steppe climate is not taken into account, since the assumption of hot climate and agriculture on areas affected by groundwater appears somewhat contradictory. For this interface, the variations among the climates are low, with the exception of the radionuclides C-14, I-129, and Cs-135, whose dose conversion factors are by far highest for tundra climate.

For C-14, the high exposure for tundra climate is due to the high consumption of fish, which accumulates C-14 considerably.

For I-129, and Cs-135 the strong increase is caused by their different behaviour in soil. Under the conditions of tundra climate, in wet and water-logged soils, the predominant iodine species is iodide which is readily available for root uptake. The transfer factors of cesium are also considerably enhanced for the low pH and high organic matter found in tundra climate, which causes high concentrations in grass and reindeer, berries and mushrooms.

For the GBI “rising groundwater” by far highest differences in dose conversion factors for the different climate states are found for Cs-135 with nearly three orders of magnitude and for I-129 with more than two orders of magnitude. The differences for all other radionuclides are below one order of magnitude.

3 Selection and justification of climate states and modelling results

3.1 Selection and justification

A systematic justification of relevant climate states for Northern Germany is necessary to implement a reference climate region approach. In this work results from the BIOCLIM project were used to select potential future reference climate states and their sequence for northern Germany.

3.1.1 Predicted climate development

In order to assess the influence of climate changes on the biosphere models as described in chapter 2, potential future climate states have to be selected and justified. For this purpose, the range of possible temperature and precipitation changes can be estimated by analysing paleoclimatic data and the results of predictive climate models /NOS 08/. Paleoclimatic data sets provide information about relevant changes in solar activity, geological processes, atmospheric as well as oceanic and glacial processes influencing the climate over longer time frames. Predictive climate models can be created with enough knowledge about those processes, their interaction and influence on climate.

In the BIOCLIM project, this was done for several European reference regions and predictive models for the next million years were developed /BIO 04/. In these predictive models, climate developments are calculated by using predicted changes in insolation, albedo of the earth surface and CO₂ content of the atmosphere. Changes in precipitation are more difficult to predict compared to temperature changes, due to highly uncertain factors influencing precipitation patterns.

Model calculations from the BIOCLIM project predict a temperature increase of 3 °C in winter and 5 °C in summer for elevated atmospheric CO₂ concentration scenarios in the near future for northern Germany. During the same time winter precipitation would increase by 1 mm/d and summer precipitation decrease by 0.3 to 1.7 mm/d /BIO 04/. These projected changes in temperature and precipitation can be added to current climate data of a reference region and compared with data from other climate stations (Fig. 3.1). These models and resulting climate changes are similar to those used by the

Intergovernmental Panel on Climate Change (IPCC) to predict climate developments for the next century /IPC 07/. If these predictions are accurate, the climate in northern Germany will change to a climate similar to current day Rome with warm and dry summers and humid winters in the short term. This result confirms the reference climate region approach.

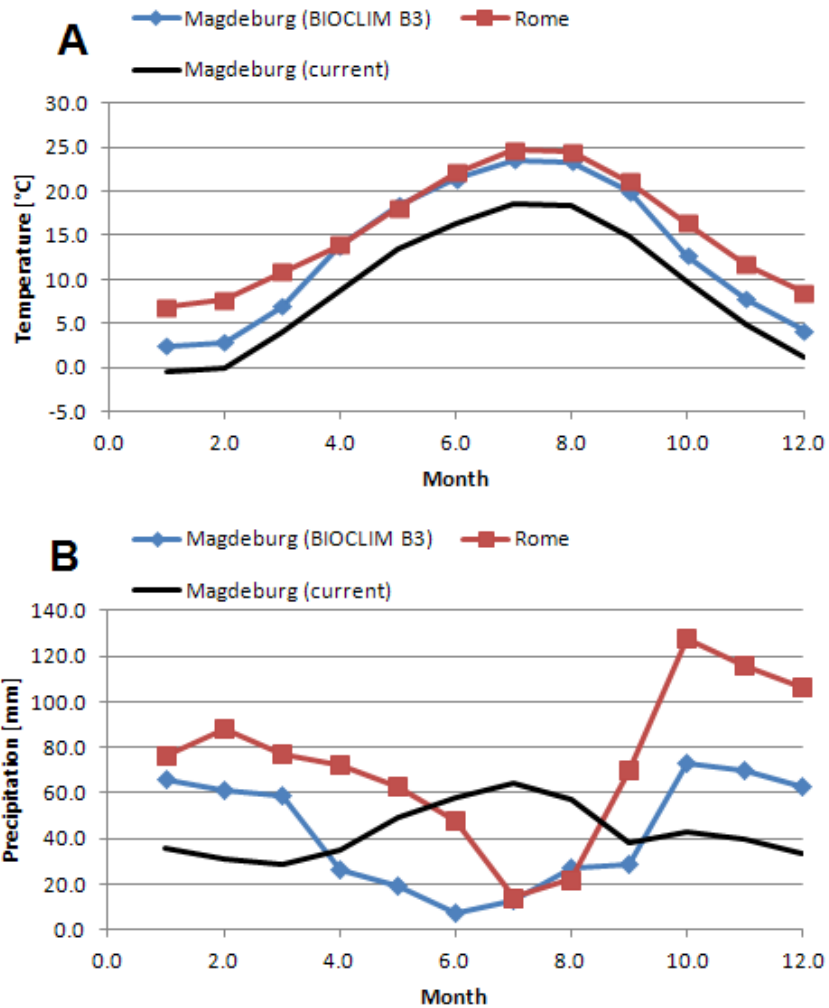


Fig. 3.1 Changes in A) temperature and B) precipitation predicted by the BIOCLIM project for northern Germany

In the long term, results from BIOCLIM in addition to model inherent uncertainties mostly assess climate developments in the next 200 000 years. BIOCLIM results can be used to set limits to potential future climate states and their possible sequence, depending on the assumed scenario (Fig 3.2). For the assumption of a natural CO₂ level the future climate is dominated by temperate conditions intersected by shorter periods of boreal climate. For increased CO₂ level scenarios subtropical climate conditions are

prevalent during this time frame. Since subtropical, temperate and boreal climate conditions might occur in Germany in the next 200 000 years, corresponding reference climate regions need to be considered. For each climate zone a dry, average and humid reference climate region needs to be selected, since precipitation amounts can only be modelled with high uncertainties. During glacial periods, no self-sustaining human populations are assumed. Due to this, no reference climate region model was created for glacial periods.

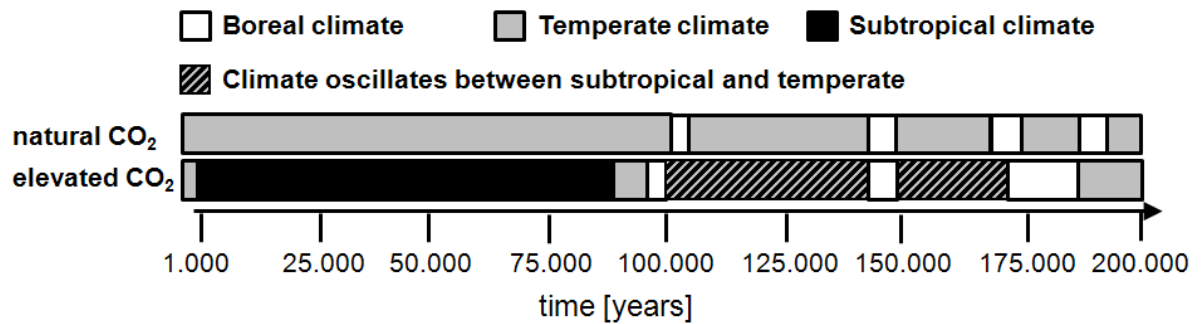


Fig. 3.2 Potential future climate development for northern Germany assuming naturally changing and elevated CO₂ concentrations in the atmosphere due to the BIOCLIM project /BIO 04/, /STA 13/

Grey depicts temperate, black subtropical and white boreal climate conditions.

3.1.2 Selected reference climate regions

For the selection of reference climate regions only European and one North African climate stations were used. This was done, since the axial tilt of the earth influences the climate and seasons. Due to this tropical climate states do not apply for northern Germany. Among the nine selected reference climate stations are three boreal, three temperate and three subtropical climate regions (Fig. 3.3, Tab. 3.1). The subtropical climate stations can be further divided into stations with Mediterranean climate, Rome and Valladolid, and with Steppe climate, Marrakesh. For each subtropical, temperate and boreal climate zone one low, medium and high precipitation climate station was selected. Climate stations with glacial conditions are excluded as reference regions from the assessment.

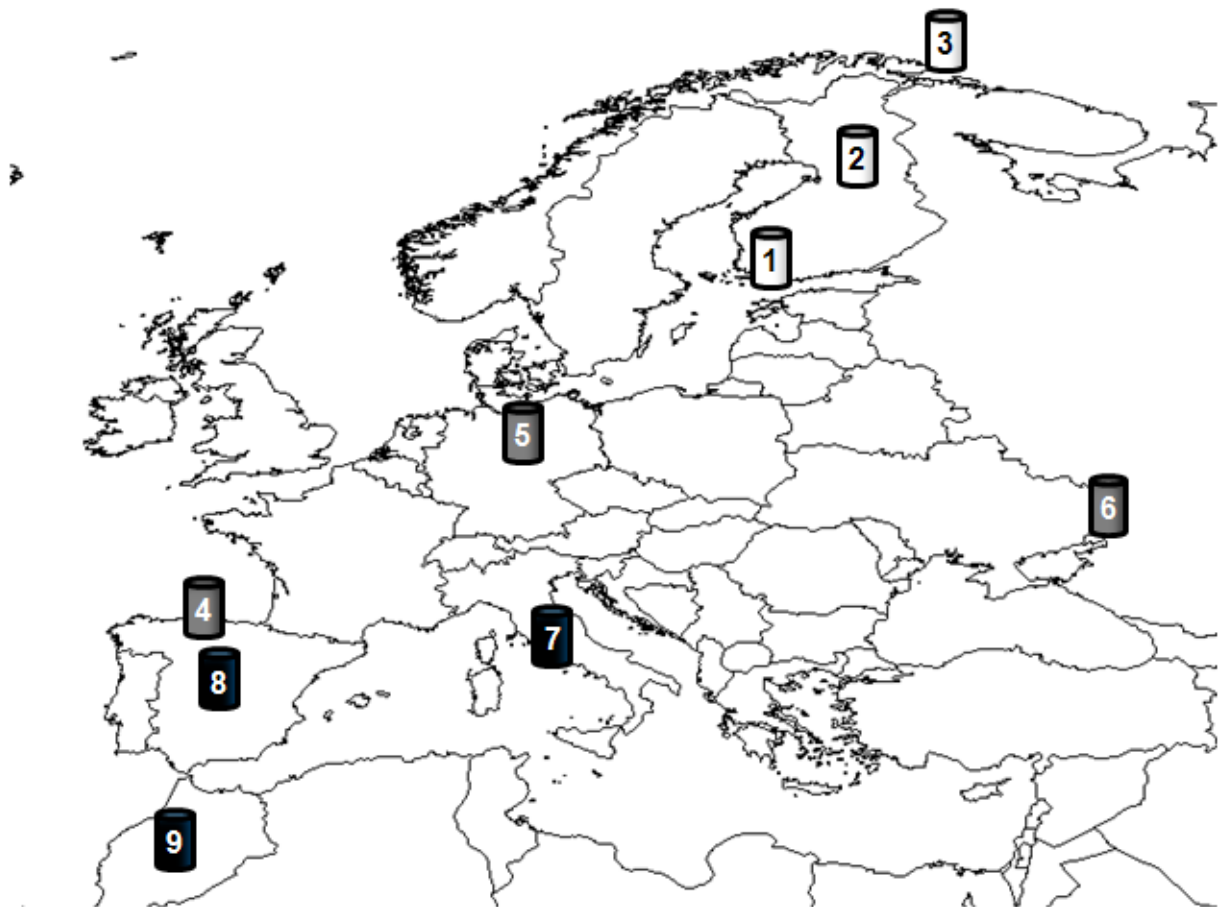


Fig. 3.3 Selection of discrete reference climate regions. Grey depicts temperate, black subtropical and white boreal climate conditions

Tab. 3.1 Köppen/Geiger climate classification and climate data for the reference climate regions

Reference climate region	Number in Map	Köppen/Geiger classification	Annual average temperature [°C]	Annual precipitation [mm]
Turku	1	Dfb boreal	4.8	576
Sodankyla	2	Dfc boreal	-0.4	508
Vardo	3	ET boreal	1.6	544
Santander	4	Cfb temperate	13.9	1198
Magdeburg	5	Cfb temperate	9.2	513
Rostov	6	Dfa temperate	8.4	483
Rome	7	Csa subtropical	15.6	874
Valladolid	8	Csb subtropical	12.1	364
Marrakesh	9	BS subtropical	19.9	241

The current conditions in northern Germany are a temperate climate with medium precipitation. Due to this, a total of nine reference climate regions can be arranged in a matrix with the German reference region in the centre. From the current German cli-

mate conditions, all realistically possible developments to higher and lower temperature or more dry and humid climates are included (Tab. 3.1). These developments cover the range of possible climate developments predicted for northern Germany by BIOCLIM models for the next 200 000 years. Since all climate states from subtropical steppe climate to tundra permafrost are included (Fig. 3.2), these climate regions should also be sufficient to cover potential development for the next 1 million years. Due to this, tundra and steppe climates were included in the assessment, since extreme climates cannot be excluded for the whole assessment time period. Desert and glaciation reference climate regions were excluded, since self-sustaining populations are special cases and even often impossible in these climates.

In previous modelling approaches it was assumed that these stylized reference climate regions and the parameters describing them are stable over long time periods, see /NOS 08/. Accordingly transitions between this climate states were not modelled. The conditions for future climate states are assumed to approach those at the present day reference climate regions. Present day parameters for the different regions like temperature, precipitation, food consumption habits, and radionuclide behaviour in soil or dust concentration in air are used for the model.

The model and results for six reference climate regions were described in a previous project /NOS 08/. Three additional reference climate regions were added to increase the resolution of the model and to fully cover the potential characteristics of potential future climates. These additional reference climate regions are:

- the subtropical reference region Valladolid, representing a development to warmer climate,
- the temperate reference region Santander, representing a development to more humid climate,
- the boreal climate region Sodankyla, representing a development to colder climate from the current conditions in Germany.

Data for temperature, precipitation, humidity and water deficit of soils is given for all selected reference regions in Tab. 3.2 and Fig. 3.4.

Tab. 3.2 Data for the nine reference stations /MUE 96/

Marrakesh	Jan	Feb	Mar	Apr	May	Jun	Jul	Aug	Sep	Oct	Nov	Dec	Year
Temperature (°C)	11.6	13.2	16.0	18.3	21.3	24.8	28.7	28.8	25.5	21.4	16.3	12.3	19.9
Precipitation (mm)	28.0	29.0	32.0	31.0	17.0	7.0	2.0	3.0	10.0	21.0	28.0	33.0	241.0
Humidity (%)	77.0	73.0	70.0	65.0	60.0	58.0	53.0	53.0	57.0	61.0	65.0	66.0	63.0
Water deficit (mm)	25.7	40.6	63.2	90.6	140.3	192.0	252.5	252.9	198.7	136.2	75.7	38.7	
Rome	Jan	Feb	Mar	Apr	May	Jun	Jul	Aug	Sep	Oct	Nov	Dec	Year
Temperature (°C)	6.9	7.7	10.8	13.9	18.1	22.1	24.7	24.5	21.1	16.4	11.7	8.5	15.6
Precipitation (mm)	76.0	88.0	77.0	72.0	63.0	48.0	14.0	22.0	70.0	128.0	116.0	106.0	874.0
Humidity (%)	77.0	73.0	71.0	70.0	67.0	62.0	58.0	59.0	66.0	72.0	77.0	79.0	69.0
Water deficit (mm)	-49.1	-52.3	-21.3	6.4	54.3	115.5	183.8	172.3	78.0	-31.8	-61.6	-73.4	
Rostov	Jan	Feb	Mar	Apr	May	Jun	Jul	Aug	Sep	Oct	Nov	Dec	Year
Temperature (°C)	-6.3	-5.5	0.2	8.6	15.9	19.6	22.7	21.8	15.8	9.3	2.0	-3.5	8.4
Precipitation (mm)	38.0	41.0	32.0	39.0	36.0	58.0	49.0	37.0	32.0	44.0	40.0	37.0	483.0
Humidity (%)	87.0	85.0	80.0	67.0	59.0	61.0	58.0	58.0	62.0	75.0	82.0	87.0	72.0
Water deficit (mm)	-51.1	-52.0	-31.6	8.6	71.6	80.8	125.9	128.0	71.1	-2.1	-37.6	-50.0	
Valladolid	Jan	Feb	Mar	Apr	May	Jun	Jul	Aug	Sep	Oct	Nov	Dec	Year
Temperature (°C)	3.3	5.1	8.6	11.0	14.1	18.5	21.3	20.4	17.8	12.9	7.7	4.4	12.1
Precipitation (mm)	30.0	26.0	42.0	30.0	35.0	33.0	13.0	13.0	28.0	34.0	40.0	40.0	364.0
Humidity (%)	84.0	78.0	69.0	64.0	62.0	57.0	51.0	55.0	63.0	71.0	80.0	85.0	68.0
Water deficit (mm)	-26.0	-8.2	3.2	35.4	54.6	100.1	155.1	141.0	91.4	35.9	-12.7	-33.3	
Magdeburg	Jan	Feb	Mar	Apr	May	Jun	Jul	Aug	Sep	Oct	Nov	Dec	Year
Temperature (°C)	-0.5	-0.1	4.0	8.8	13.4	16.4	18.5	18.3	14.9	9.7	4.8	1.2	9.2
Precipitation (mm)	36.0	31.0	29.0	35.0	49.0	58.0	64.0	57.0	38.0	43.0	40.0	33.0	513.0
Humidity (%)	84.0	82.0	76.0	70.0	67.0	67.0	70.0	71.0	74.0	79.0	85.0	87.0	76.0
Water deficit (mm)	-41.8	-33.6	-13.0	10.1	29.3	44.2	53.5	57.4	43.4	-3.6	-31.8	-38.7	
Santander	Jan	Feb	Mar	Apr	May	Jun	Jul	Aug	Sep	Oct	Nov	Dec	Year
Temperature (°C)	9.3	9.2	11.5	12.3	14.2	16.9	18.8	19.3	18.2	15.3	12.2	9.9	13.9
Precipitation (mm)	119.0	89.0	74.0	82.0	88.0	66.0	59.0	84.0	114.0	134.0	134.0	155.0	1198.0
Humidity (%)	75.0	76.0	74.0	77.0	80.0	81.0	80.0	81.0	80.0	78.0	76.0	76.0	78.0
Water deficit (mm)	-77.1	-48.9	-17.4	-23.5	-19.3	23.7	49.3	27.9	-11.4	-54.2	-75.0	-110.8	
Turku	Jan	Feb	Mar	Apr	May	Jun	Jul	Aug	Sep	Oct	Nov	Dec	Year
Temperature (°C)	-6.1	-6.5	-3.6	2.6	8.9	13.6	17.1	15.8	11.1	5.6	1.2	-2.4	4.8
Precipitation (mm)	43.0	27.0	23.0	33.0	30.0	40.0	67.0	77.0	65.0	64.0	58.0	49.0	576.0
Humidity (%)	87.0	84.0	79.0	74.0	64.0	66.0	69.0	74.0	79.0	84.0	88.0	89.0	78.0
Water deficit (mm)	-56.2	-36.4	-26.4	-19.2	22.8	41.0	38.9	11.7	-17.0	-51.3	-64.9	-63.4	
Sodankyla	Jan	Feb	Mar	Apr	May	Jun	Jul	Aug	Sep	Oct	Nov	Dec	Year
Temperature (°C)	-13.5	-13.0	-9.0	-2.1	4.9	11.3	14.7	12.0	6.2	-0.5	-5.8	-9.8	-0.4
Precipitation (mm)	27.0	26.0	20.0	31.0	31.0	56.0	74.0	71.0	57.0	43.0	39.0	31.0	508.0
Humidity (%)	87.0	85.0	78.0	71.0	61.0	60.0	65.0	74.0	81.0	87.0	91.0	89.0	77.0
Water deficit (mm)	-26.0	-24.2	-19.4	-23.5	6.4	16.1	16.6	-11.0	-38.1	-52.4	-57.1	-42.2	
Vardo	Jan	Feb	Mar	Apr	May	Jun	Jul	Aug	Sep	Oct	Nov	Dec	Year
Temperature (°C)	-4.6	-5.3	-4.0	-1.0	2.7	6.2	9.3	9.8	6.8	2.4	-0.7	-3.0	1.6
Precipitation (mm)	44.0	46.0	47.0	36.0	36.0	37.0	41.0	52.0	63.0	56.0	43.0	43.0	544.0
Humidity (%)	86.0	87.0	86.0	83.0	80.0	83.0	86.0	85.0	84.0	84.0	85.0	86.0	85.0
Water deficit (mm)	-56.2	-59.4	-59.0	-41.4	-29.1	-20.5	-12.3	-19.2	-45.0	-54.8	-50.3	-54.4	

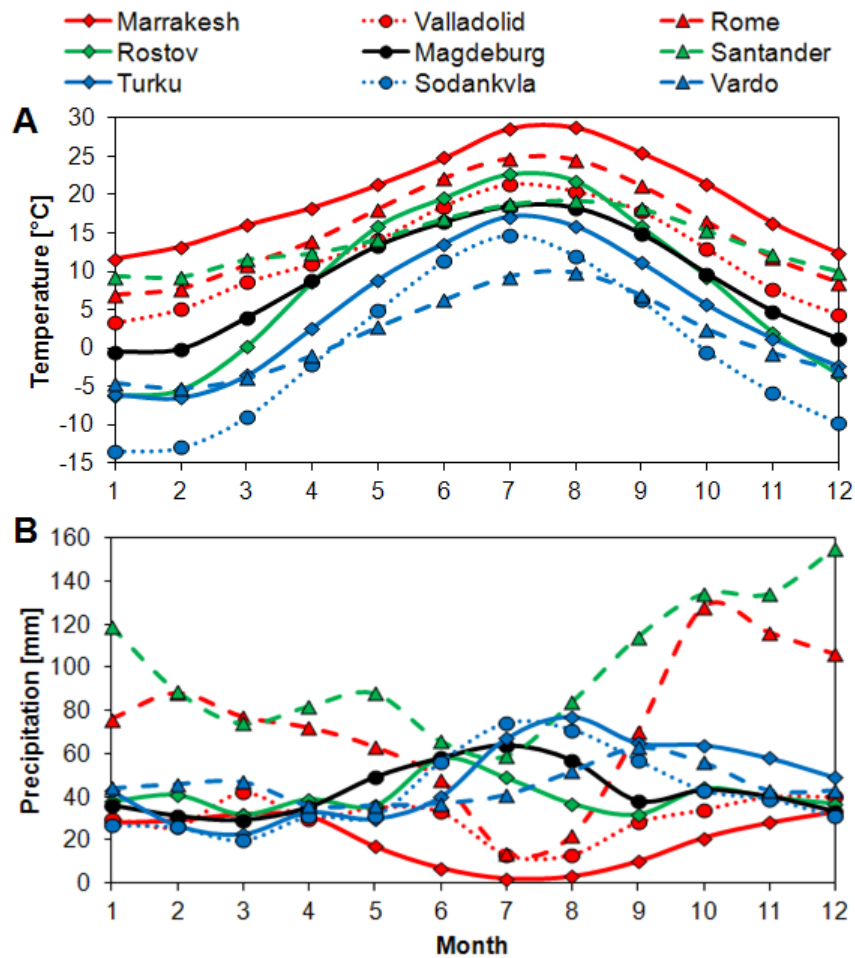


Fig. 3.4 A) Average temperature and B) average monthly precipitation at the reference climate regions

3.1.3 Model parameters for the additional reference climate regions and probabilistic models

For the new reference climate regions Santander, Valladolid and Sodankyla, several climate dependent model parameters were changed compared to the six original reference climate regions. The most important parameters are new irrigation amounts, calculated from reference region specific temperature, precipitation and humidity with equation 1, chapter 8 from /NOS 08/. Other parameters were reused from the 6 original reference climate regions if applicable. These reference climate region dependent parameters are presented in Tab. 3.3 for the three new climate regions.

Parameter values for transfer factors soil to plant used in the probabilistic and sensitivity analysis models presented in chapter 3.3 were derived from a parameter data base

/IAE 09/. This data base is an updated version of the data base /IAE 94/ used for the prior models in /NOS 08/ and the three new reference climate regions presented in chapter 3.1 and 3.2. In newer iterations of the model /STA 13/ other parameters, like food consumption rates, radionuclide migration factors in soil and agricultural yields were also updated.

Tab. 3.3 Reference climate region dependent parameters for the Valladolid, Santander and Sodankyla reference climate regions

Parameter	Valladolid	Santander	Sodankyla
Dust concentration in air	Rome Csa	Magdeburg Cfb	Turku Dfb
Feed of beef cattle	Rome Csa	Magdeburg Cfb	Turku Dfb
Food consumption rate	Rome Csa	Rome Csa	Turku Dfb
Harvest of leafy vegetables	Rome Csa	Magdeburg Cfb	Turku Dfb
Irrigation cereals [mm/y]	486	101	33
Irrigation fruit vegetables [mm/y]	613	101	33
Irrigation Grass [mm/y]	617	101	33
Irrigation leafy vegetables [mm/y]	617	101	33
Irrigation maize [mm/y]	542	101	0
irrigation potatoes [mm/y]	542	101	33
Migration in arable soil	Rome Csa	Magdeburg Cfb	Turku Dfb
Migration in pasture soil	Rome Csa	Magdeburg Cfb	Turku Dfb
Resuspension factor grass	Rome Csa	Magdeburg Cfb	Turku Dfb
Resuspension factor other	Rome Csa	Magdeburg Cfb	Turku Dfb
Transfer factor soil-Plant	Rome Csa	Magdeburg Cfb	Turku Dfb
Growing period grass	Rome Csa	Magdeburg Cfb	Turku Dfb

Radionuclide parameter data bases are used, since site specific data is not available. In these data bases, experimentally measured transfer factors for a large variety of elements, plants and soils types are summarized. For some elements, like Caesium, a large quantity of experimental data is available. For other elements few or no transfer factors were measured. This leads to a heterogeneous data source adding to uncertainty in the model. The data base provides geometric and arithmetic means as well as standard deviations and minimum and maximum values for the element specific transfer factors.

In the model presented in chapter 3, differences in radionuclide specific transfer factors from soil to plant between the reference climate regions are simulated by multiplying the transfer factor from the /IAE 94/ database with a modification factor (Tab. 11.7). For the probabilistic model used in chapter 4 and 5 different transfer factors were used for

the temperate and subtropical reference climate regions, since transfer factors for those two climates are presented separately in /IAE 09/.

3.1.4 Soil development

Soils can be classified by the World Reference Base for soil Resources (WRB) soil classification method due to soil morphology resulting from pedogenesis. Extensive soil maps are available for the WRB classification /EUR 05/. In data bases for radioecological parameters soil classification methods are often used, that distinguish soil types due to their soil texture and organic matter (OM) content. This soil texture/OM classification divides soils into sand, loam, clay and organic soils /IAE 10/. While radionuclide accumulation in different soil types is modelled for the discrete reference climate region models, further pedogenesis and resulting changes in the soil type are not considered. Top soil layers may be strongly influenced by agricultural use like ploughing and the use of fertilizers. These soils are often called anthrosols in the WRB classification due to the influence humans had on their development, when the soils have been cultivated for long time periods (Fig. 3.5A). Other examples for soils that are included in the sand subclass of the soil texture/OM criterion are soils like arenosols consisting mostly out of sand (Fig. 3.5B), cambisols which are young soils with little horizon differentiation and a high sand content (Fig. 3.5C) or podisols showing highly differentiated soil layers with a high sand content in the root zone (Fig. 3.5D). Despite the fact that anthrosols, arenosols, cambisols and podisols have very different soil properties and are the result of different pedogenic processes, they can be included in the sand soil class and use the according parameters in models. An example for an organic soil within the soil texture/OM classification is the WRB Histosol with high organic matter content (Fig. 3.5E) occurring at fens and bogs or were they were drained for agricultural use.

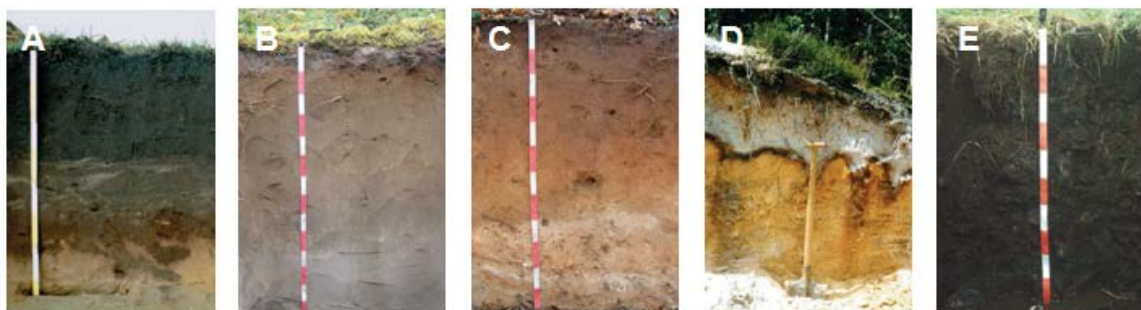


Fig. 3.5 Soil types A) anthrosol, B) arenosol, C) cambisol, D) podsol and E) histosol according to the WRB soil classification /EUR 05/

3.2 Results

To assess the potential radiation exposure of a self-sustaining hypothetical population for scenarios, where radionuclides are released from a deep geological repository, the exposure of a population to radionuclides in the biosphere needs to be modelled. To this end, the BIOMASS methodology can be used to design stylized reference biosphere systems /IAE 03/. As a source term, a normalized radionuclide activity in the near surface groundwater is used. This near surface groundwater is then used as drinking water and for irrigation of agricultural land. In addition to this, a high groundwater table may influence the root zone soil layers directly.

The endpoint of the model are biosphere dose conversion factors (BDCF) describing the exposure according to this normalized source term. The exposure of a hypothetical population can then be calculated using the radionuclide concentration in near surface groundwater derived by integrated performance assessment models. The models applied here are the same as used in our previous work /NOS 08/ and summarised in appendix A.1, see also below. Only the results from the well scenario are presented in this chapter for the three new reference climate regions. The same radionuclide selection used for the original six reference climate regions was used for the three new reference climate regions.

As described above the assessment period for a safety case for high level waste deep geological repositories is in one million years in Germany /BMU 10/. Accordingly, agricultural soil is a key compartment of radioecological models, due to accumulation of radionuclides over long time frames in soil by irrigation with contaminated groundwater. Those accumulation processes and the resulting radionuclide contamination in soils influence key model pathways like external exposure, inhalation of dust particles and ingestion of food. Since radionuclide concentration curves in near surface waters, calculated for selected scenarios, usually show long-term plateaus (see section 2), BDCF are presented for the maximum soil contamination reached after distinct times in discrete models.

The soil type influences the activity concentrations and time frames due to differences in migration rates and transfer factors soil to plant for the radionuclides. The development of Cs-135 activity in sand and organic soil for cereal cultivation due to irrigation is shown in Fig. 3.6 for the Magdeburg and Rome reference climate regions. With the current soil model, maximum activity concentrations in soil at stationary state are reached

after several hundred to several thousand years depending on soil type and radionuclide properties. The model assumes continuous irrigation and land use during the considered time frame. Due to lower migration rates of Cs-135 in organic soils compared to sand soils, the activity concentration maximum is higher for organic soils.

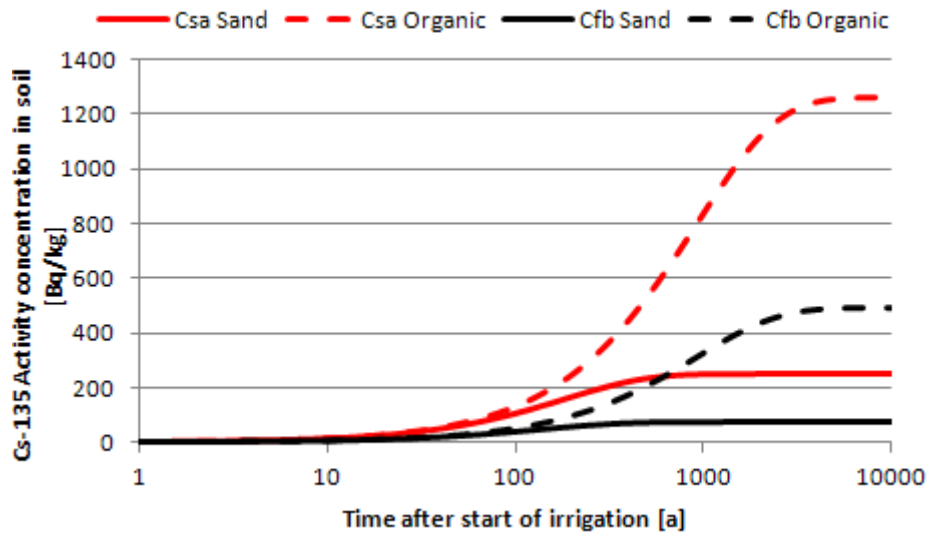


Fig. 3.6 Cs-135 specific activity concentration in sand and organic soil

Since the agricultural soil is irrigated over long time periods, an average irrigation rate over all crop types was used to determine the activity concentration in soil. The average irrigation rate was 190 mm/y for Magdeburg and 485 mm/y for Rome.

The activity concentration in plants, in this example for cereals, results from the foliar uptake of radionuclides directly from irrigation water and the root uptake from radionuclides out of the soil. Due to different transfer factors from soil to plant for the various soils and climates, the activity in, for example, cereals grown in organic soil is higher for the Cfb compared to the BS region, despite the higher activity in soil at the BS reference climate region. In sand soil such a pronounced effect cannot be seen for cereals, since a larger part of the total activity concentration derives from the foliar uptake, not being dependent on differences in the transfer factor (Fig. 3.7).

The activity concentration in cereals is initially determined by the annual foliar uptake. The contribution of foliar uptake to the activity concentration in the plant is constant during the whole time simulated in the discrete model due to constant irrigation amounts. The activity concentration in cereals during the first ten years after the start of irrigation is mostly due to foliar uptake of radionuclides from irrigation water, since radionuclide concentrations in soil are low during this time. The activity uptake by plant

roots increases with rising radionuclide concentrations in soil (Fig. 3.6). The foliar uptake of radionuclides dominates the total activity uptake especially for sand soil, where less Cs-135 activity is taken up by the plant roots than by the plant leaves. In organic soils, the contribution of root uptake to the total activity in cereals is higher than the contribution of foliar uptake at late time points (Fig. 3.7).

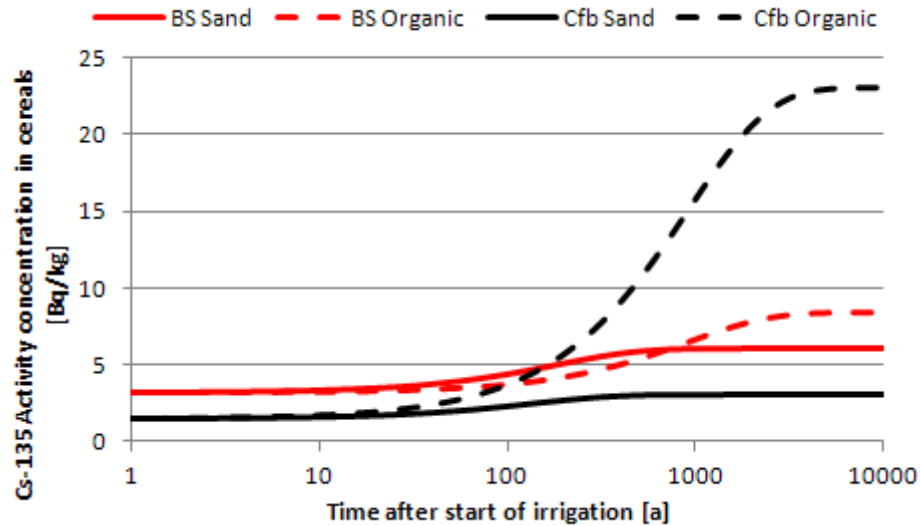


Fig. 3.7 Cs-135 specific activity concentrations in cereals

At the Csa reference climate region Rome the irrigation amount for cereals was set to 360 L/y m², at the Cfb reference climate region Magdeburg to 170 L/y m² with a radionuclide activity of 1 Bq/L, determining the foliar uptake and Cs-135 concentrations in soil.

The contribution of different food types to the ingestion BDCF are shown in Fig. 3.8 for the Rome and the Magdeburg reference climate region. These climate regions have been selected since those two reference climate regions are used for modelling the impact of climate transitions (see sections 5 and 6). The most marked difference is the increased contribution of the drinking water to the ingestion BDCF at the Magdeburg compared to the Rome reference climate region. This is an effect caused by the higher radionuclide concentration in plant and animal food at the Rome reference climate region, originating from the higher activity concentration in soil due to higher irrigation rates. In addition to this different consumption habits influence the results. The contribution of pathways to the total exposure mirrors the relevance of the corresponding parameters for the model (further discussed in section 3.3).

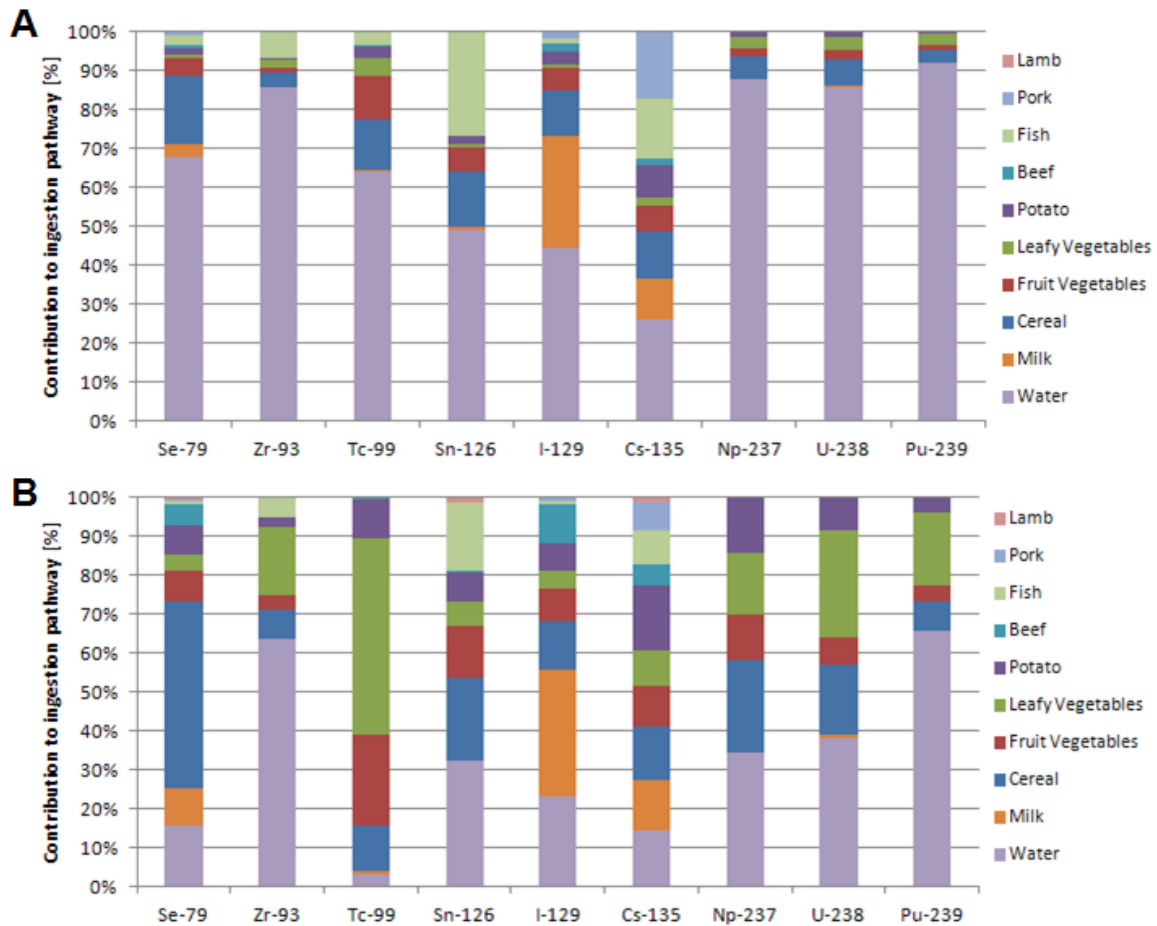


Fig. 3.8 Comparison of the contribution of food types on the ingestion BDCF of selected radionuclides for A) the Magdeburg and B) Rome reference climate region and sand soil

The analysis of the contribution of food types and exposure pathways as well as sensitivity analysis helps to identify relevant parameters significantly affecting the total BDCF. For example, for Cs-135 and I-129 activity in milk is an important factor influencing the total exposure from these radionuclides (Fig. 3.8).

In Tab. 3.4 and Tab. 3.5 the total BDCF for nine references climate regions are shown for the “well” scenario for sand and organic soil. The parameters used for the model, including the transfer factors soil to plant, are the same as in /NOS 08/ for the sandy soil. For organic soil the transfer factors soil to plant and migration factors calculated from distribution coefficients from /IAE 10/ were used.

The lowest BDCF for sandy soil can always be found in the Vardo reference climate region. Since no agriculture is done in this permafrost reference region, the soil is not

irrigated with contaminated groundwater. Due to this, the population is exposed to radionuclides only by the consumption of contaminated drinking water and fish. The highest BDCF for 12 of the 17 radionuclides can be found in the Valladolid reference climate region. This region has the highest irrigation amounts compared to the other reference climate region. At the Marrakesh reference climate region the annual precipitation is lower than at Valladolid, but since agriculture is done during the cooler and more humid autumn, winter and spring months the irrigation amounts are lower than in Valladolid. The high BDCF for Cs-135 at the Turku reference climate region can be explained by the assumed high transfer factor for caesium in boreal climates /NOS 08/. Since Sn-126 and Zr-93 are highly accumulated in fish compared to crops in sand soil, both radionuclides also have their maximum BDCF at Turku, since a large amount of fish is consumed at this reference climate region. Maximum BDCFs for Cl-36 and Se-79 are found for the Marrakesh reference climate region, due to high irrigation rates and consumption habits favouring food types with high chlorine and selenium accumulation, for example cereals.

For the organic soil, the lowest BDCF can again be found at the permafrost reference climate region Vardo. 10 of the 17 highest BDCF were calculated for the Valladolid reference climate region, 4 for Marrakesh and 1 at Turku, Rostov and Santander. Since the transfer factors for organic soil to plants differ from the transfer factors from sand soil to plants, the distribution of the maximum BDCF for organic soils across the various reference climate regions also differs from the distribution for sand soils.

The ratios between the maximum and minimum values of a radionuclide specific BDCF for the nine reference climate regions and sand soil ranges from 1.9, for Th-230 and Pu-239, to 81.4 for Nb-94 (Tab. 3.4). Since the amount of consumed drinking water does not change between the reference climate regions, low ratios are found for radionuclides where drinking water is the main contributor to the ingestion pathway and the ingestion pathway is the main contributor to the BDCF (see Fig. 3.8 and Fig. 3.9). The BDCF for Nb-94 is determined predominantly by the external exposure and the external exposure is determined by the radionuclide accumulation in soil. Due to this, the Nb-94 BDCF is correlated to different average irrigation amounts at the reference climate regions and the migration of Nb-94 in soil showing highest values for climate states with highest irrigation rates.

Since the activity concentrations in organic soil (Fig. 3.6) and in plants grown in organic soil (Fig. 3.7) are usually higher than in sand soil, the contributions of ingestion of food,

external exposure and inhalation are higher than to the contribution of ingested drinking water compared to contributions in sand soil scenarios. Due to this, variations in consumption habits of food have a higher impact on the variations of the BDCF, resulting in more extreme variations of the BDCF at the different reference climate regions (Tab. 3.5). This is exemplarily illustrated by the maximum to minimum ratio for Nb-94, which is again the highest but with a much higher value of 2490.4 for the organic soil.

The influence of the ingestion, inhalation and external exposure pathways on the total exposure is shown in Fig. 3.9 and Tab. 3.6. These three pathways are the main pathways used in most contemporary radioecological models. At the Magdeburg reference climate region, the ingestion pathway dominates the total exposure for most radionuclides except Nb-94 for sand soil scenarios. Compared to this, the inhalation pathway has a relatively larger effect on the total BDCF for the heavy radionuclides Pa-231, Th-231, Np-237, U-238, Pu-239 and Am-243 at the Rome reference climate region. This is due to the increased assumed dust concentration in air at this reference climate station because of low humidity during the summer (Fig. 3.4) /NOS 08/.

The external exposure has a contribution of more than one per cent for Sn-126, Ra-226, Pa-231, Np-237, U-238 and Am-243 at both reference climate regions for the radionuclides shown here. In addition to this, the external pathway dominates the total exposure for Nb-94.

Tab. 3.4 BDCF for different reference regions for the “well” scenario and sand soil. The BDCF are in Sv/y per Bq/L in near surface groundwater

Climate	BS	Csa	Csb	Cfb	Cfb	Dfa	Dfb	Dfc	ET	Min	Max	Ratio Max/Min
Reference region	Marrakesh	Rome	Valladolid	Santander	Magdeburg	Rostov	Turku	Sodankyla	Vardo			
Cl-36	4.4E-05	6.3E-06	7.0E-06	1.5E-06	2.2E-06	5.8E-06	1.8E-06	1.5E-06	8.1E-07	8.1E-07	4.4E-05	53.6
Ni-59	2.4E-07	2.7E-07	3.2E-07	9.1E-08	1.1E-07	2.4E-07	7.8E-08	6.4E-08	4.8E-08	4.8E-08	3.2E-07	6.8
Se-79	1.9E-05	1.3E-05	1.5E-05	2.8E-06	3.1E-06	1.8E-05	3.6E-06	3.4E-06	2.2E-06	2.2E-06	1.9E-05	8.6
Zr-93	1.2E-06	1.3E-06	1.3E-06	9.4E-07	9.3E-07	1.1E-06	1.7E-06	1.7E-06	8.0E-07	8.0E-07	1.7E-06	2.2
Nb-94	7.4E-05	8.5E-05	1.0E-04	1.4E-05	2.6E-05	7.8E-05	1.0E-05	5.1E-06	1.2E-06	1.2E-06	1.0E-04	81.4
Tc-99	1.6E-05	1.4E-05	1.6E-05	7.0E-07	7.2E-07	6.9E-06	8.7E-07	8.4E-07	4.7E-07	4.7E-07	1.6E-05	34.9
Pd-107	1.0E-07	1.1E-07	1.4E-07	5.1E-08	5.9E-08	1.0E-07	4.4E-08	3.7E-08	2.7E-08	2.7E-08	1.4E-07	5.1
Sn-126	2.3E-04	2.5E-04	2.9E-04	1.1E-04	1.3E-04	2.3E-04	4.7E-04	4.5E-04	5.2E-05	5.2E-05	4.7E-04	8.9
I-129	3.4E-04	3.4E-04	3.7E-04	1.4E-04	1.8E-04	3.1E-04	1.8E-04	1.5E-04	8.9E-05	8.9E-05	3.7E-04	4.1
Cs-135	1.0E-05	9.8E-06	1.1E-05	4.3E-06	5.5E-06	8.9E-06	6.1E-05	3.2E-05	1.7E-06	1.7E-06	6.1E-05	36.6
Ra-226	4.3E-04	4.8E-04	5.3E-04	2.7E-04	2.8E-04	3.9E-04	2.6E-04	2.4E-04	2.1E-04	2.1E-04	5.3E-04	2.5
Th-230	3.8E-04	4.0E-04	4.3E-04	2.6E-04	2.6E-04	3.4E-04	2.5E-04	2.4E-04	2.3E-04	2.3E-04	4.3E-04	1.9
Pa-231	1.2E-03	1.2E-03	1.3E-03	5.9E-04	6.0E-04	9.9E-04	5.6E-04	5.4E-04	5.2E-04	5.2E-04	1.3E-03	2.4
Np-237	2.1E-04	2.6E-04	2.9E-04	9.3E-05	9.5E-05	2.0E-04	8.9E-05	8.5E-05	8.0E-05	8.0E-05	2.9E-04	3.6
U-238	7.2E-05	9.5E-05	1.1E-04	4.1E-05	4.1E-05	6.9E-05	3.9E-05	3.7E-05	3.5E-05	3.5E-05	1.1E-04	3.0
Pu-239	3.2E-04	3.2E-04	3.4E-04	2.0E-04	2.0E-04	2.7E-04	2.0E-04	1.9E-04	1.8E-04	1.8E-04	3.4E-04	1.9
Am-243	2.8E-04	2.8E-04	3.0E-04	1.6E-04	1.7E-04	2.4E-04	1.7E-04	1.6E-04	1.5E-04	1.5E-04	3.0E-04	2.1

Tab. 3.5 BDCF for reference regions for the “well” scenario and organic soil. The BDCF are in Sv/y per Bq/L in near surface groundwater

Climate	BS	Csa	Csb	Cfb	Cfb	Dfa	Dfb	Dfc	ET	Min	Max	Ratio Max/Min
Reference region	Marrakesh	Rome	Valladolid	Santander	Magdeburg	Rostov	Turku	Sodankyla	Vardo			
Cl-36	2.9E-05	3.4E-05	4.0E-05	6.6E-05	1.3E-05	3.0E-05	5.8E-06	3.2E-06	8.1E-07	8.1E-07	6.6E-05	81.7
Ni-59	9.8E-07	1.1E-06	1.3E-06	2.4E-07	3.5E-07	8.1E-07	1.7E-07	1.0E-07	4.8E-08	4.8E-08	1.3E-06	26.5
Se-79	5.9E-05	6.2E-05	7.1E-05	1.3E-05	2.1E-05	5.1E-05	1.1E-05	6.2E-06	2.2E-06	2.2E-06	7.1E-05	32.3
Zr-93	2.4E-05	2.9E-05	3.5E-05	6.0E-06	7.0E-06	1.8E-05	3.6E-06	2.5E-06	8.0E-07	8.0E-07	3.5E-05	43.1
Nb-94	2.6E-03	2.6E-03	3.1E-03	5.4E-04	1.0E-03	2.4E-03	3.6E-04	1.5E-04	1.2E-06	1.2E-06	3.1E-03	2490.4
Tc-99	2.6E-06	3.0E-06	3.3E-06	2.2E-05	1.1E-05	2.4E-05	1.4E-05	6.2E-06	4.7E-07	4.7E-07	2.4E-05	51.9
Pd-107	7.0E-07	8.2E-07	9.6E-07	1.8E-07	2.6E-07	6.0E-07	1.1E-07	6.3E-08	2.7E-08	2.7E-08	9.6E-07	35.2
Sn-126	3.7E-03	3.8E-03	4.4E-03	8.2E-04	1.4E-03	3.3E-03	9.2E-04	6.4E-04	5.2E-05	5.2E-05	4.4E-03	84.9
I-129	2.6E-04	2.8E-04	3.1E-04	1.4E-04	1.8E-04	2.9E-04	1.4E-04	1.3E-04	8.9E-05	8.9E-05	3.1E-04	3.5
Cs-135	8.9E-05	8.0E-05	8.6E-05	1.9E-05	3.4E-05	8.4E-05	2.2E-04	9.0E-05	1.7E-06	1.7E-06	2.2E-04	130.3
Ra-226	8.0E-03	1.0E-02	1.2E-02	2.1E-03	2.5E-03	5.9E-03	1.5E-03	7.2E-04	2.1E-04	2.1E-04	1.2E-02	56.1
Th-230	1.9E-03	1.5E-03	1.8E-03	4.0E-04	4.6E-04	1.2E-03	3.1E-04	2.7E-04	2.3E-04	2.3E-04	1.9E-03	8.6
Pa-231	4.8E-02	2.7E-02	3.2E-02	2.4E-03	3.5E-03	2.3E-02	1.6E-03	9.5E-04	5.2E-04	5.2E-04	4.8E-02	93.4
Np-237	2.2E-03	2.9E-03	3.4E-03	6.1E-04	6.5E-04	1.6E-03	3.1E-04	1.7E-04	8.0E-05	8.0E-05	3.4E-03	42.0
U-238	2.3E-03	3.6E-03	4.3E-03	7.6E-04	5.3E-04	1.3E-03	4.2E-04	2.0E-04	3.5E-05	3.5E-05	4.3E-03	121.7
Pu-239	1.6E-03	1.2E-03	1.4E-03	2.6E-04	2.9E-04	8.4E-04	2.3E-04	2.0E-04	1.8E-04	1.8E-04	1.6E-03	9.0
Am-243	2.9E-03	1.9E-03	2.2E-03	3.1E-04	4.0E-04	1.5E-03	2.5E-04	1.9E-04	1.5E-04	1.5E-04	2.9E-03	19.7

Tab. 3.6 List of the contribution of exposure pathways to the total BDCF for sand soil

	Magdeburg (Cfb)				Rome (Csa)			
	Contribution [%]			Total BDCF [Sv/y per Bq/L]	Contribution [%]			Total BDCF [Sv/y per Bq/L]
	External	Ingestion	Inhalation		External	Ingestion	Inhalation	
Cl-36	0.0	100.0	0.0	2.2E-06	0.0	100.0	0.0	6.4E-06
Ni-59	0.5	99.5	0.0	1.2E-07	0.7	99.3	0.0	2.8E-07
Se-79	0.0	100.0	0.0	3.1E-06	0.0	100.0	0.0	1.3E-05
Zr-93	0.0	100.0	0.0	9.4E-07	0.0	99.5	0.5	1.3E-06
Nb-94	94.5	5.5	0.0	2.6E-05	97.7	2.3	0.0	8.5E-05
Tc-99	0.0	100.0	0.0	7.3E-07	0.0	100.0	0.0	1.4E-05
Pd-107	0.0	100.0	0.0	6.2E-08	0.0	100.0	0.0	1.2E-07
Sn-126	21.8	78.2	0.0	1.4E-04	38.8	61.2	0.0	2.6E-04
I-129	0.0	100.0	0.0	1.8E-04	0.0	100.0	0.0	3.5E-04
Cs-135	0.0	100.0	0.0	5.6E-06	0.0	100.0	0.0	1.0E-05
Ra-226	8.8	91.1	0.1	2.8E-04	17.0	82.0	0.9	4.9E-04
Th-230	0.0	98.8	1.2	2.6E-04	0.0	89.2	10.8	4.0E-04
Pa-231	1.4	94.5	4.1	6.0E-04	1.9	68.7	29.4	1.2E-03
Np-237	2.9	96.3	0.9	9.5E-05	3.6	90.9	5.5	2.6E-04
U-238	1.1	98.4	0.5	4.2E-05	1.4	95.7	2.9	9.6E-05
Pu-239	0.0	98.4	1.6	2.0E-04	0.0	86.0	14.0	3.2E-04
Am-243	2.5	95.4	2.1	1.7E-04	4.0	78.8	17.1	2.8E-04

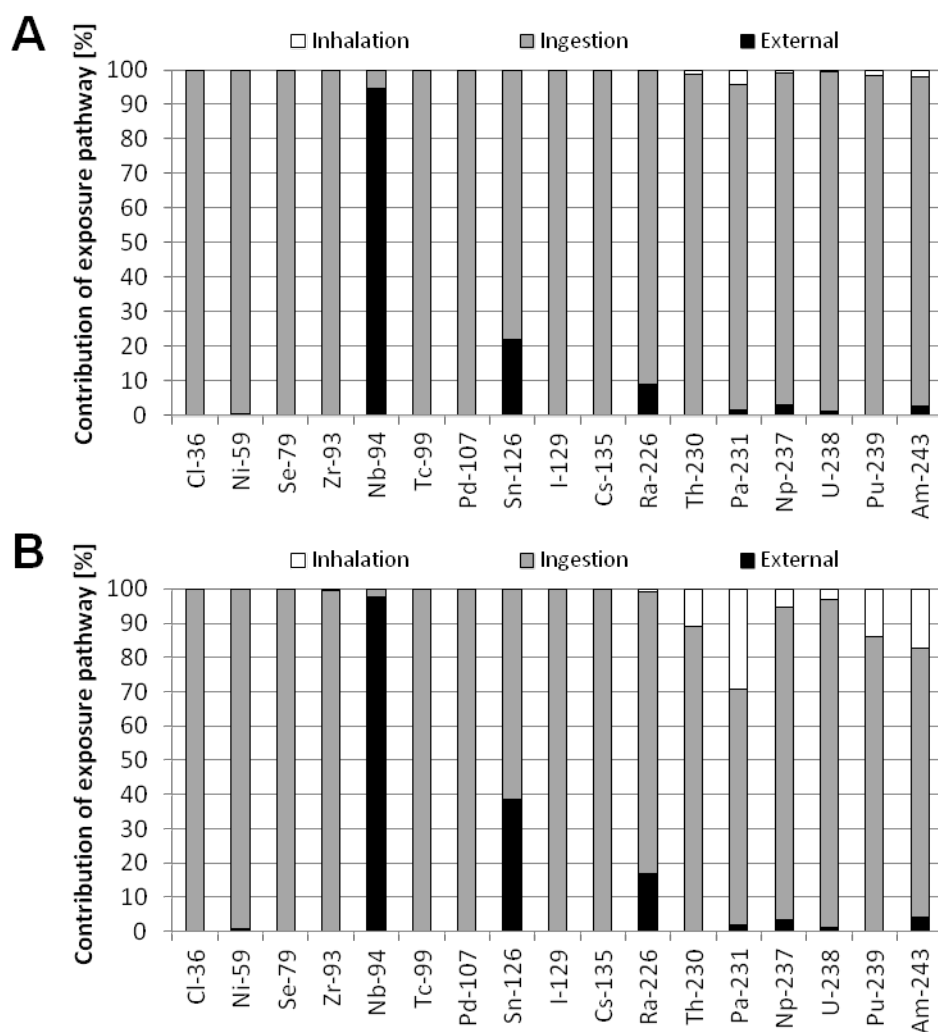


Fig. 3.9 Comparison of the contribution of exposure pathways on the total BDCF for the Magdeburg (A) and Rome (B) reference climate region

3.3 Probabilistic uncertainty and sensitivity analysis

Parameters for reference biosphere models are subject to uncertainty. In order to estimate the impact of the uncertainties on the BDCFs and to identify the most relevant parameters a probabilistic uncertainty and sensitivity analysis is performed. This analysis is restricted to the radionuclides Se-79, Tc-99, Cs-135, I-129, U-238, Np-237, Pu-239 and to the temperate and the Mediterranean climate states. The parameters used for the probabilistic model and the sensitivity analysis with their maximum, minimum and mode values are shown in Tab. 3.7 and Tab. 3.8 for the Magdeburg reference climate region and in Tab. 3.9 and Tab. 3.10 for the Rome reference climate region. The number of

simulations was set to 10 000 for the probabilistic analysis and the sample size for the sensitivity analysis to 5 000. The probability density functions (pdf) for relevant model parameters were derived from literature with either triangular or log-normal distributions. Migration factors for radionuclides in soil, transfer factors from animal feed to animal products and transfer factors soil to plant were assumed to have log normal distributions, other parameters were assumed to have triangular distributions.

Transfer factor arithmetic means, standard deviations, minimum and maximum values were directly taken from /IAE 09/ and /IAE 10/. Different radionuclide transfer factors soil to plant for subtropical, temperate and boreal climates were used when available. Parameter values for migration factors were derived from distribution coefficients for the given radionuclide /BAE 83/, /IAE 05/. The maximum values for the consumption rates were derived by using the multipliers for the 95 percentile of the according food type from the German ordination of radiation protection (Strahlenschutzverordnung) /STR 08/. Minimum and maximum values for translocation factors were set to one third and three times of the mode value, for resuspension factors to one tenth and ten times the mode. For irrigation amounts, estimated minimum and maximum values were used. Correlations between the parameters are not considered due to the amount of parameters and lacking information about correlations. This approach is simplified and should be expanded to include correlations between different parameters to increase the informative value of future model iterations.

Tab. 3.7 Parameters used for the probabilistic model and sensitivity analysis of the Magdeburg reference climate region

In this table parameters with a triangular probability density function are shown.

Parameter	Abbreviation	Unit	Radionuclide	Min	Max	Mode	
Dust concentration in air	C_Dust	µg/m ³		0	200	20	
	Consumption rate	FC_Beef	kg/y		0	60	30
		FC_Cereal			0	220	110
		FC_Fish			0	2	1
		FC_Fruity			0	225	75
		FC_Lamb			0	2	0
		FC_Leafy			0	39	13
		FC_Milk			0	390	130
		FC_Pork			0	120	60
		FC_Potato			0	165	55
		FC_Water			365	1460	730
Interception factor	IF_Cereal	dimensionless	Cs-135	1.7E-02	1.5E-01	5.0E-02	
			I-129	1.0E-02	9.0E-02	3.0E-02	
			Np-237	3.3E-02	3.0E-01	1.0E-01	
			Pu-239	3.3E-02	3.0E-01	1.0E-01	
			Se-79	1.0E-02	9.0E-02	3.0E-02	
			Tc-99	1.0E-02	9.0E-02	3.0E-02	
			U-238	3.3E-02	3.0E-01	1.0E-01	
			IF_Fruit	Cs-135	1.7E-02	1.5E-01	5.0E-02
				I-129	1.0E-02	9.0E-02	3.0E-02
				Np-237	3.3E-02	3.0E-01	1.0E-01
				Pu-239	3.3E-02	3.0E-01	1.0E-01
				Se-79	1.0E-02	9.0E-02	3.0E-02
	Tc-99	1.0E-02		9.0E-02	3.0E-02		
	IF_Grass	U-238	3.3E-02	3.0E-01	1.0E-01		
		Cs-135	1.7E-02	1.5E-01	5.0E-02		
		I-129	1.0E-02	9.0E-02	3.0E-02		
		Np-237	3.3E-02	3.0E-01	1.0E-01		
		Pu-239	3.3E-02	3.0E-01	1.0E-01		
		Se-79	1.0E-02	9.0E-02	3.0E-02		
	IF_Leafy	Tc-99	1.0E-02	9.0E-02	3.0E-02		
		U-238	3.3E-02	3.0E-01	1.0E-01		
		Cs-135	2.7E-02	2.4E-01	8.0E-02		
		I-129	1.3E-02	1.2E-01	4.0E-02		
		Np-237	5.0E-02	4.5E-01	1.5E-01		
		Pu-239	5.0E-02	4.5E-01	1.5E-01		
	IF_Maize	Se-79	1.3E-02	1.2E-01	4.0E-02		
		Tc-99	1.3E-02	1.2E-01	4.0E-02		
		U-238	5.0E-02	4.5E-01	1.5E-01		
		Cs-135	1.7E-02	1.5E-01	5.0E-02		
		I-129	1.0E-02	9.0E-02	3.0E-02		
		Np-237	3.3E-02	3.0E-01	1.0E-01		
	IF_Potato	Pu-239	3.3E-02	3.0E-01	1.0E-01		
		Se-79	1.0E-02	9.0E-02	3.0E-02		
		Tc-99	1.0E-02	9.0E-02	3.0E-02		
		U-238	3.3E-02	3.0E-01	1.0E-01		
		Cs-135	2.0E-02	1.8E-01	6.0E-02		
		I-129	1.0E-02	9.0E-02	3.0E-02		
				Np-237	4.0E-02	3.6E-01	1.2E-01
				Pu-239	4.0E-02	3.6E-01	1.2E-01
				Se-79	1.0E-02	9.0E-02	3.0E-02
				Tc-99	1.0E-02	9.0E-02	3.0E-02
				U-238	4.0E-02	3.6E-01	1.2E-01

Tab. 3.7 (cont.) Parameters used for the probabilistic model and sensitivity analysis of the Magdeburg reference climate region

Parameter	Abbreviation	Unit	Radionuclide	Min	Max	Mode
Irrigation	R_Mean	L/m ² y		0	300	190
	R_Cereal			0	300	170
	R_Fruity			0	300	210
	R_Grass			0	300	210
	R_Leafy			0	300	210
	R_Maize			0	300	210
	R_Potato			0	300	210
	R_Inhalation			4050	16200	8100
Resuspension factor	RFgrass	dimensionless		0.0006	0.0550	0.0055
	RFother			0.0001	0.0050	0.0005
Residence time	T_res	h/y		0.0000	8760.0000	1000
Translocation factor	TL_Cereal	dimensionless	Cs-135	3.0E-02	2.7E-01	9.0E-02
			I-129	3.0E-02	2.7E-01	9.0E-02
			Np-237	1.7E-03	1.5E-02	5.0E-03
			Pu-239	1.7E-03	1.5E-02	5.0E-03
			Se-79	3.0E-02	2.7E-01	9.0E-02
			Tc-99	3.0E-02	2.7E-01	9.0E-02
			U-238	1.7E-03	1.5E-02	5.0E-03
	TL_Fruity	dimensionless	Cs-135	3.3E-02	3.0E-01	1.0E-01
			I-129	3.3E-02	3.0E-01	1.0E-01
			Np-237	1.1E-03	9.9E-03	3.3E-03
			Pu-239	1.1E-03	9.9E-03	3.3E-03
			Se-79	3.3E-02	3.0E-01	1.0E-01
			Tc-99	3.3E-02	3.0E-01	1.0E-01
			U-238	1.1E-03	9.9E-03	3.3E-03
	TL_Leafy	dimensionless	Cs-135	3.3E-01	3.0E+00	1.0E+00
			I-129	3.3E-01	3.0E+00	1.0E+00
			Np-237	3.3E-01	3.0E+00	1.0E+00
			Pu-239	3.3E-01	3.0E+00	1.0E+00
			Se-79	3.3E-01	3.0E+00	1.0E+00
			Tc-99	3.3E-01	3.0E+00	1.0E+00
			U-238	3.3E-01	3.0E+00	1.0E+00
	TL_Potato	dimensionless	Cs-135	3.3E-02	3.0E-01	1.0E-01
			I-129	3.3E-02	3.0E-01	1.0E-01
			Np-237	0.0E+00	0.0E+00	0.0E+00
			Pu-239	0.0E+00	0.0E+00	0.0E+00
Se-79			3.3E-02	3.0E-01	1.0E-01	
Tc-99			3.3E-02	3.0E-01	1.0E-01	
U-238			0.0E+00	0.0E+00	0.0E+00	

Tab. 3.8 Parameters used for the probabilistic model and sensitivity analysis of the Magdeburg reference climate region

In this table parameters with a log-normal probability density function are shown.

Parameter	Abbreviation	Unit	Radionuclide	Mean	Std. Dev.	Lower trunc.	Upper trunc.			
Migration factor	Migarable	1/y	Cs-135	5.0E-04	5.0E-04	2.6E-06	2.7E-02			
			I-129	6.3E-02	6.3E-02	4.6E-04	2.4E+00			
			Np-237	1.9E-02	1.9E-02	2.2E-04	1.9E-01			
			Pu-239	6.7E-04	6.7E-04	3.9E-05	8.1E-02			
			Se-79	4.8E-02	4.8E-02	1.7E-04	6.5E-02			
			Tc-99	1.9E+0	1.9E+00	1.4E-02	2.4E+00			
			U-238	2.4E-03	2.4E-03	4.0E-06	3.3E-01			
	Migpasture			Cs-135	1.3E-03	1.3E-03	1.9E-05	6.9E-02		
				I-129	1.6E-01	1.6E-01	1.1E-03	6.1E+00		
				Np-237	4.7E-02	4.7E-02	5.6E-04	4.8E-01		
				Pu-239	1.7E-03	1.7E-03	9.7E-05	2.0E-02		
				Se-79	1.2E-02	1.2E-02	4.2E-04	1.6E-01		
				Tc-99	4.8E+0	4.8E+00	3.5E-01	6.1E+00		
				U-238	6.1E-03	6.1E-03	1.0E-05	8.3E-01		
Transfer factor	TF_Beef	dimension-	Cs-135	3.0E-02	2.3E-02	4.7E-03	9.6E-02			
			I-129	1.2E-02	1.5E-02	2.0E-03	3.8E-02			
			Np-237	1.0E-04	1.0E-04	1.0E-05	1.0E-03			
			Pu-239	6.0E-05	1.3E-04	8.8E-08	3.0E-04			
			Se-79	5.0E-03	5.0E-03	5.0E-04	5.0E-02			
			Tc-99	5.0E-03	5.0E-03	5.0E-04	5.0E-02			
			U-238	4.2E-04	2.0E-04	2.5E-04	6.3E-04			
			TF_Cereal			Cs-135	8.0E-02	1.2E-01	2.0E-03	6.6E-01
						I-129	5.8E-02	6.7E-02	1.0E-03	1.1E-02
						Np-237	8.0E-03	1.2E-02	2.5E-04	7.1E-02
						Pu-239	3.3E-05	6.6E-05	5.0E-07	3.6E-04
						Se-79	2.0E-02	2.0E-02	2.0E-03	2.0E-01
						Tc-99	1.3E+0	1.6E+00	1.8E-01	2.4E+00
			TF_Fruity			U-238	2.8E-02	2.5E-02	1.9E-04	6.2E-02
	Cs-135	1.1E-01				2.1E-01	1.2E-02	7.3E-01		
	I-129	1.0E-01				1.0E-01	1.0E-02	1.0E+00		
	Np-237	2.3E-02				1.6E-02	4.0E-03	5.7E-02		
	Pu-239	8.7E-05				5.4E-05	6.0E-06	2.0E-04		
	Se-79	3.0E-03				3.0E-03	3.0E-04	3.0E-02		
	TF_Grass			Tc-99	1.1E+0	1.1E+02	1.1E+01	1.1E+03		
				U-238	4.9E-02	6.0E-02	1.3E-03	1.6E-01		
				Cs-135	1.6E-01	2.1E-01	1.0E-02	9.9E-01		
				I-129	2.4E-03	2.5E-03	9.0E-04	5.0E-01		
				Np-237	4.8E-02	3.9E-02	7.2E-03	8.6E-02		
				Pu-239	1.6E-04	1.6E-04	5.0E-05	2.7E-04		
	TF_Lamb			Se-79	5.0E-02	5.0E-02	5.0E-03	5.0E-01		
				Tc-99	1.2E+0	1.3E+02	7.9E+00	4.7E+02		
				U-238	1.2E-01	4.9E-01	2.0E-04	5.5E+00		
				Cs-135	2.7E-01	2.6E-01	5.3E-02	1.3E+00		
				I-129	3.0E-02	3.0E-02	3.0E-03	3.0E-01		
Np-237				1.0E-03	1.0E-03	1.0E-04	1.0E-02			
Pu-239				5.3E-05	5.3E-05	2.0E-05	8.5E-05			
Se-79				5.0E-02	5.0E-02	5.0E-03	5.0E-01			
Tc-99				5.0E-03	5.0E-03	5.0E-04	5.0E-02			
U-238				1.0E-03	1.0E-03	1.0E-04	1.0E-02			

Tab. 3.8 (cont.) Parameters used for the probabilistic model and sensitivity analysis of the Magdeburg reference climate region

Parameter	Abbreviation	Unit	Radionuclide	Mean	Std. Dev.	Lower trunc.	Upper trunc.	
	TF_Leafy		Cs-135	2.4E-01	2.4E-01	2.1E-03	9.8E-01	
			I-129	4.0E-02	4.0E-02	4.0E-03	4.0E-01	
			Np-237	4.0E-02	3.3E-02	5.0E-03	8.0E-02	
			Pu-239	1.2E-04	9.3E-05	1.0E-05	2.9E-04	
			Se-79	3.0E-03	3.0E-03	3.0E-04	3.0E-02	
			Tc-99	1.2E+0	1.4E+03	4.5E+00	2.9E+03	
			U-238	2.2E-01	1.1E+00	7.8E-05	8.8E+00	
	TF_Maize			Cs-135	6.9E-02	6.2E-02	8.0E-03	2.6E-01
				I-129	1.0E-01	1.0E-01	1.0E-02	1.0E+00
				Np-237	4.8E-03	6.6E-03	1.0E-04	9.4E-03
				Pu-239	3.0E-06	3.0E-06	3.0E-07	3.0E-05
				Se-79	2.0E-02	2.0E-02	2.0E-03	2.0E-01
				Tc-99	1.7E+0	2.3E+01	5.0E-01	5.2E+01
				U-238	1.2E-01	2.3E-01	5.0E-04	7.1E-01
	TF_Milk			Cs-135	6.1E-03	6.3E-03	6.0E-04	6.8E-02
				I-129	9.1E-03	7.0E-03	4.0E-04	2.5E-02
				Np-237	5.0E-06	5.0E-06	5.0E-07	5.0E-05
				Pu-239	1.0E-06	1.0E-06	1.0E-07	1.0E-05
				Se-79	5.2E-03	4.5E-03	1.5E-03	1.6E-02
				Tc-99	1.0E-04	1.0E-04	1.0E-05	1.0E-03
				U-238	2.9E-03	2.9E-03	5.0E-04	6.1E-03
	TF_Pork			Cs-135	2.2E-01	9.0E-02	1.2E-01	4.0E-01
				I-129	4.1E-02	4.1E-02	1.5E-02	6.6E-02
				Np-237	3.0E-04	3.0E-04	3.0E-05	3.0E-03
				Pu-239	3.0E-04	3.0E-04	3.0E-05	3.0E-03
				Se-79	3.2E-01	3.2E-01	3.1E-02	3.1E-01
				Tc-99	1.0E-03	1.0E-03	1.0E-04	1.0E-02
				U-238	4.4E-02	4.4E-02	2.6E-02	6.2E-02
TF_Potato			Cs-135	1.5E-01	1.4E-01	4.0E-03	6.0E-01	
			I-129	1.0E-01	1.0E-01	1.0E-02	1.0E+00	
			Np-237	8.2E-03	6.9E-03	7.1E-04	2.7E-02	
			Pu-239	3.8E-04	4.1E-04	3.8E-06	2.0E-03	
			Se-79	3.0E-03	3.0E-03	3.0E+00	3.0E-02	
			Tc-99	4.3E-01	1.8E-01	1.8E-01	6.5E-01	
			U-238	3.3E-02	3.4E-02	4.3E-03	7.8E-02	

Tab. 3.9 Parameters used for the probabilistic model and sensitivity analysis of the Rome reference climate region

In this table parameters with a triangular probability density function are shown.

Parameter	Abbreviation	Unit	Radionuclide	Min	Max	Mode	
Dust concentration in air Consumption rate	C_Dust	µg/m ³		0	200	100	
	FC_Beef	kg/y		0	56	28	
	FC_Cereal			0	230	115	
	FC_Fish			0	1	0.5	
	FC_Fruity			0	252	84	
	FC_Lamb			0	3	1.5	
	FC_Leafy			0	112	56	
	FC_Milk			0	300	100	
	FC_Pork			0	56	28	
	FC_Potato			0	214	107	
	FC_Water			365	1460	730	
Interception factor	IF_Cereal	dimensionless	Cs-135	1.7E-02	1.5E-01	5.0E-02	
			I-129	1.0E-02	9.0E-02	3.0E-02	
			Np-237	3.3E-02	3.0E-01	1.0E-01	
			Pu-239	3.3E-02	3.0E-01	1.0E-01	
			Se-79	1.0E-02	9.0E-02	3.0E-02	
			Tc-99	1.0E-02	9.0E-02	3.0E-02	
			U-238	3.3E-02	3.0E-01	1.0E-01	
			IF_Fruit	Cs-135	1.7E-02	1.5E-01	5.0E-02
				I-129	1.0E-02	9.0E-02	3.0E-02
				Np-237	3.3E-02	3.0E-01	1.0E-01
				Pu-239	3.3E-02	3.0E-01	1.0E-01
	Se-79	1.0E-02		9.0E-02	3.0E-02		
	Tc-99	1.0E-02		9.0E-02	3.0E-02		
	U-238	3.3E-02		3.0E-01	1.0E-01		
	IF_Grass	Cs-135		1.7E-02	1.5E-01	5.0E-02	
		I-129		1.0E-02	9.0E-02	3.0E-02	
		Np-237		3.3E-02	3.0E-01	1.0E-01	
		Pu-239		3.3E-02	3.0E-01	1.0E-01	
		Se-79	1.0E-02	9.0E-02	3.0E-02		
		Tc-99	1.0E-02	9.0E-02	3.0E-02		
		U-238	3.3E-02	3.0E-01	1.0E-01		
		IF_Leafy	Cs-135	2.7E-02	2.4E-01	8.0E-02	
			I-129	1.3E-02	1.2E-01	4.0E-02	
			Np-237	5.0E-02	4.5E-01	1.5E-01	
			Pu-239	5.0E-02	4.5E-01	1.5E-01	
	Se-79		1.3E-02	1.2E-01	4.0E-02		
	Tc-99		1.3E-02	1.2E-01	4.0E-02		
	U-238		5.0E-02	4.5E-01	1.5E-01		
	IF_Maize		Cs-135	1.7E-02	1.5E-01	5.0E-02	
			I-129	1.0E-02	9.0E-02	3.0E-02	
			Np-237	3.3E-02	3.0E-01	1.0E-01	
			Pu-239	3.3E-02	3.0E-01	1.0E-01	
		Se-79	1.0E-02	9.0E-02	3.0E-02		
		Tc-99	1.0E-02	9.0E-02	3.0E-02		
		U-238	3.3E-02	3.0E-01	1.0E-01		
		IF_Potato	Cs-135	2.0E-02	1.8E-01	6.0E-02	
			I-129	1.0E-02	9.0E-02	3.0E-02	
			Np-237	4.0E-02	3.6E-01	1.2E-01	
			Pu-239	4.0E-02	3.6E-01	1.2E-01	
	Se-79		1.0E-02	9.0E-02	3.0E-02		
	Tc-99		1.0E-02	9.0E-02	3.0E-02		
	U-238		4.0E-02	3.6E-01	1.2E-01		

Tab. 3.9 (cont.) Parameters used for the probabilistic model and sensitivity analysis of the Rome reference climate region

Parameter	Abbreviation	Unit	Radionuclide	Min	Max	Mode
Irrigation	R_Mean	L/m ² y		0	800	485
	R_Cereal			0	800	360
	R_Fruity			0	800	610
	R_Grass			0	800	610
	R_Leafy			0	800	610
	R_Maize			0	800	610
	R_Potato			0	800	610
	R_Inhalation				4050	16200
Resuspension factor	RFgrass	dimensionless		0.0006	0.0550	0.0055
	RFother			0.0001	0.0050	0.0005
Residence time	T_res	h/y		0.0000	8760.0000	1000
Translocation factor	TL_Cereal	dimensionless	Cs-135	3.0E-02	2.7E-01	9.0E-02
			I-129	3.0E-02	2.7E-01	9.0E-02
			Np-237	1.7E-03	1.5E-02	5.0E-03
			Pu-239	1.7E-03	1.5E-02	5.0E-03
			Se-79	3.0E-02	2.7E-01	9.0E-02
			Tc-99	3.0E-02	2.7E-01	9.0E-02
			U-238	1.7E-03	1.5E-02	5.0E-03
	TL_Fruity	dimensionless	Cs-135	3.3E-02	3.0E-01	1.0E-01
			I-129	3.3E-02	3.0E-01	1.0E-01
			Np-237	1.1E-03	9.9E-03	3.3E-03
			Pu-239	1.1E-03	9.9E-03	3.3E-03
			Se-79	3.3E-02	3.0E-01	1.0E-01
			Tc-99	3.3E-02	3.0E-01	1.0E-01
			U-238	1.1E-03	9.9E-03	3.3E-03
	TL_Leafy	dimensionless	Cs-135	3.3E-01	3.0E+00	1.0E+00
			I-129	3.3E-01	3.0E+00	1.0E+00
			Np-237	3.3E-01	3.0E+00	1.0E+00
			Pu-239	3.3E-01	3.0E+00	1.0E+00
			Se-79	3.3E-01	3.0E+00	1.0E+00
			Tc-99	3.3E-01	3.0E+00	1.0E+00
			U-238	3.3E-01	3.0E+00	1.0E+00
	TL_Potato	dimensionless	Cs-135	3.3E-02	3.0E-01	1.0E-01
			I-129	3.3E-02	3.0E-01	1.0E-01
			Np-237	0.0E+00	0.0E+00	0.0E+00
			Pu-239	0.0E+00	0.0E+00	0.0E+00
Se-79			3.3E-02	3.0E-01	1.0E-01	
Tc-99			3.3E-02	3.0E-01	1.0E-01	
U-238			0.0E+00	0.0E+00	0.0E+00	

Tab. 3.10 Parameters used for the probabilistic model and sensitivity analysis of the Rome reference climate region

In this table parameters with a log-normal probability density function are shown.

Parameter	Abbreviation	Unit	Radionuclide	Mean	Std. Dev.	Lower trunc.	Upper trunc.			
Migration factor	Migarable	1/y	Cs-135	5.0E-04	5.0E-04	2.6E-06	2.7E-02			
			I-129	6.3E-02	6.3E-02	4.6E-04	2.4E+00			
			Np-237	1.9E-02	1.9E-02	2.2E-04	1.9E-01			
			Pu-239	6.7E-04	6.7E-04	3.9E-05	8.1E-02			
			Se-79	4.8E-02	4.8E-02	1.7E-04	6.5E-02			
			Tc-99	1.9E+00	1.9E+00	1.4E-02	2.4E+00			
			U-238	2.4E-03	2.4E-03	4.0E-06	3.3E-01			
	Migpasture			Cs-135	1.3E-03	1.3E-03	1.9E-05	6.9E-02		
				I-129	1.6E-01	1.6E-01	1.1E-03	6.1E+00		
				Np-237	4.7E-02	4.7E-02	5.6E-04	4.8E-01		
				Pu-239	1.7E-03	1.7E-03	9.7E-05	2.0E-02		
				Se-79	1.2E-02	1.2E-02	4.2E-04	1.6E-01		
				Tc-99	4.8E+00	4.8E+00	3.5E-01	6.1E+00		
				U-238	6.1E-03	6.1E-03	1.0E-05	8.3E-01		
Transfer factor	TF_Beef	dimensionless	Cs-135	3.0E-02	2.3E-02	4.7E-03	9.6E-02			
			I-129	1.2E-02	1.5E-02	2.0E-03	3.8E-02			
			Np-237	1.0E-04	1.0E-04	1.0E-05	1.0E-03			
			Pu-239	6.0E-05	1.3E-04	8.8E-08	3.0E-04			
			Se-79	5.0E-03	5.0E-03	5.0E-04	5.0E-02			
			Tc-99	5.0E-03	5.0E-03	5.0E-04	5.0E-02			
			U-238	4.2E-04	2.0E-04	2.5E-04	6.3E-04			
			TF_Cereal			Cs-135	4.8E-03	5.8E-03	1.0E-03	2.6E-02
						I-129	1.5E-04	1.5E-04	1.5E-05	1.5E-03
						Np-237	8.0E-03	1.2E-02	2.5E-04	7.1E-02
						Pu-239	3.3E-05	6.6E-05	5.0E-07	3.6E-04
						Se-79	2.0E-02	2.0E-02	2.0E-03	2.0E-01
						Tc-99	3.0E-02	3.0E-02	3.0E-03	3.0E-01
			TF_Fruity			U-238	2.8E-02	2.5E-02	1.9E-04	6.2E-02
	Cs-135	7.9E-02				1.2E-01	2.3E-03	3.0E-01		
	I-129	1.4E-03				1.1E-03	6.5E-04	2.7E-03		
	Np-237	2.3E-02				1.6E-02	4.0E-03	5.7E-02		
	Pu-239	8.2E-04				5.4E-04	4.3E-04	1.2E-03		
	Se-79	3.0E-03				3.0E-03	3.0E-04	3.0E-02		
	TF_Grass			Tc-99	3.0E-01	3.0E-01	3.0E-02	3.0E+00		
				U-238	4.9E-02	6.0E-02	1.3E-03	1.6E-01		
				Cs-135	8.3E-01	1.1E+00	6.0E-03	3.7E+00		
				I-129	2.4E-03	2.5E-03	9.0E-04	5.0E-01		
				Np-237	4.8E-02	3.9E-02	7.2E-03	8.6E-02		
				Pu-239	1.6E-04	1.6E-04	5.0E-05	2.7E-04		
	TF_Lamb			Se-79	5.0E-02	5.0E-02	5.0E-03	5.0E-01		
				Tc-99	1.2E+02	1.3E+02	7.9E+00	4.7E+02		
				U-238	1.2E-01	4.9E-01	2.0E-04	5.5E+00		
				Cs-135	2.7E-01	2.6E-01	5.3E-02	1.3E+00		
				I-129	3.0E-02	3.0E-02	3.0E-03	3.0E-01		
Np-237				1.0E-03	1.0E-03	1.0E-04	1.0E-02			
Pu-239				5.3E-05	5.3E-05	2.0E-05	8.5E-05			
Se-79				5.0E-02	5.0E-02	5.0E-03	5.0E-01			
Tc-99				5.0E-03	5.0E-03	5.0E-04	5.0E-02			
U-238				1.0E-03	1.0E-03	1.0E-04	1.0E-02			

Tab. 3.10 (cont.) Parameters used for the probabilistic model and sensitivity analysis of the Rome reference climate region

Parameter	Abbreviation	Unit	Radionuclide	Mean	Std. Dev.	Lower trunc.	Upper trunc.
Transfer factor	TF_Leafy		Cs-135	2.7E-02	3.4E-02	1.1E-03	8.9E-02
			I-129	4.1E-02	2.1E-02	1.2E-02	6.3E-02
			Np-237	4.0E-02	3.3E-02	5.0E-03	8.0E-02
			Pu-239	1.1E-03	1.3E-03	1.9E-04	2.0E-03
			Se-79	3.0E-03	3.0E-03	3.0E-04	3.0E-02
			Tc-99	8.4E-01	3.8E-01	1.7E-01	1.3E+00
			U-238	2.2E-01	1.1E+00	7.8E-05	8.8E+00
			U-238	2.2E-01	1.1E+00	7.8E-05	8.8E+00
	TF_Maize		Cs-135	5.0E-03	4.2E-03	2.0E-03	8.0E-03
			I-129	1.0E-01	1.0E-01	1.0E-02	1.0E+00
			Np-237	4.8E-03	6.6E-03	1.0E-04	9.4E-03
			Pu-239	3.0E-06	3.0E-06	3.0E-07	3.0E-05
			Se-79	2.0E-02	2.0E-02	2.0E-03	2.0E-01
			Tc-99	1.7E+01	2.3E+01	5.0E-01	5.2E+01
			U-238	1.2E-01	2.3E-01	5.0E-04	7.1E-01
			U-238	1.2E-01	2.3E-01	5.0E-04	7.1E-01
	TF_Milk		Cs-135	6.1E-03	6.3E-03	6.0E-04	6.8E-02
			I-129	9.1E-03	7.0E-03	4.0E-04	2.5E-02
			Np-237	5.0E-06	5.0E-06	5.0E-07	5.0E-05
			Pu-239	1.0E-06	1.0E-06	1.0E-07	1.0E-05
			Se-79	5.2E-03	4.5E-03	1.5E-03	1.6E-02
			Tc-99	1.0E-04	1.0E-04	1.0E-05	1.0E-03
			U-238	2.9E-03	2.9E-03	5.0E-04	6.1E-03
			U-238	2.9E-03	2.9E-03	5.0E-04	6.1E-03
	TF_Pork		Cs-135	2.2E-01	9.0E-02	1.2E-01	4.0E-01
			I-129	4.1E-02	4.1E-02	1.5E-02	6.6E-02
			Np-237	3.0E-04	3.0E-04	3.0E-05	3.0E-03
			Pu-239	3.0E-04	3.0E-04	3.0E-05	3.0E-03
			Se-79	3.2E-01	3.2E-01	3.1E-02	3.1E-01
			Tc-99	1.0E-03	1.0E-03	1.0E-04	1.0E-02
		U-238	4.4E-02	4.4E-02	2.6E-02	6.2E-02	
		U-238	4.4E-02	4.4E-02	2.6E-02	6.2E-02	
TF_Potato		Cs-135	2.0E-01	1.5E-01	4.8E-02	4.1E-01	
		I-129	1.0E-01	1.0E-01	1.0E-02	1.0E+00	
		Np-237	8.2E-03	6.9E-03	7.1E-04	2.7E-02	
		Pu-239	2.0E-03	1.8E-03	6.2E-04	4.8E-03	
		Se-79	3.0E-03	3.0E-03	3.0E+00	3.0E-02	
		Tc-99	1.5E+00	2.2E+00	8.0E-02	4.0E+00	
		U-238	3.3E-02	3.4E-02	4.3E-03	7.8E-02	
		U-238	3.3E-02	3.4E-02	4.3E-03	7.8E-02	

In the probabilistic analysis, distributions of BDCF were calculated from the pdf of the parameters listed in the above tables. These distributions are compared with the results from the deterministic model using the arithmetic or geometric means for the transfer factor and migration coefficients. For the calculation of the BDCF for the discrete model presented in section 3.2 geometric mean values from data bases are used for the parameters. The results for the deterministic models are within the range of the BDCF distributions calculated with the probabilistic models, but sometimes are at the low end of the distribution in case of the BDCF calculated with the geometric mean parameters. The distribution of the BDCF calculated with the probabilistic model depends on the on the pdf of the parameters and the influence of the various parameters and their associated pathways on the BDCF (Fig. 3.8 and Fig. 3.9). The spread of the probabilistic BDCF distributions is in most cases larger than the differences between the de-

terministic BDCF of the temperate and Mediterranean reference climate regions. These results suggest that the uncertainty of the parameters may have a larger impact on calculated BDCF than parameter changes between reference climate regions.

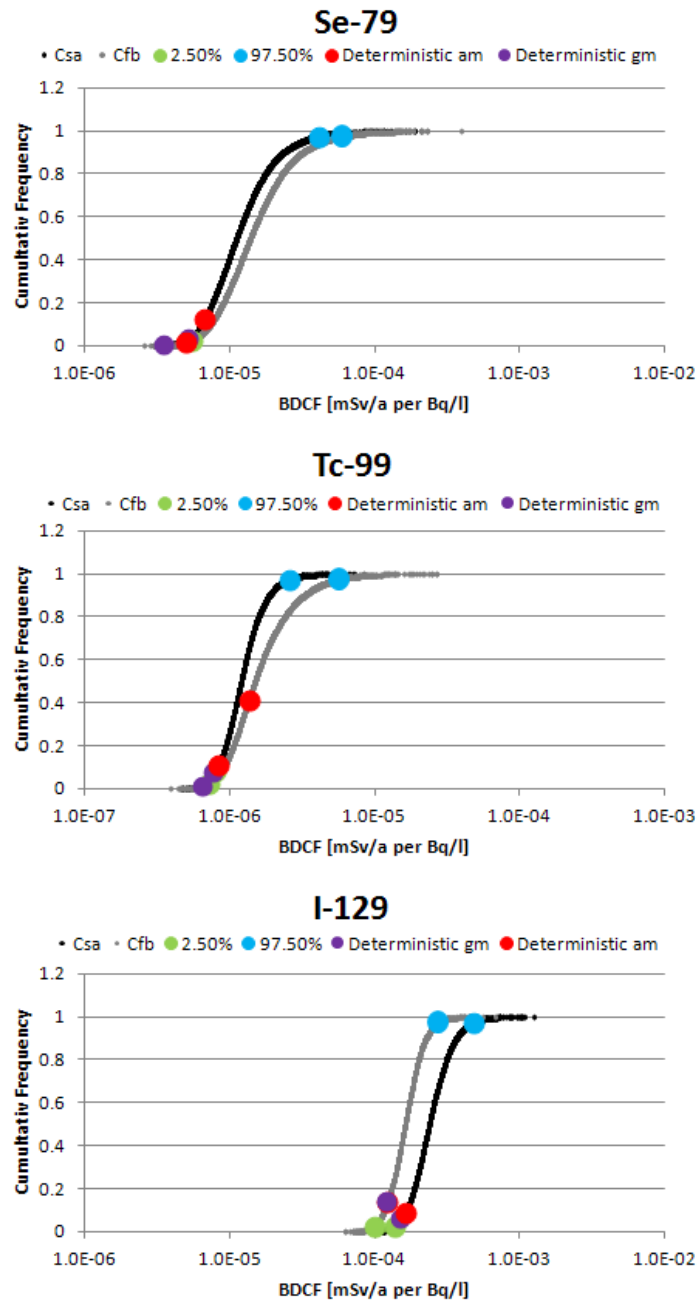


Fig. 3.10 Cumulative frequencies of BDCF for sand soil at the Magdeburg (Cfb) and Rome (Csa) reference climate regions from a probabilistic model for Se-79, Tc-99 and I-129

The values of the BDCF for the deterministic model using the geometric mean (gm) or arithmetic mean (am) are also marked in the distributions for comparison. These values for the deterministic model are not part of the probabilistic distribution. For the probabilistic analysis the number of simulations was set to 10 000.

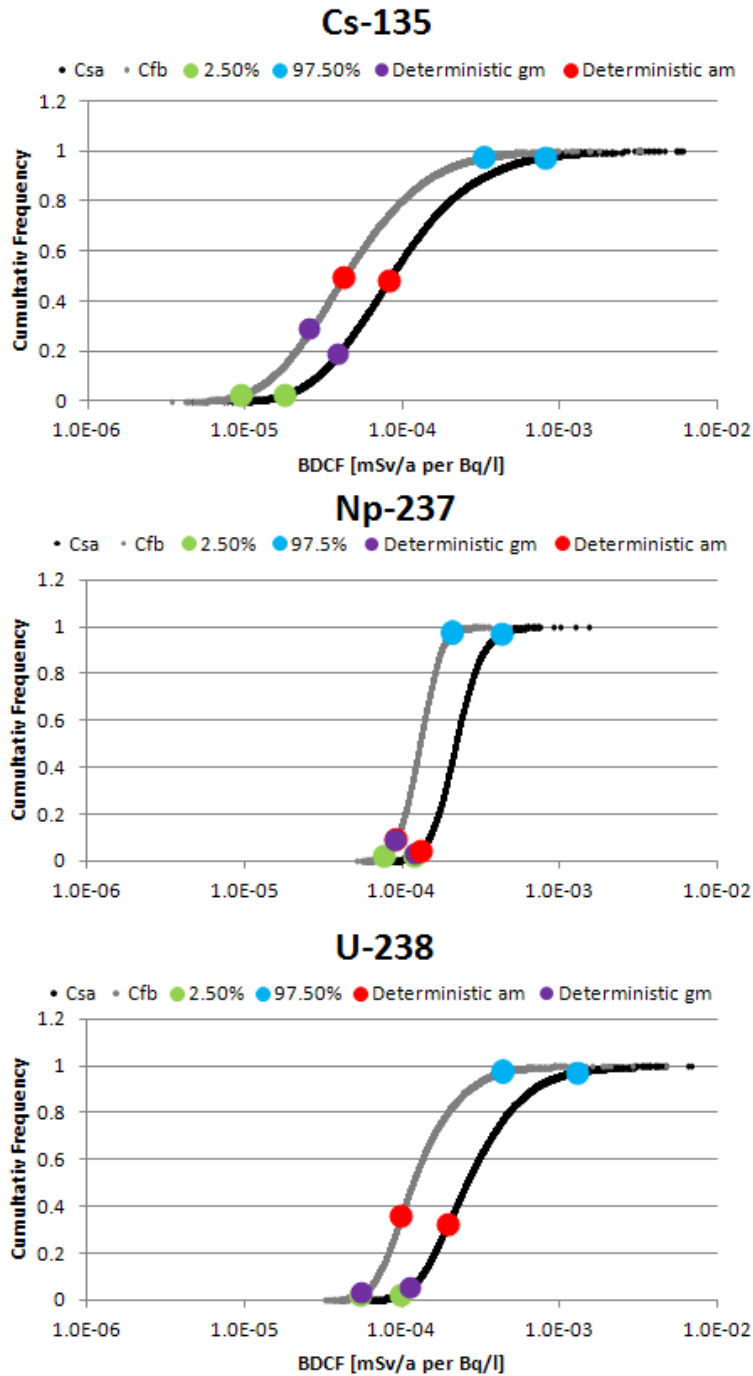


Fig. 3.11 Cumulative frequencies of BDCF for sand soil at the Magdeburg (Cfb) and Rome (Csa) reference climate regions from a probabilistic model for Cs-135, Np-237 and U-238

The values of the BDCF for the deterministic model using the geometric mean (gm) or arithmetic mean (am) are also marked in the distributions for comparison. These values for the deterministic model are not part of the probabilistic distribution. For the probabilistic analysis the number of simulations was set to 10 000.

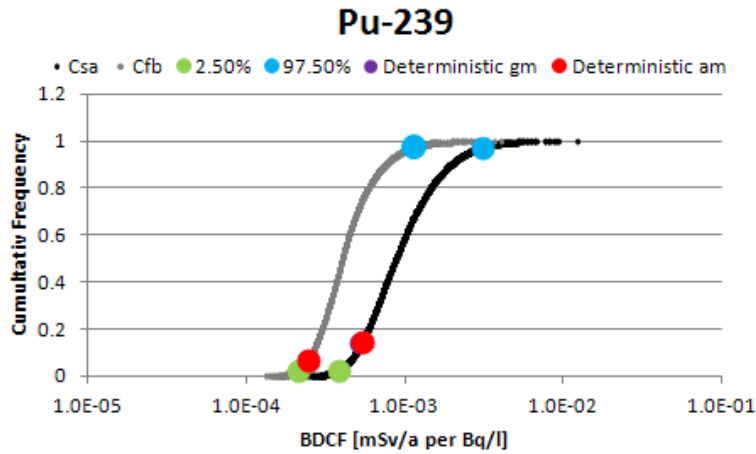


Fig. 3.12 Cumulative frequencies of BDCF for sand soil at the Magdeburg (Cfb) and Rome (Csa) reference climate regions from a probabilistic model for Pu-239

The values of the BDCF for the deterministic model using the geometric mean (gm) or arithmetic mean (am) are also marked in the distributions for comparison. These values for the deterministic model are not part of the probabilistic distribution. For the probabilistic analysis the number of simulations was set to 10 000.

Tab. 3.11 Comparison of the BDCF calculated with the deterministic models with the results from the probabilistic model

Reference region	Radionuclide	Deterministic model		Probabilistic model		
		geometric mean of parameters	arithmetic mean of parameters	2.50 %	50 %	97.50 %
Csa	Se-79	5.2E-06	6.6E-06	5.1E-06	1.1E-05	4.1E-05
Cfb		3.5E-06	4.9E-06	5.5E-06	1.4E-05	6.0E-05
Csa	Tc-99	7.9E-07	8.2E-07	6.7E-07	1.2E-06	2.5E-06
Cfb		6.4E-07	1.1E-06	7.1E-07	1.5E-06	5.6E-06
Csa	I-129	1.5E-04	1.6E-04	1.3E-04	2.4E-04	4.8E-04
Cfb		1.2E-04	1.2E-04	9.8E-05	1.6E-04	2.7E-04
Csa	Cs-135	3.9E-05	8.1E-05	1.8E-05	8.4E-05	7.9E-04
Cfb		2.6E-05	4.2E-05	9.3E-05	4.2E-05	3.3E-04
Csa	Np-237	1.2E-04	1.3E-04	1.2E-04	2.2E-04	4.2E-04
Cfb		8.9E-05	9.0E-05	7.5E-05	1.3E-04	2.1E-04
Csa	U-238	1.1E-04	1.9E-04	9.6E-05	2.5E-04	1.3E-03
Cfb		5.5E-05	9.7E-05	5.3E-05	1.2E-04	4.4E-04
Csa	Pu-239	5.2E-04	5.3E-04	3.8E-04	8.7E-04	3.1E-03
Cfb		2.4E-04	2.4E-04	2.1E-04	4.0E-04	1.1E-03

In order to evaluate the sensitivity of the respective parameters, Spearman correlation coefficients have been calculated and are shown in Fig. 3.13 – Fig. 3.19. The results are presented in the form of tornado charts. A value of 1 would signify a perfect mono-

tone relation. Negative values signify a negative correlation between the parameter and the BDCF, positive values a positive correlation. Only the ten parameters with the highest absolute correlations are shown. Most parameters show a positive correlation with the BDCF. Only the agricultural yields and the migration factors in arable and pasture soil show a negative correlation, since higher migration factors result in lower radionuclide concentration in soil and thus lower BDCF. Since different migration rates and transfer factors were used for this analysis, compared to the results shown for the deterministic models in section 3.2, it is difficult to compare the absolute values for BDCFs calculated by those two different models. The colours of the parameters in the graphs were chosen in such a way, that parameters relevant for a certain food type have the same colour. For example transfer factors from soil to cereals, interception factors for cereals and cereal food consumption rates are all in the same blue colour. This was done to facilitate the comparison of the graphs. For all radionuclides tested in this analysis the migration rates of radionuclides in soil, determining the radionuclides activity in agricultural and pasture soil, are among the parameters with the highest correlations with the BDCF.

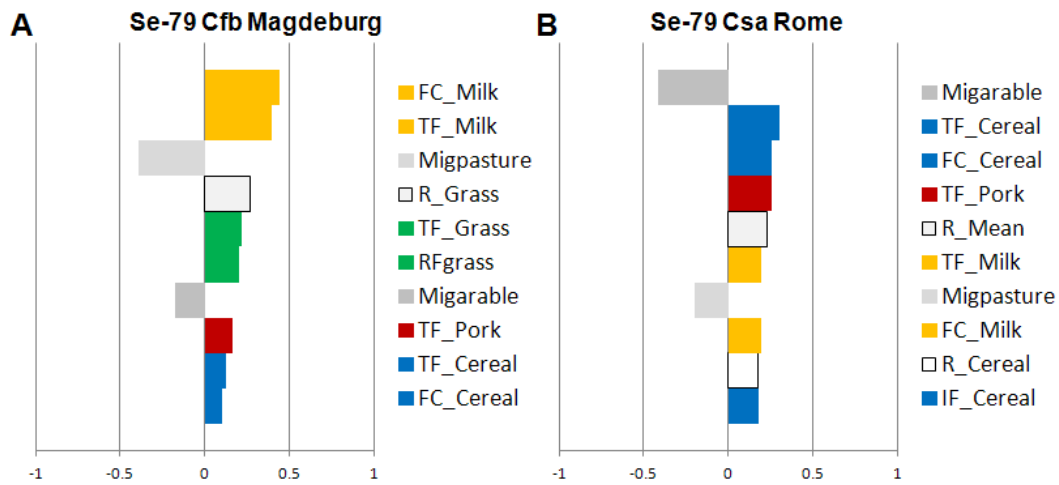


Fig. 3.13 Tornado chart for the sensitivity analysis of Se-79 for sand soil and the A) Magdeburg and B) Rome reference climate region

The tornado charts for Se-79 show that similar parameters have a high correlation with the BDCF at both analysed reference climate regions (Fig. 3.13), but the relative importance of these parameters is different. The most important parameters for Se-79 seem to be those influencing the contamination in milk and cereals and their consumption rates.

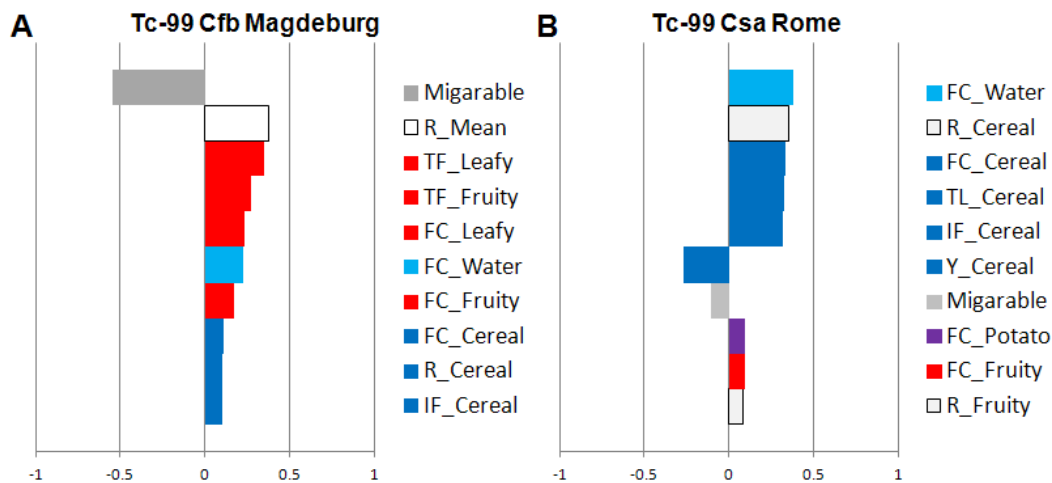


Fig. 3.14 Tornado chart for the sensitivity analysis of Tc-99 for sand soil and the A) Magdeburg and B) Rome reference climate region

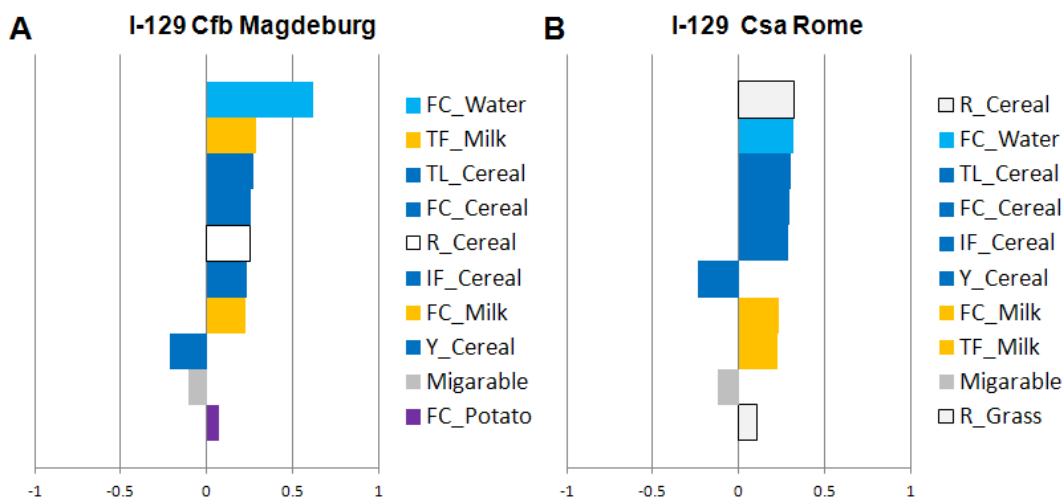


Fig. 3.15 Tornado chart for the sensitivity analysis of I-129 for sand soil and the A) Magdeburg and B) Rome reference climate region

The results for the sensitivity analysis for Tc-99 indicate that the BDCF is mainly affected by parameters influencing the radionuclide activity concentration in certain food types, like leafy vegetables, fruit vegetables and cereals (Fig. 3.14). This agrees with major contributions of those food types to the ingestion pathway calculated by the deterministic model and shown in Fig. 3.8. For the two reference climate regions, the contributions of various food types are quite different, resulting in quite different tornado charts.

The determining factors for the BDCF of I-129 are shown to be the parameters influencing the activity concentration in milk and cereals (Fig. 3.15 and Fig. 3.8). The tornado charts of both reference climate regions shown here contain almost the same parameters in a different order of importance. This agrees with the fact that the BDCF from the deterministic model only vary by a factor of 4.1 for I-129 (Tab. 3.4).

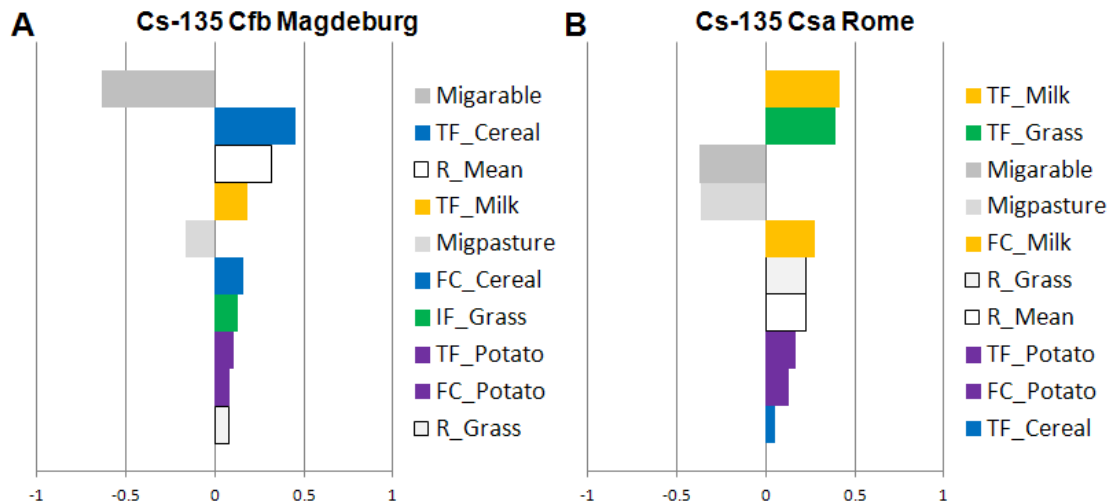


Fig. 3.16 Tornado chart for the sensitivity analysis of Cs-135 for sand soil and the A) Magdeburg and B) Rome reference climate region

For Cs-135 the milk pathway contributes in an important way to the BDCF especially at the Csa reference region (Fig. 3.16). Due to this, the parameters for grass are also important, since dairy cows feed on grass in the model. In addition to the milk parameters, parameters from the cereal pathway are important at the Cfb reference region. That is also true to a lesser degree for the Csa reference region. At both reference climate regions, parameters in the potato pathway show a good positive correlation with the BDCF. In Fig. 3.8 a high contribution of milk, cereals and potatoes to the ingestion BDCF of Cs-135 can be observed, confirming these results.

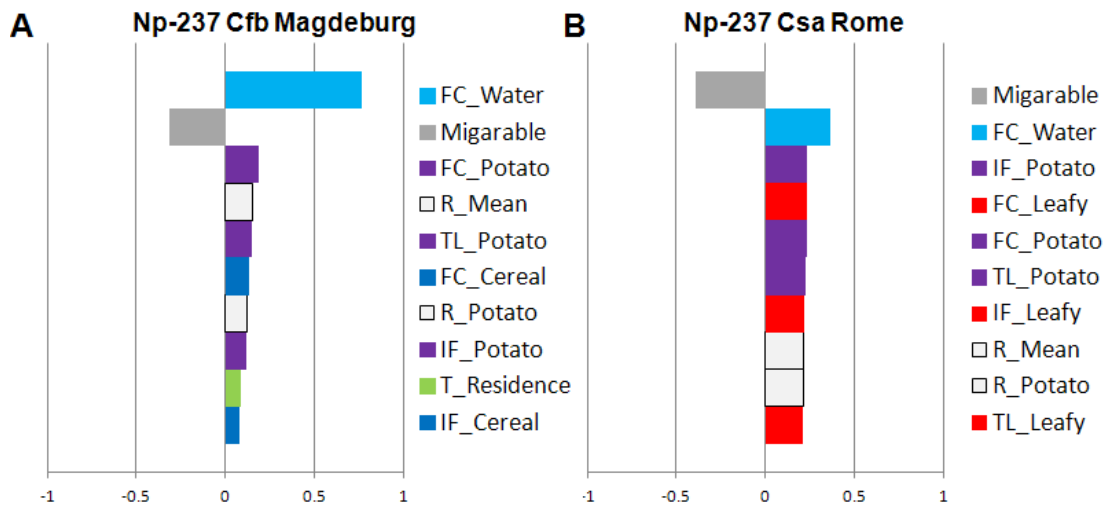


Fig. 3.17 Tornado chart for the sensitivity analysis of Np-237 for sand soil and the A) Magdeburg and B) Rome reference climate region

Fig. 3.17 shows, that for the Np-237 BDCF at the Magdeburg reference climate region the consumption rate of drinking water is the most important parameter (Fig. 3.17a). This agrees with the high contribution of drinking water to the ingestion BDCF shown in Fig. 3.8a. In contrast to this, parameters influencing the activity concentration and consumption rates of leafy vegetables and potatoes have an increased importance for the Rome reference climate region, also in accordance with the results from deterministic calculations (Fig. 3.17b and Fig. 3.8b).

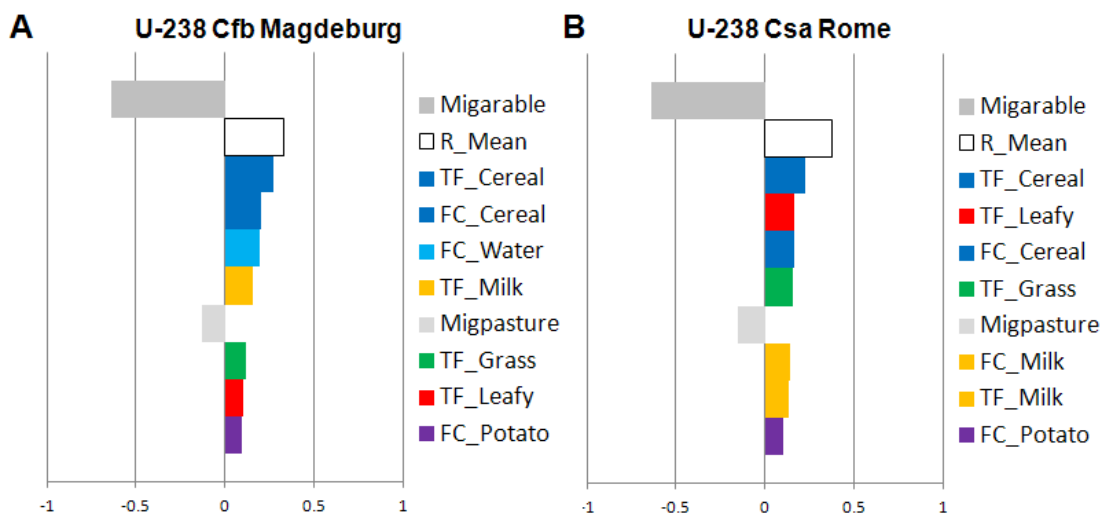


Fig. 3.18 Tornado chart for the sensitivity analysis of U-238 for sand soil and the A) Magdeburg and B) Rome reference climate region

For uranium at the Magdeburg reference climate region, the parameters influencing the radionuclide concentration in cereals and milk as well as their consumption rates have a highly positive correlation to the BDCF (Fig. 3.18a and Fig. 3.8a). At the Rome reference climate region parameters influencing the activity concentration in cereals and leafy vegetables have an increased impact and the consumption rate of water a decreased impact on the BDCF (Fig. 3.18b and Fig. 3.8b).

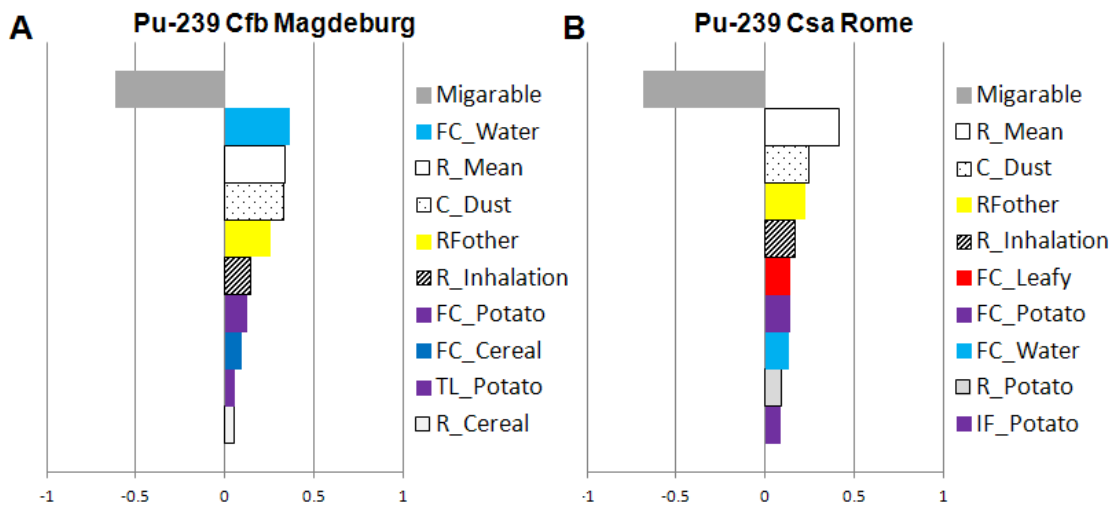


Fig. 3.19 Tornado chart for the sensitivity analysis of Pu-239 for sand soil and the A) Magdeburg and B) Rome reference climate region

Pu-239 is the only one of the radionuclides used for the sensitivity analysis that has a significant contribution of the inhalation pathway to the total BDCF (Fig. 3.9). Due to this parameters influencing the external exposure, like the dust concentration in the air and the inhalation rate are among the ten parameters with the highest absolute correlation to the BDCF (Fig. 3.19).

The sensitivity analysis results shown in this chapter demonstrate that in the model different parameters are important for different radionuclides and reference climate regions. For example, the BDCF of Tc-99 is mostly determined by water and cereal consumption rates in Mediterranean scenarios using and by parameters of the vegetable pathways in the temperate scenario. Cereals pathway parameters are also show a high positive correlation with the BDCF of the other radionuclides shown here. The grass-milk pathway has a high importance for Se-79, I-129 and Cs-137. For Pu-239 the inhalation pathway and connected parameters have a large impact on the BDCF while they are not important for the other radionuclides. All radionuclides react strongly to uncer-

tainties in the migration rates determining radionuclide concentrations in soil and consumption rates of drinking water

In conclusion, the sensitivity analysis highlights the importance of the soil model, since the migration factor, which is the most important parameter in the soil model, is always among the 10 most important parameters for the radionuclides and scenarios shown in this chapter. Transfer factors from soil to plant and consumption rates, especially for drinking water, are also highly relevant for the model results. The sensitivity analysis also confirms, that different parameters are important for different radionuclides and reference regions.

4 Identification of key transition processes affecting exposure

Climatic changes are expected to have a significant influence on the long-term radiological consequences of a radioactive waste repository. The routes and mechanisms by which persistent radionuclides are delivered to the area are strongly influenced by climate variability and global climate change. According to *Albritton et al*, climate can change over a period of time ranging from months to thousands or millions of years. The climate change referred to may be due to natural causes, e. g., changes in the sun's output, or due to human activities, e. g., changing the composition of the atmosphere. Any human-induced changes in climate will occur against the “background” of natural climatic variations /ALB 01/.

Changing climate impacts society and ecosystems in a broad variety of ways. For example climate change can increase or decrease rainfall, influence agricultural and consumption habits, affect human health, cause changes to forests and other ecosystems, or even impact the energy supply. Climate-related impacts are occurring across regions of the country and across many sectors of the economy.

The transition from one climate to another can also cause changes in the physico-chemical composition of radionuclides: some of them may become more available for plant uptake and due to this, their activity concentration in the plants increases. Other radionuclides may be stronger bound to soil and their activity concentration in plants decreases. Such changes might also cause remobilization of radionuclides from localised areas with contaminated sediments, their re-suspension and transfer to the surrounding areas.

The resulting total dose depends on many different parameters changing with climate, for example, consumption habits, transfer factor soil – plant, transfer factor feed – animal food etc.

Soil-to-plant transfer of radionuclides has long been a significant topic in radioecology for the protection of humans and the environment from the effects of ionising radiation. Climate/environmental change will impact soil-to-plant transfer of radionuclides and subsequent transfers in specific environments /DOW 08/.

4.1 Selection and justification of climate transitions

As mentioned above, the transition from one climate to the other may influence the behaviour of radionuclides in the environment, and respectively their impact on human populations. In order to select the relevant climate transitions, we have to look to the significant key processes and decide which of them can cause unexpected effects of increasing activity concentration in one or several parts of the food chain, affecting the radiation exposure of man.

The following key processes could affect radiation exposure during the transition from warm to cold and from cold to warm climate:

- Remobilisation, resuspension and transfer to the surrounding areas
- Leaching out of a marine or lake environment
- Increased precipitation could cause faster washing out of hazardous substances (water erosion)
- Changes in the physicochemical composition and following increase or decrease of bioavailability (especially for redox sensitive elements)
- Increase or decrease of soil-to-plant transfer
- Wind erosion, desertification

Climatic transitions causing radical changes in the agricultural praxis are of most interest. For example, there is no need for irrigation, if the groundwater level has risen high enough to directly supply the plants. The transfer factor soil-to-plant can differ for different climate states; moreover, by transition from a climate with rising groundwater to a climate requiring irrigation the concentration of radionuclides in plants increases because of additional foliar contamination.

Two scenarios for well and rising groundwater are described in /NOS 08/ for discrete reference climate regions under equilibrium conditions reflecting different accumulation processes of radionuclides in agricultural soil.

Fig. 4.1 shows selected transitions from one climate to another with a change of the interface between geo- and biosphere (well to rising groundwater and vice versa) where

the effects of transitions could be observed, especially for redox sensitive radionuclides. Blue arrows indicate cooling and red arrows indicate warming processes.

The most likely transitions are considered. A drop in temperature can lead to an increase in rainfall, decrease of evaporation and following rising groundwater tables. (In general also the opposite situation is possible: a decrease of temperature may lead to more arid conditions as it was reconstructed in Spain during the Medieval Climate Anomaly, ca. 900 – 1350 AD). Transitions from Semi-arid (Steppe) or Mediterranean climate to Temperate climate, from Temperate to Boreal climate, and from Boreal to Tundra may be caused by similar processes.

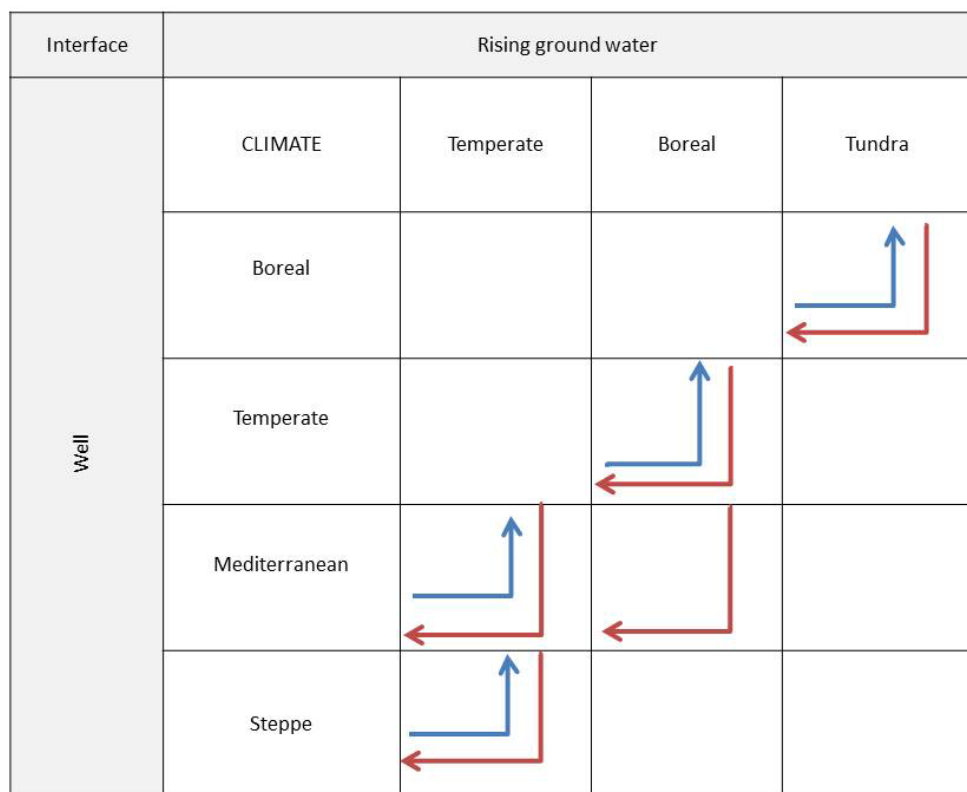


Fig. 4.1 Possible climate transitions and interface changes (blue arrow: cooling; red arrow: warming)

The increase of temperature leads to more arid conditions, the groundwater table drops, evaporation increases and the need of irrigation increases accordingly. As a result of these changes, the following climatic transitions could take place: from Temperate climate to Mediterranean or to Semi-arid (Steppe), from Boreal to Temperate or to Mediterranean and from Tundra to Boreal.

Thus, the most important transitions, the transition from temperate to a warm climate (warming) and the transition from a temperate to a cold climate (cooling) are identified.

4.1.1 Discrete climate states

The calculation of soil contamination for discrete climate states is based on the assumption that soil has been contaminated by irrigation with contaminated groundwater (well scenario) or by rising groundwater (rising groundwater scenario) and the contamination process is in equilibrium with processes of leaching and decay.

The soil contamination under equilibrium conditions can be described by the following equation:

$$C_i^s = \frac{R_i}{k_i} \quad (4.1)$$

where R_i is the input rate, and k_i is the first-order loss rate constant of radionuclide i ; in our case, k is a sum of migration and decay rates. By considering the transitions from one discrete climate state to another the setting of boundary conditions is needed:

$$C_i^s(0) \neq 0 \quad (4.2)$$

i. e. we have to take into account the initial contamination of soil caused by irrigation (cooling) or rising groundwater (warming) during the initial climate.

$$C_i^s = \frac{R_i}{k_i} + C_i^s(0) \quad (4.3)$$

It means that the soil contamination change as a step function with a time.

4.1.2 Cooling

Climate change to colder temperatures heavily entails complex changes in behaviour of radionuclides and resulting increase or decrease of soil or plant contamination.

Radionuclides remaining after the irrigation period (dry climate, well scenario) in the soil or mobilized from deeper soil layers with rising groundwater must be considered as the initial condition. The activity concentration of radionuclides in the soil for the scenario "rising groundwater" is calculated as a product of contamination of groundwater and the distribution coefficient k_d under equilibrium conditions. It is assumed that the ground is drained completely.

An increase in the radionuclide activity concentration in soil can be caused by gradually rising contaminated groundwater if the radionuclides in this groundwater are added to the already present radionuclides in soil accumulated during the irrigation phase. Such an event can occur if no outflow of water out of the system with resulting removal of radionuclides takes place. However, sustainable agriculture would not be possible under these conditions, since they would either lead to bog formation in the case of high soil water contents during long time periods, or to salting of the top soil layers in the case of evaporation of water. On the other hand, when outflow of radionuclides and water from the system takes place, the resulting radionuclide concentration should reach levels comparable to those assessed in the rising groundwater scenario for drained agricultural soil.

Climate cooling could cause changes in the agricultural practice of a population, for example, from farming and herding to hunting and gathering. A hunter-gatherer community needs a larger area per person for foraging compared to a society based on agriculture. Due to this, exposure pathways may change. Depending on the processes in the geosphere determining the surface footprint of radionuclides from a deep geological repository, fewer people may be exposed to those radionuclides in the case of hunter-gatherer communities. For example, cooling of the climate could cause an increasing role of Cs-135 in the total exposure, because it becomes more bioavailable. As special case permafrost has to be considered. Periodic freezing and thawing of deep freeze soil affects the chemical properties of soil, and has an influence on the behaviour of radionuclides /RAZ 11/. In addition to this, permafrost conditions limit the rise of contaminated groundwater to the surface and its introduction into the biosphere.

Fig. 4.2 shows the transitions in case of climate cooling:

- Steppe with Irrigation to Temperate Rising Groundwater (RGW)
- Steppe or Mediterranean with Irrigation to Temperate RGW
- Temperate with Irrigation to Boreal RGW





Interface	Rising ground water			
Well	CLIMATE	Temperate	Boreal	Tundra
	Boreal			
	Temperate			
	Mediterranean			
	Steppe			

Fig. 4.2 Transitions between discrete climates and geosphere-biosphere interfaces when the climate becomes colder

The considered transitions may be completely described by the discrete climate states under equilibrium conditions. The changes in soil conditions by decrease of the temperature do not lead to changes of physic-chemical characteristics of radionuclides, and we cannot see any unexpected effects, such as a temporary increase of bioavailability of certain radionuclides and a following increase of BDFC.

4.1.3 Warming

During the climate transition to higher temperatures, the compensation of an increased water deficit with irrigation using contaminated groundwater, change of soil conditions, changes in agricultural practices etc. may cause an increase of exposure to man. In general the behaviour of radionuclides was described with discrete climate states /NOS 08/. Fig. 4.3 shows the considered transitions between climates and interfaces if the climate becomes warmer. For these transitions unexpected effects on the exposure related to changes in radionuclides transfer from soil to plants could be possible and need to be assessed.

Interface	Rising ground water			
Well	CLIMATE	Temperate	Boreal	Tundra
	Boreal			←
	Temperate		←	
	Mediterranean	←	←	
	Steppe	←		

Fig. 4.3 Considered transitions between climates and interfaces

The following transition from one climate to another may be considered:

- Tundra RGW to Boreal with irrigation
- Boreal RGW to Temperate or Mediterranean with irrigation
- Temperate RGW to Mediterranean or Steppe with irrigation

All those transitions have one common characteristic, namely that due to increasing temperature the contaminated groundwater levels fall and agricultural land needs additional irrigation. If the irrigation occurs with this contaminated groundwater (deep well), already contaminated soil will get additional radionuclides with this irrigation water. Especially the increase of irrigation amounts in warmer and drier climates could be important for the exposure of a population in the discrete models.

Fig. 4.4 shows examples of transitions from temperate climate (rising groundwater scenario) to Mediterranean climate (irrigation) for Se-79 calculated for discrete climate states, taking into account changing of parameters (Tab. 4.1).

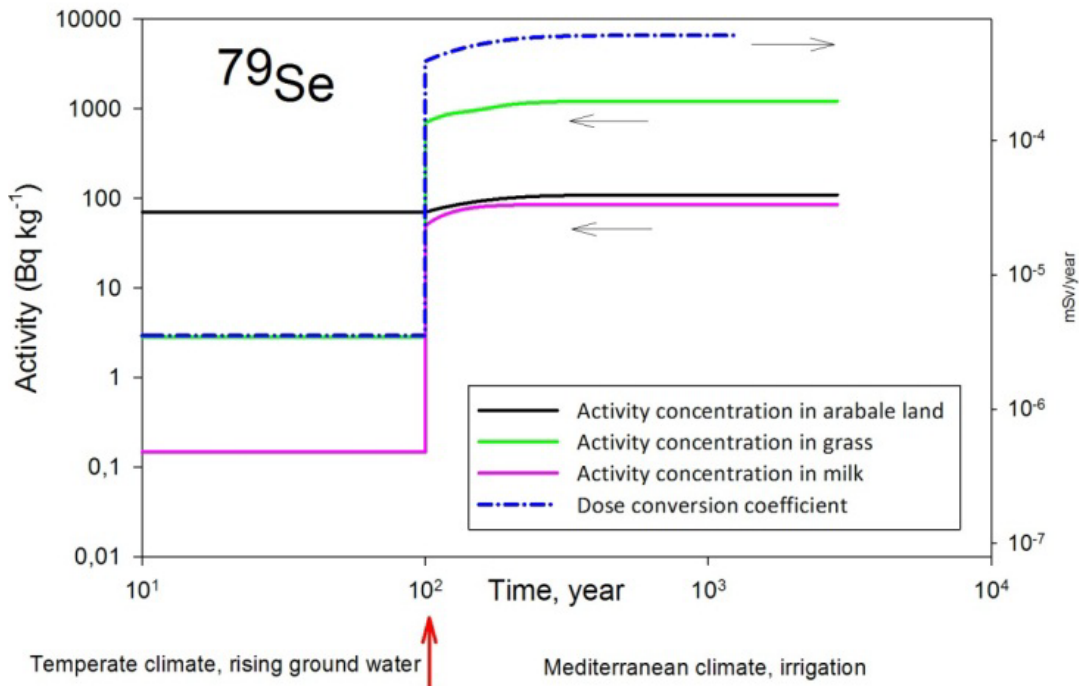


Fig. 4.4 Transitions from temperate climate (rising groundwater scenario) to Mediterranean climate (irrigation) for Se-79

Tab. 4.1 Parameters used for calculation of the transitions Fig. 4.6

Parameters	Unit	Temperate, RGW	Mediterranean, Irrigation
Migration	1/y		0.016
Transfer factor		0.02	5
Resuspension		0.0005	0.001
Interception			0.03
Translocation			1
Growing period	d		150
Yield	kg/m ² y		3
Weathering	1/d		0.0495
Soil mass	kg/m ²		350
Irrigation rates	L/m ² y		610
Initial Activity in soil	Bq/kg	70	

In the first step the dynamic processes in soil can be described with a sum of two components changing during the time, Fig. 4.5

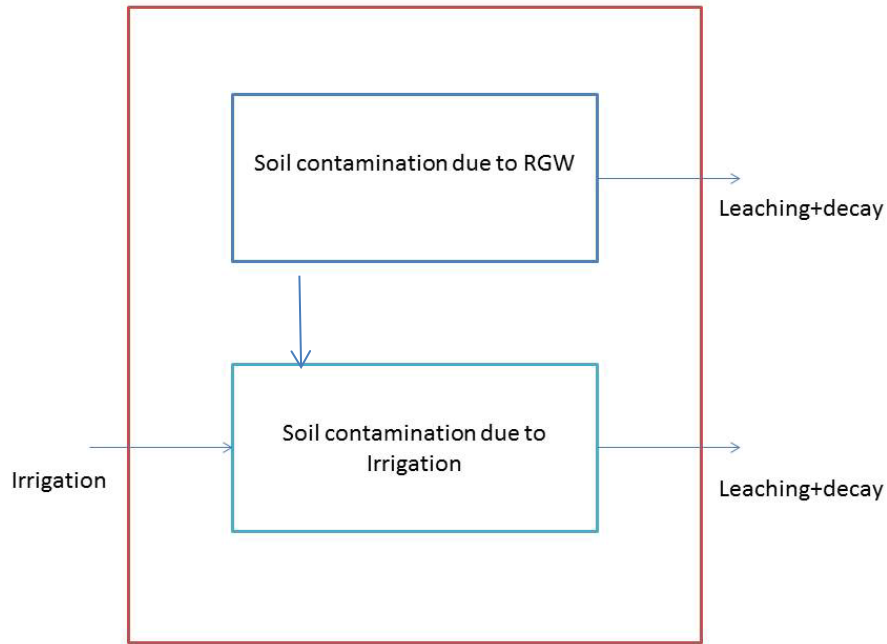


Fig. 4.5 Two compartment of soil model

For an initially contamination due to RGW the activity concentration of radionuclide i develops with time as

$$C_i^{RGW}(t) = C_i^{RGW}(0)e^{-kt} \quad (4.4)$$

The contamination of soil due to irrigation follows a saturation law:

$$C_i^{Irr} = \frac{R}{k}(1 - e^{-kt}) \quad (4.5)$$

The total activity concentration of radionuclide i is the sum of these two processes:

$$C_i^{tot}(t) = \frac{R}{k}(1 - e^{-kt}) + C_i^{RGW}(0)e^{-kt} \quad (4.6)$$

where R_i is the input rate, and k_i is a first-order loss rate constant of radionuclide i ; k is a sum of migration and decay rates.

The processes are shown in Fig. 4.6 for Se-79, initial contamination 1 000 Bq/kg, transition time 100 years. The contamination of plants increases because of increasing of the transfer factor soil to plant and additional foliar contamination and resuspension.

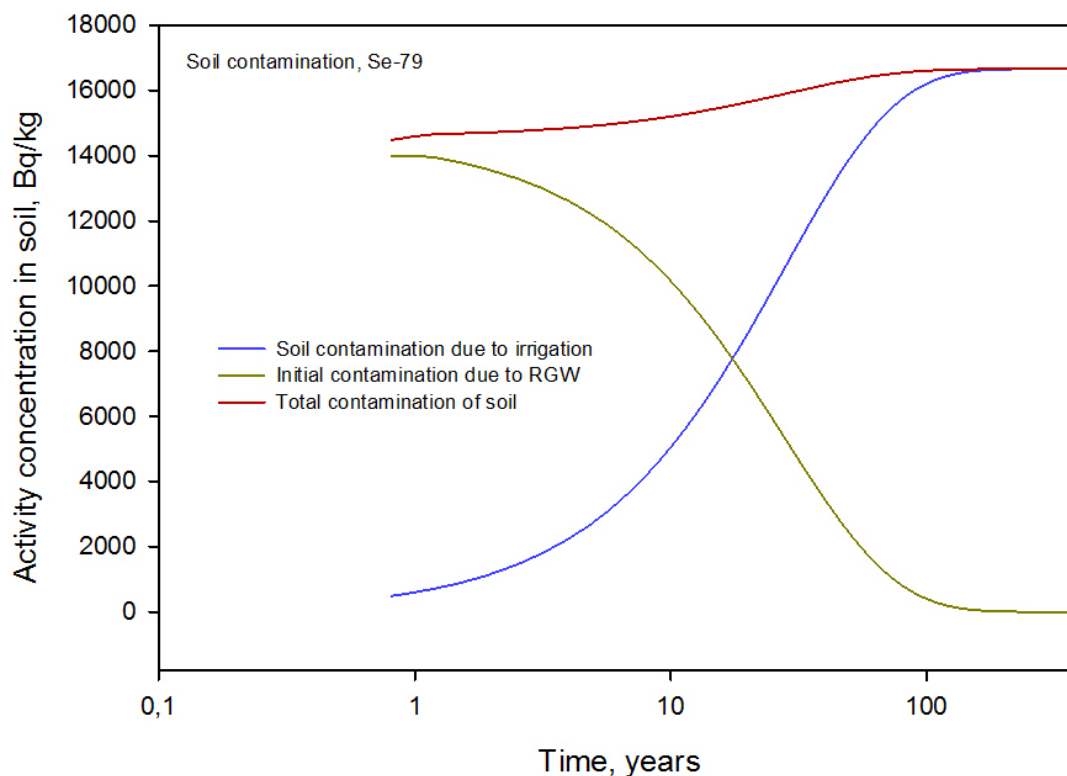


Fig. 4.6 Time course of two processes causing the contamination of agricultural land with Se-79

4.1.4 Redox sensitive radionuclides

The radionuclides Se-79, Np-237, Tc-99, U-238 are very sensitive to soil moisture (see Annex A.2) and thus, to the redox potential. Tab. 4.2 shows the distribution coefficient values for redox sensitive radionuclides, and additionally for iodine, for the minimum and maximum of possible reduction potential (Eh) in sand soil /IAE 09/. The availability of redox sensitive radionuclides increases with drying out of soil, the oxidation state changes and radionuclides become more mobile. Correspondingly, the transfer to plant increases by a factor of 10 or 100. Iodine shows a different behaviour compared to the other redox-sensitive elements, since it is more mobile in the lower oxidation state.

The chemical form, especially the oxidation state, determines solubility, sorption and subsequent mobilisation of the nuclides. Fig. 4.7 shows the expected dominant oxidation states of the radionuclides as a function of the standard redox potential in pH 7 water at equilibrium with atmospheric CO₂. The radionuclides Tc, U and Np oxidise and reach their mobile form already by Eh values of about -0.1 – 0 mV, while Se reaches its mobile form only by Eh value of about 0.5 mV.

Tab. 4.2 Values of K_d for minimum and maximum redox potential (pH=7)

Element	K_d (Eh_{min})	K_d (Eh_{max})
Technetium	11	0.01
Iodine	0.01	580
Uranium	67 000	0.7
Neptunium	1 200	1.3
Plutonium	21 000	6
Selenium	2 100	4

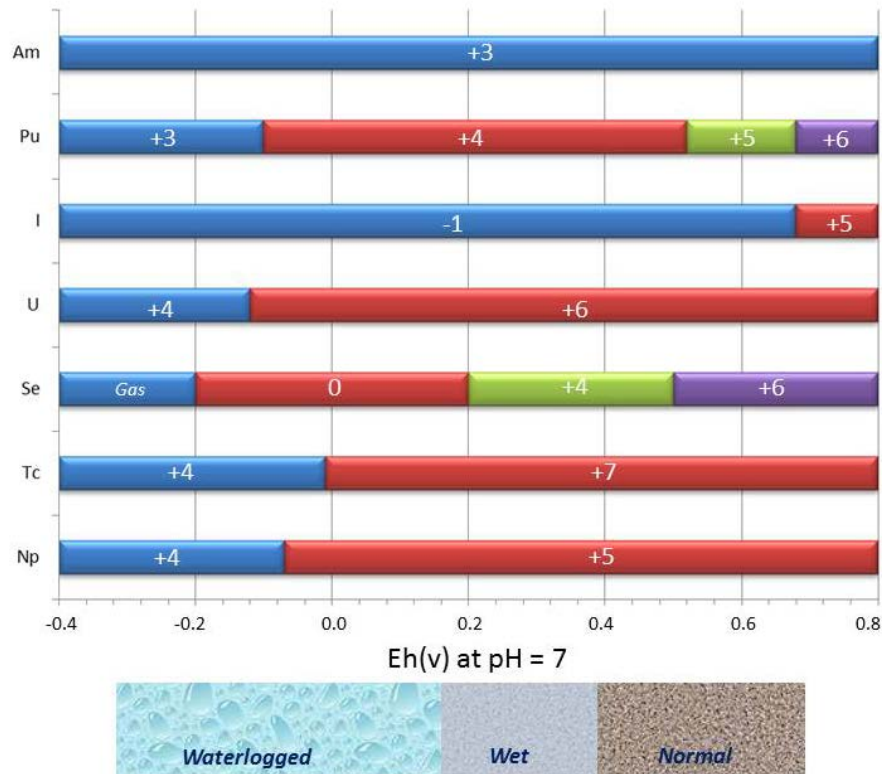


Fig. 4.7 Expected dominant oxidation states of the radionuclides as a function of standard redox potential at pH 7

4.1.5 Special scenario

As mentioned above, the redox potential of the soil influences the speciation of redox sensitive radionuclides, the migration properties of the radionuclide in soil and the uptake of radionuclides into plants. For some radionuclides an increase in mobility in soil and thus bioavailability leads to an increased uptake into plants.

Models of discrete climate states assume that the soil in all climate regions was prepared for agricultural use by drainage and ploughing. Therefore, no large differences in radionuclide behaviour are taken into account for the transition calculations described in section 4.1.3. Only changes of transfer from soil to plant caused by climatic effects are taken into account.

In an additional scenario, the land is initially very humid and very low E_h -values cause high sorption and accumulation of radionuclides in soil particles. Then this land is dried out, the redox potential increases and redox sensitive radionuclides change their speciation and their behaviour. Such processes might lead to an increased contamination of plants grown on this land.

A suitable illustration of the processes related to the changes of the redox potential is the examination of a dry lake or fen bed for agricultural purposes as pasture or ameliorated pasture. In these cases the accumulation of radionuclides in the lake or fen sediment is followed by their release and increasing mobility after agricultural processing of the dry bed of lake or fen. Ploughing of the soil leads to increased supply of oxygen to previous anoxic soil layers causing an increase in redox potential.

4.1.6 Time scale

An important question is the duration of the transition process. The assessment of the time period, when a climate change could occur is difficult and could not be precisely determined using paleoclimatic information. Time scale resolution of paleoclimatic data may not be fine enough to resolve processes taking less than 100 years. Moreover the anthropological influence could accelerate the processes of climate changes.

There are several factors affecting climate. These factors combined cause fluctuations on different time scales (Tab. 4.3). Factors that cause long-term fluctuations in climate include the Earth's orbit about the sun and changes in ocean circulation. Fluctuations on a shorter time scale can be caused by changes in clouds and water vapour, and increased concentration of greenhouse gases due to human activities /ACK 02/.

The time span of the past few million years has been punctuated by many rapid climate transitions, most of them on time scales of centuries to decades or even less. The most detailed information is available for the Younger Dryas-to-Holocene stepwise change around 11 500 years ago, which seems to have occurred over a few decades. The

speed of this change is probably representative of similar but less well-studied climate transitions during the last few hundred thousand years. These include sudden cold events (Heinrich events/stadials), warm events (Interstadials) and the beginning and ending of long warm phases, such as the Eemian interglacial /ADA 99/

An abrupt (sudden) climate change occurs when the climate system is forced to transition to a new state at a rate that is determined by the climate system itself, and which is more rapid than the rate of change of the external forcing.

Timescales of events described as 'abrupt' may vary dramatically. Changes recorded in the climate of Greenland at the end of the Younger Dryas, as measured by ice-cores, imply a sudden warming of +10 °C within a timescale of a few years. Other abrupt changes are the +4 °C on Greenland 11 270 years ago or the abrupt +6 °C warming 22 000 years ago on Antarctica. By contrast, the Paleocene-Eocene Thermal Maximum may have initiated anywhere between a few decades and several thousand years.

Tab. 4.3 Causes of climate fluctuations and approximate time lines /ACK 02/

Cause of Climate Change	Years
Human effects on land surface	1 – 100
Human effects on atmosphere	1 – 100
Volcanism	1 – 1000
Solar variability	10 – 1000
Air-sea interaction	1 – 100 000
Orbital variations	10 000 – 100 000
Plate Tectonics	100 000 – 100 000 000

5 Modelling Exposure during Transitions

To model the exposure during the transition between two climates, the following scenario is considered: the transition from temperate to Mediterranean climate for pasture on a dry bed of lake or fen before and after agricultural processing (ploughing). The pasture grass was chosen because only this allows comparing the activity concentration in plant before and after ploughing.

5.1 Drying of a Lake

In Fig. 5.1 a possible development of drying lakes and fens is represented. A lake exists as long as water inflow into the lake is greater than water loss. The in-coming water balance originates from surface and underground flow from the lake catchments, and atmospheric precipitation on the lake surface. The out-going water balance originates from surface and underground flow from the lake and evaporation from its surface. A negative water balance can cause a dry-out of the lake. The reason for such imbalance can be natural or anthropogenic.

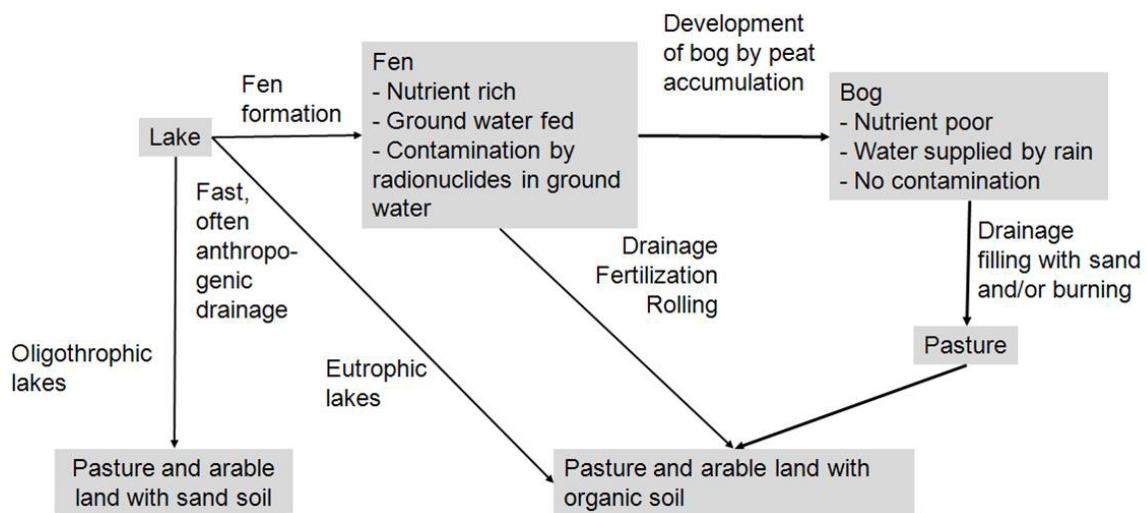


Fig. 5.1 Scheme of the drying of lakes and fens

Productivity or the nutrient richness of lakes is the basis for the trophic concept of classification. It runs from nutrient poor, super clear lakes to those that are nutrient rich and usually have very poor water clarity, i. e. from the oligotrophic lake at one end to the eutrophic lake at the other end /KEV 96/.

Oligotrophic waters: Oligotrophic lakes are clear, deep, cold and located in rocky geography. Sparse weed growth and lack of large algae blooms make these lakes low in nutrients.

Eutrophic waters: Eutrophic lakes are small, shallow, and weedy with cloudy water and a mud basin, usually located in farm land areas where nutrient rich soil is abundant and its run off causes frequent algae blooms.

Mesotrophic waters: Mesotrophic lakes are fertile with moderate weed growth, water clarity is clear to stain with the basin consisting of gravel, rock and sand.

The natural process by which lakes fill in to form dry land takes centuries, or even thousands of years. Human activities can change these lakes in less than a single generation via a process known as cultural eutrophication

To model the impact of climate change and drying of a lake, we use a scenario with an oligotrophic type of lake contaminated by radionuclides from a deep geological repository in groundwater. The soil left in the dried lake basin is assumed to be sandy soil; the corresponding parameters are used in the model scenario.

When an eutrophic lake dries out, the soil left behind has a high organic content, which is very similar to a fen and treated in section 5.2.

5.2 Drying of fen

5.2.1 Sorption of radionuclides on peat soil

Organic matter affects the behaviour of radionuclides in soil. It can accelerate or slow down their migration. The composition of organic matter of soil is very various, including incompletely decomposed plants, soil microorganisms and humus. Humus is a composition of organic compounds of different classes with various structure and molecular weight. The influence of organic matter on migration of radionuclide in soil depends on the interaction with single components of organic matter, on the physical and chemical nature of the radionuclide, and on the soil type. In general, three main characteristics of soil organic matter are important: ability of radionuclide absorption, formation of soluble complexes, and interaction with mineral particles (shielding).

Here a simplified sorption process is assumed. Tab. 5.1 shows the values of the distribution coefficient, K_d , for organic soils (geometrical mean) /IAE 09/.

Tab. 5.1 K_d values for organic soil

Radionuclide	K_d [L/kg]
Am-243	2 500
Cl-36	0.7
Cs-135	270
I-129	32
Nb-94	2 000
Ni-59	1100
Np-237	810
Pa-231	6 600
Pd-107	670
Pu-239	760
Ra-226	1 300
Se-79	1 000
Sn-126	1 600
Tc-99	3,1
Th-230	730
U-238	1 200
Zr-93	3 700

These data were determined for organic, but not for peat soil. This means that K_d for radionuclides in peat soil of fen can be several times higher.

5.2.2 Using fen for agriculture

Fen is of great value for agriculture, when transformed into arable land, pasture or hay-fields. The peat soil, as mentioned above, has very a high content of ash elements and of nitrogen. The mobilisation of the nutrients of organic substances of fen could be reached by reclamation (melioration).

The purpose of reclamation is not only the removal of excess water from the fen, but mostly regulation of water regime of fen soils through the construction of special dams, reservoirs, ponds and reservoirs, to ensure an uninterrupted supply of water to crops during the growing season.

Peat bogs are poor in potassium and phosphorus. Therefore, it is necessary to systematically add potash and phosphate fertilizers. In some cases, especially in the early years of development; the plants in the wetland soils respond very strongly to the mineral nitrogen fertilizers. If no additional fertilizers are added during intensive agricultural use, the depletion of nutrients from the soil leads to decreasing soil quality and yields /SUC 01/.

5.3 Description of the model

In the drying Lake/fen scenario, a groundwater fed sediment is assumed as initial condition. Due to the similarity of the development of a drying lake and a fen, for both scenarios the same conceptual model is used. The contamination of sediment has achieved a balance with the contamination in groundwater defined by radionuclide specific distribution coefficients. After the groundwater table falls and the evaporation increases or the lake/fen is artificially drained, the area is used for agriculture. We conservatively assume that the radionuclides are retained in the soil and do not move with groundwater. Further climate change results in an increased irrigation of the agricultural land with groundwater. The resulting area is used for agriculture by a hypothetical self-sustaining population. The agricultural and food consumption habits of the population adapt to the climate.

5.3.1 General assumptions of the model:

To describe the possible changes of climate, the parameters of existing discrete climate states have been used, see sections 1 and A.1.

- stage 1: Temperate climate, RGW scenario
- stage 2: Mediterranean climate, well scenario

In the case of a drying lake/fen a sand soil parameters are used. In both cases, the area is used for agriculture as soon as the necessary conditions are fulfilled.

The transitions have been modelled for three different transition periods: instantaneous (1 year), 10 years and 100 years and for three values of initial contamination of the soil: 10, 100 and 1 000 Bq/kg. Such initial contaminations occur in our model for a normalised radionuclide concentration in groundwater of 1 Bq/L and K_d -values of 10, 100 and

1 000 L/kg and, which are in a typical range for reducing conditions (c. f. Tab. 4.2). In stage 0 and 1, when the soil is saturated with groundwater, the total inventory of radionuclides in soil is constant after an equilibration time. It is assumed that the soil conditions and the K_d value of each element do not change with time.

Tab. 5.2 Matrix of calculation conditions

Initial contamination of soil	Duration of transition		
	Instantaneous	10 y	100 y
10 Bq/kg	✓	✓	✓
100 Bq/kg	✓	✓	✓
1 000 Bq/kg	✓	✓	✓

In stage 2 the migration of radionuclides in the soil of dried out lakes/fen is driven only by irrigation or precipitation.

5.3.2 Model concept

Fig. 5.2 shows the conceptual model presenting processes for redox sensitive radionuclides. We start with a lake/fen already dried out; the sediment of the former lake/fen has an activity concentration caused by contaminated groundwater.

From stage 1 to stage 2 the transfer factor soil-to-plant increases by one to two orders of magnitude. At the same time, the radionuclide migration in soil decreases, because of longer half-life time of radionuclides in soil. Migration in arid soils is in general significantly slower than in floodplain, lowland or in swamp. The parameters for diffusion and convective transfer are 4 – 5 times lower. For example, for Cs-135 the half-life time in arid soil is 55 – 143 years, for swamp meadow 15 – 21 years /SAN 96/. The following stages of dry lake/fen development have been considered:

- Stage 0: Lake/fen
The radionuclide concentration of the lake sediment is in balance with the concentration in groundwater, which is the only source of radionuclides and determined by the K_d value of each radionuclide. This stage has not been modelled, instead three different initial concentration in soil are assumed, which are, however, correlated to typical K_d -values under reducing conditions (see above).

- Stage 1: Dried Lake/fen bed: the groundwater level is low, but the soil is humid enough to be used as pasture
 After a period of drying out, the lake bed can be used as pasture, if the soil is still humid enough for the growth of grass and solid enough for domestic animals. Radionuclides are in reduced, immobile state corresponding to a low uptake from the soil solution into the plant (grass).
- Stage 2: Agricultural processing.
 The lake continues to dry; the moisture content falls below the wilting point. Under dry and therewith aerated conditions radionuclides become oxidised and most of them therewith more mobile. This is further facilitated by enrichment of soil with oxygen by ploughing.

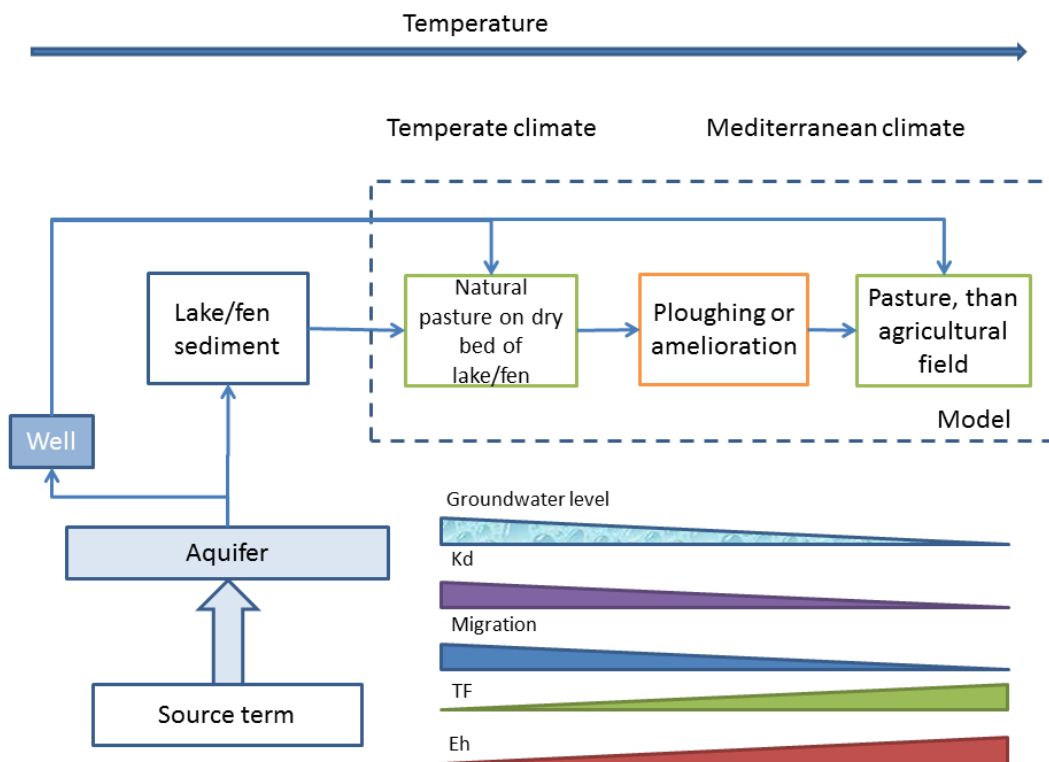


Fig. 5.2 Conceptual model for estimating the radiation exposure to man in case of agricultural use of dry lake sediment

Tab. 5.3 Characteristics of considered stages of dried-out lake/fen, chemical speciation of radionuclides

Parameter	Stage 0: Lake/fen	Stage 1: dried lake/fen bed	Stage 2 : agricultural processing
Characterisation	Temperate climate Fully saturated sediment Radionuclide accumulation in sediment	Temperate climate Rising GW, Pasture Initial soil contamination from stage 0, $C_i^s(0)$	Mediterranean climate Ploughing/harrowing Pasture Irrigation Migration Soil contamination is a sum of initial contamination from stage 1 and contamination due to irrigation
Radionuclide speciation	Reduced states	Reduced states	Oxidised states
Transfer factor		low	high
Radionuclide	immobile	immobile	mobile
Migration	no	no	yes

5.3.3 Implementation of the model

The contamination of lake sediment through rising groundwater (initial condition) is described by:

$$C_i^s(0) = C_i^{GW} \times Kd_i \quad (5.1)$$

with:

C_i^{GW} activity concentration of radionuclide i in groundwater [Bq/L]

C_i^s activity concentration of radionuclide i in soil [Bq/kg]

Kd_i distribution coefficient for radionuclide i under reduced conditions [L/kg]

For stage 2 the contamination of plants due to irrigation is formulated as:

$$C_i^p(t) = C_i^s(t) \times TF_i(t) \quad (5.2)$$

Where $C_i^s(t) = \frac{C_i^{GW}}{(\lambda_i + M_i(t))} \times (1 - e^{-(\lambda_i + M_i(t))t}) + C_i^s(0) \times e^{-(\lambda_i + M_i(t))t}$

with:

λ_i decay constant of radionuclide i [1/y]

M_i migration rate for radionuclide i in soil for Mediterranean climate [1/y]

6 Results

6.1 Lake

In order to observe the influence of the oxidation of redox-sensitive radionuclides on transfer to plants, a comparison of pasture grass contamination before (stage 1) and after (stage 2) the beginning of agricultural development of a dry lake bed was made. The pasture has been irrigated with contaminated groundwater for the whole time, before and after agricultural development.

The first calculation has been performed for sudden transitions and three values of initial contamination of soil. Tab. 6.1 shows the corresponding parameters. The time dependence of Se-79, Tc-99, Np-237 and U-238 activity concentrations in pasture grass during sudden transitions and initial sediment activity concentrations of 10, 100 and 1000 Bq/kg is shown in Fig. 6.1 to Fig. 6.4.

Tab. 6.1 Parameters used for calculation

Parameter	Transition time [y]	Temperate climate				Agricultural processing	Mediterranean climate				Function
		Value					Value				
		Se	Tc	U	Np	Se	Tc	U	Np		
Transfer factor soil – plant [Bq kg ⁻¹ /Bq kg ⁻¹]	1	0.011	26.4	0.0264	0.01056	2.2	170	0.00792	0.0528	Step	
	10									Linear	
	10									Linear	
Irrigation, [L m ⁻¹ y ⁻¹]		-				600 L/y m ²				Constant	
Migration [m ⁻¹]		-				0.036	0.17	0.0053	0.0097	Constant	
Initial contamination [Bq/kg]		10, 100, 1000				-					

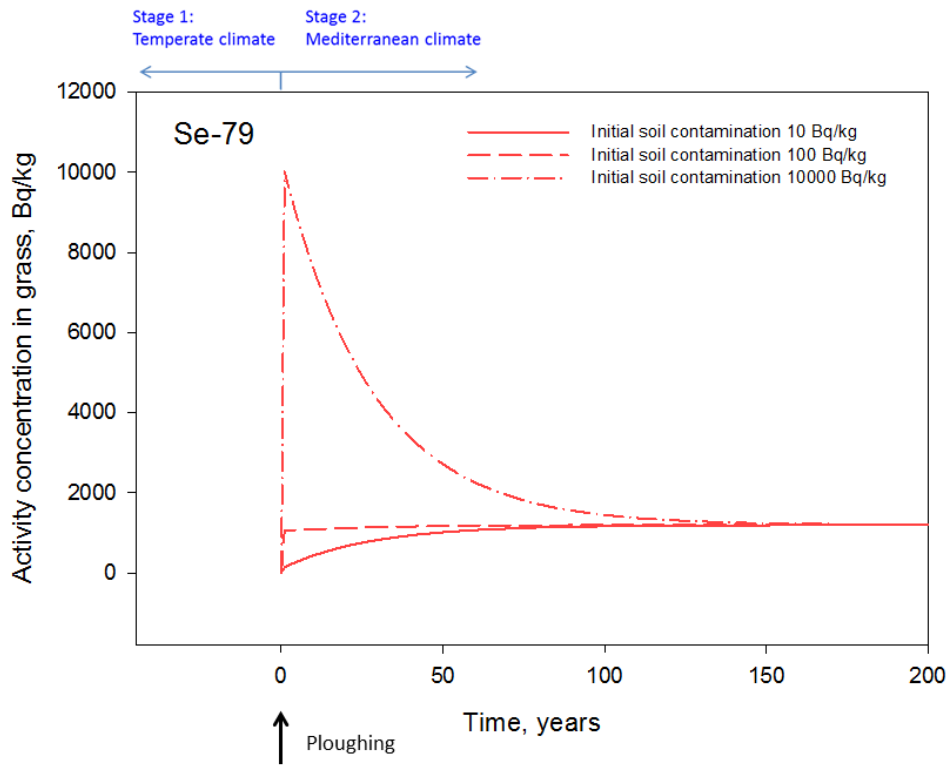


Fig. 6.1 Activity concentration of Se-79 in pasture grass; sudden transition; full irrigation

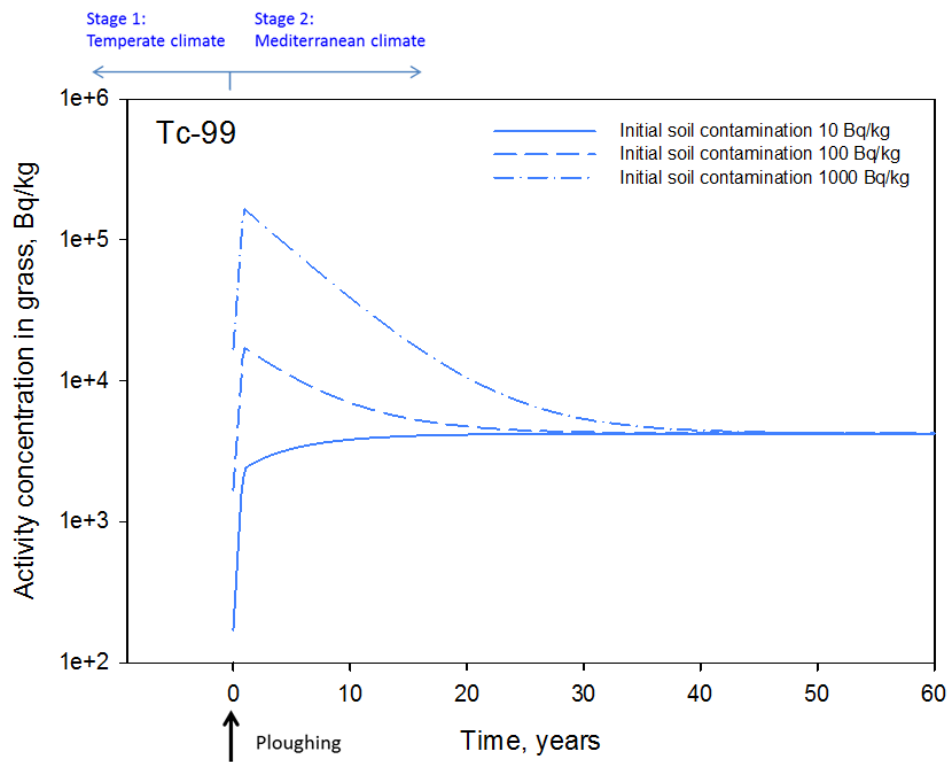


Fig. 6.2 Activity concentration of Tc-99 in pasture grass: sudden transition, full irrigation

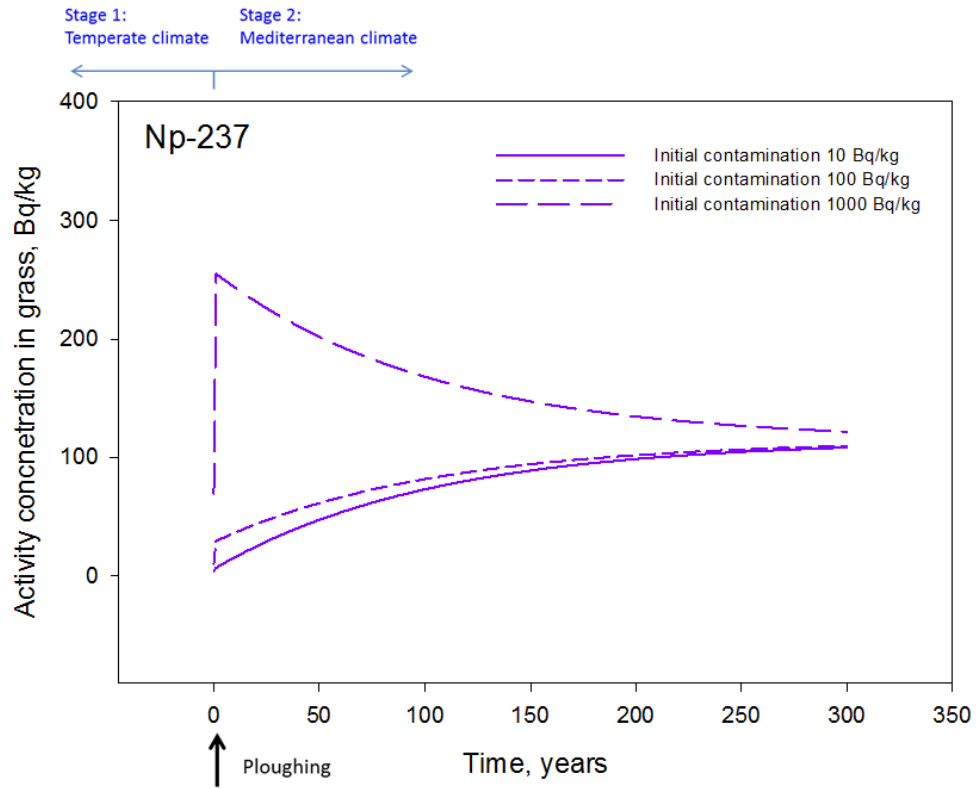


Fig. 6.3 Activity concentrations of Np-237 in pasture grass: sudden transition, full irrigation

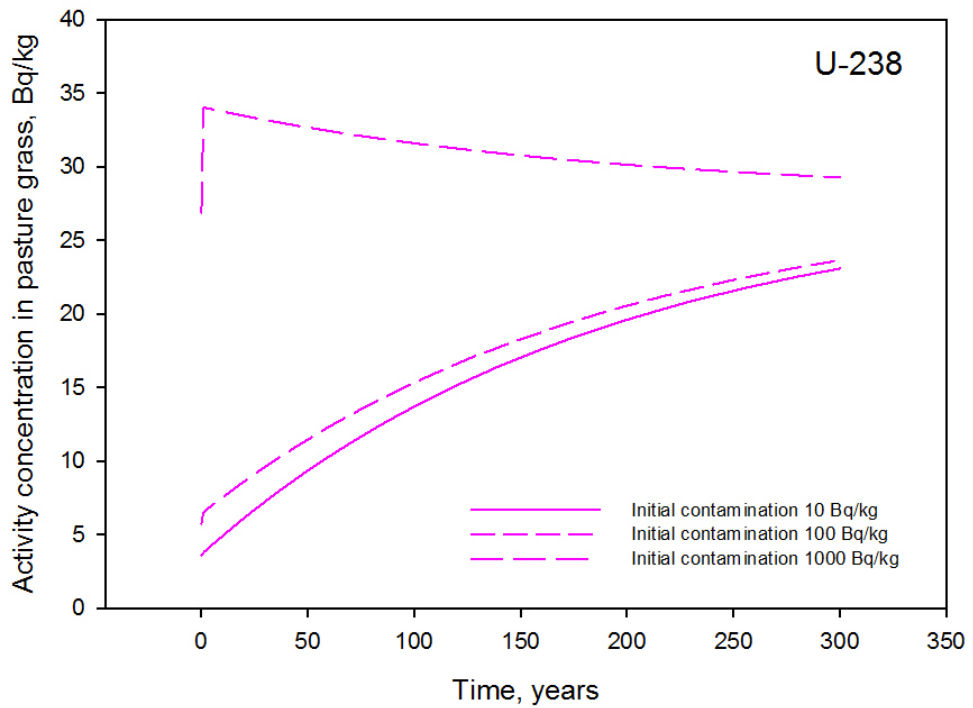


Fig. 6.4 Activity concentrations of U-238 in pasture grass: sudden transition, full irrigation

For redox sensitive radionuclides three processes play a crucial role in the contamination of pasture grass in these scenarios: the increase of transfer of radionuclides from soil to grass caused by a change of the radionuclide redox state, the initial contamination of soil due to rising GW and the additional contamination of soil due to irrigation. During the transition, the contamination of grass with such nuclides as Tc-99 and Se-79 can increase by a factor of 1 000. In case of high initial contamination, in the beginning migration is negligible and dramatically increasing transfer factors lead to high activity concentrations in pasture grass. For all scenarios the contamination of pasture grass adjust to levels similar to the corresponding discrete climate state due to the increasing role of radionuclide migration and contaminated irrigation water.

For the assessment of potential exposures to populations, exposure peaks after changes in the environment are a concern. The scenarios presented above show that for low initial sediment contamination, 10 and 100 Bq/kg, the activity concentration of pasture grass does not show a peak, except for the 100 Bq/kg contaminations with Tc-99 (Fig. 6.2). With high pre-contaminations of soil with 1 000 Bq/kg, peaks can be observed only when sudden transitions are assumed.

Very similar effects may occur with assumed transition times of 10 years, but in these cases the activity concentration in grass increases temporarily and reaches lower maximum values compared to the sudden transition scenarios. Fig. 6.5 to Fig. 6.8 show the activity concentration development in pasture grass, if the transition from temperate to Mediterranean climate takes 10 years.

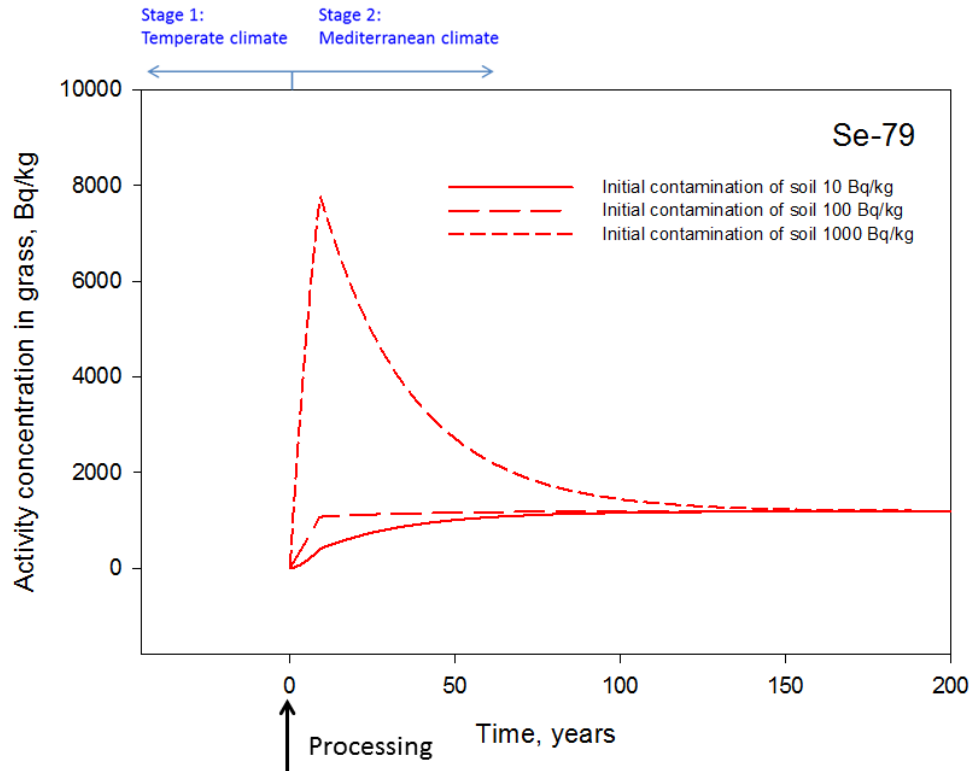


Fig. 6.5 Activity concentration of Se-79 in pasture grass; 10 years transition; full irrigation

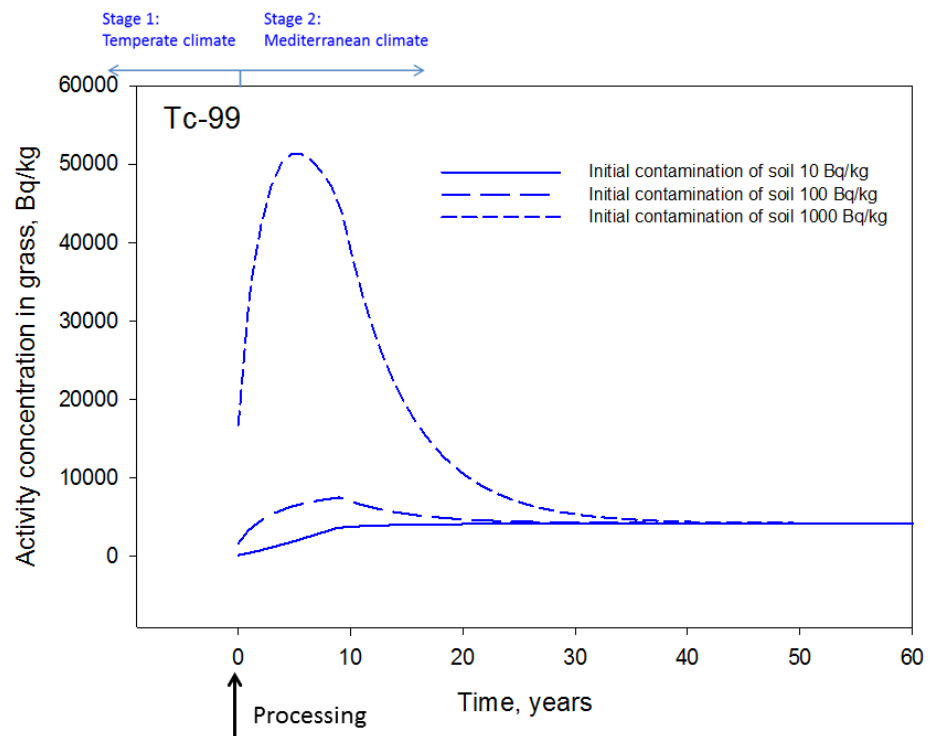


Fig. 6.6 Activity concentration of Tc-99 in pasture grass; 10 years transition; full irrigation

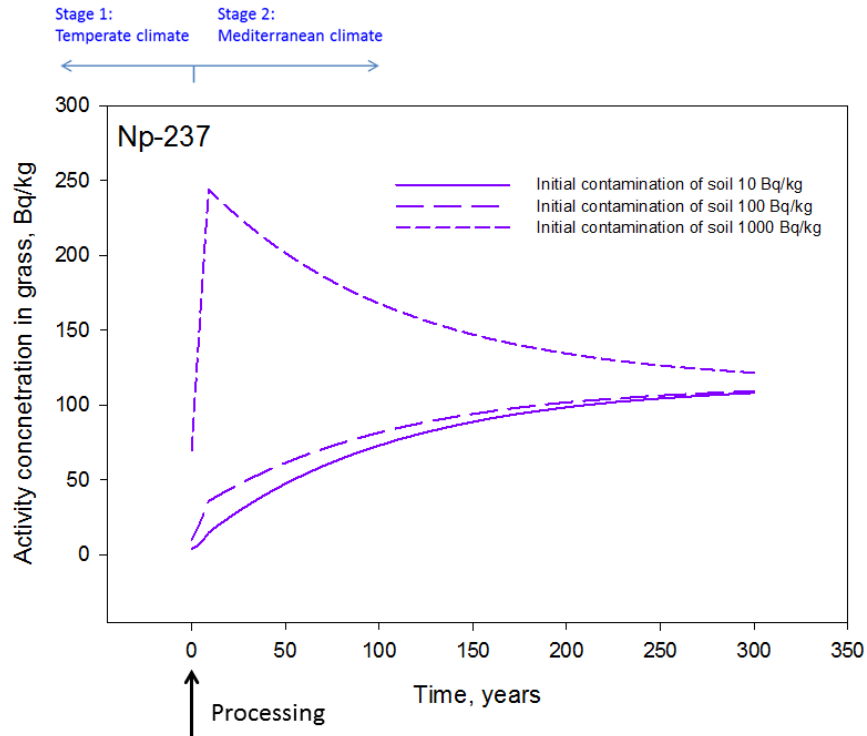


Fig. 6.7 Activity concentration of Np-237 in pasture grass; 10 years transition; full irrigation

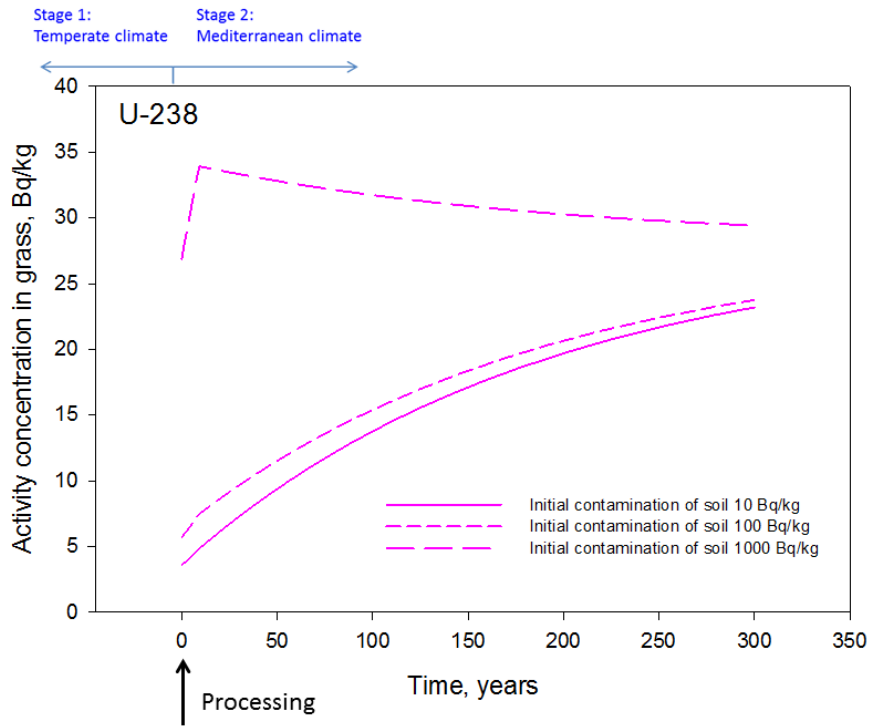


Fig. 6.8 Activity concentration of U-238 in pasture grass; 10 years transition; full irrigation

Fig. 6.9 to Fig. 6.12 present the time course of activity concentration in pasture grass, if the transition from temperate to Mediterranean climate takes 100 years. Gradual drying of a lake or fen over 100 years does not show a dramatic increase or peak in plant contamination for low initial contaminations. For the high initial concentration scenarios, less pronounced peaks and maximum concentration values compared to lower transition times develop. A smooth transition to higher or lower contamination because of irrigation water as an additional contamination source can be observed.

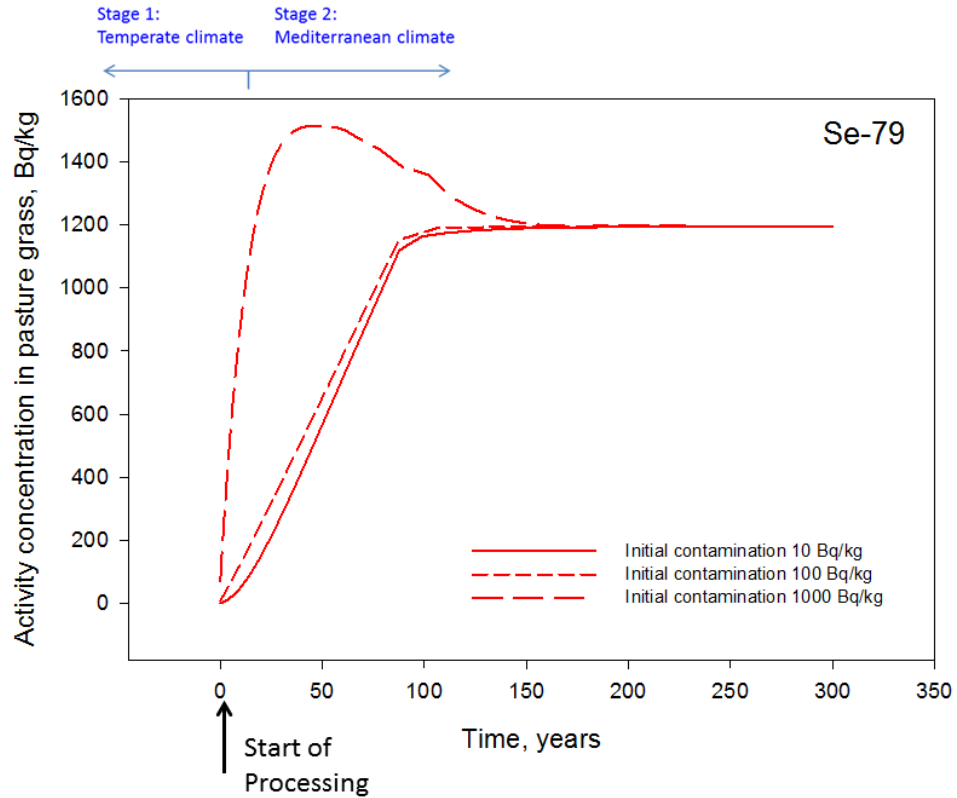


Fig. 6.9 Se-79 activity concentrations in pasture grass for three values of initial concentration, 10, 100, and 1000 Bq/kg, and transition time of 100 years

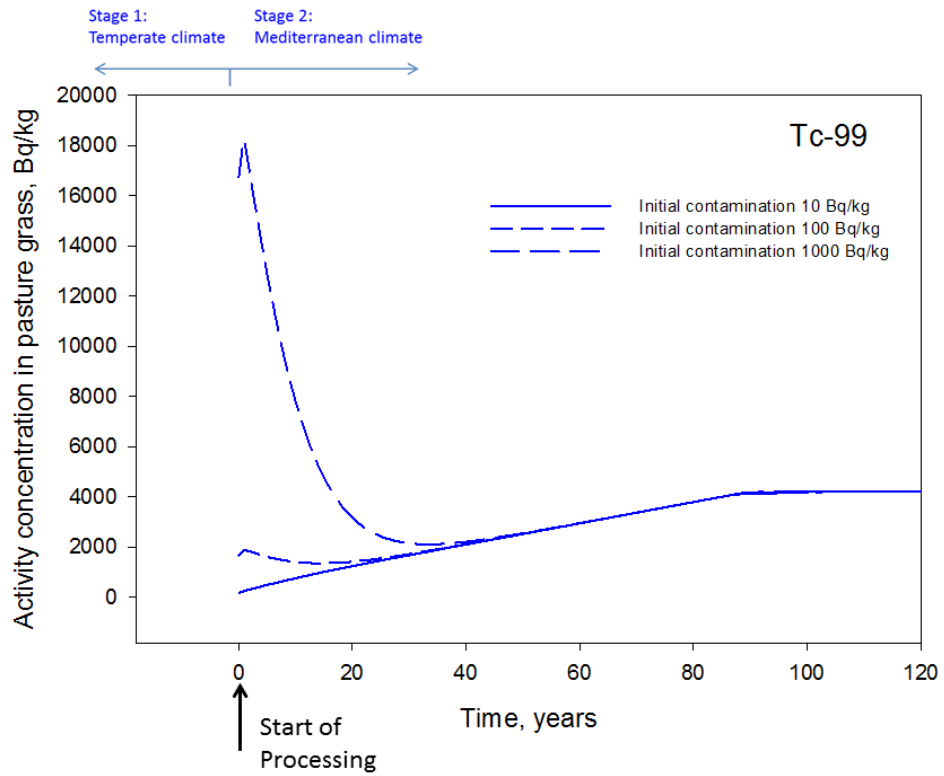


Fig. 6.10 Tc-99 activity concentrations in pasture grass for three values of initial concentration, 10, 100, and 1000 Bq/kg; transition time of 100 years

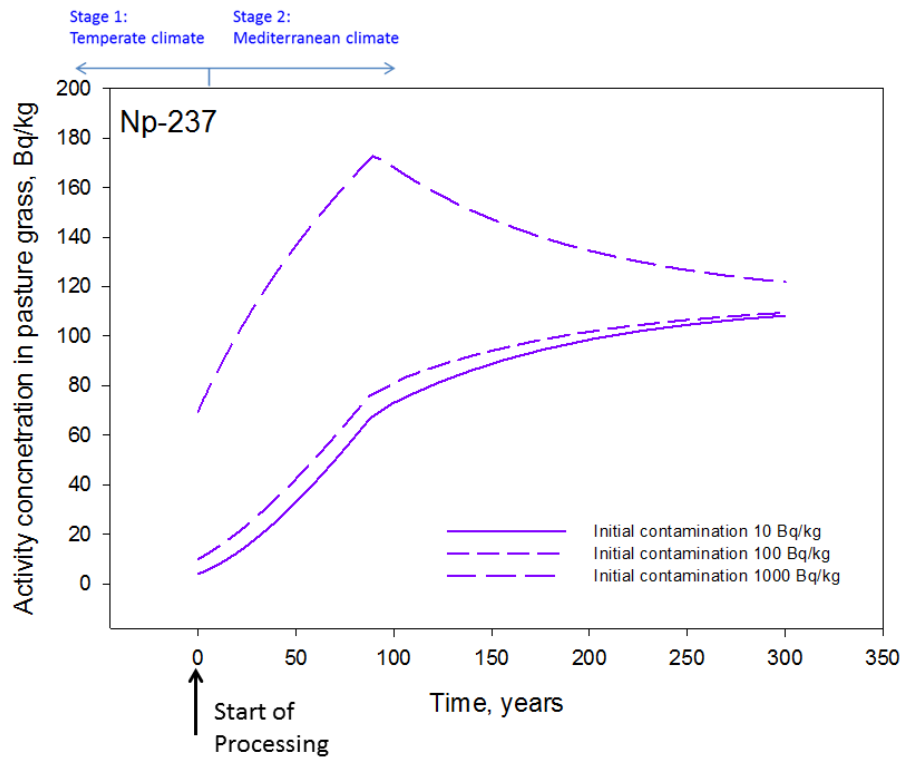


Fig. 6.11 Np-237 activity concentrations in pasture grass for three values of initial concentration, 10, 100, and 1000 Bq/kg; transition time of 100 years

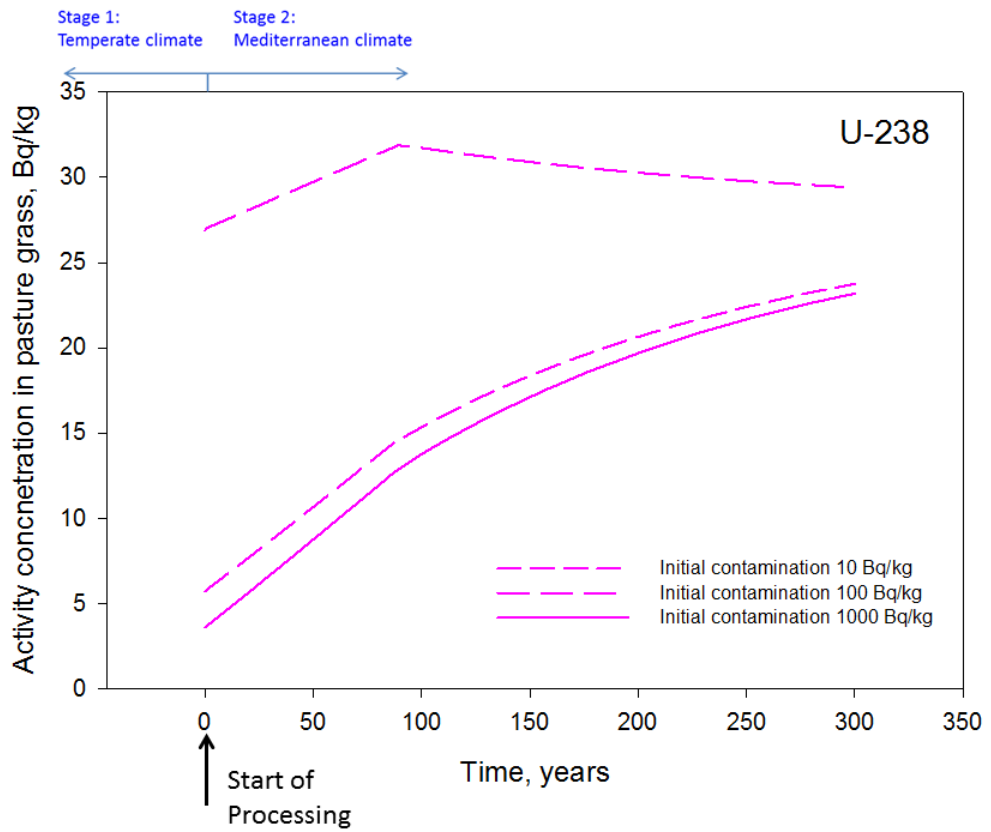


Fig. 6.12 U-238 activity concentrations in pasture grass for three values of initial concentration, 10, 100, and 1 000 Bq/kg, and transition time of 100 years

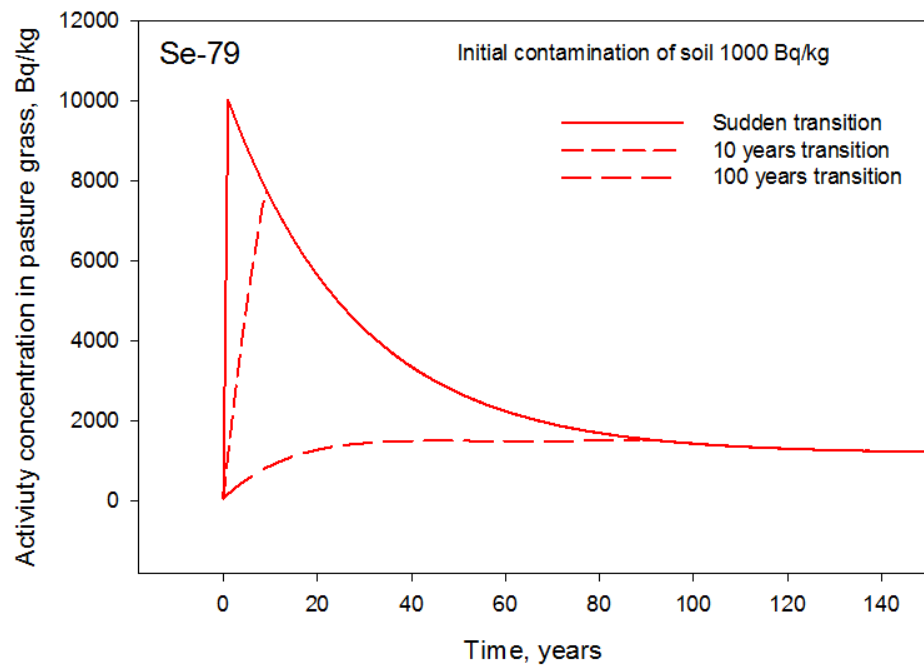


Fig. 6.13 Influence of transition time on the behaviour of activity concentration of Se-79 in pasture grass under full irrigation conditions

As shown in Fig. 6.13 and Fig. 6.14 the long-time transitions smooth the irregularities in the behaviour of the radionuclides. The peaks developing after start of the agricultural processing of the soil can only be observed in case of high soil pre-contamination. Tc-99 shows the most pronounced effects of a climate transition from temperate to Mediterranean conditions.

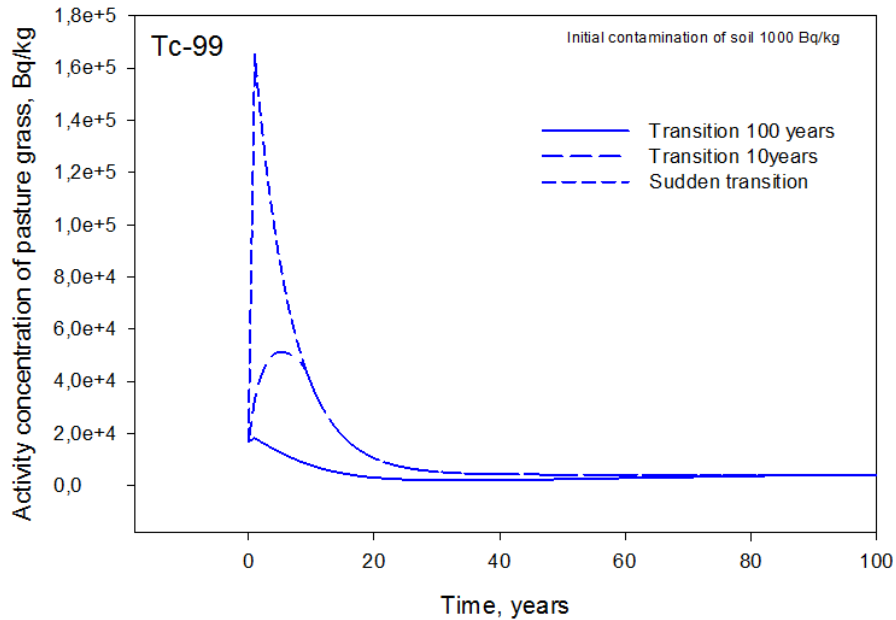


Fig. 6.14 Influence of transition time on the behaviour of activity concentration of Tc-99 in pasture grass under full irrigation conditions

6.2 Fen

The behaviour of radionuclides in dried-out fen is very similar to a dried-out lake, but the initial activity concentration in soil could be much higher for some of them, due to potentially high K_d values in organic and peat soils. /KUD 96/ reported that *in situ* measurements of radiocesium activities in flooded peat bog results in K_d values in the range $10^2 - 10^3$ L/kg.

6.2.1 Fen for agricultural use

The scarcity of radioecological data, such as transfer factors, migration rates etc. for radionuclides in peat soil, especially for redox sensitive radionuclides in available literature, does not permit to perform the calculation for fen. We can assume, that the calculation for a dried out lake with a high initial contamination of 1 000 Bq/kg (Fig. 6.13 and

Fig. 6.14) can be used to approximate the conditions for a dried out fen (cf. discussion in section 5.3.1).

Another important, but highly uncertain factor is the leaching of radionuclides in peat. We do not have any information about the speed of accumulation, saturation and leaching of radionuclides in fen sediment humic substances (HS) contained in peat form stable compounds with radionuclides and can be used as a powerful geochemical barrier. In addition, the HS show a high resistance to chemical and thermal destruction. However, under conditions of global climate fluctuation, structural parameters of the mineral matrix and their ability to absorb toxicants may change. /RAZ 11/.

When the fen is drained artificially to create agricultural land, this may happen during a short, almost instantaneous, time frame. In this a case, the drainage system will be built in a way that the groundwater sinks only to a certain depth in order to maintain a water balance useful for agriculture.

Drainage is the main danger for peats close to nature, as drained peat shrinks and the peat soil surface collapses /SOI 12/. Oxic conditions in peat soils foster the decomposition of the organic matter and mineralization of the peat. Nutrients and green-house gases like carbon dioxide (CO₂) are released and peat soils change from a carbon sink to a carbon source. Climate change can also lead to desiccation and destruction of fen soils. Intensively used peat soils can release up to 40 tons CO₂ per hectare and year. If not managed properly, the organic and nutrient content of former peat soils decreases rapidly after reclamation and the soils deplete over relatively short time frames, resulting in decreasing agricultural yields.

6.2.2 Fen peat as fuel

For more than 1,000 years, peat has been used as solid fuel for heating and for production of electricity, as medicine and fertilizer. Some publications dedicated to radionuclide concentration in fuels and ash products from peat-fired power plants appeared after Chernobyl accident, /ERL 95/, /HED 92/, /ORG 05/, but are relatively rare. Most of them are from Scandinavian countries, because of wide use of peat as fuel in this part of the world.

The peat burns in suspension at about 1 000 – 1 100 °C. Approximately 5 – 10 % of total ash produced stays in the furnace as “bottom ash” while the remaining 90 – 95 %

passes into the gas stream as “fly ash”. In case of the industrial use of peat fuel, only a small fraction of fuel gases containing small quantities of radionuclides in gaseous form passes through the grit arrestors and is discharged through the stack to the atmosphere /ORG 05/. The authors of /ERL 95/, /HED 92/, /ORG 05/ presented the measurements of activity concentration of NORM and radionuclides from Chernobyl and global fall-out in peat fuel and ash from peat-fired power plants. Tab. 6.2 shows activity concentrations of U-238 and Cs-137 in raw material, fly ash and bottom ash (from /ORG 05/). Depending on the volatility of the element in question and the temperature of the burning process, the concentration of the element in the gaseous phase, fly ash and bottom ash may change drastically.

Tab. 6.2 Activity concentration of U-series radionuclides and Cs-137 (in Bq/kg, dry weight)

Sample type	U-238	Th-234	Ra-226	Cs-137
Raw material	2.8±0.4	4.3±0.6	2.6±0.4	4.2±0.1
Fly ash	301.2±13.9	306.3±5.8	28.9±1.4	67.5±1.0
Bottom ash	77.1±13.8	33.0±5.8	14.9±1.4	4.8±0.1

The results show high activity concentration in fly ash while the bottom ash is relatively low contaminated.

/RON 01/ investigated the volatility of trace elements in a coal combustor. The authors distinguished for the considered trace elements between three groups:

- Group 1: elements are volatile and emitted almost totally in the vapour phase
- Group 2: elements are vaporized at intermediate temperature and are emitted mostly in fly ash
- Group 3: Elements hardly vaporized and so equally distributed between bottom ash and fly ashes

Se-79 may be located in group 1 and 2. We can assume, that Tc-99, highly soluble as Tc_2O_7 could also be emitted in the vapour phase (group 1), or it may react with CO and produce very volatile decacarbonyl, $Tc_2(CO)_{10}$. Ash from the combustion of peat is the complex fertilizer containing phosphorus, potassium, calcium and many trace elements (magnesium, boron, sulphur, etc.) necessary for plants. Moreover, it contains potassium and phosphorus, what are readily available for plants.

Peat soil of fen produces 15 % of ash. We assume that the ash of peat-fired power plant or of private furnace contains 100 % of nuclides considered. By initial contamination of peat soil of 10 Bq/kg burning of 1 kg of contaminated peat will produce all 10 Bq activities in 150 g of ash (Tab. 6.3).

- 1) It is assumed that the whole ash is bottom ash. For fertilising about 150 g of ash for 1 m² per application is needed, i. e. by each fertilisation about 10 Bq/m² of additional activity is added to the soil. The ash amends into the soil only once or twice a year and it means that by these hypothetical conditions the soil contamination due to ash is relatively low in comparison with contamination due to irrigation with contaminated water (600 L/m²).
- 2) It is further assumed that the whole ash is fly ash and the whole activity passes with a gas stream depositing around the stack on the ground. To calculate the fallout from 1 kg contaminated peat the following conditions have been assumed: maximum of long-time propagation factor for 20 m emission height and main wind direction in 30° sector has a value of 7·10⁻⁵ sec/m³ /BMU 05/; release rates assumed as 3·10⁻⁴ Bq/sec (1 kg of peat burns about 10 hours). If the deposition speed is 1 cm/sec, we will get additional contamination in soil about 6·10⁻³ Bq/m² per years in main wind direction, which can be neglected, compared to the input from irrigation.

Tab. 6.3 Additional contaminations to agricultural soil for using bottom ash from burned peat as fertiliser. The data from Tab. 6.2 are used for the calculation of the concentrations in bottom ash

Parameter	Unit	Bottom ash	Fly ash
Activity in ash	[Bq]	10	10
Weight of ash	[g]	150	150
Fertilisation per application	[g/m ²]	150	-
Max long-time propagation factor for 20 m emission height, main wind direction in 30° sector	[sec/m ³]	-	7·10 ⁻⁵
Release rates (1 kg of peat brick burns about 10 hours)	[Bq/sec]	-	3·10 ⁻⁴
Speed of fallout	[cm/sec]	-	1
Additional contamination of soil	[Bq/m ²]	10	6·10 ⁻³

6.3 Calculation of the Biosphere Dose Conversion Factor (BDCF) for transition between two climates

With an increase of temperature and decrease of groundwater level, the dry lake ground may be used differently. Fig. 6.15 shows schematically the potential agricultural use of a dry lake for different time periods.

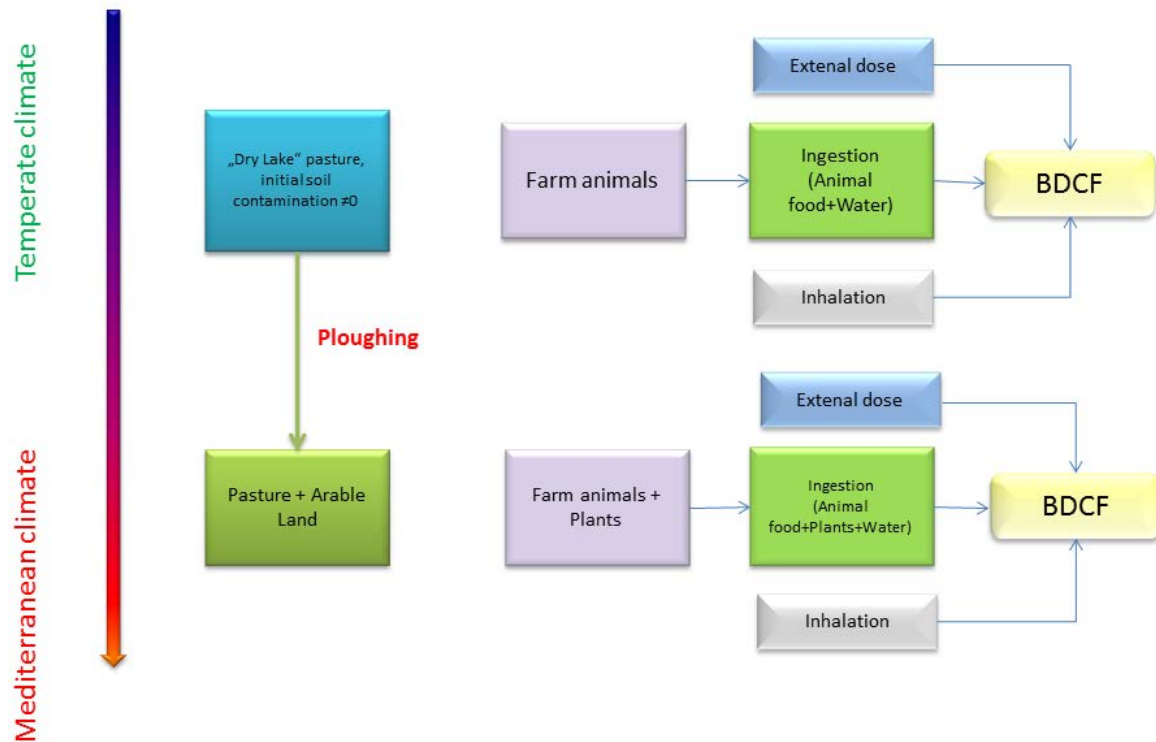


Fig. 6.15 Possible use of a contaminated dry lake

In order to understand how the transition from temperate to Mediterranean climate and following changes in contamination of pasture grass influence the exposure to men, the corresponding BDCFs have been calculated. Hypothetically, one could imagine a population which provides itself with the necessary food using a large dried-up lake as agricultural holding. The use of this lake ground depends on climate change, starting with a grazing area, then ploughing and using the arable land. Corresponding to agricultural use, the contribution of exposure pathways changes so that there is a need to predict a likely future exposure from each pathway and compare it with exposure calculated for discrete climate states.

For the first period (stage 1), assuming a dry lake pasture pre-contaminated by groundwater with only animal food production, calculations have been made using pa-

rameters corresponding to temperate climate. For the second period (stage 2) with Mediterranean climate – including the transition period – ploughing, cultivation of cereals, maize etc. as well as animal and plant food production has been assumed. In addition to this, the other agricultural lands used by the hypothetical population are cultivated under the same model relevant conditions as the former lake/fen bed. Fig. 6.16 demonstrates BDCFs for the time before, during and after transition.

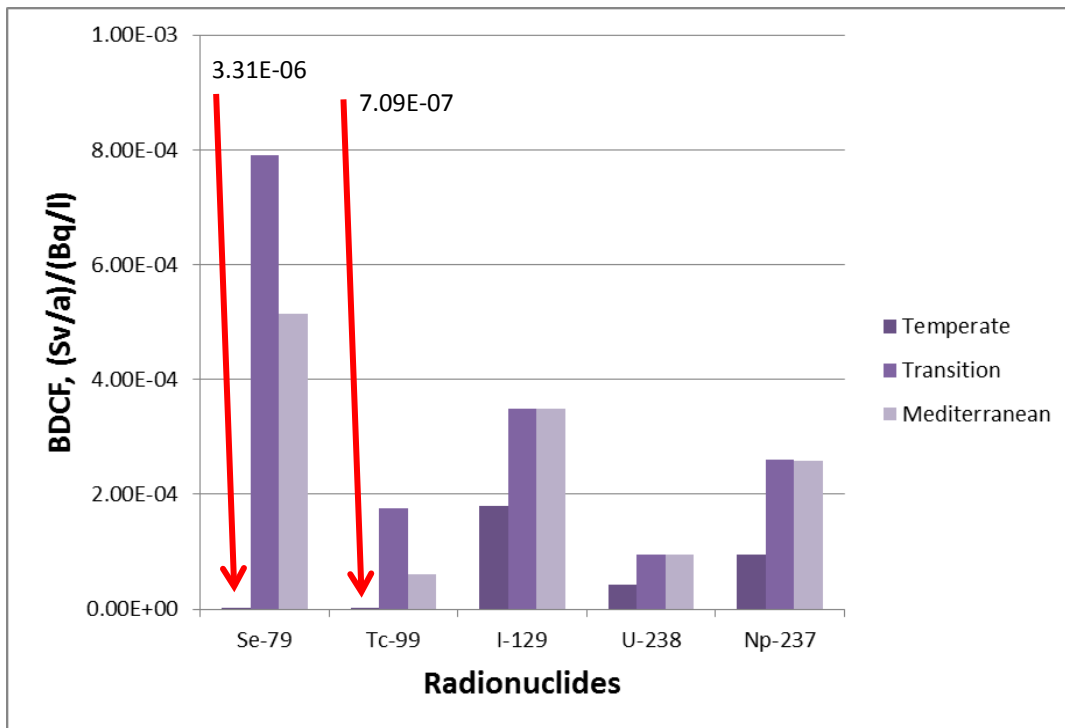


Fig. 6.16 BDCF calculated for the time before (Temperate), during (Transition), and after transition (Mediterranean)

For the transition state the peak activity concentrations in grass after an initial soil contamination of 1 000 Bq/kg and a sudden transition described in section 6.1 are used. It can be seen that only Se-79 and Tc-99 show a relevant increase of exposure during the transition phase compared to the BDCF before and after the transition.

It should be noted that depending on the radionuclide, different exposure pathways dominate the total exposure (Fig. 3.8 and Fig. 3.9). For most of radionuclides the dominant pathway is ingestion of drinking water, fruits or vegetables (see Tab. 6.4). These pathways are independent of the contamination of pasture grass which explains that the BDCFs for the transition and Mediterranean state do not differ for the radionuclides U-238 and Np-237. Milk plays a certain role in the total exposure of Cs-135 and I-129,

but these radionuclides are not assumed to change their speciation during the climate transition Temperate-Mediterranean.

In the case of Se-79, the contaminated pasture grass causes an increase in BDCF due to the relatively high importance of beef and milk for the exposure to this radionuclide. For Tc-99 the high peak of activity concentration in grass for this scenario (Fig. 6.2) results only in a moderate increase of exposure during the transition compared to the discrete Mediterranean BDCF, since the exposure pathways involving grass only play a negligible role in the total exposure (Fig. 3.8).

Despite of relatively conservative assumptions (e. g. instantaneous transition, high pre-contamination) the transitions play a role only for a few radionuclides. The highest impact for Se-79 and Tc-99 is only of a factor 3.

Tab. 6.4 Dominant exposure pathways for selected radionuclides

Radionuclide in abstracted water	Dominant exposure pathways
Cl-36	fruit, eggs, drinking water
Se-79	fruit, beef
Tc-99	fruit, drinking water, green vegetables
I-129	fruit, drinking water, green vegetables
Np-237+	fruit, drinking water
Th-229	dust inhalation, fruit, drinking water
Pu-239	dust inhalation, fruit, drinking water
U-238	fruit, drinking water, dust inhalation
Th-230	dust inhalation, fruit, drinking water
Ra-226+	fruit, external irradiation, drinking water

6.4 Desertification

Desertification is land degradation in arid, semi-arid and dry sub-humid areas resulting from various factors, including climatic variation and human activities /UNC 92/. Manifestations of desertification include accelerated soil erosion by wind and water, increasing salinization of soil and near-surface groundwater supplies, a reduction in species diversity and plant biomass, and reduction in the overall productivity of arid ecosystems, with an attendant impoverishment of the human community dependent of this

ecosystem. A combination of climatic stress and arid environment degradation can lead in turn to extreme social disruption, migrations and famine /WIL 96/.

Climate has a major impact on arid soils, vegetation, water resources and human land use. Arid soils are inherently vulnerable to desertification processes, since they have already low levels of biological activity, organic matter and aggregate stability. The sparser the plants cover, the greater the susceptibility of arid soils to accelerated erosion by wind and water /WIL 96/.

The process of reducing and cessation of agricultural land use leads, on the one hand, to omitting of major exposure pathways such as ingestion, and corresponding reduction of total BDCF. On the other hand, the inhalation pathway becomes more important especially during dust storms.

Climate variability affects also the live and traditional farming of populations using arid environments. Nomads in arid environments have a great dependence on pastoralism, as well as being hunters and gatherers who survive by harvesting natural resources. Nomadism occurs mostly in marginal regions bordering deserts that are characterised by marked rainfall seasonality and tendency towards drought, creating a precarious balance between livestock and resources /WIL 96/. Fig. 6.17 shows a marked seasonality and a tendency towards drought limits the productive capacity of the land, creating a precarious balance between livestock and resources /DIX 90/.

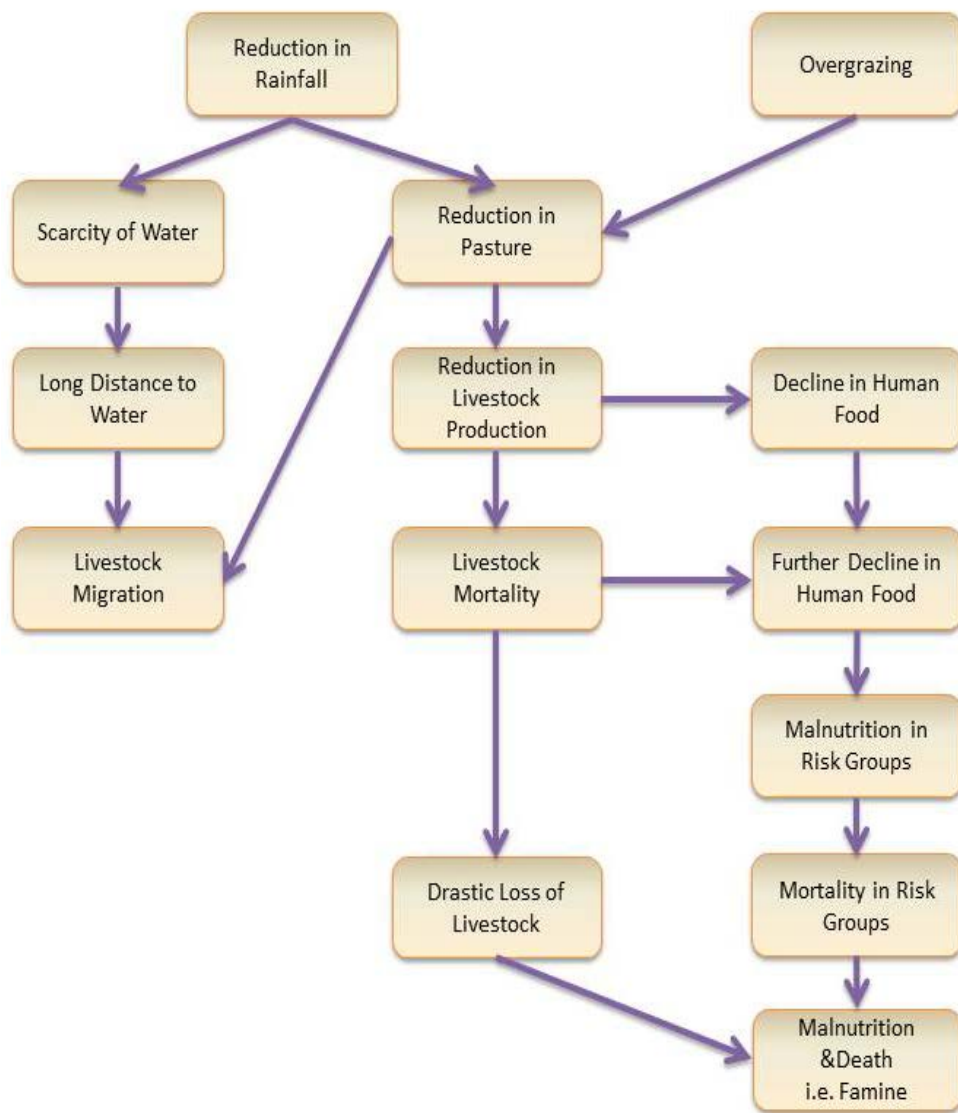


Fig. 6.17 Marked seasonality and a tendency towards drought limits the productive capacity of the land, creating a precarious balance between livestock and resources /DIX 90/

7 Summary and conclusions

Changes in climate can significantly impact biosphere processes and exposure pathways of radionuclides, which need to be addressed in a safety case for radioactive waste repositories. The work presented here is a continuation of the study described in /NOS 08/. In order to quantify the impacts biosphere models are developed and biosphere dose conversion factors (BDCFs) are calculated. The approach considers a normalised radionuclide concentration in a surface-near aquifer, from where the radionuclides enter the biosphere. There are two scenarios assumed in the model used in this work: groundwater raises to the soils used for agriculture (RGW scenario) or the soils are contaminated by irrigation with groundwater (well scenario). Both of these possibilities were treated in /NOS 08/ for six discrete climate states, for which representative analogue climate stations were proposed.

In the work presented here, in a first step a critical justification of the climate states covering the potential future climate evolution in Northern Germany is performed. For this purpose, data from the BIOCLIM project was used to select possible future climate states and their potential sequence. When BIOCLIM and IPCC forecasts for temperature and precipitation developments to warmer climates are used on current climate data sets from northern Germany, a development to a Mediterranean dry summer, wet winter climate data can be seen. Three additional climate states are selected to comprehensively cover colder and warmer climates with different amounts of precipitation, which might develop in the far future. Particularly the calculations for the subtropical reference region Valladolid, showed slightly higher BDCFs compared to the climate stations considered in /NOS 08/.

In the second step a global uncertainty and sensitivity analysis is performed, varying a broad range of parameters of the biosphere models for the temperate and the Mediterranean climate. The uncertainty analysis, namely the spread of the BDCF distributions, seems to indicate, that the impact of uncertainties in the parameters is comparable or even higher for some radionuclides than the impact of different climates as calculated for the nine reference climate stations. However, the uncertainty analysis can be regarded as a first estimation. More emphasis to derive probability density functions (pdfs) for the parameters and an approach for the treatment of correlations between the parameters is needed. The results of the sensitivity analysis agree well with the observations from the deterministic calculations, i. e. the most important exposure path-

ways and the respective model parameters observed in the deterministic calculations showed up as the most sensitive ones in the sensitivity analysis.

In a further step, we tried to quantify the impact of climate transitions, i. e. whether processes occurring during climate transition might lead to an increased release or accumulation of radionuclides, which in turn could increase radiation exposures more than the effects calculated for discrete climate states. The evaluation, which was not meant to be comprehensive at this stage, aimed to identify such processes. In our analysis we found the most relevant processes during the transition to warmer climates. Real peaks of the BDCFs compared to the discrete climate states are mainly expected for redox sensitive radionuclides, which may change their chemical speciation under drier, more oxidised conditions and thereby become more available to plants. The two scenarios drying of a lake and drying of a fen have been chosen to investigate such transition states.

In order to quantify the effects for the transition, which are a sequence of quite complex processes, we tried to keep the models as simple as possible. The model calculations show that the contamination of plants could significantly increase due to an increasing mobility of redox-sensitive radionuclides. This effect was observed by simulating changes in activity concentrations in grass grown on the bed of a dried-out lake and a dried-out fen, respectively. An effect on the total BDCF could only be observed for the redox sensitive radionuclides Se-79 and Tc-99, where the exposure pathways related to the contamination of soils are highly contribute to the BDCF. For these calculations high pre-contamination of the soil and a sudden transition between the redox states are assumed. With lower pre-contamination of the soil, the effects of the change in speciation on the exposure decrease since other, soil independent pathways like foliar uptake of radionuclides from irrigation water or use as drinking water increase in relative importance. As the duration of the described transition processes is difficult to judge, the calculations were made assuming three different time frames for the transition period: 1, 10, and 100 years, respectively. Long time frames tend to smooth out peaks and reduce maxima.

The investigations presented here tried to estimate the impact of future climates and climate transition on processes in the biosphere and resulting potential radiation exposure to mankind by the use of generic, stylised models. The bandwidths covered by calculations for the different discrete climate states are in a similar range as the bandwidths derived from parameter uncertainties. The models also allowed calculating tran-

sition states for climate changes, which are of complex nature. The results indicate that climate transitions could cause radiation exposures increased compared to discrete climate states but not more than a factor of ten. Relatively high accumulations of redox-sensitive radionuclides in plants are smoothed, because other exposure pathways not related to radionuclide mobilisation in soils contribute to the overall BDCFs.

References

- /AAR 69/ Aarkrog, A.; Lippert, J.: The direct contamination of rye, barley, wheat and oats with Sr-85, Cs-134, Mn-54 and Ce-141. *Rad. Bot.* 9:357-366; 1969.
- /AAR 71/ Aarkrog, A.; Lippert, J.: Direct contamination of barley with Cr-51, Fe-59, Co-58, Zn-65, Hg-203, and Pb-210. *Rad. Bot.* 11:463-472; 1971.
- /AAR 72/ Aarkrog, A.: Direct contamination of barley with Be-7, Na-22, Cd-115, Sb-125, Cs-134 and Ba-133. Risø, Denmark: Risø National Laboratory, Risø-R-256:163-175; 1972.
- /AAR 75/ Aarkrog, A.: Radionuclide levels in mature grain related to radiostrontium content and time of direct contamination. *Health Physics* 28, 557-562, 1975.
- /ACH 80/ Achtnich, W.: *Bewässerungslandbau*. Ulmer Verlag, 1980.
- /ACK 02/ Ackerman, S.; Knox, J.: *Meteorology: Understanding the Atmosphere*. Brooks Cole; 1st edition. ISBN-13: 978-0534371999. 512 pages, 2002.
- /ADA 99/ Adams, Jonathan , Mark Maslin, Ellen Thomas. Sudden climate transitions during the Quaternary. *Progress in Physical Geography*. Vol. 23, 1-36, March 1999.
- /ALB 01/ Albritton et al.: "Technical Summary", Box 1: What drives changes in climate?, in IPCC TAR WG1 2001.
- /AMA 09/ AMAP Assessment: Radioactivity in the Arctic. Arctic Monitoring and Assessment, Programme (AMAP), Oslo, Norway. xii + 92 pp., 2009.
- /AMI 89/ AMIRO, B.D.; Johnston, F.L.: Volatilization of iodine from vegetation. *Atmospheric Environment* 23: 533538, 1989.
- /ANG 80/ Angeletti, L.: La contamination des paturages par l'iode 131, deuxième partie et fin. Données expérimentales concernant le depot sec et humide de l'iode sur le ray-grass. CEA-R-5056. 20 pp., 1980.

- /ASH 06/ Ashworth, D.J.; Shaw, G.: Soil migration, plant uptake and volatilization of radio-selenium from a contaminated water table. *Science of total environment*, 370, 506–514, 2006.
- /BAE 83/ Baes, C., Sharp, R.: A Proposal for Estimation of Soil Leaching and Leaching Constants for Use in Assessment Models. *J. Environ. Qual.* 12, 17-28, 1983.
- /BEC 03/ Becker, A.: Beitrag zur Erstellung einer Referenzbiosphäre zur Berechnung der in der Nachbetriebsphase eines Endlagers für radioaktive Stoffe hervorgerufenen potentiellen Strahlenexposition unter Berücksichtigung des Einflusses des Klimas BMU – 2003-623, 2003.
- /BIO 04/ BIOCLIM: Modelling sequential BIOSphere systems under CLIMate change for radioactive waste disposal, EC-Contract FIKW-CT-2000-00024, 2004.
- /BMU 05/ BMU (Bundesminister für Umwelt, Naturschutz und Reaktorsicherheit): Allgemeine Verwaltungsvorschrift zu § 47 Strahlenschutzverordnung: Ermittlung der Strahlenexposition durch die Ableitung radioaktiver Stoffe aus kerntechnischen Anlagen oder Einrichtungen. *Bundesanzeiger* 42 (Nr. 64a), 1990, Überarbeiteter Entwurf vom Mai 2005.
- /BMU 10/ BMU, Sicherheitsanforderungen an die Endlagerung wärmeentwickelnder radioaktiver Abfälle, Bundesministerium für Umwelt, Naturschutz und Reaktorsicherheit, Berlin, 2010.
- /BUN 92/ Bunzl, K.; Kracke, W.; Schimmack, W.: Vertical migration of $^{239/240}\text{Pu}$, ^{241}Am and ^{137}Cs fallout in a forest soil under spruce. *Analyst.* 117, 469-474, 1992.
- /BUN 94/ Bunzl, K.; Förster, H.; Kracke, W.; Schimmack, W.: Residence times of fallout $^{239/240}\text{Pu}$, ^{238}Pu , ^{241}Am and ^{137}Cs in the upper horizons of an undisturbed grassland soil. *J. Environm. Radioact.* 22, 11-27, 1994.
- /BUN 95a/ Bunzl, K.; Kracke, W.; Schimmack, W.; Auerswald, K.: Migration of $^{239/240}\text{Pu}$, ^{241}Am and ^{137}Cs in the various horizons of a forest soil under pine. *J. Environm. Radioact.* 28, 17-34, 1995.

- /BUN 95b/ Bunzl, K.; Kofuji, H.; Schimmack, W.; Tsumura, A.; Ueno, K.; Yamamoto, M.: Residence times of global weapons testing fallout Np-237 in a grassland soil compared to Pu-239/240, Am-241 and Cs-137. *Health Physics*, 68, 89-93, 1995.
- /CHA 02/ Charman, D.: *Peatlands and environmental change*. J. Wiley & Sons, London & New York, 301 p., 2002.
- /COP 09/ Coppin, F.; Chabroulet, C.; Martin-Garin A.: Selenit interaction with some particulate organic and mineral fraction isolated from a natural grassland soil. *European Journal of soil science*, 60, 369-376, 2009.
- /CRO 05/ Crossland, I.; Pinedo P.; Kessler, J.H.; Torres-Vidal, C.; Walters, B.: "Reference biospheres" for solid radioactive waste disposal. *J. Environmental Radioact.* 84, 135-150, 2005.
- /CUV 03/ Ćuvardiĉ M.S.: Selenium in soil, *Proceedings for Natural Sciences, Matica Srpska, Novi Sad, No.104*, 23 – 37, 2003.
- /DEL 05/ Delaune, R. D.; Reddy K. R.: Redox Potential. In *Encyclopedia of Soils in the Environment*. D. Hillel (ed). Academic Press. pp. 366-371, 2005.
- /DIX 90/ Dixon, C.: *Rural Development in the Third World*. London: Rutledge, 1990.
- /DOW 08/ Dowdall, M.; Standring, W.; Shaw, G.; Strand, P.J: *Environ Radioact.*; 99(11):1736-45. Epub Aug 3. 2008.
- /EPA 12/ US-EPA: Jim Amon, Wright state University: What is a fen? <http://www.aswm.org/science/images/fen.jpg>, Access date November 2012.
- /EUR 05/ European Commission: *Soil Atlas of Europe*. European Soil Bureau Network. 2005.
- /ERL 95/ Erlandsson, B., Hedwall, R.: Radionuclide concentration in fuels and ash products from biofuel heating plants, Report 02/95, LUNFD6/(NFFR-3067), Lund 1995.

- /ERT 92/ Ertel, J.; Paretzke, H.G.; Ziegler, H.: Cs-137 penetration by contact exchange through isolated plant cuticles: cuticles as asymmetric transport membranes. *Plant, Cell and Environ.* 15, 211-219, 1992.
- /FAO 07/ FAOSTAT: <http://faostat.fao.org>. 2007.
- /FAO 10/ FAOSTAT: FAO Statistical Yearbook 2010.
- /FES 02/ Fesenko, S. V.; Spiridonov, S. I.; Sanzharova, N. I.; Anisimov, V. S.; Aleksakhin, R. M.: *Russian Journal of Ecology*, Vol. 33, No. 3, 2002, pp. 170–177. Translated from *Ekologiya*, No. 3, pp. 185–192, 2002.
- /FRA 82/ Franke, G.: *Nutzpflanzen der Tropen und Subtropen*. Hirzel Verlag Leipzig, 1982.
- /GEI 83/ Geisler, G.: *Ertragsphysiologie von Kulturarten des gemäßigten Klimas*. Verlag Paul Parey, Berlin und Hamburg 1983.
- /GIL 74/ Gillette, D.; Blifford, I.; Fryrear, D.: The influence of wind velocity on the size distributions of aerosols generated by the wind erosion of soils. *Journal of Geophysical Research* 79, 4068-4075, 1974.
- /HED 92/ Hedwall, R.; Erlandsson, B.: Radioactivity in peat fuel and ash from a peat-fired power plant, *J. Environ. Radioactivity* 16, 205-228, 1992.
- /HJE 09/ Hjerpe, T.; Ikonen, A.; Broed, R.: *Biosphere Assessment Report. POSIVA 2010-03*. 2009.
- /HOF 95/ Hoffman, F.O.; Thiessen, K.M.; Rael, R.M.: Comparison of interception and initial retention of wet-deposited contaminants on leaves of different vegetation types, *Atmospheric Environment* 29, 1771-1775, 1995.
- /HU08/ Hu, Q.H. ; Zavarin, M. ; Rose, T.P. : Effect of reducing groundwater on the retardation of redox-sensitive radionuclides. *Geochemical Transactions* 9:12, doi:10.1186/1467-4866-9-12, 2008.

- /IAE 94/ IAEA: Handbook of parameter Values for the prediction of radionuclides transfer in temperate environment. Technical report, Series No.364, IAEA, Vienna, 1994.
- /IAE 03/ IAEA: "Reference Biospheres" for solid radioactive waste disposal: Report of BIOMASS Theme 1 of the BIOSphere Modelling and ASSESSment (BIOMASS) Programme. 2003.
- /IAE 05/ IAEA: Derivation of Activity Concentration Values for Exclusion, Exemption and Clearance, Safety Report Series No. 44, Vienna, 2005.
- /IAE 06/ IAEA: Classification of Soil Systems on the Basis of Transfer Factors of Radionuclides from Soil to Reference Plants. TECDOC- 1497, IAEA, Vienna (2006).
- /IAE 09/ IAEA: Quantification of radionuclide transfer in terrestrial and freshwater environments for radiological assessments TECDOC-1616, 2009.
- /IAE 10/ IAEA: Handbook of parameter values for the prediction of radionuclide transfer in terrestrial and freshwater environments, Technical Reports Series No. 472, Vienna 2010.
- /IPC 07/ IPCC: IPCC Fourth Assessment Report (AR4) Climate Change 2007: Impacts, Adaption and Vulnerability. Intergovernmental Panel on Climate Change, Cambridge University Press, Cambridge, UK. 2007.
- /KEV 96/ Kevern, N.R.; King, D.L.; Ring, R.: Lake classification systems – part 1. by The Michigan Riparian February <http://www.mlswa.org/lkclassif1.htm>. 1996.
- /KOC 01/ Koch-Steindl, H., Proehl G.: Radiat Environ Biophys 40, 93–104, 2001.
- /KUD 96/ Kudelsky, A.; Smith, J.; Ovsianikova, S.; Hilton, J.: The mobility of Chernobyl-derived ¹³⁷Cs in a peatbog system within the catchment of the Pripyat River, Belarus. Science of the Total Environment, 188 (2-3). pp. 101-113. ISSN 0048-9697, 1996.

- /LEC 08/ Leclerc, E.; Colle, C.; Madoz-Escande, C.; Choi, Y.H.: Translocation. In: International Atomic Energy Agency: Radioecological models and parameters for radiological assessments, TECDOC, 2008.
- LEE 96/ Lee, J.L.; Phillips, D.L.; Dodson, R.F.: Sensitivity of the US Corn Belt to climate change and elevated CO₂: II. Soil erosion and organic carbon. *Agricultural Systems*, 52, 503-521, 1996.
- /LEM 04/ Lemly, A.D.: Recommendation for Pre-Mine Assessment of Selenium Hazards Associated with coal mining in West Virginia. 2004, (http://www.ohvec.org/issues/mountaintop_removal/articles/EIS_lemly%20.pdf).
- /LID 11/ Lidman, F.; Mörth, C.-M.; Björkvald, L.; Laudon, H.: Selenium dynamics in boreal streams: the role of wetlands and changing groundwater tables. *Environmental Sci. Technol*, 45, 2677 – 2683, 2011.
- /LIV 88/ Livens, F.; Baxter, M.: Chemical association of artificial radionuclides in West Cumbrian soils. *J. Environmental Radioactivity*, 7, 75-86, 1988.
- /LOS 97/ Losi, M. E.; Frankenberger, W. T. jr.: Bioremediation of Selenium in Soil and Water. *Soil Science*, 162(10), 692-702, 1997.
- /MAY 91/ Mayland, H.F.; Gough L.P.; Stewart, K.C.: Selenium Mobility in soils and its absorption, translocation, and metabolism in plants. USGS Circular No. 1064. pp. 55-64, 1991.
- /MUE 93/ Müller, H.; Pröhl, G.: ECOSYS – A dynamic model for assessing radiological consequences of nuclear accidents. *Health Physics*, 64, 232-252, 1993.
- /MUE 96/ Müller, M.: *Handbuch ausgewählter Klimastationen der Erde*. 5 ed. Gerold Richter, 1996.
- /MUR 04/ Muramatsu, Y.; Yoshida, S.; Fehn, U.; Amachi S. Ohmomo Y.: Studies with natural and anthropogenic iodine isotopes: iodine distribution and cycling in the global environment. *J. Environ. Radioact.*, 74, 221-232, 2004.

- /NAS 12/ NASA: Satellite views of Lake Chad, Afrika.
<http://climate.nasa.gov/blogs/index.cfm?FuseAction=ListBlogs>. Access date November 2012.
- /NEE 91/ Neemann, W.: Bestimmung des Bodenerodierbarkeitsfaktors für winderosionsgefährdete Böden Norddeutschlands – Ein Betrag zur Quantifizierung der Bodenverluste; Geologisches Jahrbuch, Reihe F, Heft 25, 1991.
- /NOS 08/ Noseck, U., Fahrenholz, C., Flügge, J., Fein, E., Schneider, A., Pröhl, G.: Impact of climate change on far-field and biosphere processes for a HLW repository in rock salt. FKZ 02E 9954 (BMW), GRS-241. Gesellschaft für Anlagen und Reaktorsicherheit (GRS) mbH, 2008.
- /NWM 11/ NWMO: OPG's Deep Geological Repository For Low & Intermediate Level Waste: Postclosure Safety Assessment. Quintessa Ltd., Geofirma Engineering Ltd. and SENES Consultants Ltd., 2011.
- /OLY 05/ Olyslaegers, G., Zeevaert, T., Pinedo, P., Simon, I., Proehl, G., Kowe, R., Chen, Q., Mobbs, S., Bergstroem, U., Hallberg, B., Katona, T., Eged, K., Kanyar, B.: A comparative radiological assessment of five European biosphere systems in the context of potential contamination of well water from the hypothetical disposal of radioactive waste. *J Radiol Prot* 25, 375-391, 2005.
- /ORG 05/ Organo, C.; Lee, E.M.; Menezes, G.; Finch, E.C.: Investigation of occupational radiation exposures to NORM at an Irish peat-fired power station and potential use of peat fly ash by the construction industry. *J. Radiol. Prot.* **25** (2005) 461–474.
- /POC 75/ *Pochvovedenie*, 2nd ed. Moscow, 1975 (in Russian).
- /PRO 96/ Pröhl, G.; Hoffman, F.O.: "Radionuclide, interception and loss processes in vegetation, Modelling of radionuclide interception and loss processes in vegetation and of transfer in semi-natural ecosystems. IAEA-TECDOC-857, 9-47, Vienna 1996.

- /PRO 08/ Pröhl, G.: Interception of dry and wet deposited radionuclides by vegetation. *J. Environ. Radioact.* 100, 675-682 (2009), 2008.
- /RON 01/ Rong, Y.; Gauthier, D.; Flamant, G.: Volatility and chemistry of trace elements in a coal combustor. *Fuel*, 80, 2217-2226, 2001.
- /RAZ 11/ Razvorotneva, L.I.; Gilinskaya, L.G.; Markovich, T.I.: The influence of freeze – thaw process on the stability of natural geochemical barriers during sorption of radionuclides on them. *Vestnik Otdelenia nauk o Zemle RAN*, VOL. 3, NZ6081, doi:10.2205/2011NZ000211, 2011.
- /SAN 96/ Sanzharova, N.I.; Kotik, V.A.; Arkhipov, A.N.; Sokolik, G.A.; Ivanov, Y.A.; Fesenko, S.V.; Levchuk, S.E.: The quantitative parameters of the vertical migration of radionuclides in the soils in different types of meadows. *Radiation Biology. Radiology*, vol. 36 (4), 488 – 496, 1996.
- /SAN 08/ Sanzharova, N.; Shubina, O.; Vandenhove, H.; Olyslaegers, G.; Fesenko, S.; Uchida, S.; Tagami, K.; Reed, E.; Velasco, H.; Ayub, J.; Choi, Y.H.; Shang, Z.R.: Agricultural ecosystems: root uptake. In: International Atomic Energy Agency: Radioecological models and parameters for radiological assessments, 2008.
- /SCH 77/ Schönherr, J.: Plant cuticles are polyelectrolytes with isoelectric points around three. *Plant Physiol.* 59, 145-150, 1977.
- /SCH 02/ Scheffer, F.; Schachtschabel, P.: *Lehrbuch der Bodenkunde*. Ferdinand Enke Verlag 2002.
- /SCO 07/ Scott Van Pelt, R.; Zobeck, T.M.; Ritchie, J.C.; Gill, T.: Validating the use of ¹³⁷Cs to estimate rates of soil redistribution by wind. *CATENA*, 70, 455-464, 2007.
- /SEB 98/ Seby, F.; Potin-Gautier, M.; Giffaut, E.; Donard, O.F.X.: Assessing the speciation and the biogeochemical processes affecting the mobility of selenium from a geological repository of radioactive wastes to the biosphere. *Analysis*, 26, 193 – 198, ©EDP Sciences, Wiley-VCH, 1998.

- /SEI 86/ Seinfeld, J.: Atmospheric chemistry and physics of air pollution. John Wiley & Sons, New York, 1986.
- /SHA 95/ Sharmasarkar, Sh.; Vance, G.F., Reddy, K.J.; Zhang, R.; Spackmann, L.K.: Understanding selenium mobility by sorption and extraction coal mine spoil. In: Proceeding of the 12th Annual National Meeting of the American Society for Surface Mining and Reclamation, June 3-8-95, Gillette, Wyoming, 1995.
- /SHA 02/ Sharmasarkar, Sh.; Vance, G.F.: Selenite_selenate sorption in surface coal mine environment. Advances in Environmental Research 7, 87-95, 2002.
- /SHA 10/ Shaw, G.: Selenium (2010): Encyclopedia of Inorganic Chemistry, John Wiley&Sons, Ltd.
- /SIE 09/ Sierra Club: Toxic Selenium: How Mountain top Removal Coal Mining Threatens People & Streams, April 2009,
<http://www.sierraclub.org/coal/downloads/Seleniumfactsheet.pdf>.
- /SKB 11/ SKB: Long-term safety for the final repository for spent nuclear fuel at Forsmark: Main report of the SR-Site project, TR-11-01, Technical Report. Svensk Kärnbränslehantering AB. 2011.
- /SOI 12/ Soil of the Year 2012 – Lowland Peat Soil.
http://eusoils.jrc.ec.europa.eu/Awareness/Documents/Material/SoiloftheYear_2012.pdf. Date of access: December 2012.
- /STA 13/ Chr. Staudt; N. Semioshkina; J.C. Kaiser Modelling the impact of climate change in Central Europe with biosphere models for long-term safety assessment of nuclear waste repositories. Journal of Environmental Radioactivity 115. 214-223, 2012.
- /STO 05/ Stoller-Navarro Joint Venture (SNJV): Phase II Contaminant Transport Parameters for the Groundwater Flow and Contaminant Transport Model of Corrective Action Unit 98: Frenchman Flat, Nye County, Nevada. Las Vegas, NV: S-N/99205-043. 2005.
[http://www.osti.gov/energycitations/product.biblio.jsp?osti_id=875996]
website.

- /STR 08/ StrlSchV, 2008. Strahlenschutzverordnung vom 20. Juli 2001 (BGBl. I S. 1714; 2002 I S. 1459), zuletzt geändert durch Artikel 2 des Gesetzes vom 29. August 2008 (BGBl. I S. 1793).
- /UNC 01/ UNCCD: Global alarm: Dust and sandstorms from the world's drylands. Editors: Yang Youlin, Victor Squires and Lu Qi., Asia RCU of the UNCCD, United Nations Building, Rajadamnern Avenue, Bangkok 10200, Thailand, 2001.
- /UNC 92/ UN conference on environment and development, Rio de Janeiro, 1992.
- /UNI 89/ United States Public Health Service: Toxicological Profile for Selenium. Agency for Toxic Substances and Disease Registry, December 1989.
- /VAN 95a/ Vance, G.F.; Sharmasarkar, Sh.; Reddy, K.J.; Spackmann, L.K.: Abandoned Coal Mine Land Research program. Final report. The importance of solid and solution selenium speciation in mobility and plant uptake of selenium from Wyoming coal mine land reclamation, 1995.
- /VAN 95b/ Vance, G.F.; Schladweiler, B.K.; Pasch, R.N.; Page, M.S.; Carroll, P.K.: Abandoned Coal Mine Land Research program. Final report. Relationship between soil selenium concentrations and selenium uptake by vegetation on surface coal mine lands in Wyoming, 1995.
- /VID 08/ Vidal, M.; Rigol, A.; Gil-García, C.J.: Agricultural ecosystems: radionuclide mobility in soil. In: International Atomic Energy Agency: Radioecological models and parameters for radiological assessments. 2008.
- /VOG 08/ Vogler E.: Biogeochemistry of Radioselenium in Soils. Term Paper, Institute of Biogeochemistry and Pollutant Dynamics, Department Environmental Sciences, ETH Zurich, 2008.
- /VOI 91/ Voigt, G.; Müller, H.; Pröhl, G.: Experiments on the seasonality of the cesium translocation in cereals, potatoes and vegetables. Radiat. Environm. Biophysics, 30, 295-303, 1991.
- /WIK 12/ [/http://en.wikipedia.org/wiki/Tulare_Lake](http://en.wikipedia.org/wiki/Tulare_Lake). Date of access: November 2012.

- /WIL 96/ Williams, M.A.J.; Balling jr, R.C.: Interactions of desertification and climate. Prepared for World meteorological organisation UN Environmental Programme, ARNOLD, ISBN 0 340 63217 8; ISBN 92-0-113009-9, 1996.
- /ZOB 00/ Zobeck, T.M.; Parker, N.C.; Haskell, S.; Guoding, K.: Scaling up from field to region for wind erosion prediction using a field scale wind erosion model and GIS, Agriculture. Ecosystem and Environment, 82, 247-259, 2000.

List of figures

Fig. 2.1	Effective dose rate calculated for /BEX 08/	3
Fig. 2.2	Principal geosphere-biosphere interfaces for radionuclides entering biosphere.....	5
Fig. 2.3	Conceptual model for estimating the radiation exposure to man, if radionuclides enter the biosphere via well water	6
Fig. 2.4	Conceptual model for estimating the radiation exposure to man if radionuclides enter the biosphere via rising groundwater.....	7
Fig. 2.5	Processes involved in the transfer of radionuclides to plants subsequent to irrigation with contaminated groundwater.....	9
Fig. 2.6	Processes involved in the transfer of radionuclides to plants due to rising of contaminated groundwater	9
Fig. 3.1	Changes in A) temperature and B) precipitation predicted by the BIOCLIM project for northern Germany	16
Fig. 3.2	Potential future climate development for northern Germany assuming naturally changing and elevated CO ₂ concentrations in the atmosphere due to the BIOCLIM project /BIO 04/, /STA 13/.....	17
Fig. 3.3	Selection of discrete reference climate regions. Grey depicts temperate, black subtropical and white boreal climate conditions	18
Fig. 3.4	A) Average temperature and B) average monthly precipitation at the reference climate regions.....	21
Fig. 3.5	Soil types A) anthrosol, B) arenosol, C) cambisol, D) podsol and E) hisotosol according to the WRB soil classification /EUR 05/	23
Fig. 3.6	Cs-135 specific activity concentration in sand and organic soil	25
Fig. 3.7	Cs-135 specific activity concentrations in cereals	26
Fig. 3.8	Comparison of the contribution of food types on the ingestion BDCF of selected radionuclides for A) the Magdeburg and B) Rome reference climate region and sand soil	27
Fig. 3.9	Comparison of the contribution of exposure pathways on the total BDCF for the Magdeburg (A) and Rome (B) reference climate region	33

Fig. 3.10	Cumulative frequencies of BDCF for sand soil at the Magdeburg (Cfb) and Rome (Csa) reference climate regions from a probabilistic model for Se-79, Tc-99 and I-129.....	43
Fig. 3.11	Cumulative frequencies of BDCF for sand soil at the Magdeburg (Cfb) and Rome (Csa) reference climate regions from a probabilistic model for Cs-135, Np-237 and U-238.....	44
Fig. 3.12	Cumulative frequencies of BDCF for sand soil at the Magdeburg (Cfb) and Rome (Csa) reference climate regions from a probabilistic model for Pu-239.....	45
Fig. 3.13	Tornado chart for the sensitivity analysis of Se-79 for sand soil and the A) Magdeburg and B) Rome reference climate region	46
Fig. 3.14	Tornado chart for the sensitivity analysis of Tc-99 for sand soil and the A) Magdeburg and B) Rome reference climate region	47
Fig. 3.15	Tornado chart for the sensitivity analysis of I-129 for sand soil and the A) Magdeburg and B) Rome reference climate region	47
Fig. 3.16	Tornado chart for the sensitivity analysis of Cs-135 for sand soil and the A) Magdeburg and B) Rome reference climate region	48
Fig. 3.17	Tornado chart for the sensitivity analysis of Np-237 for sand soil and the A) Magdeburg and B) Rome reference climate region	49
Fig. 3.18	Tornado chart for the sensitivity analysis of U-238 for sand soil and the A) Magdeburg and B) Rome reference climate region	49
Fig. 3.19	Tornado chart for the sensitivity analysis of Pu-239 for sand soil and the A) Magdeburg and B) Rome reference climate region	50
Fig. 4.1	Possible climate transitions and interface changes (blue arrow: cooling; red arrow: warming).....	55
Fig. 4.2	Transitions between discrete climates and geosphere-biosphere interfaces when the climate becomes colder.....	58
Fig. 4.3	Considered transitions between climates and interfaces.....	59
Fig. 4.4	Transitions from temperate climate (rising groundwater scenario) to Mediterranean climate (irrigation) for Se-79.....	60
Fig. 4.5	Two compartment of soil model	61

Fig. 4.6	Time course of two processes causing the contamination of agricultural land with Se-79.....	62
Fig. 4.7	Expected dominant oxidation states of the radionuclides as a function of standard redox potential at pH 7	63
Fig. 5.1	Scheme of the drying of lakes and fens	67
Fig. 5.2	Conceptual model for estimating the radiation exposure to man in case of agricultural use of dry lake sediment.....	72
Fig. 6.1	Activity concentration of Se-79 in pasture grass; sudden transition; full irrigation.....	76
Fig. 6.2	Activity concentration of Tc-99 in pasture grass: sudden transition, full irrigation.....	76
Fig. 6.3	Activity concentrations of Np-237 in pasture grass: sudden transition, full irrigation	77
Fig. 6.4	Activity concentrations of U-238 in pasture grass: sudden transition, full irrigation	77
Fig. 6.5	Activity concentration of Se-79 in pasture grass; 10 years transition; full irrigation	79
Fig. 6.6	Activity concentration of Tc-99 in pasture grass; 10 years transition; full irrigation.....	79
Fig. 6.7	Activity concentration of Np-237 in pasture grass; 10 years transition; full irrigation	80
Fig. 6.8	Activity concentration of U-238 in pasture grass; 10 years transition; full irrigation	80
Fig. 6.9	Se-79 activity concentrations in pasture grass for three values of initial concentration, 10, 100, and 1000 Bq/kg, and transition time of 100 years.....	81
Fig. 6.10	Tc-99 activity concentrations in pasture grass for three values of initial concentration, 10, 100, and 1000 Bq/kg; transition time of 100 years	82
Fig. 6.11	Np-237 activity concentrations in pasture grass for three values of initial concentration, 10, 100, and 1000 Bq/kg; transition time of 100 years.....	82

Fig. 6.12	U-238 activity concentrations in pasture grass for three values of initial concentration, 10, 100, and 1 000 Bq/kg, and transition time of 100 years.....	83
Fig. 6.13	Influence of transition time on the behaviour of activity concentration of Se-79 in pasture grass under full irrigation conditions.....	83
Fig. 6.14	Influence of transition time on the behaviour of activity concentration of Tc-99 in pasture grass under full irrigation conditions	84
Fig. 6.15	Possible use of a contaminated dry lake.....	88
Fig. 6.16	BDCF calculated for the time before (Temperate), during (Transition), and after transition (Mediterranean).....	89
Fig. 6.17	Marked seasonality and a tendency towards drought limits the productive capacity of the land, creating a precarious balance between livestock and resources /DIX 90/.....	92
Fig. A.1	Average transfer factors soil-plant for sand, loam, clay and organic soils	133
Fig. A.2	Average K_d -values for sand, loam, clay and organic soils	133
Fig. A.3	Se redox potential – pH diagram for an aqueous medium at 25 °C and 1 bar pressure for a dissolved Se activity of 10^{-7} mol L ⁻¹ /SEB 98/	149
Fig. A.4	Biogeochemical cycle of selenium /SEB 98/	151
Fig. A.5	Scheme of Se oxides presence in soil depending on pH and soil moisture.....	152
Fig. A.6	Contents of total and water-soluble Se in the profiles of the examined soils in the Vojvodina Province /CUV 03/	152
Fig. A.7	E_h -pH diagram for technetium. The dotted line delineates redox limits of soils and micro-organisms	153
Fig. A.8	Scheme of Tc oxides presence in soil depending on pH and soil moisture.....	154
Fig. A.9	E_h -pH diagram for neptunium. The dotted line delineates redox limits of soils and micro-organisms	155
Fig. A.10	E_h -pH diagram for uranium. The dotted line delineates redox limits of soils and micro-organisms	158

Fig. A.11	E _h -pH diagram for iodine; the dotted line delineates redox limits of soils and micro-organisms	159
Fig. A.12	Change of ⁹⁹ Tc K _d values under five different redox conditions for different aquifer materials	164
Fig. A.13	Change of iodine K _d values under five different redox conditions for different aquifer materials	164
Fig. A.14	Change of ²³⁷ Np K _d values under five different redox conditions for different aquifer materials	165
Fig. A.15	Change of ²³⁸ U K _d values under five different redox conditions for different aquifer materials	165
Fig. A.16	Change of ²⁴² Pu K _d values under five different redox conditions for different aquifer materials	166
Fig. A.17	Soil Textural Triangle: Based on the triangle, a loamy soil has 40 % sand, 20 % clay and 4 % silt; a sandy loam has 60 % sand, 10 % clay and 30 % silt.....	168
Fig. A.18	Lake Oroumeih, Iran; Left: August 1985; Right: August 2010	169
Fig. A.19	Lake Chad, Africa. Left: December 8, 1972; Middle: December 14, 1987; Right: December 18, 2002 /NAS 12/	170
Fig. A.20	Tulare Lake basin: Map of the watercourses.....	171
Fig. A.21	Schematic location and characteristics of a fen (from /EPA 12/)	172

List of tables

Tab. 2.1	Climates, analogue stations and GBIs considered in /NOS 08/.....	4
Tab. 2.2	Contamination pathways considered	8
Tab. 2.3	Plant and animal products considered for the different climates.....	11
Tab. 3.1	Köppen/Geiger climate classification and climate data for the reference climate regions.	18
Tab. 3.2	Data for the nine reference stations	20
Tab. 3.3	Reference climate region dependent parameters for the Valladolid, Santander and Sodanykla reference climate regions.	22
Tab. 3.4	BDCF for different reference regions for the “well” scenario and sand soil. The BDCF are in Sv/y per 1 Bq/L in near surface groundwater.....	30
Tab. 3.5	BDCF for reference regions for the “well” scenario and organic soil. The BDCF are in Sv/y per 1 Bq/L in near surface groundwater.....	31
Tab. 3.6	List of the contribution of exposure pathways to the total BDCF for sand soil.	32
Tab. 3.7	Parameters used for the probabilistic model and sensitivity analysis of the Magdeburg reference climate region.....	35
Tab. 3.8	Parameters used for the probabilistic model and sensitivity analysis of the Magdeburg reference climate region.....	37
Tab. 3.9	Parameters used for the probabilistic model and sensitivity analysis of the Rome reference climate region.	39
Tab. 3.10	Parameters used for the probabilistic model and sensitivity analysis of the Rome reference climate region.	41
Tab. 3.11	Comparison of the BDCF calculated with the deterministic models with the results from the probabilistic model.....	45
Tab. 4.1	Parameters used for calculation of the transitions Fig. 4.6.....	60
Tab. 4.2	Values of K_d for minimum and maximum redox potential (pH=7).	63
Tab. 4.3	Causes of climate fluctuations and approximate time lines	65
Tab. 5.1	K_d values for organic soil	69

Tab. 5.2	Matrix of calculation conditions	71
Tab. 5.3	Characteristics of considered stages of dried-out lake/fen, chemical speciation of radionuclides.....	73
Tab. 6.1	Parameters used for calculation.....	75
Tab. 6.2	Activity concentration of U-series radionuclides and Cs-137 (in Bq/kg, dry weight)	86
Tab. 6.3	Additional contaminations to agricultural soil for using bottom ash from burned peat as fertiliser. The data from Tab. 6.2 are used for the calculation of the concentrations in bottom ash.....	87
Tab. 6.4	Dominant exposure pathways for selected radionuclides	90
Tab. A.1	Leaf area indices (LAI) for present day conditions as function of time and value chosen for the model	121
Tab. A.2	Interception factors $f_{w,rj}$ calculated by equation (X)	121
Tab. A.3	Classification of elements concerning their mobility in plants	123
Tab. A.4	Translocation factors averaged over the irrigation period.....	124
Tab. A.5	Transfer factors soil-plant and half-lives in the upper soil layer for present day conditions	127
Tab. A.6	Possible modifications in relation to present conditions at the reference site.....	129
Tab. A.7	Modification factors (to be applied to transfer factor soil-plant for present day conditions) to estimate the root uptake of radionuclides for the other climates	135
Tab. A.8	Modification of further parameters for the other climates.....	135
Tab. A.9	Transfer factors soil-plant for tundra climate	136
Tab. A.10	Feeding rations for calculating activities in animal food products	138
Tab. A.11	Transfer factors feed-animal products.....	139
Tab. A.12	Element independent parameters to estimate the activity in lake water .	141
Tab. A.13	Concentration factors water-fish and K_d water-sediment	141
Tab. A.14	Food intake rates for the different climate states considered. RG = Rising Groundwater	143

Tab. A.15	Dose coefficients for ingestion, inhalation and internal exposure	144
Tab. A.16	Parameters for estimating exposures from inhalation of resuspended particles	145
Tab. A.17	Common compounds of Se in the environment /LOS 97/.....	150
Tab. A.18	Summary of reported K_d values for Se /VOG 08/	162
Tab. A.19	Radionuclide sorption on different rock (compiled from /STO 08/)	163
Tab. A.20	Particle sizes of various soils	167
Tab. A.21	Soil parameters	168
Tab. A.22	Characteristics of peat soils /FES 02/	173

A Annexes

A.1 Model approaches for exposure calculation

In this section, the model approaches are described that are applied to estimate exposures to humans, if the radionuclides enter the biosphere via the geosphere-biosphere interface “well” and “rising groundwater”, which have been applied to the deterministic calculations. In the first part, the models and parameters are described to estimate the activities in plant and animal foodstuffs. In the second part, the approaches to calculate dose conversion factors for reference persons are described.

A.1.1 Activity in foods

The activity in plant food products is due to direct contamination of the foliage during irrigation and due to uptake of radionuclides from the soil. Plant contamination due to foliar uptake is only relevant, if the contaminated groundwater is used as irrigation water; i. e., this contamination is not relevant, if the radionuclides enter the biosphere due to contamination of surface soil as a consequence of high groundwater table.

A.1.1.1 Interception

During the irrigation of plants, a certain fraction of radionuclides applied with the irrigation water is retained by the foliage of plants. This fraction is quantified by the interception factor f_w , which is calculated according to /MUE 93/, /HOF 95/, /PRO 96/:

$$f_{w,rj} = \frac{LAI_j \cdot k_{rj} \cdot S_j}{R} \cdot \left[1 - \exp\left(-\frac{\ln(2)}{3 \cdot k_{rj} \cdot S_j} \cdot R\right) \right] \quad (\text{A.1})$$

with

$f_{w,rj}$	interception factor for nuclide r and plant j [-]
LAI_j	leaf area index for plant j at time of application (m ² leaf area per m ² soil area)
S_j	water storage capacity of the foliage for plant j (mm)
k_{rj}	retention factor for nuclide r and plant j [-]
R	amount of irrigation for plant j (mm)

The expression above is valid for a wide range of irrigation amounts. The exponential term describes accounts for the built-up of a water film on plant leaves with increasing amount of irrigation. In the case of relatively high irrigation amounts, this term approaches 1 and can be neglected. For low amounts of rainfall and fully developed plant canopies it may occur that f_w yields values higher than 1.0. In this case the value is set to 1.0.

The most important factors for the estimation of the interception factor are the parameters S , LAI and k . According to the review in /PRO 08/, measured values for S for grass, cereals and maize are in the range of 0.1 to 0.3 with a mean of about 0.2. For all other plants (potatoes, root, fruit and leafy vegetables a value of 0.3 is assumed for S /MUE 93/. The leaf area index LAI is defined as the ratio of leaf area (single-sided) and soil area; i.e, it quantifies the size of the interface plant-irrigation water. It represents the surface of plants which is able to retain irrigation water. The leaf area varies considerably throughout the growing period. From planting or sprouting the it increases rapidly until flowering. During the maturing phase the leaf area decreases again.

Data for LAI are summarised as function of time after start of growth for present day conditions in Tab. A.1 /MUE 93/. The values vary from year-to-year due to weather variations and to agricultural practices as fertilization, choice of varieties and the time of seeding. In the model, average values for LAI for the irrigation period are used. The irrigation water is applied in specific periods that depend on crop and climate. During these periods, the applications are evenly distributed, which justifies the use of an average value.

The element dependent retention factor k describes the ability of an element to be fixed on the leaves. A value of $k < 1$ means that the fraction of the element intercepted by the foliage is lower than the intercepted fraction of water in which this element is dissolved. A value of $k > 1$ means that the interception fraction of the element is higher than the interception of water. The retention factor k is controlled by the chemical form. Usually anions have k -values below 1; cations above 1 /ANG 80/, /HOF 95/. The lower values for anions are presumed to be due to the predominantly negative charge of the leaf surfaces /SCH 77/, /ERT 92/. For the radionuclides in anionic form (I, Cl, Se, Tc), a value for $k = 0.5$ seems to be appropriate /PRO 90/. According to /HOF 95/, for all cations with more than one positive valency (Ni, Mo, Zr, Nb, Pd, Sn, Sm, Pb, Po, Ra, Ac, Pa, Th, U, and the transuranics) a value of $k = 2.0$ is selected. Little information is available about monovalent cations such as cesium and rubidium. The observations of

/PRO 90/, /PRO 96/ suggest a k -value of 1.0. For the calculation of the interception, it has been assumed that per irrigation event 20 mm of water are applied. The resulting interception factors are summarised in Tab. A.2.

Tab. A.1 Leaf area indices (LAI) for present day conditions as function of time and value chosen for the model

Plant	Time after start of growth [d]				Model value
	<i>LAI</i>				
Grass	0	60	230	231	5
	0,3	5,5	5,5	0,3	
Cereals	0	66	112	113	5
	0	6	1	0	
Potatoes	0	42	73	118	4
	0	4	4	0	
Fruit vegetables	0	77	169	200	5
	0	5	5	0	
Leafy vegetables	0	30	213	214	5
	0	5	5	0	

Tab. A.2 Interception factors $f_{w,rj}$ calculated by equation (A1)

Interception factor	Cl, Se, Tc, I	Cs	Ni, Zr, Nb, Pd, Sn, Ra, Th, Pa, U, Np, Am, Pu
Grass	0,025	0,05	0,1
Maize	0,025	0,05	0,1
Cereals	0,025	0,05	0,1
Potatoes & roots	0,03	0,06	0,12
Leafy vegetables	0,038	0,075	0,15
Fruit vegetables	0,038	0,075	0,15

A.1.1.2 Weathering and translocation

For estimating the contamination of plant products subsequent to radionuclide deposition on the foliage, two kinds of plants have to be distinguished with regard to their usage as food:

- plants that are used completely as grass, maize silage, and leafy vegetables,
- other crops, (e. g. cereals or potatoes) , where only a specific part can be used.

For the first group, the contamination at time of harvest is given by the initial contamination at the time of deposition, by loss of activity by weathering (by rain and wind) and by growth dilution during the time between deposition and harvest:

$$C_{rj}(\Delta T) = \frac{C_{wr} \cdot f_{w,rj} \cdot I_j}{E_j} \cdot \exp[-(\lambda_w + \lambda_r) \cdot \Delta T] \quad (\text{A.2})$$

with

- $C_{rj}(\Delta T)$ concentration of activity of nuclide r in plant type j at harvest (Bq kg^{-1})
- C_{wr} activity of nuclide r in irrigation water (Bq m^{-3})
- $f_{w,rj}$ interception factor for nuclide r and plant j
- E_j yield of plant type j at time of harvest (kg m^{-2} fresh weight)
- I_j irrigation water applied during an irrigation event to plant j ($\text{m}^3 \text{m}^{-2}$)
- λ_w weathering rate (d^{-1})
- λ_r radioactive decay constant (d^{-1}) of nuclide r
- ΔT time between application of irrigation water and harvest (d)

For the weathering rate, a value equivalent to a half-life of 14 d is applied as suggested by the review in /IAE 96/. For plants that are used partly only, the systemic transport from leaves to edible organs (translocation) subsequent to foliar contamination is a key process. It is quantified by the translocation factor, which is defined as the fraction of the activity initially retained by the foliage of the plant and the activity transferred to the edible parts of the plants until harvest:

$$T_{r,j} = \frac{A_{rj}}{C_{rj}} \quad (\text{A.3})$$

with

- T_{rj} translocation factor for nuclide r and plant j
- A_{rj} activity of nuclide r on plant j initially after irrigation (Bq m^{-2})
- C_{rj} concentration of activity of nuclide r in plant type j at harvest (Bq kg^{-1})

The translocation factor is dependent on the plant type and the time span ΔT from deposition to harvest. In Tab. A.3, the elements considered are classified according to their mobility within the plant. This classification is based on several studies /AAR 69/, /AAR 71/, /AAR 72/, /AAR 75/, /VOI 91/. However, no details on the mobility of nickel,

palladium, tin and niobium could be found in the literature. By default, these elements are considered to be mobile, which is a conservative assumption.

The most reliable data for the translocation are available for the mobile element cesium and the immobile element strontium. Therefore, as long as no other quantitative data are available, the translocation data for cesium are considered to be representative for mobile elements. However, the translocation of cesium appears to be relatively high among the mobile elements /LEC 08/. The strontium data are assumed to be typical for the translocation of immobile elements.

Tab. A.3 Classification of elements concerning their mobility in plants

Mobile elements	Immobile elements
Nickel	Zirconium
Selenium	Samarium
Rubidium	Lead
Molybdenum	Polonium
Niobium	Radium
Technetium	Actinium
Palladium	Thorium
Tin	Protactinium
Iodine	Uranium
Cesium	Transuranics

The contamination of the edible plant parts at time of harvest is given by:

$$C_{rj}(\Delta T) = \frac{C_{wr} \cdot f_{w,rj} \cdot I_j}{E_j} \cdot T_{rj} \cdot \exp(-\lambda_r \cdot t) \quad (\text{A.4})$$

with

$C_{rj}(t)$ concentration of activity of radionuclide r in the edible part of plant type j resulting from foliar deposition and translocation (Bq kg^{-1})

E_j yield of edible part of plant type j (kg m^{-2})

$T_{rj}(t)$ translocation factor for nuclide r and plant type j [-]

t time between deposition and harvest (d)

The translocation of radionuclides also depends on the growth state of the plant. For mobile elements, the maximum can be observed during flowering and begin of the de-

velopment of fruit, tubers or grain. However, in this model, the time-dependence of the translocation is not taken into account, since the irrigation occurs more or less uniformly through the whole irrigation period and averaged values can be used. For immobile elements, translocation is very low; it is superimposed by the deposition directly on the edible parts which also causes a contamination of the edible parts. Otherwise, edible plant parts that grow in soil (e. g. potato tubers) are not contaminated by immobile radionuclides that are deposited on the foliage. The translocation factors applied in this study (Tab. A.4) are derived from /MUE 93/ as an average over the irrigation period.

Tab. A.4 Translocation factors averaged over the irrigation period

Translocation factor	Mobile elements Cl, Ni, Se, Tc, Pd, Sn, I, Cs	Immobile elements Zr, Nb, Ra, Th, Pa, U, Np, Am, Pu
Cereals	0,09	0,005
Potatoes & roots	0,1	0
Fruit vegetables	0,1	0,0033

A.1.1.3 Plant contamination by uptake from soil

The contamination of soil is caused by the application of contaminated irrigation water and by rising of contaminated groundwater. The activity in plants resulting from root uptake is calculated from the activity concentration in the soil, using the transfer factors TF_{rj} which is the ratio of the activity concentration in plants and of the average activity content in the upper 25 cm soil layer. The transfer factors are experimentally derived.

The transfer factor includes all factors influencing the root uptake such as soil type, pH-value, status of the supply with nutrients and sorption capacity of the soil. Furthermore, the transfer factor is based on the total activity in the soil. The activity fractions in the soil being really available for root uptake are not explicitly considered. However, for many radionuclides, considerable fractions are not accessible, because they are strongly bound to soil particles or precipitated as insoluble compounds. All these factors cause a large variability in activity concentration of plants growing on different soils but with the same activity concentration in the root zone.

Nevertheless, the transfer factors are widely used to quantify radionuclide uptake by crops from soil due to its simple determination and application. Therefore, nearly all information on root uptake is available in terms of transfer factors.

An additional radionuclide uptake process is resuspension, i. e. a transfer of activity from soil to the lower parts of the plant. The plant contamination due to resuspension is estimated from the mass of the soil that is attached to the plant and an element-dependent enrichment factor.

The activity uptake by both processes is described with the equation

$$C_{p,rj} = (TF_{rj} + f_{e,r} \cdot R_j) \cdot C_{s,r} \quad (\text{A.5})$$

with

- $C_{p,rj}$ activity of radionuclide r in plant j resulting from root uptake (Bq kg⁻¹ fresh mass)
- TF_{rj} soil-plant transfer factor for radionuclide r and plant j
- $f_{e,r}$ enrichment factor for radionuclide r
- R_j mass load of soil for plant j (g soil per g plant)
- $C_{s,r}$ activity of radionuclide r in the rooting zone of soil (Bq kg⁻¹ dry mass).

The enrichment factor quantifies the enhancement of the activity concentration of resuspended soil compared to the mean activity concentration in soil. The enrichment is due to the fact that resuspension occurs especially with the fine-grained soil fractions as silt and clay, where radionuclides are preferentially bound to due to the high sorption capacity of these fractions. Therefore, the activity concentration in these soil fractions might be considerably increased compared to the mean soil contamination. The lower the clay and silt content, the higher is the enrichment of activity in the clay and silt fraction.

In general, the enrichment factor is greater than 1 for cationic radionuclides. The enrichment in resuspended soil depends on the specific soil conditions. As discussed above it increases with decreasing clay content. The enrichment factor is applied to the mean activity concentration in soil. According to investigations of /LIV 88/, the typical enrichment of cationic radionuclides in soil fractions that is most likely to be resuspended /GIL 74/ is about a factor of 3. This value is applied for Zr, Sn, Cs, Ra, Th, Pa, U, Np, and Pu. For the anionic elements (Cl, Se, Tc, I) the enrichment factor is assumed to be 1.

The transfer factors soil-plant are summarised in Table 10 for present day conditions. They were selected from /SAN 08/ assuming sandy soils as they are found in the Gorleben region.

The concentration of activity in soil is calculated from the annual activity applied with irrigation water. The activity is assumed to be mixed homogeneously within the upper soil layer due to soil cultivation. Activity is lost due to physical decay and migration to deeper soil layers. The activity concentration of the mother nuclide after the irrigation period T is then:

$$C_{sr}(T) = \frac{A_r}{L \cdot \rho} \cdot \{1 - \exp[-(\lambda_{s,r} + \lambda_r) \cdot t]\} \quad (\text{A.6})$$

with

- A activity annually applied during irrigation ($\text{Bq m}^{-2} \text{y}^{-1}$)
- L depth of rooting zone (m) (arable land: 0.25 m, pasture 0.1 m)
- ρ soil density (kg m^{-3} dry matter)
- t time since deposition (d)
- λ_r decay constant of radionuclide r
- λ_s loss rate due to migration (y^{-1})

The half lives equivalent to the loss rates are estimated according to /PRO 05/ and are also listed in Tab. A.5. They are based on experimental studies /BUN 92/, /BUN 94/, /BUN 95a/, /BUN 95b/ and they include both, migration of radionuclides in soluble form and fixed to small soil particles.

Tab. A.5 Transfer factors soil-plant and half-lives in the upper soil layer for present day conditions

Radio-nuclide	Transfer factors soil-plant TF_{rj} (Bq/kg fresh mass plant per Bq kg ⁻¹ dry mass soil)						Half-life in soil (a)	
	Grass	Maize	Cereals	Pota-toes & roots	Leafy veget.	Fruit veget.	Arable land (25 cm)	Pasture (10 cm)
Cl-36	2	2	2	2	2	2	1	0.5
Ni-59	0.01	0.05	0.05	5·10 ⁻³	5·10 ⁻³	5·10 ⁻³	100	40
Se-79	0.05	0.02	0.02	3·10 ⁻³	3·10 ⁻³	3·10 ⁻³	50	20
Zr-93	2·10 ⁻³	5·10 ⁻⁴	1·10 ⁻³	1·10 ⁻⁴	4·10 ⁻⁴	4·10 ⁻⁴	100	40
Nb-94	4·10 ⁻³	4·10 ⁻³	4·10 ⁻³	1·10 ⁻³	2·10 ⁻³	5·10 ⁻⁴	100	40
Tc-99	1	0.1	0.1	0.1	1	0.3	5	2
Pd-107	0.03	0.03	0.03	5·10 ⁻³	0.02	5·10 ⁻³	100	40
Sn-126	5·10 ⁻³	5·10 ⁻³	5·10 ⁻³	1·10 ⁻³	3·10 ⁻³	1·10 ⁻³	100	40
I-129	0.1	0.01	0.01	0.01	0.01	0.01	100	40
Cs-135	0.05	0.02	0.02	0.05	0.05	0.02	100	40
Ra-226	0.02	1·10 ⁻³	1E-3	0.01	0.01	0.01	100	40
Th-230	0.01	5·10 ⁻⁴	2·10 ⁻³	2·10 ⁻⁴	1·10 ⁻⁴	2·10 ⁻⁴	200	80
Pa-231	5·10 ⁻⁴	2·10 ⁻⁴	2·10 ⁻⁴	1·10 ⁻⁴	3·10 ⁻⁴	1·10 ⁻⁴	200	80
U-238	2·10 ⁻³	2·10 ⁻³	2·10 ⁻³	1·10 ⁻³	5·10 ⁻³	1·10 ⁻³	200	80
Np-237	0.01	3·10 ⁻³	3·10 ⁻³	2·10 ⁻³	2·10 ⁻³	2·10 ⁻³	100	40
Am-243	2·10 ⁻⁴	2·10 ⁻⁵	2·10 ⁻⁵	1·10 ⁻⁴	1·10 ⁻⁴	1·10 ⁻⁴	200	80
Pu-239	1·10 ⁻⁴	1·10 ⁻⁵	1·10 ⁻⁵	1·10 ⁻⁵	1·10 ⁻⁴	1·10 ⁻⁵	200	80

For dose estimations, the behaviour of long-lived radionuclides in soil is of particular importance, since the soil acts – once contaminated – as a potential long-term source for radionuclides in food and feed. In this study, the applied transfer factors were determined at different sites under present day conditions. However, these conditions will change in the far future, in particular under significantly different climate conditions. Therefore, potential changes in soil properties and their input on radionuclide behaviour is discussed in the following. Basically, the behaviour of radionuclides is nonetheless controlled by physical, biological and chemical constraints with universal and infinite validity /KOC 01/:

- The speciation of radionuclides in soil is mainly controlled by the interaction of redox potential, pH, content and composition of the organic matter and sorption to mineral soil constituents. E. g., for redox sensitive elements like Se, Tc, U, and Np

the most mobile forms are found in more or less well aerated soils ($E_h > 100$ mV) and under moderate pH (5 – 8), that are typical for intensively managed farmland. Chlorine is very mobile and subject to intensive leaching and good bioavailability over a wide range of E_h /pH combinations.

- Sustainable farming practices try to optimise and preserve optimal growth conditions. Depending on soil type and texture, the optimal plant growth is found for E_h -values between 100 and 600 mV, and for pH from 5.5 to 7.5. With the exception of iodine, these conditions coincide with those under which mobile forms are found.
- An important part of the exposure scenarios is the irrigation of crops with contaminated water. However, the irrigation of soils with a redox potential persistently lower than 100 mV is unlikely, since such soils are either water-logged or have severe structural problems /SCH 02/.
- The upper limit of the optimal redox potential is near the maximum that can be achieved under normal atmospheric conditions; this will also be a constraint for any future conditions.

Assuming agricultural practices, which aim at sustainable land use and optimal conditions for cultivation of crops, it is unlikely that radionuclides in future behave completely different than observed today on sites that are considered to be an appropriate analogue for future soil systems. Therefore, present day data are in principal appropriate to estimate root uptake also under sustainable future agricultural systems.

A.1.1.4 General interactions of climate and soil processes

However, the question is in how far the environmental conditions change and which consequences on the long-term radionuclide behaviour may be expected. Although it is impossible to predict the detailed changes at a given site, some trends can be identified.

The development of soil is driven by the interaction of the host material with climatic and anthropogenic factors. The host material from which soils are formed will not change, but on the long-term, climate and soil management may differ from present conditions, therefore the discussion will be limited to these factors. A lot has been speculated about future climatic changes and it is not intended to continue this debate here. The subject of interest in this context is, how different climatic conditions would

be able to change soils characteristics and, consequently, would alter radionuclide turnover, irrespective of the probability with which such a change may occur.

The soils are affected by climate change, directly via changes of water balance and temperature, indirectly via changes of the growth conditions for plants and the activity of soil organisms, and due to modifications of soil management. The adaptation of soils as a response to changing environmental conditions need different time periods. Soil characteristics, such as redox potential, water content and temperature may change within days or weeks. Changes of the organic matter content and quality happen within decades to centuries, whereas changes in weathering and pedogenesis occur over longer time frames, say within millennia. Such time scales have to be taken into consideration regarding further climatically induced alteration of soils.

Tab. A.6 Possible modifications in relation to present conditions at the reference site

Issue	Possible modification in relation to conditions at reference site	
Climate	Steppe (BS), Mediterranean (Csa) Boreal (Dfa)	Boreal (Dfc), Tundra (ET)
Development of climate	Increased temperature and aridity	Decreased temperature, higher humidity
General development of soil	Lower decomposition of organic matter Increase of pH	Increasing content of organic matter, Decrease of pH
Migration in soil	Reduced water leaching due to low precipitation and high evaporation	Increased leaching of water, precipitation comparable to present Gorleben site conditions, but evaporation is lower
Specific behaviour of radionuclides		
Selenium	More available Se-forms as selenate and selenite predominate	Lower root uptake due to predominance of less available Se-forms as selenide and elemental Se
Iodine	No clear trend	Higher uptake on water-logged soils due to existence of iodide
Uranium	Tends to form mobile uranyl complexes	U(IV) in wet soils, strongly bound to organic matter and precipitates
Neptunium	Trend to mobile Np(V) forms	Trend to form less available Np(IV) in wet soils, complexation by inorganic and organic ligands
Technetium	Trend to mobile and available pertechnetate	Trend to less available forms under reductive conditions
Radium	No clear trend	Strongly bound to organic matter

To account for possible changes of soil characteristics for different climatic states, it has to be differentiated in particular between increasing and decreasing temperatures as well as arid and humid conditions. General trends are compiled in Tab. A.6. These developments may be slightly modified by site-specific factors as specific annual course of temperature and precipitation, the soil type, the topography and the site-specific water balance and the soil use.

Increase of temperature

Under humid conditions, increasing temperatures lead to an acceleration of all soil processes. The soil formation driven by weathering of soil minerals, leaching of weathering products and the decrease of soil pH-value are faster at a high temperature and at humid conditions. The higher turnover of organic matter could lead to a mobilisation of radionuclides incorporated in the humus fraction and to an increased biological availability. Due to the potentially higher leaching, the migration to deeper soil layers may be enhanced as well.

Under dryer arid conditions with increased temperatures decomposition of organic matter is reduced and weathering slower compared to present day conditions. In general, the mobilisation of radionuclides sorbed to organic and mineral soil components should decrease. Aridity is associated with a predominantly upward movement of soil water caused by the high evapotranspiration, which causes an accumulation of cations and anions in the upper soil layer. Due to the increase of salinity, the pH potentially rises. The decrease of infiltration reduces migration of radionuclides into deeper soil layers. In general, the radionuclide turnover in soil is reduced.

Decrease of temperature

In colder climate conditions with enhanced humidity, the degradation of organic matter is inhibited and the sorption and incorporation of radionuclides to the organic soil fraction potentially increases. On the other hand, the pH value tends to decrease due to the leaching of alkaline cations. With increasing soil acidity, the formation of low molecular weight organic acids (e. g., fulvic acids) is promoted which act as complexing agents. This process could potentially increase mobility and so the loss to deeper soil layers. However, it depends on the site and which of these two processes is more important.

In cool and dry climates the soil productivity drops drastically and – compared to temperate climates – the possibilities for land-use are limited to an extensive management.

In general, the soil processes, such as decomposition of organic matter, weathering of the parent material, and leaching are inhibited.

Soil erosion

Erosion processes cause a relocation of soil material due to wind and rain. In case of a contaminated area that is surrounded by uncontaminated or less contaminated land, erosion causes an enhanced activity loss for the contaminated land, since the activity losses from the contaminated land are not compensated by activity inputs from the outside. At the reference site in the Gorleben area, due to the flat terrain, erosion by water is not relevant. However, the sandy soils in this area are very vulnerable to wind erosion due to the soil texture and the relatively low precipitation.

According to /SCH 02/ about $3 \text{ t ha}^{-1} \text{ y}^{-1}$ may be lost due to wind erosion on sandy soils in Northern Germany. This corresponds for a 25 cm soil layer (density: 1.6 kg dm^{-3}) to an annual loss rate of 0.00085 y^{-1} ; i. e. which is equivalent to a half-life of around 800 a. Thus, for temperate climates, activity loss due to wind erosion is less relevant. It should be noted that relevant soil losses due to wind erosion occur during very single events that may be very seldom; however, during those events large amounts of soil might be removed. It needs the coincidence of dried up sandy soils, a poor vegetation cover and high wind speeds to enable relevant wind erosion. For example on four sites in Northern Germany, soil losses from $16 - 170 \text{ t ha}^{-1} \text{ y}^{-1}$ were observed during one single day on sandy podsols /NEE 91/. For all cultivated crop land in the United States mean soil losses due to wind erosion of $7.8 \text{ t ha}^{-1} \text{ y}^{-1}$ have been estimated /LEE 96/.

For arid regions, soils are much more vulnerable to wind erosion, since usually during relatively long periods soils are dried up and have no or only a thin vegetation cover. /ZOB 00/ estimated wind erosion losses on irrigated land in Texas. Highest erosion rates were found for sandy soils, ranging from $38 - 570 \text{ t ha}^{-1} \text{ y}^{-1}$ depending on crop type. On clay and loamy soils, wind erosion is by more than a factor 10 less. In a semi-arid dry farming region in Texas with predominantly sandy and loamy soils, erosion rates were determined of about $50 \text{ t ha}^{-1} \text{ y}^{-1}$ /SCO 06/.

Consequence for transfer, erosion and migration

Higher mobility of radionuclides in soil may generally induce two processes: First, the potential root uptake of radionuclides increases. Second, the potential loss of radionuclides to deeper soil layers increases as well. These two processes compensate each other at least to some extent. From this point of view, it is unlikely that changing climat-

ic conditions would impact the total transfer of radionuclides to plants in a way that the results would drastically enhance or decrease the integrated uptake of radionuclides by plants. An exception is cesium: On acid soils, low in potassium and clay and high in organic matter, the opposite observations are made. Under these conditions, high uptake by plants is observed although the migration to deeper soil layers is low. Cesium is prevented from leaching due to the incorporation in organic matter and micro-organisms.

A recently finished compilation of transfer factors soil-plant is given in /IAE 08/. It is a comprehensive summary of transfer factors on the base of about 9 000 single data. The data in this compilation are categorised according to soil type and crop. The soil type is characterised by the soil texture; so, the transfer factors are given for sand, loam, clay and organic soils. However, the number of data varies considerably dependent on crop and radionuclide. Most data are available for grass and cereals, the radionuclides with most entries are cesium and strontium. Unfortunately, many of the radionuclides relevant for waste disposal are less well studied. In Fig. A.1 the average transfer factors for different radionuclide and different soil types are plotted. For this comparison cereal data were used, because the most comprehensive data set was available for this crop. Despite the large underlying data set, there are still gaps; e. g., there are no data for uranium and thorium in organic soils or plutonium in sandy soils. The figure indicates that for cationic elements (U, Th, Cs, Am, Np, Pu) transfer factors in general decrease in the order sand > loam > clay. This is an expected result, since the cation exchange capacity increases in the same order. The differences between the different soil types are in the order of a factor 2 – 5. For anionic radionuclides (Cl, Se, Tc, I), the soil texture is less important. Especially selenium, technetium and iodine are subject to a pronounced speciation that is controlled by redox potential and pH /KOC 01/ (see also above).

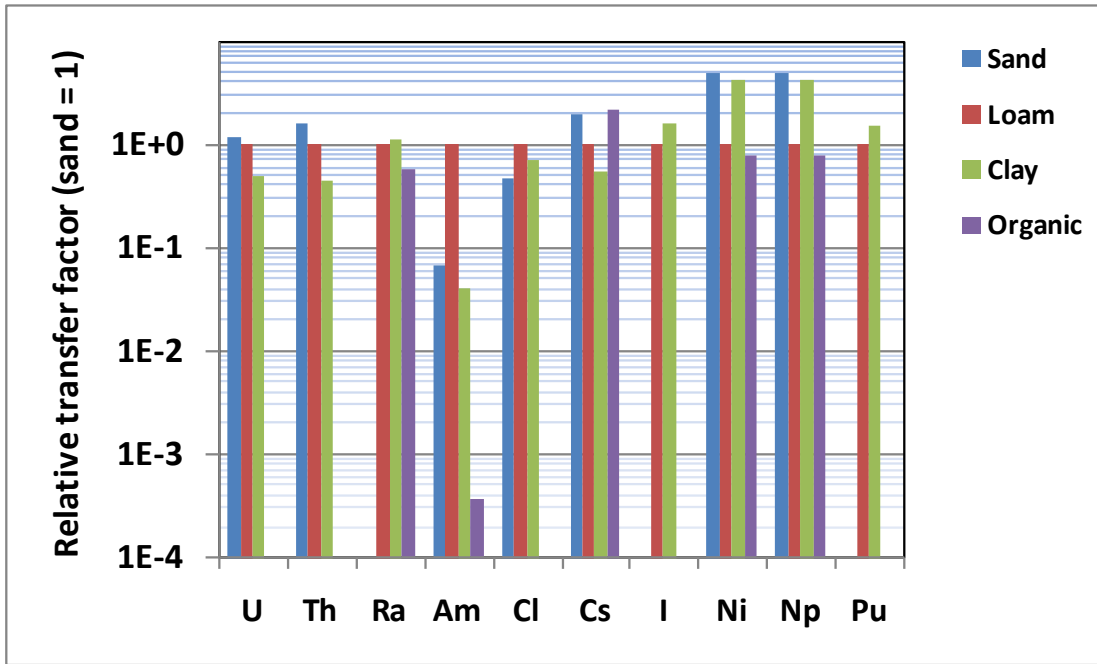


Fig. A.1 Average transfer factors soil-plant for sand, loam, clay and organic soils

In Fig. A.2 the K_d -values are plotted for the different soil types /VID 08/. The K_d -value increases with the strength of the sorption of a radionuclide to soil. It is not a direct measure of the bio-availability of a radionuclide; however, increasing K_d -values usually indicate decreasing root uptake and decreasing loss rates from the upper soil.

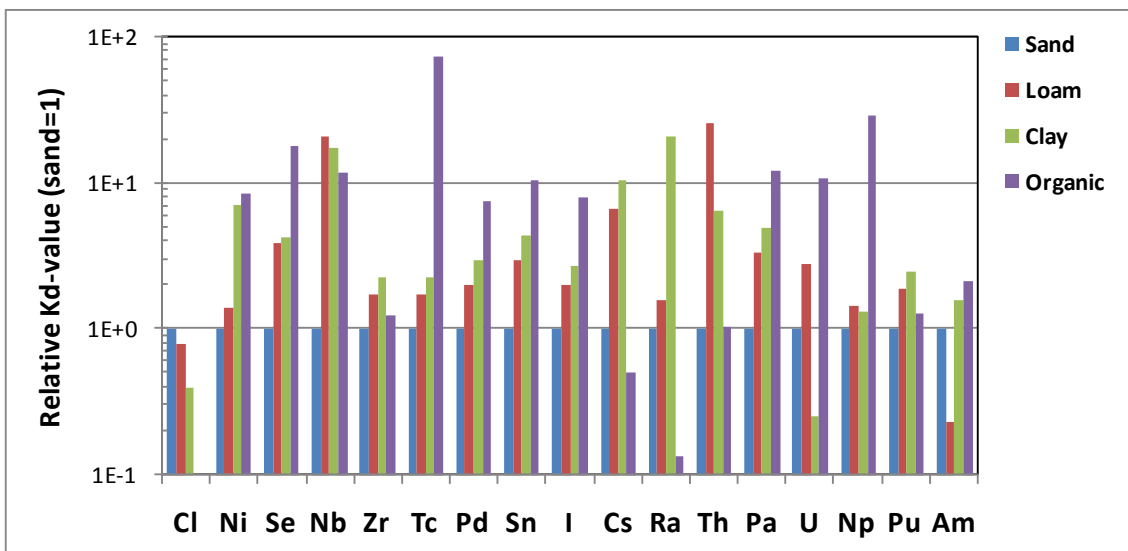


Fig. A.2 Average K_d -values for sand, loam, clay and organic soils

The results are in general consistent with those drawn from the comparison of transfer factors: For cationic radionuclides, K_d -values typically increase in the order sand > loam

> soil. In some cases, highest K_d -values are found for organic soils (Se, Tc, Np, Pd, Sn, I, Pa, Np, Am). However, the sorption strength of radionuclides to organic matter is lower than to inorganic soil constituents; i. e. a high K_d -value does not necessarily mean a low root uptake. The exchange between radionuclides pools that differ in bioavailability may be easier than in organic soils. As a result, the root uptake in organic soils may be high although the K_d -value is high. Furthermore, the fulvic and humic acids act as complexing agents that keep radionuclides in a relative mobile and available form, although the K_d -values may be relatively high.

In order to quantify the impact of climatic conditions, the transfer factors used in the models are modified according to Tab. A.7. Parameters for erosion and migration are modified as shown in Tab. A.8. The vulnerability of soil to wind erosion increases with aridity and dryness of a site. The modification factors for erosion are consistent with the wind erosion rates discussed above.

For the migration in soil, the water infiltration is the driving force; i. e. with increasing aridity, migration of radionuclides to deeper layers decreases. In continuously arid regions, there is no migration at all. However, with increasing aridity, there is a trend to salinisation of the upper soil: Due to the low humidity, there is an upwards movement of water, which evaporates at the surface and the salts originally dissolved remain at the surface. With the application of irrigation water, this process may even be intensified, since there is an additional input of minerals with the irrigation water. In the Mediterranean climate, this problem is less severe, since there is sufficient precipitation during winter, which leads a relevant downward migration of water (and therewith enriched salts) in soil. In areas with pronounced aridity, excess irrigation water has to be applied during the cold season to enforce dissolution of salts and a downward movement of the water in order to prevent salinisation /BOG 81/. Therefore, to enable sustainable agriculture, leaching of radionuclides will occur in any case, but it will be less than under temperate climates. The reduction factors listed in Tab. A.7 and Tab. A.8 should be considered as a first rough estimate.

It should be noted that the loss processes – migration and erosion – compensate each other – at least to some extent. Under dry conditions, migration to deeper soil layers is in general less than under humid climates, but the radionuclide loss due to wind erosion is higher and vice versa. Mushrooms and berries are specific to the tundra climate. The transfer factors soil-plant applied are summarised in Tab. A.9

Tab. A.7 Modification factors (to be applied to transfer factor soil-plant for present day conditions) to estimate the root uptake of radionuclides for the other climates

Radionuclide	Modification factor			
	Well		Rising groundwater	
	Steppe(BS), Mediterranean (Csa) Boreal (Dfa)	Boreal (Dfc), Tundra (ET)	Temperate (Cfb) Boreal (Dfa)	Boreal (Dfc), Tundra (ET)
Cl-36	1	1	1	1
Ni-59	1	1	1	1
Se-79	10	1	1	0.3
Zr-93	0.5	1	1	1
Nb-94	0.5	1	1	1
Tc-99	10	0.1	1	0.1
Pd-107	0.5	1	1	1
Sn-126	0.5	1	1	1
I-129	0.5	1	10	10
Cs-135	0.5	50	0.5	50
Ra-226	0.5	0.5	1	0.5
Th-230	0.5	1	1	1
Pa-231	0.5	1	1	1
U-238	3	1	1	1
Np-237	5	1	1	1
Am-243	0.5	1	1	1
Pu-239	0.5	1	1	1

Tab. A.8 Modification of further parameters for the other climates

Climate	Value
Erosion (y^{-1})	
Temperate (Cfb)	$5 \cdot 10^{-4}$
Mediterranean (Csa)	$2 \cdot 10^{-3}$
Steppe (BS)	$5 \cdot 10^{-3}$
Boreal (Dfa)	$2 \cdot 10^{-3}$
Boreal (Dfc)	$5 \cdot 10^{-4}$
Tundra (ET)	$5 \cdot 10^{-4}$
Migration (relative values)	
Temperate (Cfb)	1
Mediterranean (Csa)	0.5
Steppe (BS)	0.2
Boreal (Dfa)	0.5
Boreal (Dfc)	1
Tundra (ET)	1

Tab. A.9 Transfer factors soil-plant for tundra climate

Radionuclide	Transfer factors soil-plant TF_{rj} (Bq kg ⁻¹ fresh mass plant per Bq kg ⁻¹ dry mass soil)	
	Mushrooms	Berries
Cl-36	2	2
Ni-59	$5 \cdot 10^{-3}$	$5 \cdot 10^{-3}$
Se-79	$3 \cdot 10^{-3}$	$3 \cdot 10^{-3}$
Zr-93	$4 \cdot 10^{-4}$	$4 \cdot 10^{-4}$
Nb-94	$2 \cdot 10^{-3}$	$5 \cdot 10^{-4}$
Tc-99	0.1	0.3
Pd-107	0.02	$5 \cdot 10^{-3}$
Sn-126	$3 \cdot 10^{-3}$	$1 \cdot 10^{-3}$
I-129	0.1	0.1
Cs-135	10	1.0
Ra-226	0.1	0.01
Th-230	0.01	$2 \cdot 10^{-4}$
Pa-231	$3 \cdot 10^{-4}$	$1 \cdot 10^{-4}$
U-238	0.05	$1 \cdot 10^{-3}$
Np-237	$2 \cdot 10^{-3}$	$2 \cdot 10^{-3}$
Am-243	$1 \cdot 10^{-4}$	$1 \cdot 10^{-4}$
Pu-239	0.01	$1 \cdot 10^{-5}$

Soil contamination due to rising groundwater

In case of a high groundwater table, irrigation of plants is usually not necessary. However, under those circumstances, soils may be contaminated due to rising groundwater. Since the contamination of surface soils is a long-term process, equilibrium conditions between the activity in soil and water are assumed. Then, the contamination of soil C_s can be estimated from the water contamination C_w and the distribution coefficient K_d . The contamination of plants results from the soil contamination and element-specific transfer factors soil-plant TF_{rj} (see above):

$$C_{p,r} = C_{w,r} \cdot K_{d,r} \cdot TF_{rj} \quad (\text{A.7})$$

During continuous humid conditions, radionuclides would accumulate in the upper soil horizon, since the rising water transports radionuclides to the soil surface. The water evaporates and the radionuclides remain. However, wet and water-logged soils are dif-

difficult to use for agricultural purposes due to problems in mechanical soil cultivation. Such soils are often very wet, which impedes their cultivation. Therefore, on the long term, such soils can only be used, if due to the implementation of drainage, the soil is dewatered to avoid water logging with all its related problems. This also causes – at least temporarily – a downward movement of the soil water, which is a driving force for radionuclide leaching /VID 08/.

A.1.1.5 Transfer of radionuclides to animal products

The intake of radionuclides by animals with water, feed and soil causes a contamination of animal food products. The concentration of the activity in meat and milk can be estimated from the intake of activity by animals, considering the kinetics of the radionuclides in the animals' metabolism. Subsequent to intake and resorption in the gut, radionuclides are distributed in the animals' body while part of it is excreted via urine and faeces. After a single intake, the time-dependence of the activities in the different organs is very pronounced. However, in case of a long-term contamination of groundwater as expected in a release scenario, radionuclides are taken up over a long period. Under those conditions it is justified to assume that steady state conditions of the activity are achieved in tissues and organs.

The intake rate of activity is calculated from the activity concentrations in the different foodstuffs and the feed consumption rates:

$$A_{drk} = C_w \cdot I_w + \sum_{m=1}^M C_{rm} \cdot I_{mk} \quad (\text{A.8})$$

with

- A_{drk} activity intake rate of nuclide r by animal k (Bq d^{-1})
- C_w activity concentration of nuclide r in water (Bq kg^{-1})
- I_w water intake of animal k (L d^{-1})
- C_{rm} activity concentration of activity of nuclide r in feedstuff m (Bq kg^{-1})
- I_{mk} intake rate of feedstuff m by animal k (kg d^{-1})

For grass and forage, the soil intake of cattle is considered by the factor S_j . This parameter is defined as the amount of soil that is ingested by cattle per unit of grass or forage intake. Since during the soil ingestion of animals, no fractionation occurs as dur-

ing the resuspension, it is assumed that the contamination of soil ingested is equal to the mean activity in the soil; therefore the enrichment factor is not applied. The resuspension and soil ingestion by cattle is formally used as the transfer factor for root uptake. The feed and water intake of the animals is summarised in Tab. A.10 /PRO 05/. The data represent typical values. However, feeding regimes of animals cover a wide range of possibilities and depend on the specific conditions at a site or farm.

Tab. A.10 Feeding rations for calculating activities in animal food products

Animal	Feed	Climate					
		Tempe- rate Cfb	Medit. Csa	Steppe BS	Boreal Dfa	Boreal Dfc	Tundra ET
Lactating cow	Grass	70	70	70	70	70	70
	Water	75	75	75	75	75	75
Beef	Grass	0	25	25	25	50	-
	Maize	25	10	10	10	0	-
	Cereals	0	0	0	0	1	-
	Water	40	40	40	40	40	-
Pork	Cereals	4	4	4	4	4	-
	Water	8	8	8	8	8	-
Lamb	Grass	5	5	5	5	5	-
	Water	4	4	4	4	4	-
Reindeer	Grass	-	-	-	-	-	70
	Water	-	-	-	-	-	40

The transfer to the animal products under equilibrium conditions is described by the transfer factor fodder-animal product TF_{ik} , which is defined as the ratio of concentration of activity in the animal product (Bq kg^{-1}) and the daily intake of activity by the animal (Bq d^{-1}) for equilibrium conditions. Then, the concentration of activity in milk, meat and eggs is given by:

$$C_{rk} = A_{drk} \cdot TF_{rk} \quad (\text{A.9})$$

with

C_{rk} activity concentration of nuclide r in animal product k at equilibrium (Bq kg^{-1} , Bq L^{-1})

TF_{rk} transfer factor feed - animal product k for the radionuclide r (d L^{-1} , d kg^{-1})

As discussed above equilibrium conditions can be assumed which allows the application of transfer factors without consideration of the time-dependence of activities in animal food products. The transfer factors are summarised in /PRO 05/, /PRO 96/ IAE 08/.

Tab. A.11 Transfer factors feed-animal products

Radio-nuclide	Transfer factors feed (d L ⁻¹ , d kg ⁻¹)				
	Milk	Beef	Pork	Lamb	Reindeer
Cl-36	0.02	0.02	0.3	0.3	0.02
Ni-59	1·10 ⁻³	5·10 ⁻³	0.01	0.05	5·10 ⁻³
Se-79	1·10 ⁻³	5·10 ⁻³	0.01	0.05	5·10 ⁻³
Zr-93	1·10 ⁻⁶	1·10 ⁻⁶	5·10 ⁻⁶	1·10 ⁻⁵	1·10 ⁻⁶
Nb-94	1·10 ⁻⁶	1·10 ⁻⁶	3·10 ⁻⁶	1·10 ⁻⁵	1·10 ⁻⁶
Tc-99	1·10 ⁻⁴	5·10 ⁻⁴	1·10 ⁻³	5·10 ⁻³	5·10 ⁻⁴
Pd-107	1·10 ⁻³	1·10 ⁻³	3·10 ⁻³	0.01	1·10 ⁻³
Sn-126	5·10 ⁻⁴	1·10 ⁻³	3·10 ⁻³	0.01	1·10 ⁻³
I-129	5·10 ⁻³	0.02	0.03	0.03	0.02
Cs-135	5·10 ⁻³	0.02	0.4	0.5	0.02
Ra-226	3·10 ⁻⁴	3·10 ⁻³	2·10 ⁻³	5·10 ⁻⁴	3·10 ⁻³
Th-230	5·10 ⁻⁶	1·10 ⁻⁵	3·10 ⁻⁵	1·10 ⁻⁴	1·10 ⁻⁵
Pa-231	5·10 ⁻⁶	1·10 ⁻⁵	3·10 ⁻⁵	1·10 ⁻⁴	1·10 ⁻⁵
U-238	1·10 ⁻⁴	1·10 ⁻⁴	3·10 ⁻⁴	1·10 ⁻³	1·10 ⁻⁴
Np-237	5·10 ⁻⁶	1·10 ⁻⁴	3·10 ⁻⁴	1·10 ⁻³	1·10 ⁻⁴
Am-243	1·10 ⁻⁶	1·10 ⁻⁴	3·10 ⁻⁴	1·10 ⁻³	1·10 ⁻⁴
Pu-239	1·10 ⁻⁶	1·10 ⁻⁴	3·10 ⁻⁴	1·10 ⁻³	1·10 ⁻⁴

A.1.1.6 Contamination of fish

Under equilibrium conditions, the activity concentration in fish is estimated from the activity in water, the element-specific concentration factor water-fish according to:

$$C_{f,r} = C_{w,r} \cdot CF_{wf,r} \quad (\text{A.10})$$

with

- $C_{f,r}$ activity concentration in fish (Bq kg^{-1})
 $CF_{wf,r}$ concentration factor water-fish (L kg^{-1})
 $C_{w,r}$ activity concentration in water (Bq L^{-1})

The activity concentration in the lake water is estimated from the activity of the inflowing water, the turnover of the water body λ_t and the sedimentation rate λ_{sed} . The activity of the inflowing water is assumed to be the same as that of the contaminated near-surface water.

$$C_{Lw} = \frac{C_w}{\lambda_{\text{sed}} + \lambda_t} \quad (\text{A.11})$$

with

- λ_t rate for the loss due to turnover (d^{-1})
 $\lambda_{r,s}$ rate of nuclide r for the loss due to sedimentation (d^{-1})

The sedimentation rate λ_{sed} is estimated from the particulates suspended in water and the distribution coefficient water-sediment:

$$\lambda_s = \frac{S_a \cdot K_{d,ws}}{d \cdot (1 + C_p \cdot K_{d,ws})} \quad (\text{A.12})$$

with

- λ_s sedimentation rate (d^{-1})
 S_a annual sedimentation ($\text{kg m}^{-2} \text{y}^{-1}$)
 $K_{d,ws}$ distribution coefficient water-sediment ($\text{m}^3 \text{kg}^{-1}$)
 d depth of the water body (m)
 C_p particulate concentration in water (kg m^{-3})

The nuclide-independent parameters to estimate the activity in lake water are listed in Tab. A.12. The K_d -values and the concentration factors water-fish are summarised in Tab. A.13. The values represent a simplified reference lake /PRO 05/. The turnover rate is only 2 y^{-1} , and the depth of the water is only 3 m. These assumptions are cautious.

Tab. A.12 Element independent parameters to estimate the activity in lake water

Parameter	Unit	Value
Turnover of water	y^{-1}	2
Sedimentation rate	y^{-1}	0.2
Annual sedimentation	$\text{kg m}^{-2} \text{y}^{-1}$	5
Annual sedimentation	m y^{-1}	0.005
Sediment density	kg m^{-3}	1 000
Depth of water body	m	3
Particulate concentration	kg m^{-3}	0.1

Tab. A.13 Concentration factors water-fish and K_d values

Radionuclide	Concentration factor water-fish (L kg^{-1})	K_d -water sediment ($\text{m}^3 \text{kg}^{-1}$)
Cl-36	50	0.1
Ni-59	100	30
Se-79	200	0.1
Zr-93	200	10
Nb-94	200	30
Tc-99	15	0.1
Pd-107	10	30
Sn-126	3 000	30
I-129	10	10
Cs-135	1 000	10
Ra-226	70	30
Th-230	100	30
Pa-231	10	30
U-238	50	30
Np-237	30	30
Am-243	30	30
Pu-239	30	30

A.1.2 Dose calculation

A.1.2.1 Calculation of the ingestion dose

The annual effective dose is calculated for an adult reference person. It is the sum of the contributions from ingestion, inhalation, and external exposure. The annual ingestion dose is calculated from the activity intake with food and water exposure $D_{ing,n}$ due to ingestion of the foodstuff n is given by

$$D_{ing,n} = V_{n,r} \cdot C_{nr} \cdot g_{ing,r} \quad (\text{A.13})$$

with

$V_{n,r}$ annual intake rate of foodstuff n (kg d^{-1})

$C_{n,r}$ annual average of food activity in food n (Bq kg^{-1})

$g_{ing,r}$ ingestion dose coefficient for effective dose for ingestion of nuclide r (Sv Bq^{-1})

The intake rates for the different climate states are summarised in Tab. A.14. The data represent present day average intake rates for countries which are located in the climate zones considered as reference for the different climates.

Tab. A.14 Food intake rates for the different climate states considered. RG = Rising Groundwater

Food item	Food intake rates (L y ⁻¹ , kg y ⁻¹)						
	Well; RG	Well, GW	Well	Well	Well, GW	Well	GW
	Temperate Cfb	Mediterr. Csa	Steppe BS	Boreal Dfa	Boreal Dfc	Tundra ET	Tundra ET
Drinking water	730	1 100	1 100	730	730	730	730
Cereals	110	115	105	110	71	-	-
Potatoes/root veg.	55	107	93	55	84	-	113
Leafy vegetables	13	56	34	13	51	-	7.7
Fruit vegetables	75	84	12	75	-	-	16
Milk	130	100	87	130	115	37a	37
Beef	30	28	22	30	72	110 a	110
Pork	60	28	22	60	0	0	-
Lamb	0	1.5	12	0	0	0	-
Fish	1	0	0	1	14	0	36.5
Fungi	-	-	-	-	-	-	7.7
Berries	-	-	-	-	-	-	16
Reindeer	-	-	-	-	-	-	110
Reference	/PRO 05/		/EUR 91/	/PRO 05/		/TRA 02/	
Analogue station	Germany	Spain	Greece	Germany	Sweden	Kola peninsula	

For the temperate climate, German intake rates are applied as a reference. To represent the Mediterranean climate, Spanish data are used. No data are available for Steppe climate which is represented by the site Marrakesh. In lieu, Greek data were used, which are thought to be appropriate in view on climatic conditions. The data for tundra were surveyed by an investigation of laps on the Kola Peninsula. The water intake is assumed to be 2 L d⁻¹, which is consistent with the physiological water demand /KLE 99/. In warmer climates, water demand and intake are higher. Therefore, for the Mediterranean climate, and the Steppe climate a daily water consumption of three litres is assumed. In view of various sources that contribute to water intake, this is a very cautious assumption. The dose coefficients for ingestion and inhalation are taken from /BMU 02/ (Tab. A.15).

Tab. A.15 Dose coefficients for ingestion, inhalation and internal exposure

Dose coefficient	Ingestion (Sv Bq ⁻¹)	External exposure (Sv s ⁻¹ pro Bq m ⁻²)	Inhalation (Sv Bq ⁻¹)	Inhalation class
C-14 (organic)	5.8·10 ⁻¹⁰		-	
C-14 (anorganic)	2.9·10 ⁻¹¹	0	6.2·10 ⁻¹²	
Cl-36	9.3·10 ⁻¹⁰	0	7.3·10 ⁻⁰⁹	M
Ni-59	6.3·10 ⁻¹¹	3.1·10 ⁻¹⁹	4.4·10 ⁻¹⁰	
Se-79	2.9·10 ⁻⁰⁹	0	2.6·10 ⁻⁰⁹	M
Zr-93	1.1·10 ⁻⁰⁹	4.6·10 ⁻¹⁹	1.0·10 ⁻⁰⁸	M
Nb-94	1.7·10 ⁻⁰⁹	1.5·10 ⁻¹⁵	1.1·10 ⁻⁰⁸	
Tc-99	6.4·10 ⁻¹⁰	0	4.0·10 ⁻⁰⁹	M
Pd-107	3.7·10 ⁻¹¹	0	8.5·10 ⁻¹¹	
Sn-126	7.1·10 ⁻⁰⁸	1.9·10 ⁻¹⁵	3.1·10 ⁻⁰⁸	M
I-129	1.1·10 ⁻⁰⁷	2.0·10 ⁻¹⁷	3.6·10 ⁻⁰⁸	F
Cs-135	2.0·10 ⁻⁰⁹	0	6.9·10 ⁻¹⁰	F
Ra-226	2.8·10 ⁻⁰⁷	1.6·10 ⁻¹⁵	3.5·10 ⁻⁰⁶	M
Th-230	3.1·10 ⁻⁰⁷	3.8·10 ⁻¹⁹	4.3·10 ⁻⁰⁵	M
Pa-231	7.1·10 ⁻⁰⁷	4.0·10 ⁻¹⁶	1.4·10 ⁻⁰⁴	M
U-238	4.8·10 ⁻⁰⁸	1.6·10 ⁻¹⁵	2.9·10 ⁻⁰⁶	M
Np-237	1.1·10 ⁻⁰⁷	2.1·10 ⁻¹⁶	2.3·10 ⁻⁰⁵	M
Am-243	2.0·10 ⁻⁰⁷	2.0·10 ⁻¹⁶	4.1·10 ⁻⁰⁵	
Pu-239	2.5·10 ⁻⁰⁷	3.2·10 ⁻¹⁹	5.0·10 ⁻⁰⁵	M

A.1.2.2 Inhalation dose due to resuspended soil particles

The resuspension of contaminated soil particles depends on a variety of factors such as weather, particle size spectrum in air, characteristics of the surface (soil, vegetation, urban environment) and climatic conditions. These influencing factors lead to a pronounced variability of resuspension. The key assumption for the estimation of exposure due to inhalation of resuspended particles for an adult reference person is that the inhaled particles have the same activity concentration as the soil from which it is resuspended.

The effective dose is estimated according to:

$$D_{inh,r} = C_{s,r} \cdot L_s \cdot I_A \cdot f_{e,r} \cdot g_{inh,r} \quad (\text{A.14})$$

with

- $D_{inh,r}$ effective annual inhalations dose due to nuclide r (Sv y^{-1})
 $C_{s,r}$ activity concentration of the soil (Bq kg^{-1})
 L_s dust in air ($g\ m^{-3}$)
 I_A breathing rate ($m^3\ y^{-1}$)
 $f_{e,r}$ enrichment factor for the resuspendable soil fraction
 $g_{inh,r}$ inhalation dose coefficient for effective dose of the radionuclide r (Sv Bq^{-1})

The breathing rate for an adult person is 8 100 $m^3\ y^{-1}$ /BMU 05/. The dust concentration in air in rural areas is about 20 $\mu g\ m^{-3}$ for temperate climates /SEI 86/. For dry conditions, resuspension and wind erosion are higher /SEI 86/. Respective values given in Tab. A.16 are in consistence with the assumptions on activity loss by wind erosion.

The dose coefficients for inhalation are taken from /BMU 02/ (Tab. A.15). The dose coefficients are derived for a particle size around 1 μm . The particle size spectrum of resuspended material covers a wide range from less than 1 μm to some ten μm . Most particles have diameters below 10 μm /SEI 86/, which is considered as the respirable fraction. This assumption is cautious because it implies that the total resuspended activity contributes to the inhalation dose.

Tab. A.16 Parameters for estimating exposures from inhalation of resuspended particles

Parameter	Value
Dust concentration ($\mu g\ m^{-3}$)	
Temperate (Cfb)	20
Mediterranean (Csa)	100
Steppe (BS)	200
Boreal (Dfa)	100
Boreal (Dfc)	20
Tundra (ET)	20
Enrichment factor	
Cl, Se, Tc, I	1
Zr, Sn, Cs, Ra, Th, Pa, U, Np, Pu	3

A.1.2.3 External exposure

The external exposure from activity deposited on soil during the application of irrigation water is calculated from the activity in soil, the effective thickness of the soil layer, the exposure time during which the reference person stays on contaminated soil and the dose coefficient for external exposure.

$$D_{ext,r} = C_{s,r} \cdot d_{b,r} \cdot T_{ext} \cdot g_{ext,r} \quad (\text{A.15})$$

with

$D_{ext,r}$ annual effective dose due to external exposure (Sv y^{-1})

$d_{b,r}$ effective thickness of the soil layer that contributes to external exposure from radionuclide r in soil (m)

$g_{ext,r}$ dose coefficient for external exposure from the ground (Sv s^{-1} per Bq m^{-2})

T_{ext} exposure time (s y^{-1})

The parameter $d_{b,r}$ is a nuclide-dependent correction factor that is necessary because dose coefficients for external exposure relate to a planar radionuclide source on the soil surface, but the radionuclides are homogeneously distributed over the soil profile.

The application of these dose coefficients to radionuclides at a depth < 0.5 cm overestimates the external exposure, since the radiation is shielded by the overlying soil layers. The shielding effect increases with the penetration depth of the radionuclides. Furthermore, the photon energy is important: Low-energy photons are attenuated by a few mm of soil, whereas the mean free path of high energy photons is several cm.

The parameter $d_{b,r}$ gives the thickness of a soil layer to calculate the equivalent activity inventory per unit area for the applications of the dose coefficients of a planar radionuclide source.

A.2 Characteristics of considered radionuclides

The redox potential of soil, water and marine systems is a measure of electrochemical potential or electron availability within these systems /DEL 05/. Redox potential measurements allow for rapid characterisation of the degree of reduction and for predicting stability of various compounds that regulate nutrients and metal availability in soil and sediment.

A.2.1 Selenium

Selenium is a naturally occurring element that is widely but unevenly distributed in the earth's crust and is commonly found in sedimentary rock. Selenium is not often found in its pure form but is usually combined with other substances. Much of the selenium in rocks is combined with sulphide minerals or with silver, copper, lead, and nickel minerals. When rocks change to soils, the selenium combines with oxygen to form several substances, the most common of which are sodium selenite and sodium selenate. Some selenium compounds are gases; but hydrogen selenide is probably the only gaseous selenium compound that might pose a health concern in occupational settings.

Plants easily take up selenate compounds from water and change them to organic selenium compounds such as selenomethionine. Selenium is an essential element for humans and animals. Humans and animals can use both inorganic and organic selenium compounds. In the body, selenium helps prevent damage by oxygen to tissues, as does vitamin E. Selenium, however, is harmful to humans and animals when eaten in amounts that are not much higher than the amounts needed for good nutrition /UNI 89/.

Well fertilized agricultural soil generally shows selenium concentrations of about 400 mg/ton, since the element is naturally present in phosphate fertilizers and is often added as a trace nutrient. One of the leading sources of selenium contamination is coal mining and ash from coal fired power plants. When coal mining disturbs layers of earth containing high levels of selenium, runoff can carry this toxin to surface water or cause it to leach into groundwater. Once coal is burned, selenium is concentrated in the remaining ash. Ash disposal can also release toxic levels of selenium /SIE 09/.

In the late 1970's the landmark pollution episode took place at Belews Lake, North Carolina. Selenium released in the waste from coal-fired power plant entered the lake,

killed the fish community, and caused residual impact for many years after selenium inputs were stopped /LEM 04/.

Problems with Se occur also in the process of surface coal mining; overburden materials are brought to the earth's surface where they are exposed to oxidizing conditions. The oxidizing conditions decrease the stability of the Se containing sulphides and organic matter, which can eventually increase dissolved Se concentrations in backfill materials. Increased dissolved Se in backfill materials can potentially enhance Se mobility into groundwater environments.

During surface mining activities, materials previously in reducing environments become exposed to atmospheric conditions, thus increasing the potential of elevated levels of mobile and plant-available Se. Furthermore, the solubility and mobility of Se in areas disturbed by mining may result in higher levels of Se in surface water, groundwaters, and in resaturated backfill environments. The post mining land use of a majority of the abandoned and reclaimed coal mine lands is grazing land, pastureland and/or wildlife habitats. If Se mobilization is not attenuated, affected abandoned and reclaimed areas may not be suitable for post-mining land use or may require special resource management consideration.

Some plants can build up selenium to levels that are harmful to livestock feeding on these plants. In these areas, humans can be exposed to too much selenium if they eat locally grown grains and vegetables that have built up high levels of selenium. In fresh water containing high levels of selenium (e. g., agricultural water drainage basins in the San Joaquin Valley in California), fish may contain selenium at levels of more than 5 ppm. At one time in the Kesterson Reservoir in the San Joaquin Valley, some fish were found to contain 50 – 370 ppm selenium. The Kesterson Reservoir received sub-surface runoff water containing selenium from nearby agricultural areas, but has now been drained and filled /VAN 95a/, /VAN 95b/, /SHA 95/, /SHA 02/.

Selenium is highly sensitive to redox conditions and its biogeochemical properties differ considerably between different selenium species. The behaviour of Se compounds in soil is very complex and depends on a number of factors, including pH and chemical and mineralogical composition of soil, microbial interactions and the nature of absorbing surface. However, perhaps the most important influence on Se behaviour is the soil redox potential, E_h . Generally, the more reducing (low redox potential) the soil conditions, the more immobile Se becomes /ASH 06/. Selenium availability to vegetation is

also influenced by soil pH and redox potential (E_h), mode of occurrence, soil weathering, physiography and climate /MAY 91/, /SHA 10/. Soil temperature, moisture, concentrations of water-soluble selenium, the season of the year, organic matter content and microbial activity determine how fast selenium will move through soil. In other words, these factors determine its mobility. The major influences on uptake are soil pH and salinity /MAY 91/, /SHA 10/.

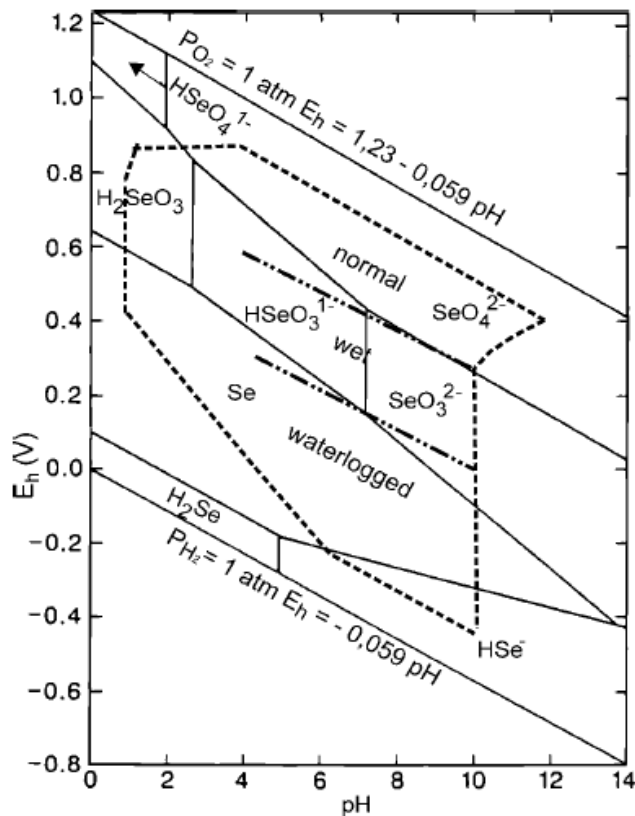


Fig. A.3 Se redox potential – pH diagram for an aqueous medium at 25 °C and 1 bar pressure for a dissolved Se activity of 10^{-7} mol L⁻¹ /SEB 98/

Four oxidation states of Se, Fig. A.3, may be present in soil and other environmental samples, which form different mineral and organic compounds /LID 11/, /COP 09/:

- Selenate (SeO_4^{2-}): weakly sorbed and generally soluble
- Selenite (HSeO_3^- and SeO_3^{2-}): more strongly sorbed than Se(VI), less soluble than Se(VI)
- Se(0): elemental Selenium, occurs in colloidal form only, very low soluble
- Selenide: co-precipitates with pyrite, very low soluble
- DMS: Dimethylselenide, volatile species

Tab. A.17 gives a summary of the most common Se compounds in the environment and where they are found. Speciation of Se is a key factor controlling its behaviour in soil, which depends on numerous factors (e. g. pH and soil solution composition) and is controlled by biotic or abiotic soil properties.

Tab. A.17 Common compounds of Se in the environment /LOS 97/

Compound (oxidation state)	Formula	Occurrence conditions
Selenide (-II)	Se^{2-}	Reducing environment, e. g., soils. Forms metal complexes; highly immobile
Dimethylselenide (DMSe)	$(\text{CH}_3)_2\text{Se}$	Gas formed by volatilization from soil bacteria and fungi
Dimethyldiselenide(DMDSe)	$(\text{CH}_3)_2\text{Se}_2$	Gas formed by volatilisation from plants and from microorganisms when Se is present at high concentrations (> 100 ppm)
Hydrogen selenide	H_2Se	Gas, unstable in moist air; decompose to Se(0) in water
Elemental selenium	$\text{Se}(0)$	Stable in reducing environments; (a) red crystalline alpha and beta monoclinic; (b) red glossy or black amorphous forms, all insoluble in water; oxidation/solubilisation very slow
Selenite(IV)		
Trimethylselenonium (TMSe ⁺)	$(\text{CH}_3)_3\text{Se}^+$	TMSe ⁺ is an important urinary metabolite of dietary Se and is made rapidly unavailable to plants by fixation and volatilisation
Seleneous acid	H_2SeO_3^-	Seleneous acid is protonated in acid/neutral conditions. Se(IV) is easily reduced to Se(0) by ascorbic acid (vitamin C) or sulphur dioxide in acidic environments by microorganisms. Readily available by Fe oxides, amorphous Fe hydroxides, and aluminium sesquioxides in soils
Selenium dioxide	SeO_2	Gaseous SeO_2 is formed as a product of fossil fuel combustion (sublimation temperature, 300 °C): dissolves in water to form seleneous acid
	HSeO_3^-	Common in soil
Selenate (VI)		
Selenic acid	SeO_4^{3-} H_2SeO_4^- HSeO_4^{2-}	Se(VI) is stable in well-oxidized environment, and very mobile in soils, hence easily available to plants. Slowly converted to more reduced forms: Not as strongly absorbed as Se(IV).

Elementary Se and selenide are fixed on minerals and not available for plants. In comparison with these two forms, selenite and selenate have a potential to be soluble, mobile and bioavailable, but in different ways. Selenite is absorbed much more strongly than selenate leaving selenate as the major form available for plant uptake /MAY 91/. The mobility of Se has the potential to increase with time in an oxidizing environment.

Fig. A.4 shows the biochemical cycle of selenium in a geological repository of radioactive waste /SEB 98/. Selenite is one of the most probable forms of Se in suboxic soils /COP 09/ and can be strongly associated with different solid phases including minerals. Metallic oxy-hydroxides (Fe, Al and Ti), particularly, are known to sorb significant amounts of Se(IV), as is also the case for some clay minerals. Soil organic matter can greatly modify the surface reactivity of inorganic minerals; these soils are the most reactive soils for Se retention and give partition coefficients ($L\ kg^{-1}$) of 1 800, 740, 490 and 150 for organic, clay, loam and sand soils, respectively /IAE 94/.

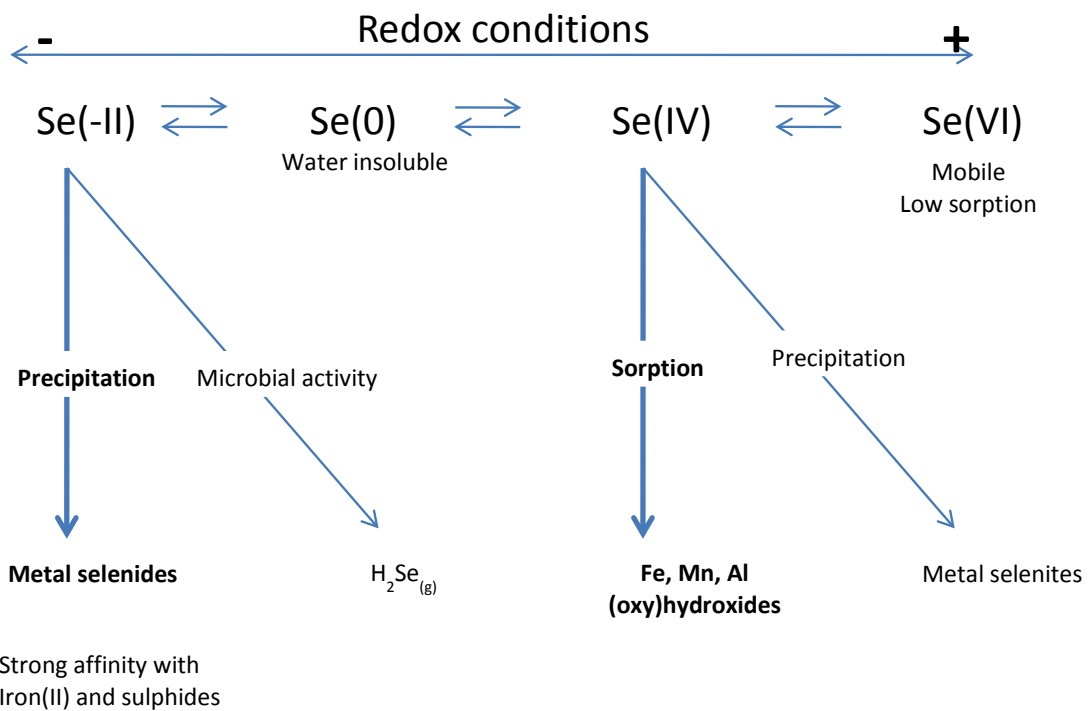


Fig. A.4 Biogeochemical cycle of selenium /SEB 98/

The scheme in Fig. A.5 shows, which Se oxides are present simultaneously in soil by pH's corresponding to agricultural conditions, and changing soil moisture. In the dry/normal soils, selenate and selenite could be find; in wet soils selenite and Se(0) could be located and in waterlogged soils mainly selenide could be found.

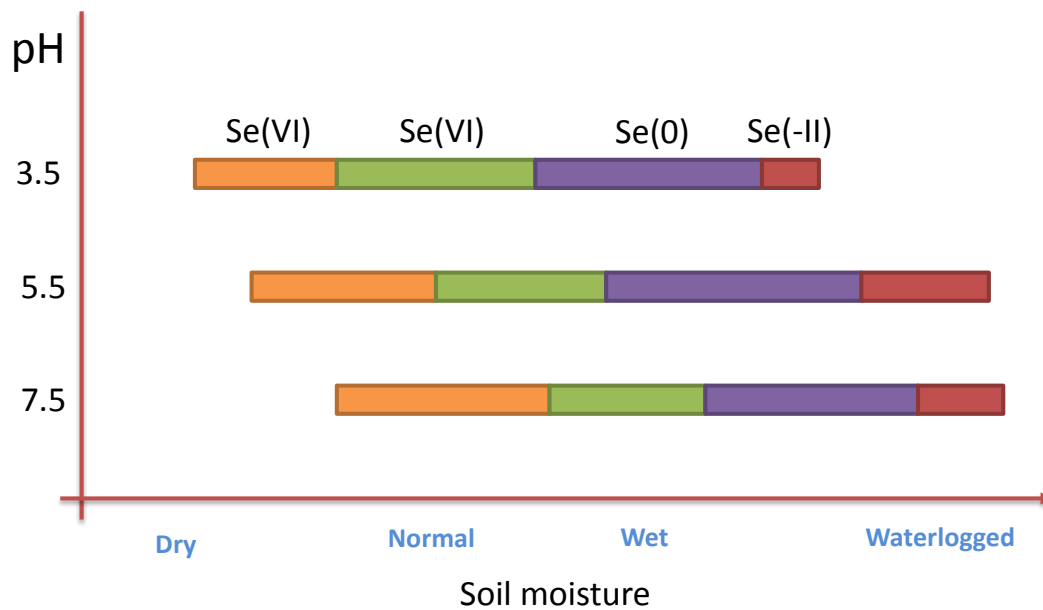


Fig. A.5 Scheme of Se oxides presence in soil depending on pH and soil moisture

Fig. A.6 illustrates the relationship of total Se to water-soluble Se in the profiles of different soil types. Total Se content in soil is not always in correlation with its content in plants because Se solubility is affected by several factors: soil reaction, the contents of sesquioxides, clay and organic matter /CUV 03/. The water soluble Se fraction is considered to be most available to plants. With exception of Solonchak and Arenosoils (low water-holding capacity), the content of water-soluble Se decreases with the depth of soil.

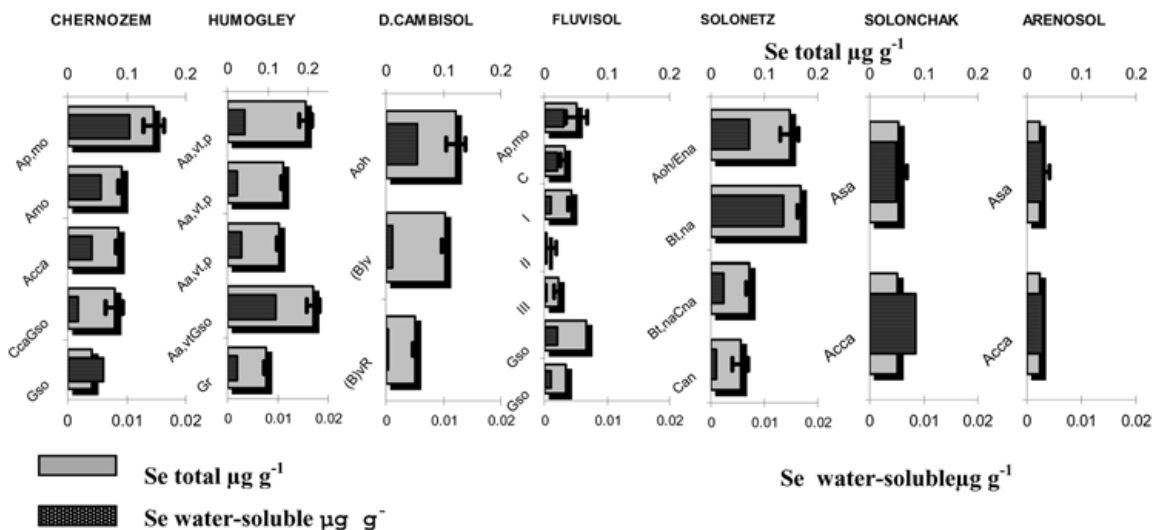


Fig. A.6 Contents of total and water-soluble Se in the profiles of the examined soils in the Vojvodina Province /CUV 03/

Selenite is the predominant form in humid regions and acidic soils. It is adsorbed on sesquioxides and clay minerals and thus not readily available to plants. In well aerated alkaline soil in semiarid regions, Se is found in the form of selenate, which is not absorbed, does not form insoluble salts and is readily available to plants. Selenium is expected to show a very complex behaviour under climate changing conditions.

A.2.2 Technetium

Technetium is a radioactive element of potential long-term importance in the environment because the half-life of the long-lived isotope ^{99}Tc is 210 000 y. The heptavalent oxidation state is common for technetium. In this state, technetium can be present as the pertechnetate (TcO_4^-) anion, which is highly soluble in water, and is thus potentially mobile in biogeochemical cycles. /KOC 01/.

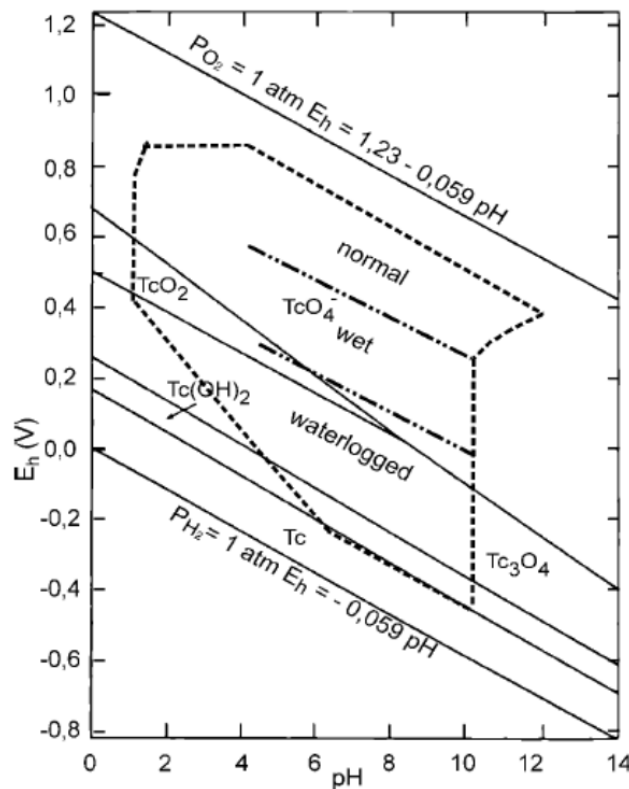


Fig. A.7 E_h -pH diagram for technetium. The dotted line delineates redox limits of soils and micro-organisms

Technetium can be found in the valences 0, +2, +3, +4 and +7, the most important forms in soil are the +4 and +7 forms. The behaviour of technetium in the soil is mainly controlled by the redox potential of the soil. The dependence of the speciation of tech-

netium on both pH and E_h is illustrated in Fig. A.7. In well aerated soils, pertechnetate (+7) is the stable technetium speciation. It behaves similar to anions, such as sulphate, selenate and molybdate. This means that sorption to soil components can be considered negligible. Migration experiments using soil columns show that there is only little delay of the migration of pertechnetate compared to that of tritium, therefore the pertechnetate mobility in soil is very high. At pH 7, pertechnetate in soil can only be found at an $E_h > 200$ mV. If the E_h drops below this value, the pertechnetate is reduced to TcO_2 , which has been clearly verified by sorption experiments with technetium in groundwater/sediment systems. Low redox potentials occur in water-logged soils or in compacted soils where the aeration is inhibited. Oxygen deficiencies may also be induced by a high oxygen demand due to an enhanced degradation of organic matter. Various investigations suggest that pertechnetate is reduced by soil organisms. Bacteria that are able to reduce sulphate have been shown to be able to reduce pertechnetate into Tc (+4), as well. Therefore, technetium is often associated with organic matter. However, it is also possible that technetium accumulates in soil horizons with reducing conditions as found in gley soils.

The scheme on Fig. A.8 shows, which Tc oxides present simultaneously in soil by pH's corresponded to agricultural conditions, and changing soil moisture.

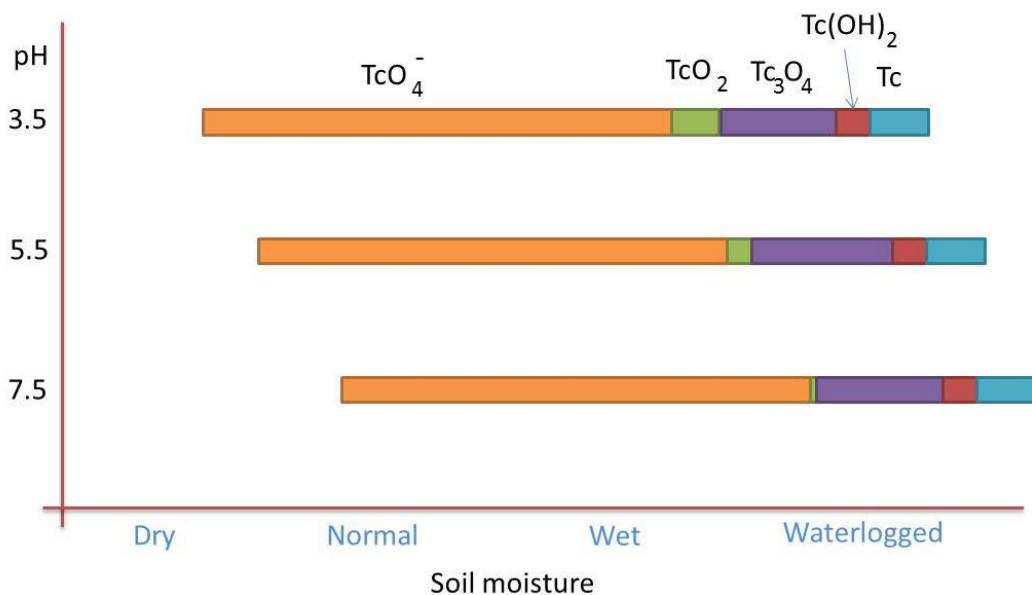


Fig. A.8 Scheme of Tc oxides presence in soil depending on pH and soil moisture

A.2.3 Neptunium

Neptunium is an important constituent in nuclear waste and one of the most problematic actinides for long-term storage of nuclear waste. While the initial neptunium concentration in spent nuclear fuel is relatively small (0.03 %), its concentration increases with time due to the radioactive decay of ^{241}Am ($t^{1/2} = 432.7$ years). Because of its long half-life ($2.14 \cdot 10^6$ years), ^{237}Np will become the major contributor to the radiation inventory of nuclear waste repositories after about 100 000 years. The critical role of neptunium in nuclear waste disposal and risk assessments attracts great attention to its geochemical behaviour.

Apart from the limited existence of neptunium in the vicinity of natural nuclear reactors, like Oklo, natural neptunium is absent in the environment. Traces of manmade neptunium are found in the environment that originates from weapon fallout. According to Bunzl et al., between 1954 and 1983, approximately 0.18 Bq/m^2 of ^{237}Np were deposited on a site in South Germany. Neptunium occurs in the oxidation states +3, +4, +5, +6 and +7. The Eh-pH diagram for neptunium is shown in Fig. A.9 /KOC 01/.

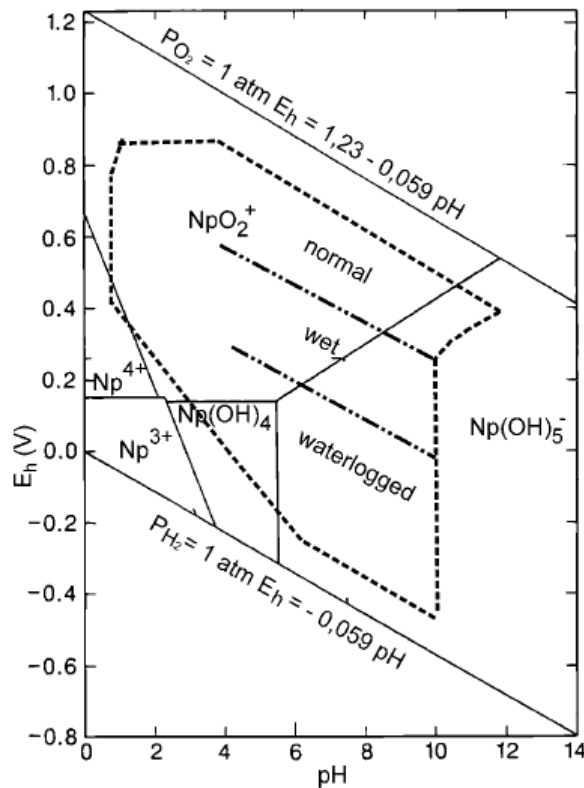


Fig. A.9 Eh-pH diagram for neptunium. The dotted line delineates redox limits of soils and micro-organisms

The 4- and 5-valent neptunium species are primarily relevant for the soil conditions. Neptunium (+5) is stable over a wide range of Eh and pH values and for the conditions of the temperate climate it is the most important species in soil. Below Eh values of about 200 mV and moderate temperate pH values, neptunium is reduced to Np (+4) which is sorbed considerably more strongly on mineral surfaces than Np (+5). The pentavalent neptunium species is classified as potentially mobile in the geosphere. In sorption experiments of various groundwater-sediment samples, under aerobic conditions (Eh > 300 mV, pH > 7) sorption ratios were found to be below 5 ml/g, whereas under anaerobic conditions at Eh values of < 100 mV, sorption ratios might increase to above 1 000 ml/g. NpO_2^+ is sorbed in the soil to aluminium and especially iron oxides as well as to clay, silt and organic matter. Neptunium forms various complexes with inorganic and organic ligands. The stability of neptunium complexes depends from the complex forming ligand and decreases in the order CO_3^{2-} , OH^- , HPO_4^{2-} , SO_4^{2-} , Cl^- and NO_3^- , whereby the stability of the pentavalent neptunium is weaker than of Np (+4). Furthermore, neptunium is complexed more effectively by the carboxyl groups (e. g. of fulvic and humic acids), than by alcoholic and hydroxylic groups. The stability of humic complexes decreases in the order thorium (+4) → americium (+3) → europium (+3) → uranium (+6) → neptunium (+5), as a result of strength of electrostatic interaction between actinide and carboxyl group and net charge of the actinide. Fig. A.9 demonstrates that the relative low sorption of Np (+5) causes a theoretically higher mobility in soils compared to other actinides, especially in the range of Eh-pH conditions of arable soils. At sites in the vicinity of the reprocessing plant at Sellafield, the mobility of neptunium on acid, well aerated soils was higher than that of americium, plutonium and cesium. Neptunium had migrated into the deeper soil to a greater extent and had been less adsorbed to organic matter and iron oxides than americium, plutonium or cesium. In contrast, Bunzl et al compared the mobility of fallout neptunium, americium and plutonium on a brown earth sample and found little variation among these elements. The higher neptunium mobility on acid soils with a high Eh is probably due to the dominance of Np (+5) which is less adsorbed to inorganic and organic soil constituents than other actinides.

A.2.4 Uranium

Uranium is a ubiquitous element. It is found in nearly all rocks and soils in concentrations of 1 – 10 mg/kg. Uranium occurs in valences of +3, +4, +5 and +6. The E_h -pH diagram of uranium is given in Fig. A.10 /KOC 01/.

It is evident that for the conditions in soil, the valences +4 and +6 are most important. Uranium (+4) dominates at $E_h < 200$ mV, which is typical for water-logged to wet soils, whereas uranium (+6) predominates in sufficiently aerated soils. Detailed investigations about the speciation of uranium in soils are very scarce. More knowledge has been gained during geochemical investigations of uranium. Uranium (+4) is rather insoluble; it can be complexed in only small amounts by various inorganic ligands such as fluoride, chloride, sulphate and phosphate. The solubility of uranium (+6) is much higher, it can be complexed by fluoride, sulphate, carbonate as well as phosphate. The mobility of uranium in groundwater and soils is markedly enhanced due to the formation of uranium-carbonate-complexes, a main inorganic form of transport at pH values > 6.5 . Furthermore, a variety of sorption reactions are involved in the dynamic of uranium in soil. Uranium interacts with all components of the soil matrix such as clay minerals, aluminium and iron oxides, the organic matter and micro-organisms. The bivalent uranyl-ion $[UO_2^{2+}]$ is sorbed to the negatively charged surfaces of clay minerals, sesquioxides and organic compounds. The sorption is controlled by pH, the zero point of charge of the sorbing clay minerals and the concentration of potential complexing ligands in the soil solution. Uranium may be sorbed to clay minerals at different binding sites.

In general, there is a competition between the sorption to Fe/Al oxides and hydroxides and the complexation of uranium. With increasing pH, more negatively charged binding sites are available on mineral surfaces, e. g. iron oxides and aluminium oxides due to the release of protons. On the other hand, with rising pH, there is a trend to increasing carbonate concentration, which is the most important complexing agent for uranium. Above pH 6, the fraction of uranium (+6) that is complexed by carbonates increases, which tends to enhance the uranium mobility in soil. In uranium-rich shaley soils of an intensively managed and irrigated agricultural area of Colorado, USA, an enhanced leaching of uranium with the drainage water could be observed. This was due to the solubility of the parent material consisting mainly of gypsum which forms soluble uranium compounds. In contrast, uranium applied with phosphate fertilizer was found to be a rather insoluble Ca-P-U precipitate. Furthermore, the uranium mobility in soil is affected by the sorption to or incorporation in micro-organisms. Uranium (+6) may be reduced and precipitated enzymatically to uranium (+4) by sulphate or iron-reducing bacteria. This occurs mainly when E_h values drop below -100 mV. On normal arable soils, such conditions may happen during time periods with enhanced wetness, e. g. after flooding (at sites near rivers) or after heavy rainfall. Organic compounds e. g. siderophores, extracted by plant roots, bacteria or fungi that are able to complex iron, may

act as complexing agents for uranium as well. Such processes may cause enhanced uranium mobility in the rooting zone.

In long-term investigations on the fate of uranium in soil applied with phosphate fertilizer, typical amounts of phosphates caused an increase of the uranium content of soil. However, this increase was limited to the upper soil layer. A detailed analysis showed that most of the uranium was associated with organic matter, indicating the importance of the organic matter for the long-term behaviour of uranium.

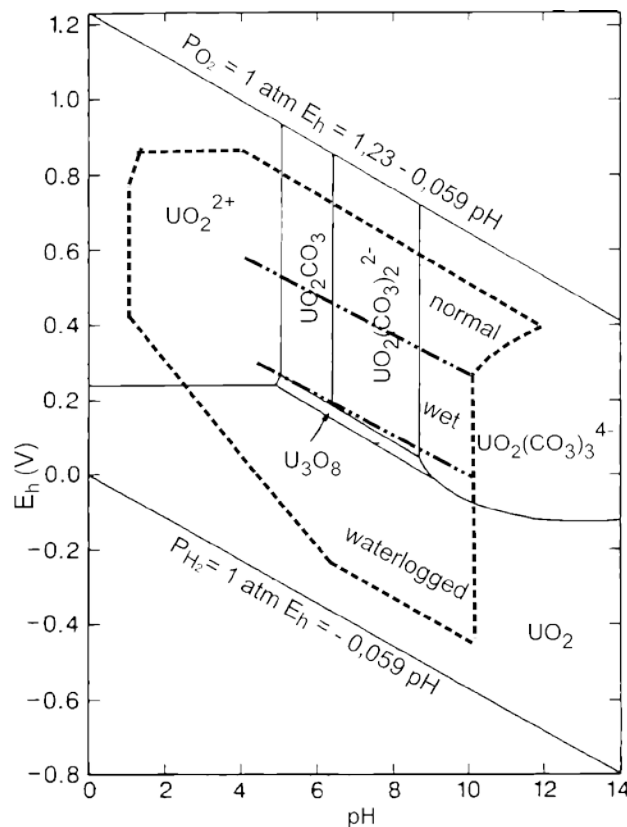


Fig. A.10 E_h -pH diagram for uranium. The dotted line delineates redox limits of soils and micro-organisms

A.2.5 Iodine

Iodine is a ubiquitous element and the concentrations found in soil are in the range of approximately 0.5 – 5 mg/kg. Iodine is released from the sea; therefore, in general, the iodine content of soils decreases with increasing distance from the sea. The E_h -pH diagram for iodine is given in Fig. A.11. Iodine is found in an elemental form I_2 (0), as iodide I^- (-1) and iodate IO_3 (+5). However, iodate is stable only in soils with high pH and

a very high E_h , therefore it is of limited relevance for the iodine speciation in soil. The most important iodine species is iodide, which is stable over a wide range of redox potentials (-200 to $+500$ mV). A considerable sorption of iodide on mineral constituents is limited to soils containing higher amounts of anion adsorbing minerals, e. g. allophane and halloysite. Sorption experiments with two Japanese soils rich in allophanes but varying in pH value, showed that iodine sorption is unspecific and increases with decreasing pH value according to the reaction: $\text{Al-OH} + \text{H}^+ \rightarrow \text{Al-OH}_2^+$. The iodate sorption appears to be similar to the phosphate sorption, where the anions are complexed by ligand exchange with aluminium and iron oxides.

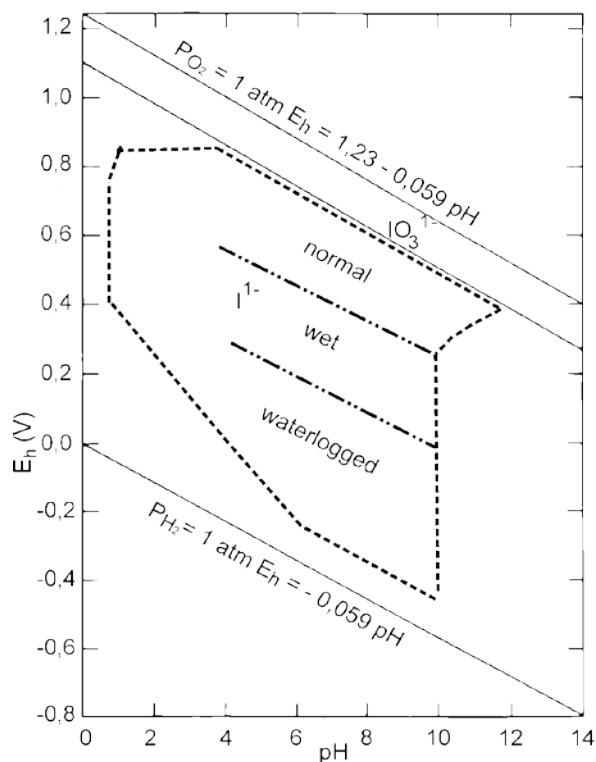


Fig. A.11 E_h -pH diagram for iodine; the dotted line delineates redox limits of soils and micro-organisms

Kaplan et al. reported on sediments low in organic matter of an arid environment, where appreciable amounts of iodide were sorbed on the clay mineral illite. However, the iodide and iodate adsorption is limited to soils with specific clay minerals. For middle European conditions, this process is of minor importance. The behaviour of iodine is closely linked with the dynamics of the organic matter in soil. Depth profiles of iodine in soils show an accumulation in the upper layer that is enriched in organic carbon. Several investigations indicate that iodide is incorporated into the organic material by the microbiological activity. Even in well drained sandy soils a very low mobility of io-

dine was observed. Results of batch experiments showed an increase of the K_d value with increasing organic matter in soil. It is not clear what kind of specific processes are involved in the iodine fixation by organic matter. Experiments show that the iodine fixation on non-sterilized soils is much faster than in sterilized ones. A further process potentially important for the long-term fate of iodine in soil is the volatilization of iodine. Volatile iodine species are I_2 and CH_3I . Measurements by *Muramatsu et al.* /MUR 04/ indicate that 90 % of the volatile iodine in soil consists of methyl iodide. It was also found that the exudation of methyl iodide from water-logged soil is much higher than for well aerated soils.

Anaerobic soil conditions may cause a mobilisation of iodine. Gaseous iodine is also released from vegetation, mainly under reducing soil conditions. *Amiro* estimated that in terrestrial ecosystems, the contribution of gaseous iodine releases of living vegetation to the stable iodine concentration in the atmosphere may probably amount to 0.1 % /AMI 89/. In this way, a direct radioactive iodine transfer from soil to other compartments would be feasible. On flooded rice fields, an increase of solubility can be observed resulting in a dropdown of the K_d value (solid/liquid) from about 6 L/kg at drained conditions to 0.6 L/kg in flooded soils, leading also to a higher transfer factor of iodine in rice plants. In lysimeter experiments, *Pel* compared the iodine uptake by plants for varying water tables. The highest iodine uptake was found in water-logged soils, indicating the remobilisation of iodine from the organic matter. In water-logged soils the microbiological activity decreases due to the lack of oxygen. Iodine is thought to be incorporated into the microflora, during the degradation of which iodine is released into the soil solution in anaerobic periods. This finding is consistent with the results of *Behrens*, who found a close relationship between the redox potential and the iodine sorption to organic matter.

A.2.6 Cesium

Characteristically for cesium is its absorption by mineral part of soil. The element is embedded in the crystalline lattice of clay minerals, strongly bound to fine disperse part of soil. The cesium is absorbed most intense in vermiculite, phlogopite, hydroflogopite, askanit, humbrin. For example, seven years after Chernobyl, the proportion of cesium-137, fixed in mineral soil increased in the gray forest soils in 2.5 times, in podzol 4.5 times, in chernozem 7 times and can reach 80 – 95 % of the whole content of this element in the soil. Cesium binds strongly to soil organic matter, forming, in particular,

humates and fulvates, which are characterized by a much greater mobility. Water-soluble organic substances formed during the decomposition of vegetation also increase the mobility of the metal. There are two mass transport mechanisms of caesium into the soil: fast (due to movement with fine particles) and slow (due to the movement of water-soluble forms). In the loamy soils only a slow migration has been observed; in sandy loam and sand the slow and fast, with a predominance of the last.

The accumulation of Cs in floodplain soils due to the additional introduction of the mechanical suspensions during the floods has been observed. Cs in floodplain soils are generally retained in the upper 5 cm layer. However, in cases where the surface horizons of floodplain soils are light-textured layers with low humus content, Cs leached from these horizons in the lower and retained there. Cs migration capacity increased also in some peat soils. Japanese researchers say evidence of penetration of ¹³⁷Cs in the rock (unweathered basalt) to a depth of 3 – 5 cm.

A.2.7 K_d model

Radioactive contaminants can be fixed in soil by ion exchange. The intensity of such an interaction can be characterised by the distribution coefficient K_d . K_d is the ratio of concentration of radionuclides absorbed in soil and concentration of these radionuclides in solution after the system has reached equilibrium.

A high value of K_d means that the contaminant is bound by soil minerals and its migration is low, and *vice versa*. K_d is a most common parameter describing the migration of contaminants in soil.

Despite of the wide use of this parameter, the applicability of K_d is limited. The K_d is strongly depended on the physic-chemical conditions of the local soils, and can vary inside one place by a factor of up to 1 000 (Table 11.2). The adsorption of radionuclides depends on many different factors: vital functions of plants and bacteria; oxidation stage of radionuclides (can change with time); the content of clay, sand and organic matter in soil etc. Moreover, five different methods of K_d measurements could also show different results. More complex models could overcome these limits, but they need much more detailed information about the investigated territories. Tab. A.18 shows reported example K_d values for various oxidation levels of Se.

Tab. A.18 Summary of reported K_d values for Se /VOG 08/

Reference	Soil type	Se species considered	Solid/liquid partitioning value (K_d) [L/kg]	Comment
Yi-Lin Jan et al. (2006)	sorption on granite in groundwater system	Se(IV)	5.7	batch experiment
	sorption on granite in seawater system	Se(IV)	8.6	batch experiment
Wang et al. (2005)	calcareous soil, pH = 7.8	Se(IV)	34.8	batch experiment
	calcareous soil, pH = 7.8	Se(IV)	21.5	column experiment
Dong et al.(1999)	red earth, pH = 7.0	Se(IV)	477	batch experiment
Sheppard and Thibault (1990)	sandy soil	not specified	150	
	loamy soil	not specified	490	
	clayey soil	not specified	740	
	organic soil	not specified	1 800	
Thorne et al. (2001)	brown acidic soil	not specified	18	
	colluvial soil	not specified	35	
	brown rendzina soil	not specified	70	
	organic soil	not specified	170	
Singh et al. (1981)	mineral soil	Se(IV)	3.9	data cited by Thorne et al. (2001)
	mineral soil	Se(VI)	26	
	calcareous soil	Se(IV)	14	
	calcareous soil	Se(VI)	40	
	high organic carbon	Se(IV)	40	
	high organic carbon	Se(VI)	73	
	saline soil	Se(IV)	0.26	
	saline soil	Se(VI)	9.2	
	alkal. soil (pH = 10)	Se(IV)	6.4	
alkal. soil (pH = 10)	Se(VI)	8.8		

Tab. A.19 shows the range in measured K_d values for six radionuclides for representative geologic media, including alluvium, carbonate rock, and volcanic tuffs (devitrified, vitric, and zeolitic) encountered at the NTS /HU 08/. Generally speaking, the largest K_d

values are observed in the zeolitic tuff and in alluvium, and the smallest values in vitric tuff. Sorption of Pu and Am onto carbonate rock is appreciable, and Np sorption to carbonate rock is higher than other rock types.

Tab. A.19 Radionuclide sorption on different rock (compiled from /STO 08/)

Radionuclide sorption on different rock						
Element	Sample type	Number of Samples	Distribution Coefficients (mL/g)			
			Min	Max	Mean	StD
Technetium	Alluvium	17	0	12	2.16	3.48
	All tuffs		0	0		
Iodine	Alluvium	14	0	24.5	5.74	4.03
	All tuffs		0	0		
Uranium	Alluvium	48	0.9	60	6.36	5.04
	Carbonate rock		0	132		
	Devitrified tuff	75	0	15	2.51	2.29
	Vitric tuff	59	0	12	1.89	1.7
	Zeolitic tuff	176	0	9 423	45	423
Neptunium	Alluvium	30	1.83	22	8.57	5.08
	Carbonate rock		< 100	5 000		
	Devitrified tuff	421	0	2 353	19	166
	Vitric tuff	400	0	526	3.17	29
	Zeolitic tuff	430	0	22	3	2
Plutonium	Alluvium	24	230	21 000	4 091	4 448
	Carbonate rock		100	10 000		
	Devitrified tuff	118	6	1 900	125	168
	Vitric tuff	71	23	1 810	516	472
	Zeolitic tuff	110	19	2 000	260	242
Americium	Alluvium	24	3 200	1 400	174,4	214
	Carbonate rock		150	300		
	Devitrified tuff	35	79	12 000	1 845	1 834
	Vitric tuff	8	860	2 050	1 354	398
	Zeolitic tuff	25	470	33 000	5 204	7 757

In the same publication /STO 05/ are presented measured K_d of each radionuclide onto four different aquifers under six different redox conditions (Fig. A.12 to Fig. A.16):

- The first batch test (Test A) was carried out under atmospheric conditions.
- Tests B and C were conducted under a gas composition of about 1 and 0.1 % O_2 .
- Tests D and E were all conducted at 0.1 % O_2 level, with test tubes further spiked with a reductant ($FeCl_2$ for Test D or Na_2S for Test E).

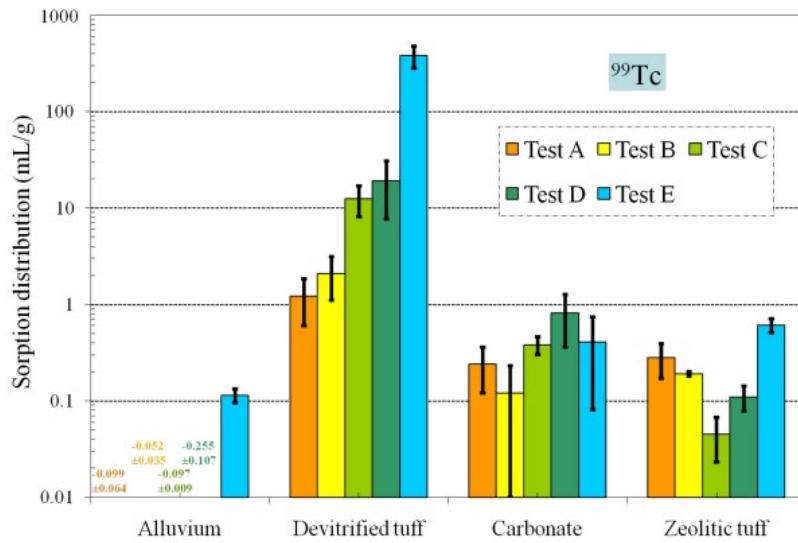


Fig. A.12 Change of ^{99}Tc K_d values under five different redox conditions for different aquifer materials

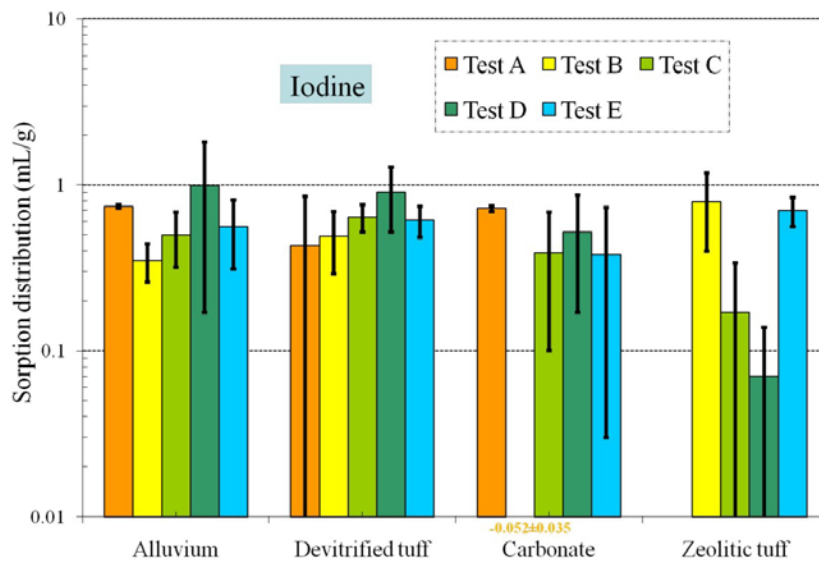


Fig. A.13 Change of iodine K_d values under five different redox conditions for different aquifer materials

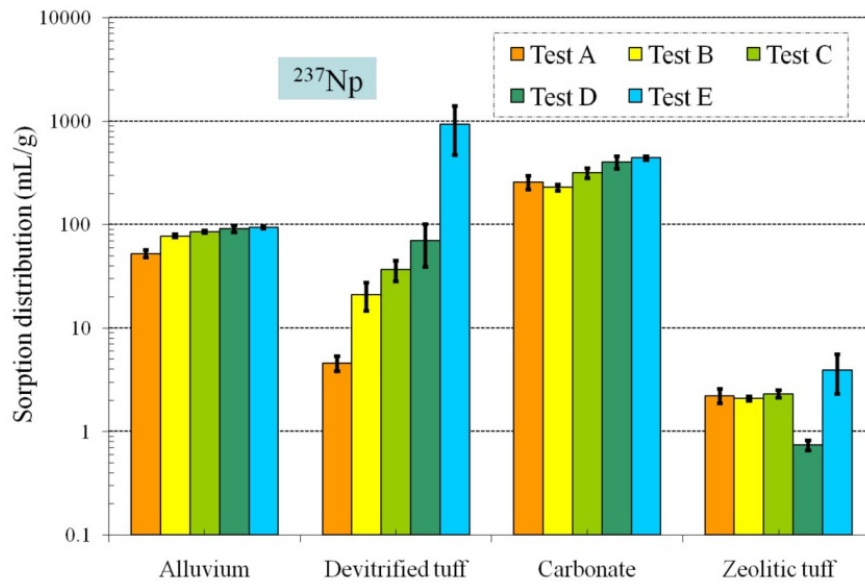


Fig. A.14 Change of ^{237}Np K_d values under five different redox conditions for different aquifer materials

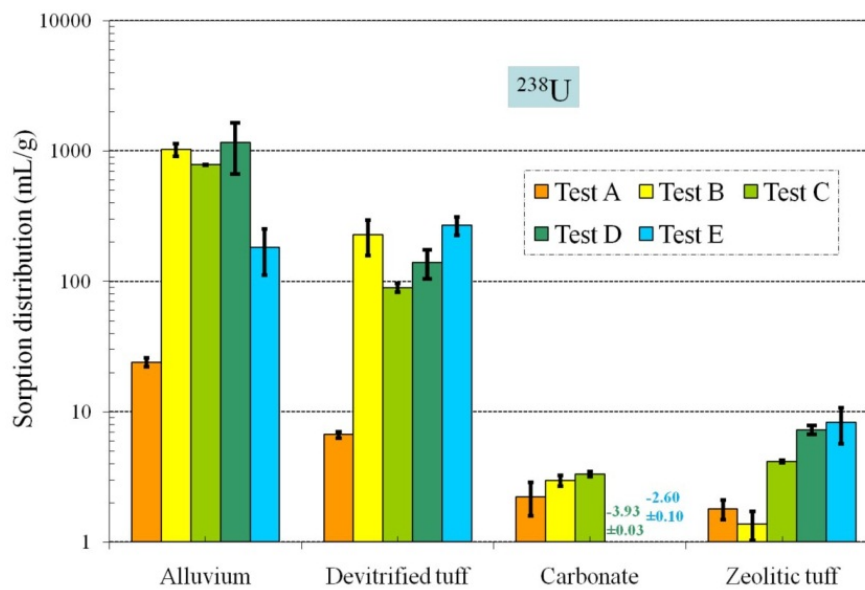


Fig. A.15 Change of ^{238}U K_d values under five different redox conditions for different aquifer materials

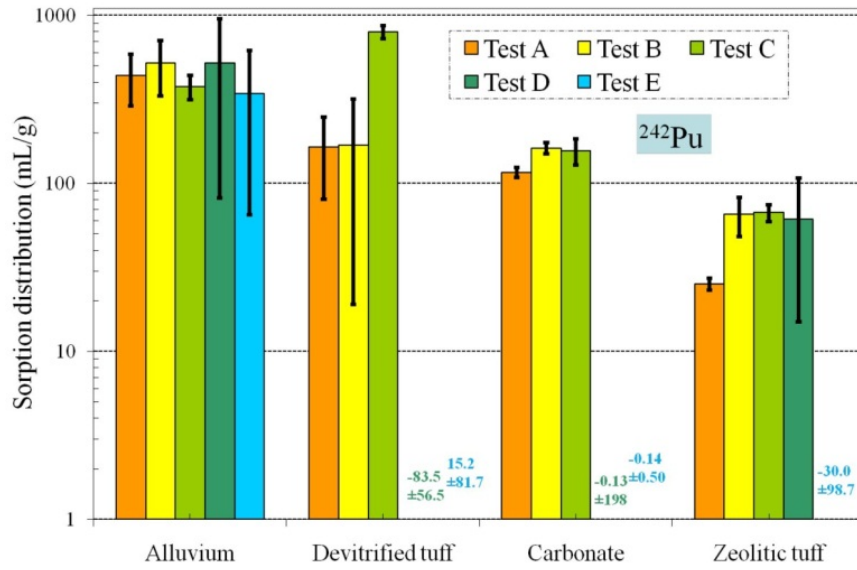


Fig. A.16 Change of ^{242}Pu K_d values under five different redox conditions for different aquifer materials

A.3 Soil classification (FAO)

Corresponding to the soil texture, the following soil types are considered: sand, loam, clay and organic. *Texture* refers to the size of the particles that make up the soil (Tab. A.20). The terms *sand*, *silt*, and *clay* refer to relative sizes of the soil particles. Sand, being the larger size of particles, feels gritty. Silt, being moderate in size, has a smooth or floury texture. Clay, having the smaller size of particles, feels sticky.

Soils were grouped according to the percentages of sand and clay in the mineral matter, and the organic matter (OM) content in the soil. This defined the 'texture/OM' criterion, which is similar to the criterion followed in TRS-364 /IAE 94/. For the mineral soils, the following three groups were created according to the percentages of sand and clay in the mineral matter: sand (sand fraction $\geq 65\%$, clay fraction $< 18\%$), clay (clay fraction $\geq 35\%$) and loam (all other mineral soils). A soil was included in the 'organic' group if the organic matter content was $\geq 20\%$. Finally, an 'unspecified' soil group was created for soils without characterization data, and for mineral soils with unknown sand and clay contents. More details of the typical textures of the mineral soil classes are given in the accompanying TECDOC /IAE 10/.

Tab. A.20 Particle sizes of various soils

Soil	Particle Diameter [mm]
Clay	below 0.002
Silt	0.002 to 0.05
Very fine sand	0.05 to 0.10
Fine sand	0.10 to 0.25
Medium sand	0.25 to 0.5
Coarse sand	0.5 to 1.0
Very coarse sand	1.0 to 2.0 _d

The *Soil Texture Triangle* gives names associated with various combinations of sand, silt and clay. A *coarse-textured* or *sandy* soil is one comprised primarily of medium to coarse size sand particles. A *fine-textured* or *clayey* soil is one dominated by tiny clay particles. Due to the strong physical properties of clay, a soil with only 20 % clay particles behaves as sticky, gummy clayey soil. The term *loam* refers to a soil with a combination of sand, silt, and clay sized particles. For example, a soil with 30 % clay, 50 % sand, and 20 % silt is called a *sandy clay loam*. Tab. A.21 shows the usual ranges of values for various soil parameters for the soil groups adopted /IAE 09/.

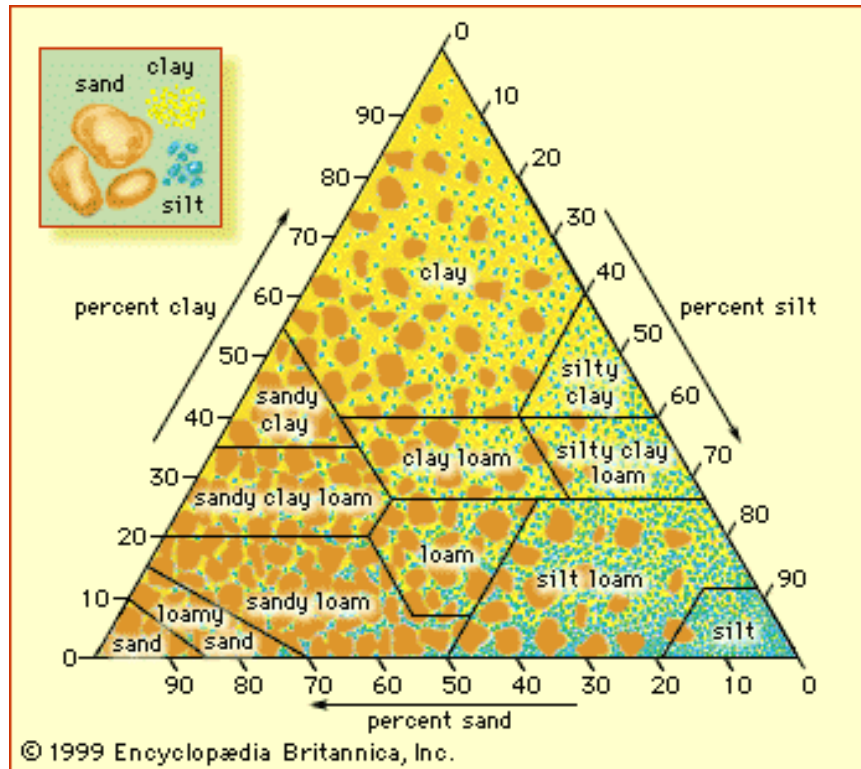


Fig. A.17 Soil Textural Triangle: Based on the triangle, a loamy soil has 40 % sand, 20 % clay and 4 % silt; a sandy loam has 60 % sand, 10 % clay and 30 % silt

Tab. A.21 Soil parameters

Soil Group	pH	%OM	CEC, [mol _c /kg]	Sand content in the mineral matter fraction	Clay content in the mineral matter fraction
Sand	3.5 – 6.5	0.5 – 3.0	3.0 – 15.0	≥ 65	< 18
Loam	4.0 – 6.0	2.0 – 6.5	5.0 – 25.0	65 – 82	18 – 35
Clay	5.0 – 8.0	3.5 – 10.0	20.0 – 70.0	-	≥ 35
Organic	3.0 – 5.0	≥ 20	20.0 – 200	-	-

A.4 Examples of dried out Lakes

One example of a naturally drying lake is the Nördlinger Ries in Germany. The town Nördlingen, 30 km from Munich, is located on the bed of an ancient meteorite lake. The basin of this lake has a diameter of 22 km. On the bottom of this basin, there is sediment with 35 m thickness, and a crater with 700 m depth and 10 km diameter. The impact of the meteorite occurred 15 million years ago. There are many examples of artificial drying of lakes in case of shortage of agricultural lands. In Italy, not far away from Rome, the basin Fuchino is situated. In the past it was a big karsts lake with about 150 km² surface. During the last century the lake was drained, and now there are plantations of tomatoes, maize, beets etc. Flat low-lying areas build by lake sediments are very valuable arable lands.

The process of drying of lakes out could be observed now in different parts of the Earth. Iran's Lake Oroumeih (also spelled Urmia) is the largest lake in the Middle East and the third largest saltwater lake on Earth. But dams on feeder streams, expanded use of groundwater, and a decades-long drought have reduced it to 60 percent of the size it was in the 1980s. Light blue tones in the 2010 image (Fig. A.18) represent shallow water and salt deposits. Increased salinity has led to an absence of fish and habitat for migratory waterfowl. At the current rate, the lake will be completely dry by the end of 2013.

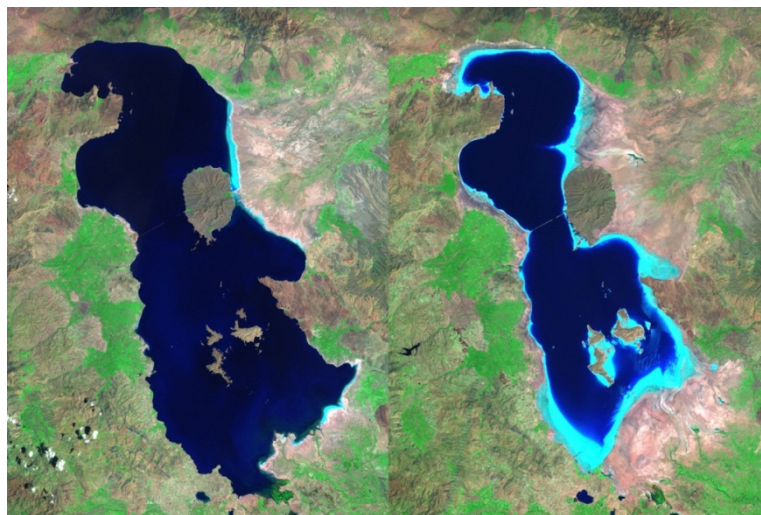


Fig. A.18 Lake Oroumeih, Iran; Left: August 1985; Right: August 2010

Persistent drought has shrunk Lake Chad (Fig. A.19), once the world's sixth largest lake, to about one-twentieth of the size it was in the 1960s. Only 16 to 26 feet (5 to 8

meters) deep in “normal” times, small changes in depth have resulted in large changes in area. As the lake has receded, large wetland areas (shown in red) have replaced open water /NAS 12/

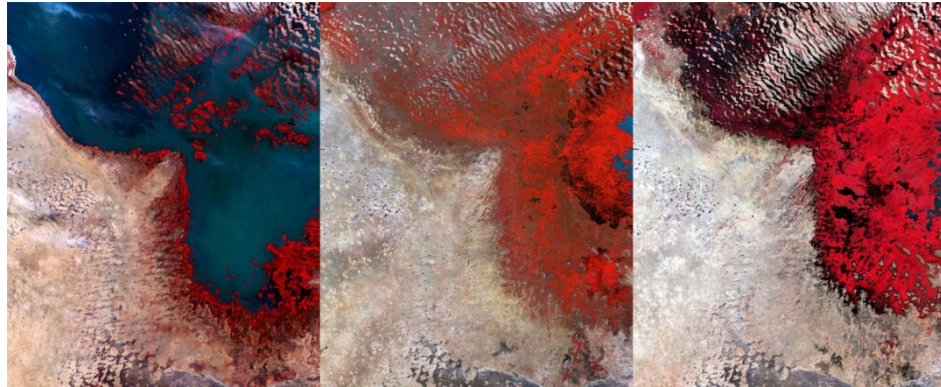


Fig. A.19 Lake Chad, Africa. Left: December 8, 1972; Middle: December 14, 1987; Right: December 18, 2002 /NAS 12/

Another example of anthropogenic impact on lakes is Tulare Lake, see Fig. A.20 /WIK 12/, a fresh-water dry lake with residual wetlands and marshes in southern San Joaquin Valley, California. Until the late 19th century, Tulare Lake was the largest freshwater lake west of the Mississippi River and the second largest freshwater lake in the United States based upon surface area, but it dried up after its tributary rivers were diverted for irrigation.

Tulare Lake was completely dry by the end of the 19th century. The Kaweh, Kern, Kings and Tule Rivers were dammed upstream in the Sierra Nevada Mountains, turning their headwaters into a system of reservoirs. In the San Joaquin Valley, canals were built to deliver that water and divert the remaining flows for agricultural irrigation and municipal water uses.

The lake bed is now a shallow basin of fertile soil, within the Central Valley of California and the most productive agricultural region of the United States. After a century of irrigation, however, soil salination is becoming a concern.

Although now dry, the lake occasionally reappears during floods following unusually high levels of snow melt, as it did in 1997.

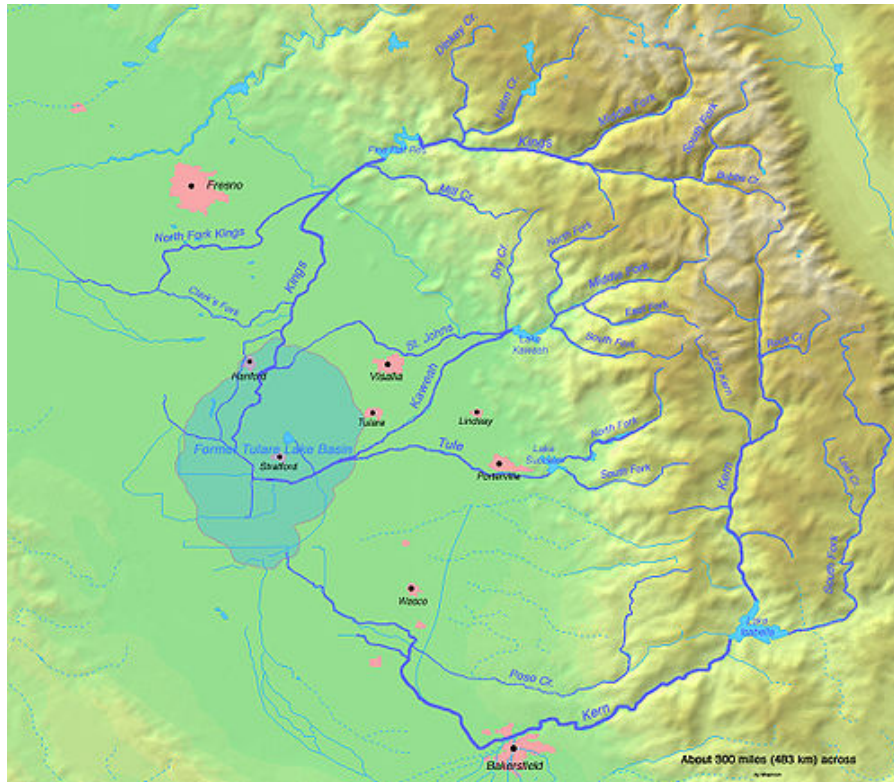


Fig. A.20 Tulare Lake basin: Map of the watercourses

An open question for the radioecological modelling of a dried lake bed as a biosphere for agriculture is the behaviour of redox sensitive radionuclides such as ^{79}Se and ^{99}Tc . Their availability for plant uptake strongly depends on soil humidity which is determined by climate change. To consider possible use of dried-out lakebeds for agricultural purpose in the future, we have to take into account the behaviour of redox sensitive radionuclides, ^{79}Se , ^{99}Tc , ^{237}Np , and ^{129}I etc. In reducing environments, these materials become exposed to changing soil and atmospheric conditions due to agricultural activity (ploughing), leading to an up to 1 000 times increase of their mobility and availability for plants.

A.4.1 Peatland classification

From the various criteria, water supply and nutrient status are the most fundamental for classifying Peatlands. A gradient exists from nutrient-rich, alkaline water (fens) to nutrient-poor, acidic water (bogs), and so Peatlands generally are divided in two broad classes /CHA 02/:

Ombrotrophic: Raised or blanket bogs that receive all water and nutrients from direct precipitation. Neither groundwater nor runoff from surrounding land reaches the surface of the bog. Rain and snow provide the water source, and nutrients are derived from whatever is blown in-dust, leaves, bird droppings and feathers, spider webs, animal fur, etc. Water chemistry tends to be acidic, and nutrients for plant growth are in short supply. Few plants can survive such extreme conditions, namely *Sphagnum* (peat moss) and pine.

Minerotrophic: Fens located in depressions that receive surface runoff and/or groundwater recharge from surrounding mineral-soil sources. Nutrients are more abundant and water is more alkaline, which is suitable for the growth of a wide range of plants and which give rise to greater floristic diversity compared to bogs. The terms *oligotrophic* and *eutrophic* refer to more nutrient-poor and more alkaline, calcium-rich fens, respectively.

Fens are located in depressions and are characterized by flat or concave surface. In addition to precipitation, their nutrition is provided by groundwater or river water which both, have a significant high content of mineral nutrients. Therefore, autotrophic vegetation, i. e. sedges, horsetails, mosses, green and wood-alder, birch, develops there.

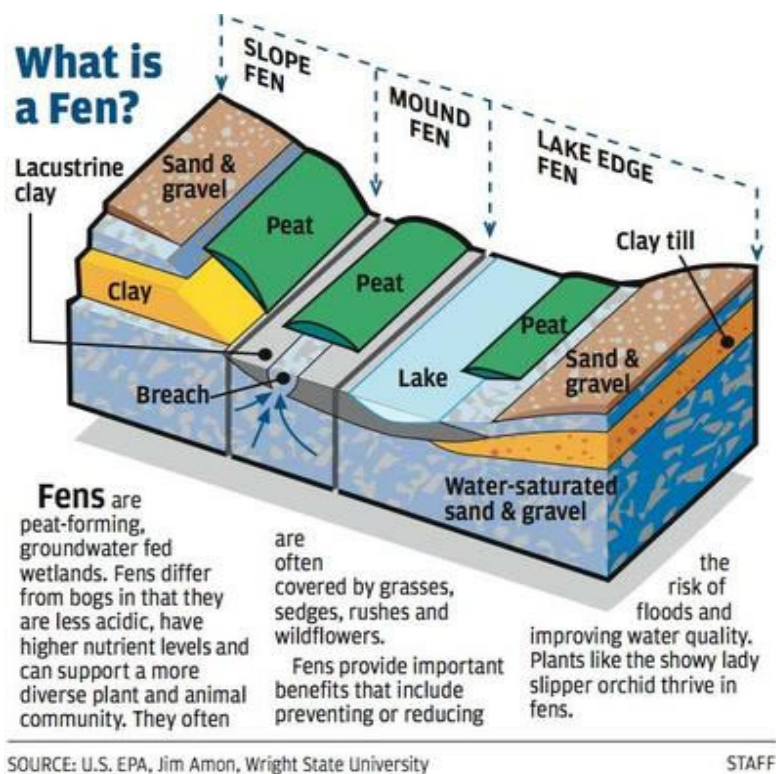


Fig. A.21 Schematic location and characteristics of a fen (from /EPA 12/)

Peatlands, formed from the remnants of autotrophic plants often have a high ash content and low calorie. Fens are often formed on the site of a lake (Fig. A.21), and may gradually develop into a bog. The intensity of the overgrowth and eutrophication of the reservoir depends on the topography of its bed and banks. A widespread process of overgrowth and eutrophication in lakes with a flat bottom and gently sloping beaches is the intensive process of sedimentation with the formation of a variety of sludges.

Dying vegetation falls to the bottom of the reservoir, which is collected and subjected to only a slight degradation due to lack of oxygen in the water leading to an accumulation of organic material and a shallowing of the lake. By the incomplete decomposition by microorganisms and accumulation of organic matter, a loose type of sediment called sapropel is formed. As the shallowing of the lake increases, coastal plants are moving closer to the centre of the reservoir forming a fen. The partially decayed organic matter accumulating in a fen is called peat /CHA 02/. Peat soils can have a wide range of physicochemical characteristics (Tab. A.22). The moisture capacity is 500 – 700 per cent of the dry weight, and the bulk density is 0.15 – 0.20 /POC 75/.

Tab. A.22 Characteristics of peat soils /FES 02/

Type of peat deposit	pH (salt)	Hydrolytic acidity	UEA	Humus [%]	Ash content [%]
		mg equiv per 100 g soil			
Low bog(fen)	5.7 – 5.9	40 – 42	141	44 – 45	15.1
Transitional bog	5.2 – 5.5	65 – 70	136	37 – 45	12.5
Raised bog	3.8 – 3.9	150 – 170	101	50 – 57	6.4

Peat soils of fen are formed in areas fed by abundant underground waters and surface runoff. They are weakly acidic or neutral. The ash content is 6 – 12 percent in normal soils and 30 – 50 percent in high-ash types.

A.5 Group of population considered in reference biosphere assessment

In the reference biosphere model a hypothetical population is assumed. Since the size of the region contaminated with radionuclides from a deep geological repository is not known, no predictions about the size of the population are made. In the discrete models, the hypothetical population obtains all of its food and drinking water from the region affected by radionuclides and is self-sustaining. It is assumed, that the agricultural and consumption habits of the population adapt to the prevailing climate.

The population lives in the contaminated region. Due to this, every member of the population inhales contaminated air all the time and works 1000 hours on contaminated soil during every year. The population is assumed to consist of adults. Other age groups are not included in this assessment.

The consumption habits for the hypothetical population in the transition models are the same as in the discrete models of the same climate region, but not all food is produced on contaminated soil at first. When the lake is still present, only contaminated fish is caught from the lake. When the dried out lakebed is used as a pasture in the first stages of agricultural development, only grass and domestic animals eating this grass are contaminated with radionuclides. In addition to this, the drinking water from wells is also contaminated. The other food types are imported out from uncontaminated areas. In the later stages of the model, the population is assumed to produce all necessary food types on contaminated soil as a conservative assumption.

Glossary

Analogue station: Since the impact of climate change on a given biosphere is subject to large uncertainties it is assumed, that a biosphere subject to certain future changes in climate develops to a biosphere similar to a contemporary biosphere that is subject to a climate similar to the predicted one.

BDCF: Biosphere Dose Conversion Factors (BDCF) are one possible result of radio-ecological models. They are used, when actual radionuclide concentrations in near surface groundwater are not known and a standardized radionuclide concentration in near surface groundwater, for example 1 Bq/L, is used in the model. When the radionuclide concentration for a certain radionuclide in near surface groundwater has been determined, it can be multiplied with the radionuclide specific BDCF to determine an exposure to a hypothetical population.

BIOCLIM: In the BIOCLIM project climate models and scenarios were created to determine possible climate developments in the northern hemisphere and different regions in Europe for the next one million years. The climate models were created by analysing paleoclimatic data and the influence of different factors, like insolation and CO₂ content of the atmosphere, on the climate. In addition to this, potential impacts of climate change on biosphere features influencing the exposure of a population to radionuclides from a deep geological repository were analysed for different regions in Europe.

BIOMASS: BIOMASS describes the development of reference biosphere model systems according to a fixed methodology /IAE 03/. The methodology begins with defining the assessment context and the identification and justification of the biosphere systems. Those biosphere systems are then described in further detail and potentially exposed groups are considered. Finally the model is developed, calculations are done and further iterations can be used to refine the model.

BIOMOSA: Parallel to the BIOMASS project the BIOMOSE project was carried out. In this project, modelling approaches and results of models from different European countries were compared.

Climate state: A climate state defines climate conditions at a certain location. The climate conditions can be defined by certain parameters, like temperature and precipitation, as well as its location in the Köppen/Geiger climate classification system.

Discrete climate state/model: Discrete climate states and models assume that the climate does not change during the model time frame. This is usually done, since processes during the change of climate which may influence modelling results are poorly understood. To increase the knowledge and better define those processes is one of the main motivations for the project presented in this work.

Exposure pathway: An exposure pathway is a potential pathway through which radionuclides move from near surface groundwater through the biosphere to an exposed population.

Reference biosphere: A reference biosphere provides a systematic framework of features events and processes for the creation of radioecological models.

Reference climate region: A reference climate region represents a set of features events and processes defining a biosphere model for a certain climate state.

Self-sustaining hypothetical population: A self-sustaining hypothetical population represents a small group of humans exposed to radionuclides from a deep geological repository. This population derives all its food and drinking water from a contaminated region, lives and works on contaminated land and inhales contaminated soil particles. The population is unaware of the contamination and due to this, no countermeasures to reduce contamination are taken.

Soil texture/OM criterion: The soil texture organic matter (OM) criterion is used by IAEA publications to allocate measured soil dependent radionuclide parameters to different soil types for a data base. Those types are sand, loam, clay and organic soil.

WRB soil types: The World reference Base for Soil Resources (WRB) is a taxonomic soil classification system. The classification is based on soil morphology as a result of pedogenesis.

**Gesellschaft für Anlagen-
und Reaktorsicherheit
(GRS) mbH**

Schwertnergasse 1
50667 Köln

Telefon +49 221 2068-0

Telefax +49 221 2068-888

Forschungszentrum

85748 Garching b. München

Telefon +49 89 32004-0

Telefax +49 89 32004-300

Kurfürstendamm 200

10719 Berlin

Telefon +49 30 88589-0

Telefax +49 30 88589-111

Theodor-Heuss-Straße 4

38122 Braunschweig

Telefon +49 531 8012-0

Telefax +49 531 8012-200

www.grs.de